Studies Toward the Chemistry of N-Confused Porphyrins

by

Ziwei Xiao

B. Sc. Peking University, 1996

M. Sc. The Ohio State University, 1998

A THESIS SUBMITTED IN PARTIAL FULFILMENT OF
THE REQUIREMENTS FOR THE DEGREE OF
DOCTOR OF PHILOSOPHY
in
THE FACULTY OF GRADUATE STUDIES

Department of Chemistry

We accept this thesis as conforming

to the required standard

THE UNIVERSITY OF BRITISH COLUMBIA

January 2003

In presenting this thesis in partial fulfilment of the requirements for an advanced degree at the University of British Columbia, I agree that the Library shall make it freely available for reference and study. I further agree that permission for extensive copying of this thesis for scholarly purposes may be granted by the head of my department or by his or her representatives. It is understood that copying or publication of this thesis for financial gain shall not be allowed without my written permission.

Department of Chemistry

The University of British Columbia
Vancouver, Canada

Date Apr. 14. 2003

Abstract

The objectives of this work were to study the chemistry of N-confused porphyrins, which is a porphyrin isomer with an inverted pyrrole ring, and to develop new photosensitizers based on N-confused porphyrins for photodynamic therapy (PDT).

Alkylation reactions of N-confused porphyrins were studied. N-confused tetraarylporphyrins reacted with CH_3I in the presence of Na_2CO_3 to yield N,N'-dimethylated N-confused porphyrin salts **103 - 107**, which are mixtures of structural isomers. The structures of the major isomers (**III**) were determined by X-ray diffraction and NMR spectroscopic analyses. These N,N'-dimethylated N-confused tetraarylporphyrin salts can generate singlet oxygen when irradiated with light of the appropriate wavelengths and are potential photosensitizers for PDT.

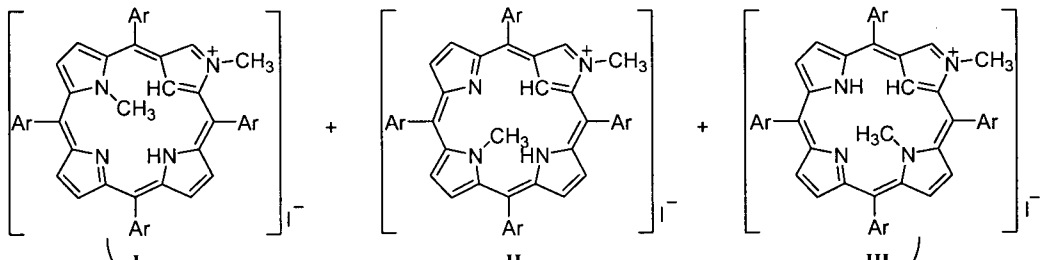

103 Ar = phenyl
104 Ar = *p*-tolyl
105 Ar = *p*-methoxycarbonylphenyl
106 Ar = *p*-methoxyphenyl
107 Ar = *m*-methoxyphenyl

The peripheral carbon-nitrogen double bonds of Ni(II) N-confused porphyrins are partially isolated from the 18 π conjugated aromatic system and reacted as dienophiles in Diels-Alder reactions with *o*-benzoquinodimethane yielding novel Ni(II) N-confused isoquinoporphyrins **133 (a-c)**. Ni(II) N-confused tetraphenylisoquinoporphyrin, **133a**, was structurally characterized by X-ray diffraction analysis.

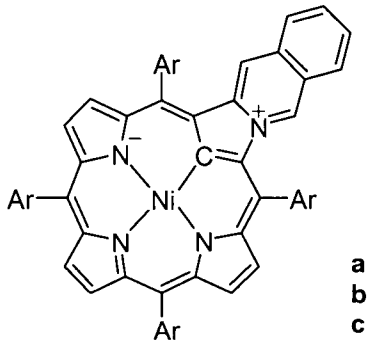

a Ar = phenyl
b Ar = *p*-tolyl
c Ar = *p*-ClC_6H_4

133(a-c)

Reaction of Ni(II) N-confused tetrakis(*p*-tolyl)porphyrin with $NaOCH_3$ and DDQ resulted in the inner C(21) cyanide addition product **146**. Minor product **145** was presumably formed by subsequent nucleophilic addition of CH_3O^- to **146** at C(3) followed by oxidation with DDQ. Structures of both complexes **145** and **146** were determined by X-ray diffraction analyses.

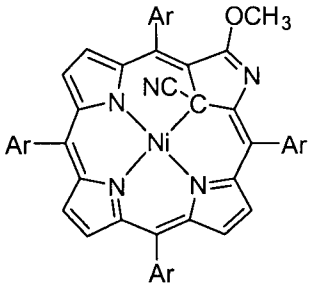

145

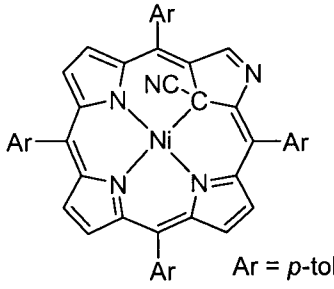

Ar = *p*-tolyl

146

The Ni(III) complex of N-confused porphyrin inner C-oxide **153** was synthesized from oxidation of the precursor Ni(II) N-confused porphyrin using OsO_4. This Ni(III) complex has been structurally characterized.

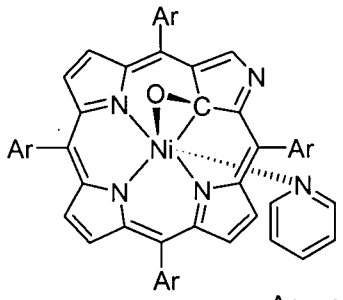

Ar = *p*-tolyl

153

Table of Contents

List of Tables

List of Figures

List of Schemes

List of Abbreviations

AMD	age-related macular degeneration
Anal.	analytical
BPDMA	benzoporphyrin derivative monoacid ring A
br	broad (NMR)
Calcd	calculated
conc.	concentrated
COSY	correlated spectroscopy
d	doublet
DDQ	2,3-dichloro-5,6-dicyano-1,4-benzoquinone
DFT	density functional theory
DMAD	dimethylacetylene dicarboxylate
DMF	N,N-dimethylformamide
DPBF	1,3-diphenylisobenzofuran
EI	electron impact ionization
EPR	electron paramagnetic resonance
equiv.	equivalent
FAB	fast atom bombardment
h	hour(s)
HMBC	heteronuclear multiple bond connectivity
HMQC	heteronuclear multiple quantum coherence
HRLSIMS	high resolution liquid secondary ionization mass spectrometry
HSQC	heteronuclear single quantum coherence
LSIMS	liquid secondary ionization mass spectrometry
m	meta
m	multiplet
m/e	mass/charge
min	minute(s)

MS	mass spectrometry
MSA	methanesulfonic acid
N_2CP	doubly N-confused porphyrin
NBS	N-bromosuccinimide
NCP	N-confused porphyrin
NCS	N-chlorosuccinimide
NCTAP	N-confused tetraarylporphyrin
NCTPP	N-confused tetraphenylporphyrin
NCTTP	N-confused tetra(*p*-tolyl)porphyrin
NFP	N-fused porphyrin
NIS	N-iodosuccinimide
NMR	nuclear magnetic resonance
NOE	nuclear Overhauser effect
o	ortho
OEP	2,3,7,8,12,13,17,18-octaethylporphyrin
ORTEP	Oak Ridge thermal ellipsoid plot
p	para
PDT	photodynamic therapy
p-TsOH	toluene *p*-sulfonic acid
r. t.	room temperature
s	singlet
t	triplet
TBAB	tetrabutylammonium bromide
TFA	trifluoroacetic acid
TLC	thin layer chromatography
TPP	*meso*-tetraphenylporphyrin
TTP	*meso*-tetra(*p*-tolyl)porphyrin
UV-vis	ultraviolet-visible

Nomenclature

Porphyrins and N-Confused Porphyrins

The parent porphyrin system is called porphine. The numbering of ring positions, including the nitrogens and the use of letters denoting individual rings, is shown below. Positions 1, 4, 6, 9, 11, 14, 16, and 19 are termed "α" positions, 2, 3, 7, 8, 12, 13, 17, and 18 are "β" positions and 5, 10, 15, and 20 are "*meso*" positions.

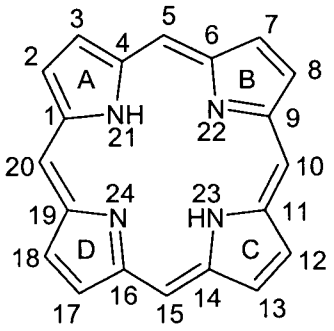

porphine

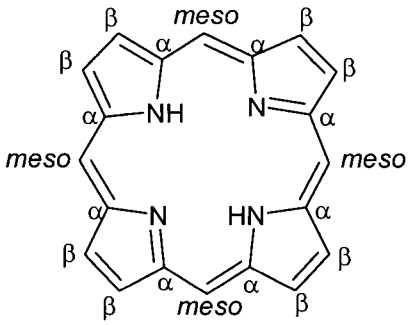

porphine

N-confused porphyrin is named as 2-aza-21-carbaporphyrin and the numbering is shown below.

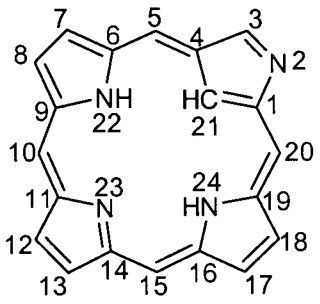

N-confused porphyrin

Acknowledgements

I would like to thank Dr. David Dolphin for advice, guidance and academic freedom to explore porphyrin chemistry. I also owe gratitude to members of Dolphin's group, past and present, who offered me invaluable assistance. I greatly appreciate the help from Mr. Jack Chow, Dr. Alison Thompson, Dr. Yuichi Terazono, and Dr. Ethan Sternberg for their ideas and advice.

Special thanks go to Dr. Elizabeth Cheu, Mr. Andrew Tovey, Dr. Sharon Hannah and Dr. Ji-Young Shin for kindly proof-reading sections of this thesis. Dr. Cheu has been especially helpful offering invaluable critique.

I am grateful to Dr. Brian Patrick for the X-ray crystal structures, Ms. Liane Darge and Ms. Marietta Austria for taking NMR spectra, Mr. Peter Borda for microanalyses, and Dr. Nick Burlinson for his advice and helpful discussions on NMR spectroscopy. Services provided by staff in mass spectrometry and glassblowing as well as administrative staff are sincerely appreciated.

I have to thank my parents, Mr. Hanhua Xiao and Ms. Nengguang Liu, who brought me to the world of science. Their constant support and encouragement have been invaluable and are deeply appreciated.

Finally I would like to thank my wife Jiangjiao, who has been very supportive to me toward completion of this thesis work.

Chapter 1

Introduction

1.1 Porphyrin and Porphyrin Related Macrocycles

Porphyrins are aromatic tetrapyrrolic macrocycles consisting of four pyrrole units joined through four methine bridges (Figure 1.1).[1] Although they have 22 π-electrons, only 18 of these π-electrons are involved in a cyclic delocalized pathway, which fulfills the requirement of Huckel's rule (4n + 2, n = 4). X-ray diffraction analyses of both free base porphyrins and metalloporphyrins have shown the planarity of the porphyrin skeleton, which is a requirement for aromatic character.[2,3] Signals for the *meso*-H atoms of typical porphyrins in ^{1}H NMR spectra appear at about 10 ppm, while signals for the two inner pyrrole protons are observed between -2 to -5 ppm, suggesting a strong ring current.[3] Saturation of the two cross-conjugated double bonds at the β positions does not affect the aromaticity; consequently these two bonds are relatively reactive. Reduction of one of these double bonds leads to formation of a chlorin and a further one bond reduction leads to formation of either a bacteriochlorin or an isobacteriochlorin (Figure 1.1).[3]

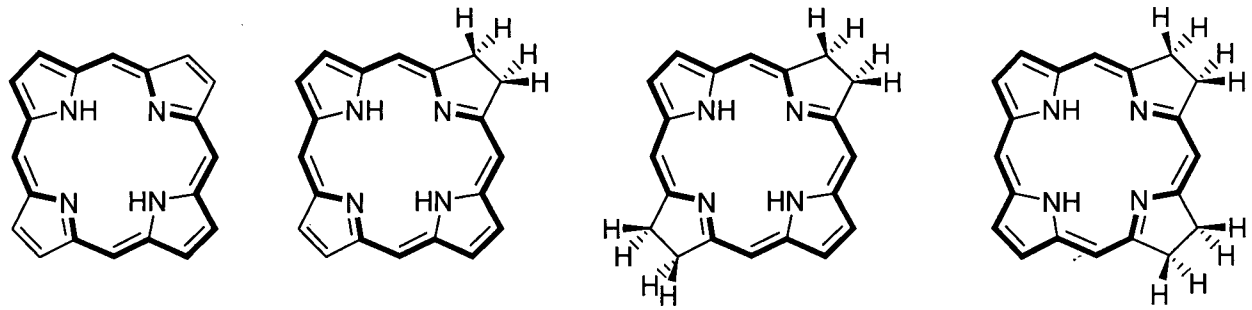

Figure 1.1 Porphyrin and porphyrin related macrocycles.

The four nitrogen atoms in a porphyrin are ideally arranged to chelate metal cations and thus readily form metal porphyrin complexes. Metalloporphyrins have been extensively studied, and most metals and some semimetals have been inserted into porphyrins, including all metals in the third to fifth row of the periodic table.[3,4] Metalloporphyrins play important roles in a wide variety of biological processes, for example, iron complexes of protoporphyrin-IX, **1**, and chlorophylls **2** (Figure 1.2).[5] The Fe(II) complex of protoporphyrin-IX is the prosthetic group of hemoglobin and myoglobin.[5] Both hemoglobin and myoglobin reversibly bind O_2. Hemoglobin transports O_2 in blood plasma and myoglobin stores O_2 in cellular tissues.[5] The Fe(III) complex of protoporphyrin-IX forms the prosthetic group of catalases and peroxidases, which are essential components of the biological defense against oxygen toxicity by removing reactive intermediates such as superoxide (O_2^-) and peroxide (O_2^{2-}).[5] Chlorophylls play a key role in the harvesting of light energy during photosynthesis.[5]

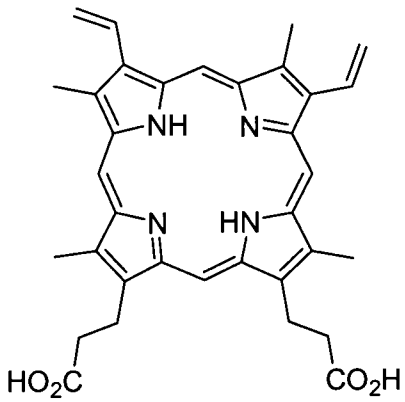

protoporphyrin-IX **1**

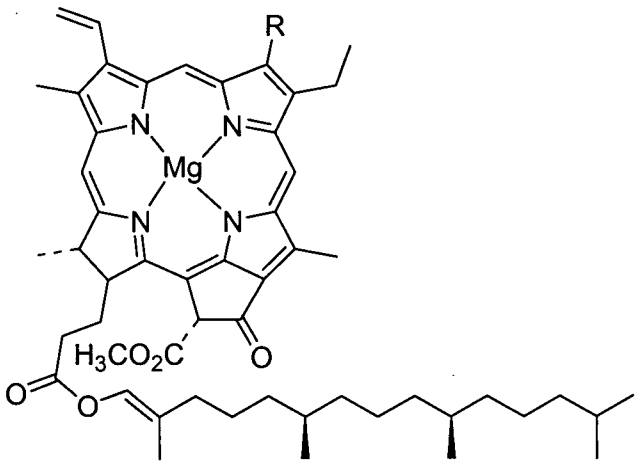

chlorophyll-a **2a** R = CH_3
chlorophyll-b **2b** R = CHO

Figure 1.2 Protoporphyrin-IX **1** and chlorophylls **2**.

Porphyrins have an intense absorption (molar extinction coefficient between 100,000 - 400,000 $M^{-1}cm^{-1}$) around 400 nm in the visible region, referred to as the Soret or B band.[3,6] Porphyrins also have lower intensity absorption bands between 450 and 650 nm, called Q-bands.[3] Compared to those of porphyrins, the Soret band of chlorins is weaker, whilst the lowest energy Q-band of chlorins is normally red-shifted about 20 - 30 nm and has a 10 times greater intensity (Figure 1.3).

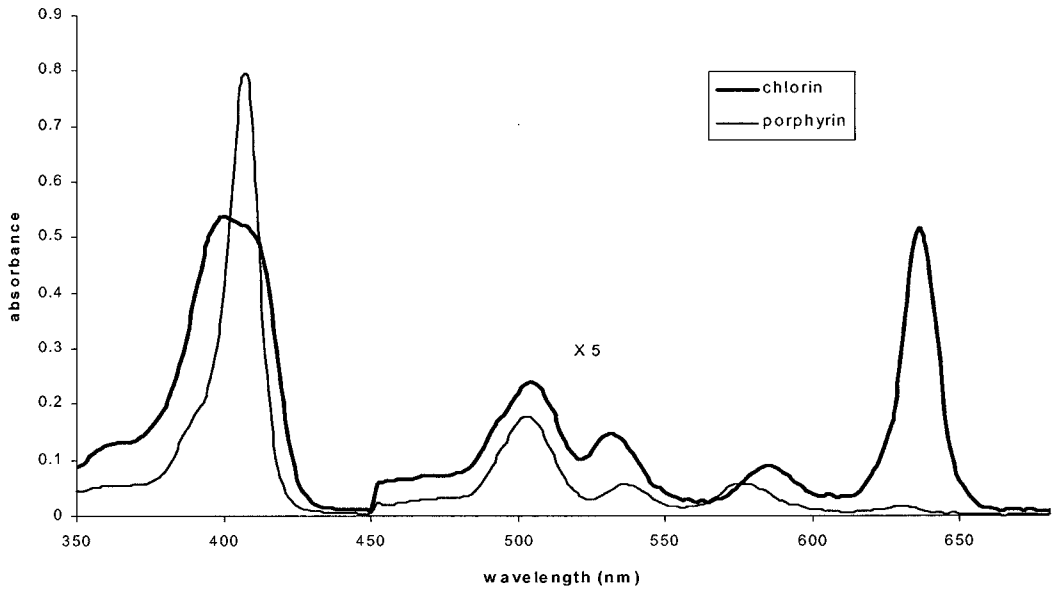

Figure 1.3 UV-vis spectra of a porphyrin and a chlorin (absorbance between 450 and 680 nm is shown with a 5 times greater intensity for clarity).

1.2 Photodynamic Therapy (PDT)

Photodynamic therapy (PDT)[7,8] is "a medical treatment which employs the combination of light and a drug to bring about a cytotoxic or modifying effect to cancerous or otherwise unwanted tissue".[7] PDT employs the use of a photosensitizer. This photosensitizer can be excited by irradiation and transfers energy to a desired reactant. PDT is used to treat diseases which involve rapid cell growth, such as cancerous tissues or abnormal blood vessels.[7] The first step involves intravenous administration of the photosensitizer which attaches to lipoproteins in the bloodstream. As rapidly dividing cells have more lipoproteins than normal cells, the photosensitizer concentrates in these tissues.[7,8] The photosensitizer is then activated with a laser at a particular wavelength where the photosensitizer absorbs extensively compared to endogenous chromophores. Once activated, the photosensitizer converts triplet oxygen to singlet oxygen, which readily reacts with many cell components resulting in cell death.[7,8]

Porphyrin and porphyrin related macrocycles have been extensively studied as potential PDT agents as they may absorb at ideal wavelengths for maximal therapeutic effect. At present, most photosensitizers in clinical trials for PDT are porphyrin related macrocycles.[9]

1.2.1 Mechanism of Photosensitization

The process of photosensitization is shown in a modified Jablonski diagram (Figure 1.4).[9-11] After absorption of light, the photosensitizer is converted from its ground singlet state (S_0) into excited singlet states (S_n). An excited singlet state molecule can lose energy *via* internal conversion ($S_m \rightarrow S_n$ + heat, $m > n$) until it reaches the first excited singlet state (S_1), which normally has a very short lifetime (~10^{-6} s).[9] The first excited singlet state (S_1) can return to the

ground singlet state (S_0) through either internal conversion or fluorescence.[11] The first excited singlet state can also be transformed into an electronically excited triplet state (T_1) through a spin forbidden process, intersystem crossing ($S_1 \rightarrow T_1$ + heat). The triplet state can return to the ground singlet state through either phosphorescence or energy transfer.[11] With phosphorescence being spin forbidden, the triplet state usually has a longer lifetime (~10^{-2} s) than that of an excited singlet state.[9]

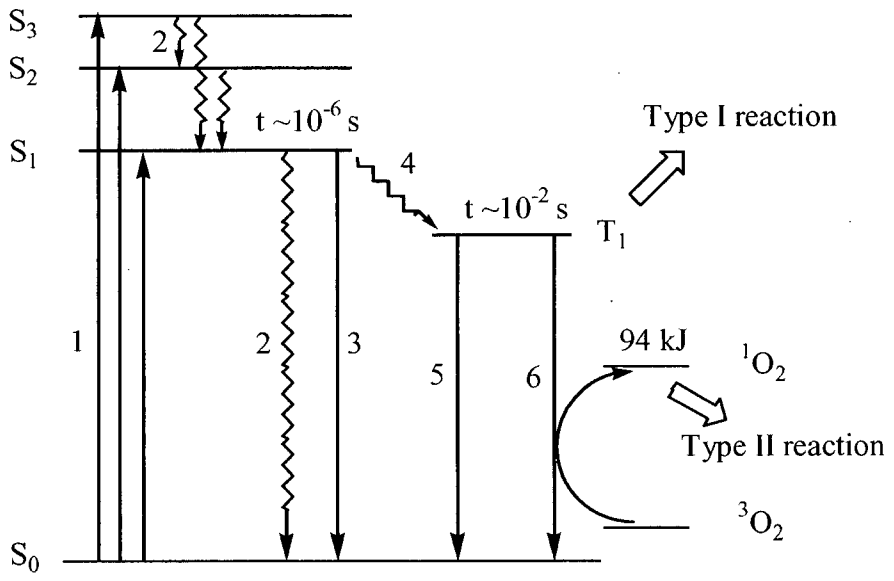

1. Absorption; 2. Internal Conversion; 3. Fluorescence;
4. Intersystem Crossing; 5. Phosphorescence; 6. Energy Transfer

Figure 1.4 Modified Jablonski diagram.[9-11]

The triplet state photosensitizer (^{3}sensitizer) can undergo energy transfer *via* two types of reactions. It can abstract an electron or hydrogen atom from a substrate (Type I Reaction):[9-11]

$$^3\text{sensitizer} + \text{substrate} \rightarrow \text{sensitizer}^- + \text{substrate}^+_{(ox)}$$

$$^3\text{sensitizer} + \text{RH} \rightarrow \text{sensitizerH}\cdot + \text{R}\cdot$$

The anionic photosensitizer can react with O_2 to generate a superoxide anion (O_2^-).[9-11]

$$\text{sensitizer}^- + O_2 \rightarrow \text{sensitizer} + O_2^-$$

The free substrate radical (R·) generated from hydrogen atom abstraction can react with O_2 and ultimately produce hydroperoxides.[9-11]

$$R\cdot + O_2 \longrightarrow RO_2\cdot \xrightarrow{\text{sensitizerH}\cdot \text{ (or other H donor)}} RO_2H + \text{sensitizer}$$

Both superoxide anion and hydroperoxides are very reactive species and can react further with a variety of substrates.[9-11]

The triplet state photosensitizer can also return to the ground state through reaction with triplet oxygen ($^3O_2$) giving singlet oxygen ($^1O_2$) (Type II Reaction).[9-11] Singlet oxygen is a powerful oxidant which reacts with biological substrates in a variety of ways, for example (Scheme 1.1):[10,11]

A. Addition to the diene systems in heterocycles to give endoperoxides.

B. Hydrogen abstraction and addition ("ene" reactions with compounds with allylic hydrogen atoms).

C. [2 + 2] addition to double bond followed by the cleavage of that bond.

D. Oxidation of sulfides to sulfoxides.

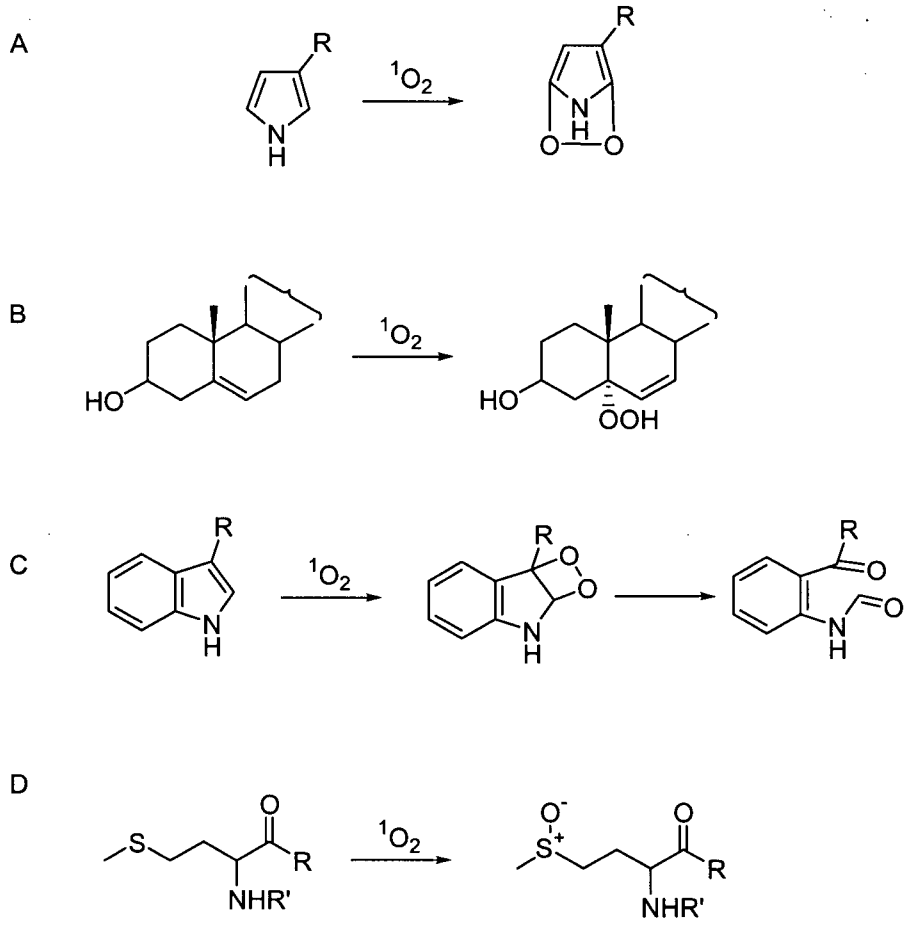

Scheme 1.1 Reactions of singlet oxygen with biological substrates.

These reactions result in destruction of biological substrates such as membranes, enzymes, proteins and nucleic acids.[11] It is generally agreed that singlet oxygen is the key agent of cellular damage in PDT,[9] although there is indication that the superoxide ion may also be involved in some aspects of PDT damage.[9]

1.2.2 Desirable Properties of a PDT Drug

Ideally, a PDT drug, as drugs in general, should be easily and economically synthesized. Furthermore, a PDT drug should have strong absorption at wavelengths between 650 and 800 nm for the following reasons:

- The presence of endogenous chromophores such as hemoglobin results in very poor penetration of tissues by light at wavelengths below 650 nm.[7]
- A compound which absorbs light above 800 nm may not have a large enough energy gap between its triplet state and ground state to generate singlet oxygen.[7]

The criteria mentioned above are considered in this thesis work. Other desirable properties, such as high light toxicity,[7] low dark toxicity,[7] rapid clearance after injection,[7] localizing specifically in tumours,[7] and ease of formulation,[7] are hard to control at the organic synthetic level.

1.3 From Porphyrins to Chlorins

As the lowest energy Q-band of chlorins is normally red-shifted 20-30 nm and has a 10 times greater absorption intensity compared to that of porphyrins, chlorins are better candidates as photosensitizers for PDT.[7] Many methods have been developed to convert porphyrins to chlorins, for example, Diels-Alder reactions of porphyrins with β-vinyl groups as dienes,[7,12,13] dihydroxylation with OsO_4,[14] cycloaddition reactions of porphyrins as dienophiles or dipolarophiles,[15,16] diimide reductions[17] and cyclopropanations with carbenes.[18]

1.3.1 Diels-Alder Reactions of Porphyrins as Dienes

Porphyrins with β-vinyl groups can act as dienes and react with various dienophiles to yield the corresponding chlorins. For example, the benzoporphyrin derivative monoacid ring A (BPDMA, **4**) was derived initially from the Diels-Alder reaction of protoporphyrin-IX dimethyl ester **3** with dimethylacetylene dicarboxylate (DMAD) (Scheme 1.2).[7,12,13] BPDMA has been approved in more than 60 countries to treat age-related macular degeneration (AMD)[7], the major cause of vision loss in people over the age of 60 in developed countries.

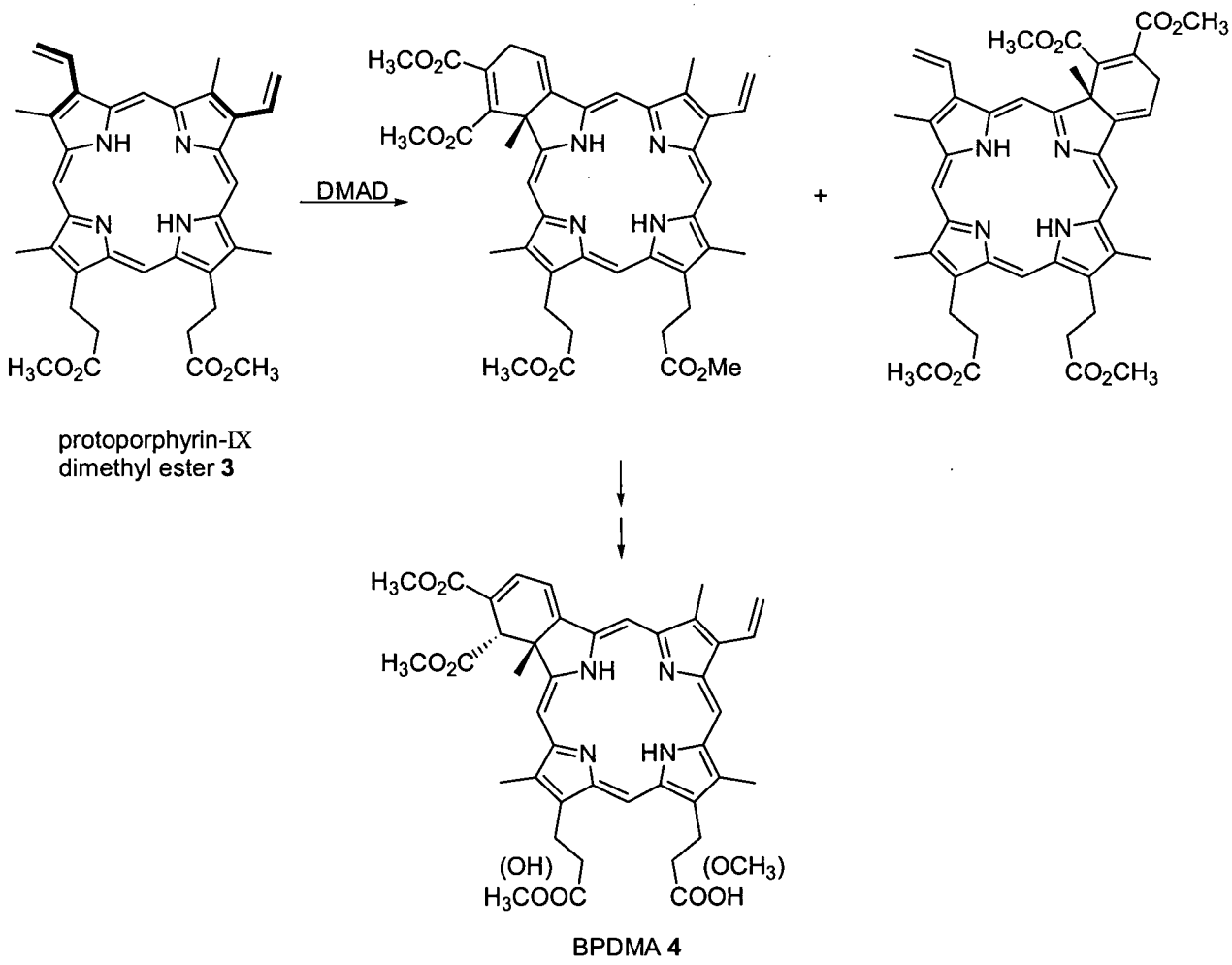

Scheme 1.2 Synthesis of BPDMA, **4**.

1.3.2 Dihydroxylation of Porphyrins with OsO_4

Dihydroxychlorins can be obtained by oxidation of porphyrins with OsO_4. For example, *meso*-tetraphenylporphyrin (TPP, **5a**) reacts with OsO_4 giving *meso*-tetraphenyl-2,3-*cis*-dihydroxy-2,3-chlorin, **6** (49 %) (Scheme 1.3).[14]

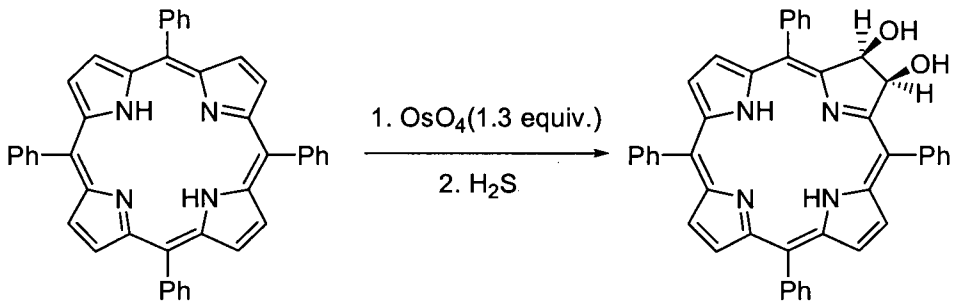

TPP **5a** **6**

Scheme 1.3 Dihydroxylation of TPP with OsO_4.

1.3.3 Cycloaddition Reactions of Porphyrins as Dienophiles or Dipolarophiles

Diels-Alder reactions of *meso*-tetraarylporphyrins **5 (a-d)** as dienophiles with *o*-benzoquinodimethane, **8**, were investigated by Cavaleiro *et al.*[15] TPP, **5a**, reacts with *o*-benzoquinodimethane, generated *in situ* from the sulfone **7**, to yield chlorin **9a** (26 %), naphtho[2,3-b]porphyrin, **10a** (20 %), and compound **11a** (20 %) (Scheme 1.4). Similar results are obtained when *meso*-tetraarylporphyrins **5 (b,c)** are used.[15]

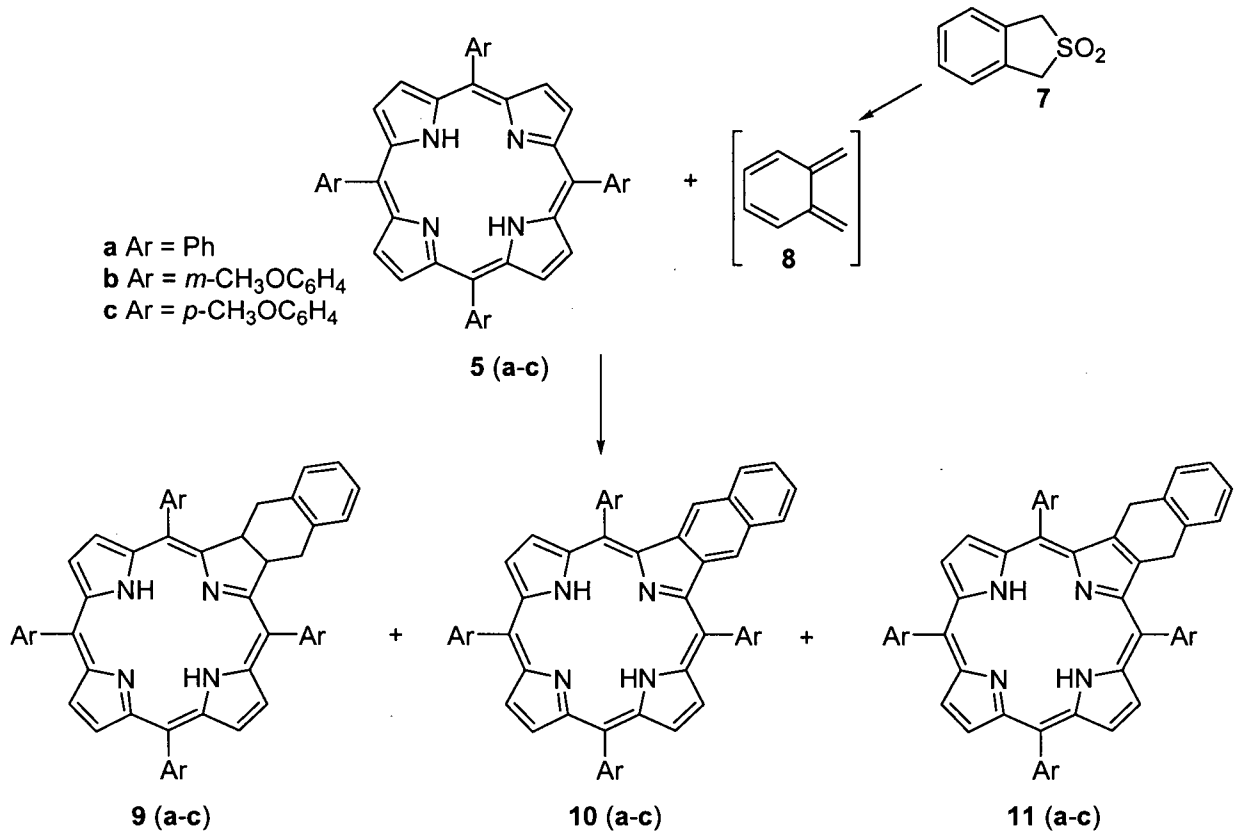

Scheme 1.4 Diels-Alder reactions of tetraarylporphyrins **5 (a-c)** with *o*-benzoquinodimethane.

When *meso*-tetrakis(pentafluorophenyl)porphyrin, **5d**, is used, chlorin **9d** (35 %) and two bacteriochlorin isomers **12** are obtained (Scheme 1.5). Porphyrin **5d** is electron-deficient and *o*-benzoquinodimethane is known to react more easily with electron-deficient dienophiles, which might explain why there can be addition of two equivalents of *o*-benzoquinodimethane to porphyrin **5d**.

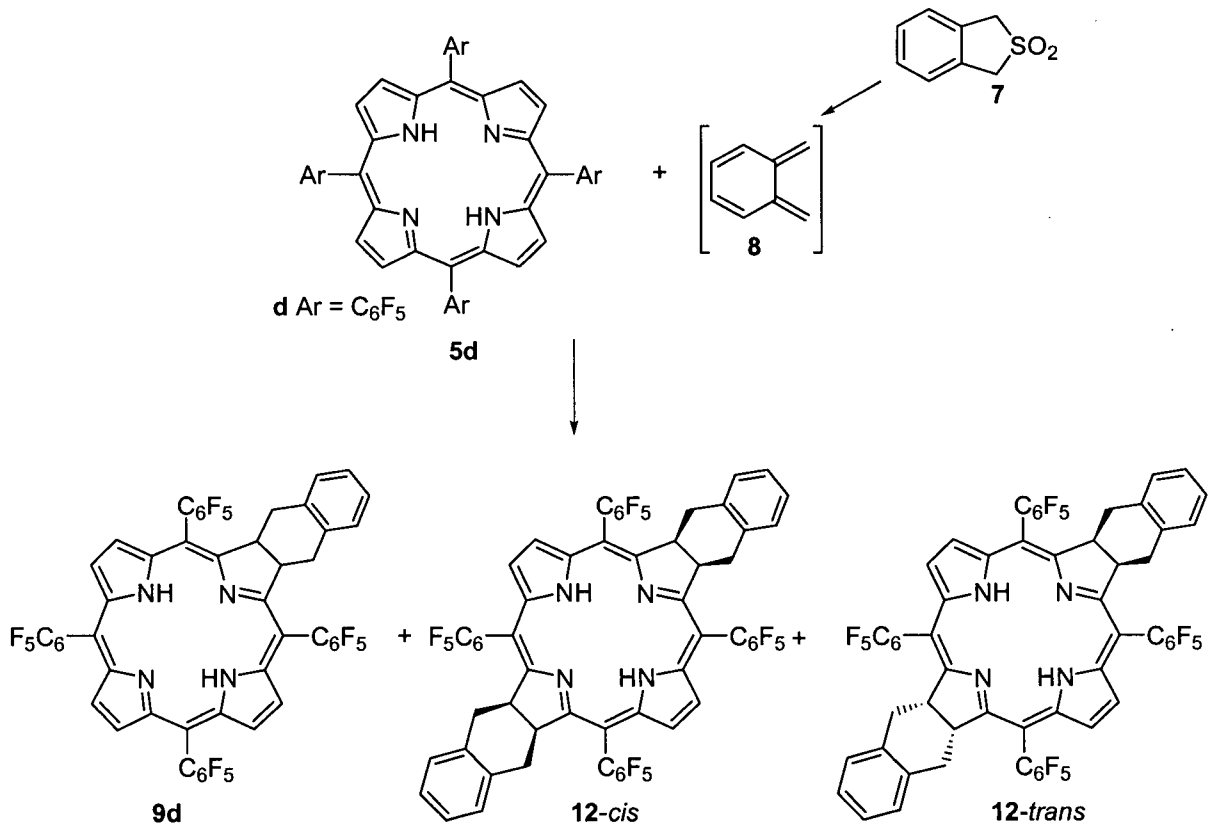

Scheme 1.5 Diels-Alder reactions of *meso*-tetrakis(pentafluorophenyl)porphyrin, **5d**, with *o*-benzoquinodimethane.

The 1,3-dipolar cycloaddition reaction of porphyrin **5d** as dipolarophile with azomethine **13** (Scheme 1.6) yields chlorin **14** (61 %) and isobacteriochlorin **15** (11 %).[16] There are four possible bis-adducts, *cis* or *trans* bacteriochlorins and isobacteriochlorin. The formation of bis-adducts in this reaction is regio- and stereoselective, yielding mainly *trans*-isobacteriochlorin **15**. Isobacteriochlorin **15** can also be obtained by the reaction of chlorin **14** with azomethine **13**.

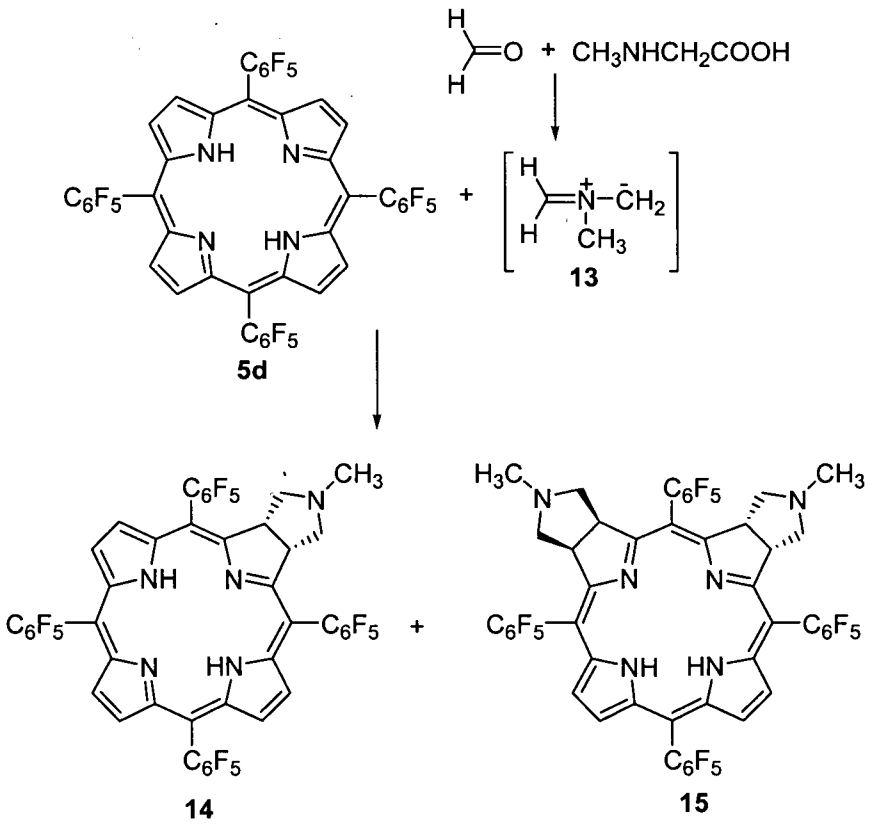

Scheme 1.6 1,3-Dipolar cycloaddition reaction of porphyrin **5d** with azomethine **13**.

1.4 N-Confused Porphyrins

1.4.1 Introduction

N-confused porphyrin (NCP) is a porphyrin isomer with an inverted pyrrole ring (Figure 1.5). Preparations of N-confused porphyrins were first independently reported by the groups of Furuta[19] and Latos-Grażyński[20] in 1994. In both cases, N-confused tetraarylporphyrins **16 (a,b)** were obtained through acid catalyzed condensation of pyrrole and aryl aldehyde with a yield of about 5 %.

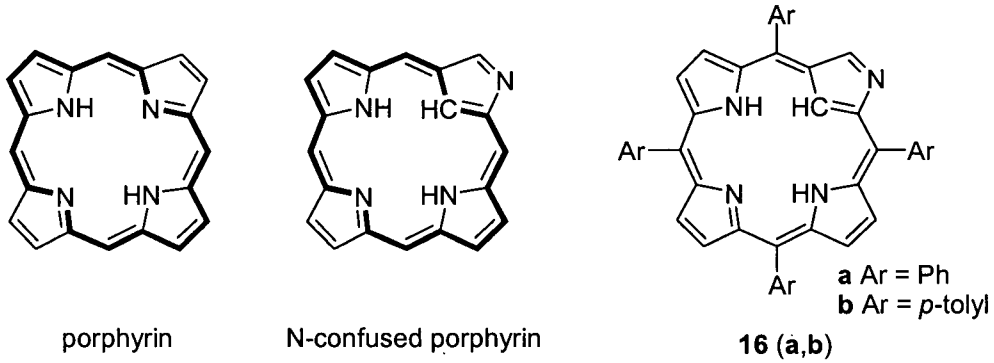

porphyrin N-confused porphyrin **16 (a,b)**

Figure 1.5 Porphyrin and N-confused porphyrins.

Similar to porphyrins, N-confused porphyrins have an 18 π-electron pathway and are aromatic (Figure 1.5). The ^{1}H NMR spectrum of N-confused tetraphenylporphyrin (NCTPP, **16a**) reveals characteristic high-field signals for the inner NHs and CH (at -2.5 and -5.1 ppm, respectively), as a result of the aromatic ring current.[19]

The Soret band and Q-bands in the electronic absorption spectrum of NCTPP in CH_2Cl_2 are broadened and red-shifted (λ_{max} = 438 and 725 nm, respectively), as compared to those of

TPP (419 and 647 nm),[19] suggesting a potential application of NCPs as photosensitizers in PDT (Figure 1.6).

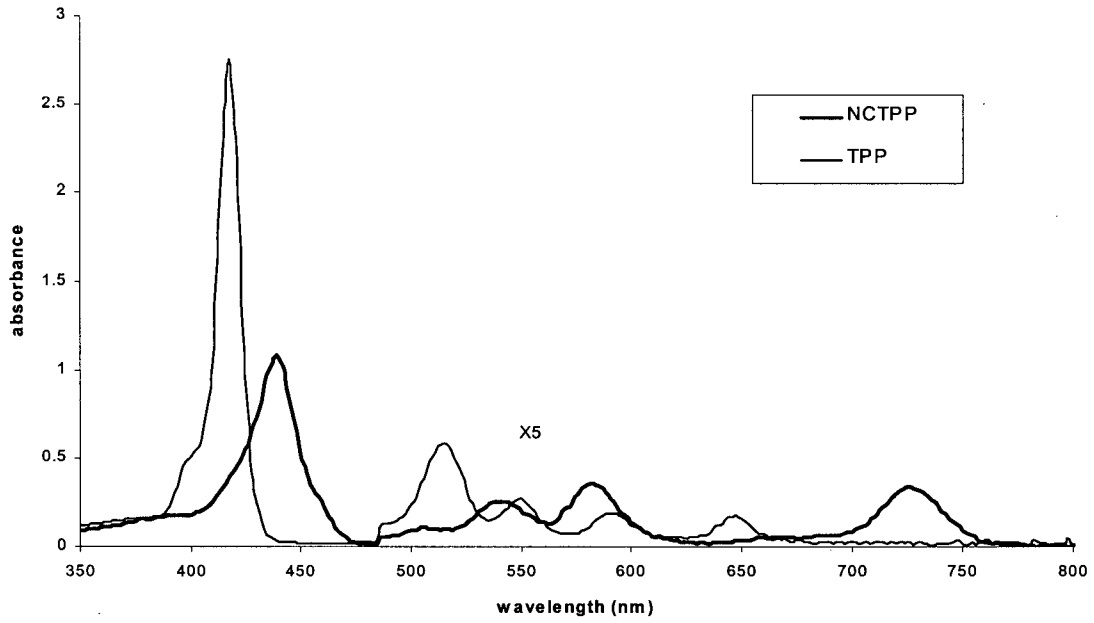

Figure 1.6 UV-vis spectra of NCTPP and TPP (absorbance between 484 and 800 nm is shown with a 5 times greater intensity for clarity).

As reported by Latos-Grażyński *et al.*,[20] Ni(II) can be inserted into N-confused tetra(*p*-tolyl)porphyrin (NCTTP, **16b**) under mild conditions to yield (NCTTP)Ni^{II}. The most notable feature of this complex is the coordination through the unprotonated inner carbon, suggested by the disappearance of the C(21)H proton resonance in the ^{1}H NMR spectrum of (NCTTP)Ni^{II}.

N-confused porphyrins have been extensively studied since the first reports on their preparations.[21-31] Many synthetic methods were developed.[21-24] Different reactions of NCPs have been studied, including its alkylation reactions and coordination chemistry.[25-29] Other porphyrin analogues with a CH in the inner macrocycle have been synthesized.[30,31]

1.4.2 Structural Features of N-confused Porphyrins

The structure of NCTPP was determined by single crystal X-ray diffraction analysis (Figure 1.7).[19] Crystals of NCTPP were obtained from a CH_2Cl_2/CH_3OH solution of NCTPP. Unlike TPP, the skeleton of NCTPP deviates from planarity.[19] The confused pyrrole ring is tilted from the reference N(2)N(3)N(4) plane by 26.9°.[19] Two adjacent and opposite pyrrole rings are tilted by 13.4°, 7.8°, and 5.8°, respectively. This deviation from planarity appears to result from mutual repulsion of the three inner hydrogen atoms.[19]

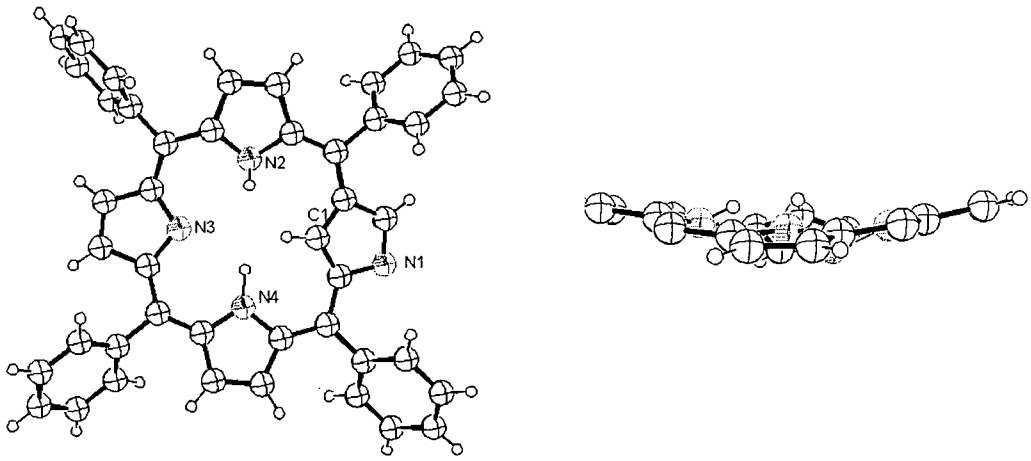

Figure 1.7 ORTEP drawings of NCTPP (obtained from a CH_2Cl_2/CH_3OH solution) showing thermal ellipsoids at the 50 % probability level: top view (left) and side view (right). Solvent in both views and phenyl groups in the side view have been omitted for clarity.

The structures and electronic energies of hypothetical tautomers of N-confused porphyrins (Figure 1.8) were investigated by Szterenberg and Latos-Grażyński using density functional theory (DFT).[32] Porphyrin was included to evaluate the relative stability of NCP with

respect to porphyrin. Tautomer 2-NH-CPH_2 was suggested by Ghosh to promote the hypothetical carbene-like coordination of C(21) and to explain the unexpectedly labile inner C-H bond.[33,34] The calculated total electronic energies are presented in Table 1.1. Tautomer 21-CPH_2 in both solid state and $CHCl_3$ solution has been reported by the groups of Latos-Grażyński[20] and Furuta,[19] and is calculated to be the most stable tautomer.[32] There is only a small calculated energy difference between 21-CPH_2 and 21-H-21-CPH or 2-NH-CPH, suggesting the possibility of equilibria with the less stable tautomers.[32] The energy of 2-NH-CPH_2 at 34.56 kcal/mol (B3LYP/6-31G**//B3LYP/6-31G) with respect to 21-CPH_2 is high compared to that of either 21-H-21-CPH or 2-NH-CPH, but is quite moderate considering its carbenic nature.[32]

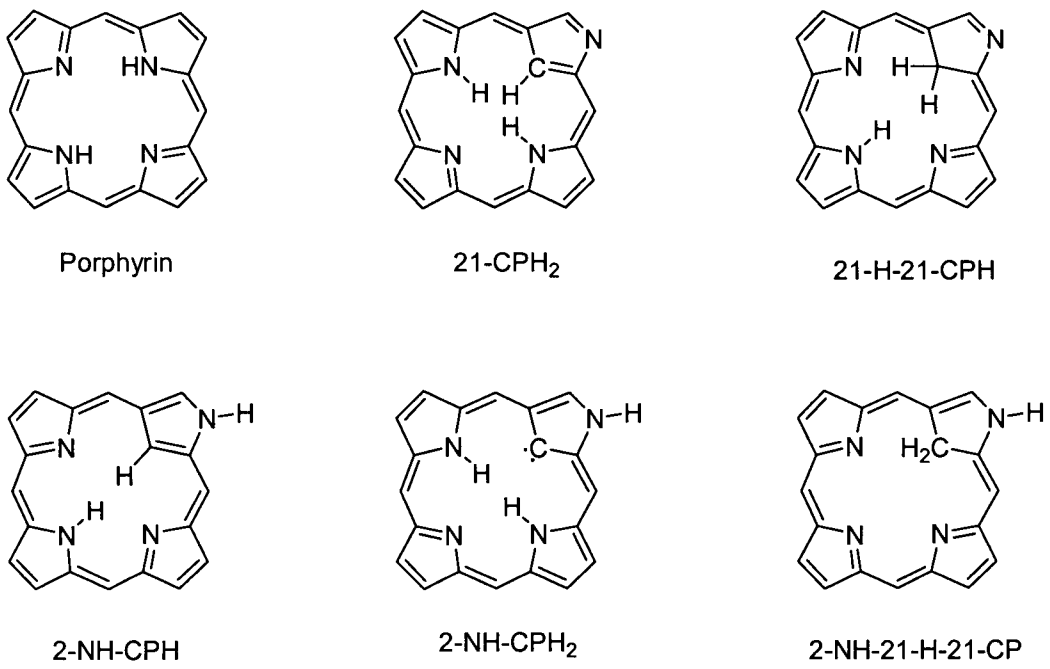

Figure 1.8 Porphyrin and hypothetical tautomers of N-confused porphyrin.

Table 1.1 Calculated relative electronic energies (kcal/mol) for porphyrin and hypothetical tautomers of N-confused porphyrin.

macrocycle	B3LYP/3-21G// B3LYP/3-21G	B3LYP/6-31G// B3LYP/6-31G	B3LYP/6-31G**// B3LYP/6-31G
Porphyrin	-22.95	-21.08	-20.41
21-CPH_2	0	0	0
21-H-CPH	6.20	8.22	3.00
2-NH-CPH	3.39	4.56	4.56
2-NH-CPH_2	31.44	33.82	34.56
2-NH-21-H-CP	41.31	43.93	36.00

Calculations employing DFT on 2-NH-CPH and 2-NH-CPH_2 relative to 21-CPH_2 were carried out also by Ghosh *et al.*[35] and the results were similar to those described above.

The presence of a type 2-NH-CPH tautomer was first reported by Furuta *et al.*[36] A color difference of NCTPP in $CHCl_3$ (red) and DMF (green) was observed. The ^1H NMR spectra of NCTPP in $CDCl_3$ and DMF-d_7 were examined. The type 21-CPH_2 tautomer, predominant in $CDCl_3$, has signals at -4.99 and -2.41 (2H) ppm, respectively, for inner CH and NHs.[19] On the other hand, the ^1H NMR spectrum of NCTPP in DMF-d_7 shows singlet signals at 0.76, 2.27, and 13.54 ppm, assigned to the inner CH, inner NH and outer NH, respectively, suggesting existence

of the type 2-NH-CPH tautomer, which should be stabilized by the hydrogen-bond between the peripheral NH and DMF.[36] The structure of a type 2-NH-CPH tautomer was explicitly determined by X-ray diffraction analysis with a crystal obtained from a DMF-MeOH solution of NCTPP (Figure 1.9).[36] The porphyrin skeleton is planar with four pyrrole rings tilted at 4.7°, 0.2°, 2.8°, and 0.9°, respectively, from the reference N(2)N(3)N(4) plane. The distance between the peripheral N of NCP and O of the associated DMF molecule is 3.101 Å, within hydrogen-bonding distances.

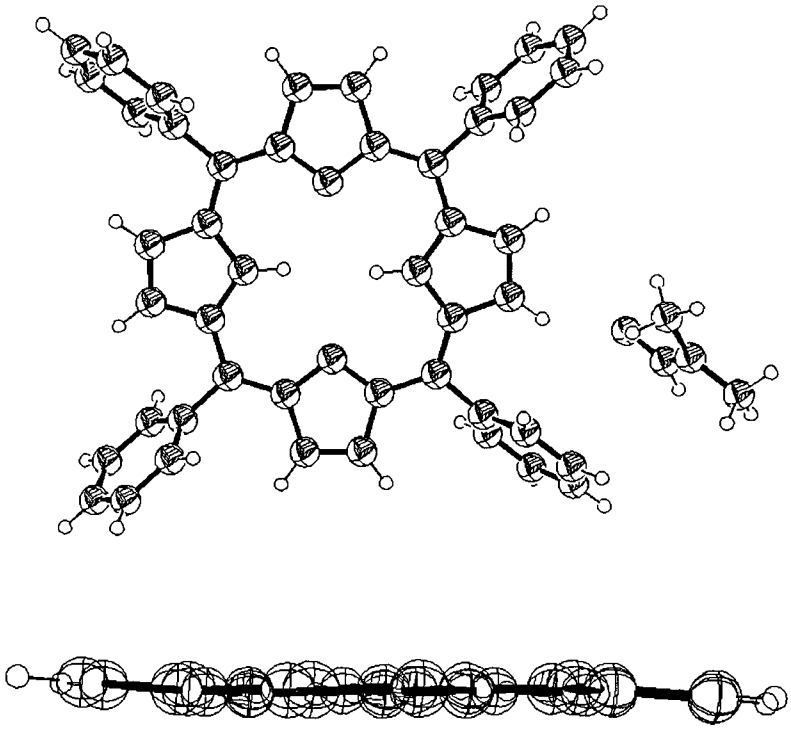

Figure 1.9 ORTEP drawings of NCTPP obtained from DMF-MeOH showing thermal ellipsoids at the 50 % probability level: top view (up) and side view (down). For clarity, phenyl groups have been omitted in the side view.

1.4.3 Preparation of N-Confused Porphyrins

N-confused porphyrins were initially synthesized from acid catalyzed condensation of pyrrole and aryl aldehyde, with Latos-Grażyński *et al.* using an excess of pyrrole and $BF_3 \cdot Et_2O$,[20] and Furuta *et al.* using a 1:1 ratio of starting materials with HBr as a catalyst.[19] In both cases, N-confused porphyrins were obtained in ~5 % yield.

Latos-Grażyński *et al.* suggested that two helical conformations of tetrapyrromethane differing only by a single 180° rotation of the terminal pyrrole are intermediates of this reaction (Scheme 1.7).[20] Both intermediates are susceptible to electrophilic attack at either the α or β positions, and upon oxidation afford tetra(*p*-tolyl)porphyrin (TTP) or NCTTP, respectively.

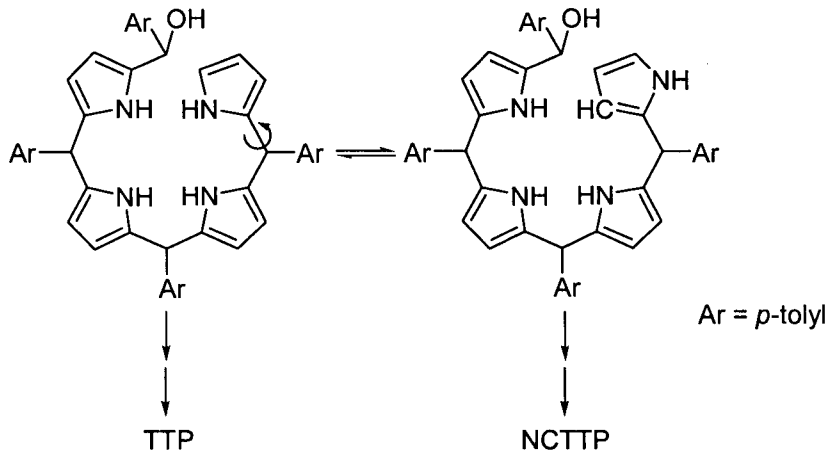

Scheme 1.7 Mechanism of NCTTP formation as suggested by Latos-Grażyński.

The effects of the use of various acids as catalysts for the preparation of N-confused porphyrins by condensation of pyrrole and aryl aldehyde were studied by Lindsey *et al.* and it was found that the highest yield was obtained using methanesulfonic acid (MSA).[21] For

example, a 1.5 L preparative scale reaction employing 10 mM of pyrrole and benzaldehyde and 7 mM of MSA affords NCTPP in the yield of 35 % (800 mg).[21]

A lower yield was obtained using dipyrromethane **17** as starting material with toluene *p*-sulfonic acid (*p*-TsOH) as a catalyst (Scheme 1.8). NCTPP was obtained in 7 % yield.[22]

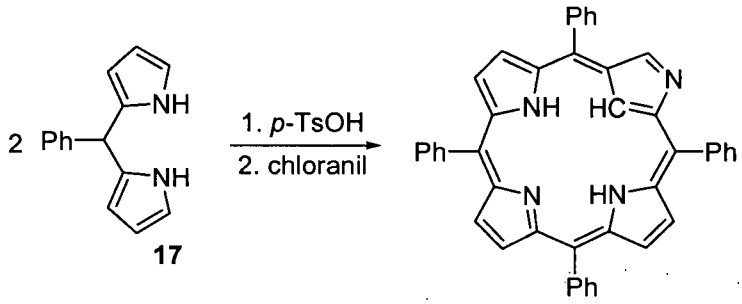

Scheme 1.8 Synthesis of NCTPP from dipyrromethane **17**.

The methods described above are simple but only useful for *β*-unsubstituted "symmetric" (excluding the asymmetric effect from the inverted pyrrole) N-confused tetraarylporphyrins (NCTAP). Other methods were developed to prepare *β*-substituted asymmetric N-confused porphyrins.[23,24] For example, a MacDonald [2+2] synthesis was reported by Dolphin *et al.* to generate N-confused porphyrin **18** (Scheme 1.9).[23]

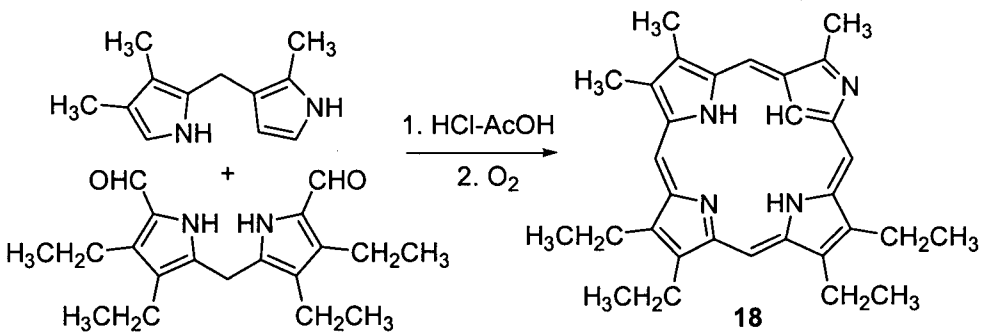

Scheme 1.9 MacDonald [2+2] synthesis of N-confused porphyrin **18**.

Lash *et al.* reported that condensation of pyrrole **19 (a-c)** with tripyrrane **20** yielded N-confused porphyrins **21 (a-c)** (Scheme 1.10).[24] The yield is high when the pyrrole contained a 5-alkyl substituent (28 - 47 %).[24] This is an example of a [3 + 1] methodology.[24]

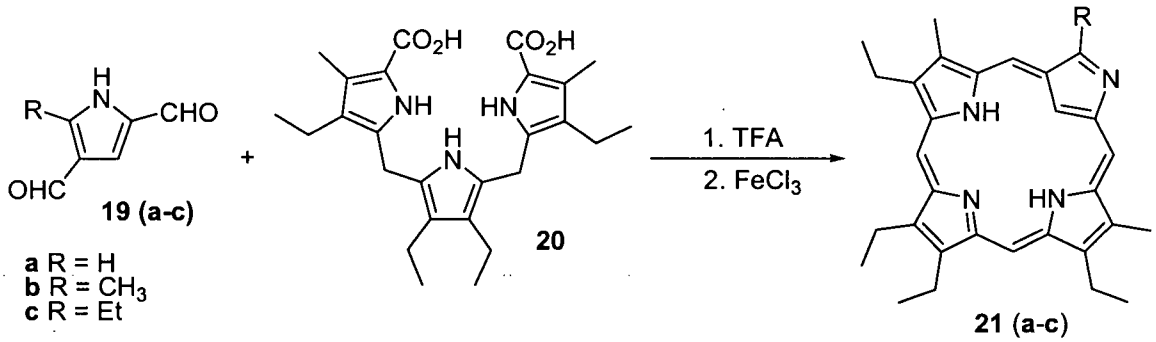

Scheme 1.10 Synthesis of N-confused porphyrins **21 (a-c)** by a [3 + 1] methodology.

A doubly N-confused porphyrin (N_2CP), 2-ethoxy-5,10,15,20-tetrapentafluorophenyl-3,7-diaza-21,22-dicarbaporphyrin, **23**, can be prepared in ~2 % yield by condensation of perfluorobenzaldehyde and dipyrromethane **22** in chloroform containing a trace of EtOH with $BF_3{\cdot}Et_2O$ as the acid catalyst followed by oxidation with 2,3-dichloro-5,6-dicyano-1,4-benzoquinone (DDQ) (Scheme 1.11).[37]

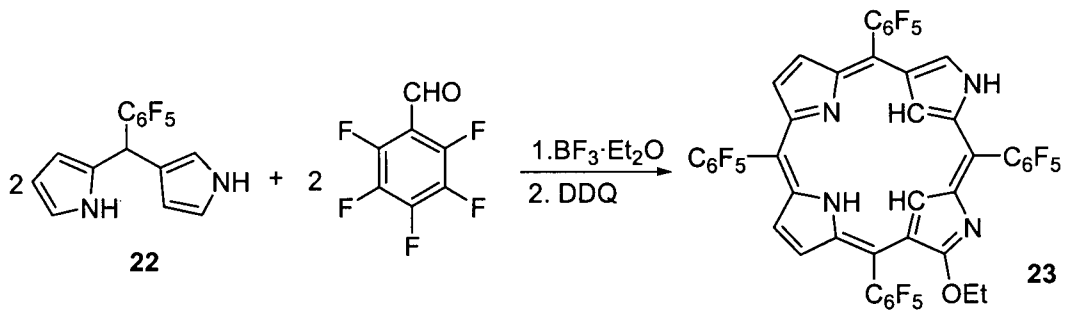

Scheme 1.11 Synthesis of doubly N-confused porphyrin **23**.

1.4.4 Reactivity of N-Confused Porphyrins

Unlike porphyrins, N-confused porphyrins have a peripheral nitrogen atom, which is less sterically hindered and much more nucleophilic than the inner nitrogen atoms in porphyrin, and consequently, the peripheral nitrogen atom can be easily methylated.[25] The inner carbon atom in Ni(II) N-confused porphyrins is nucleophilic as well and can also be methylated.[26]

N-confused porphyrins can act as either a di-anionic or tri-anionic ligand, while doubly N-confused porphyrins can act as a di-anionic, tri-anionic or tetra-anionic ligand (Figure 1.10).[28] The peripheral nitrogen atom of NCP is protonated when NCP acts as a di-anionic ligand. A variety of N-confused porphyrin complexes have been prepared.[27-29]

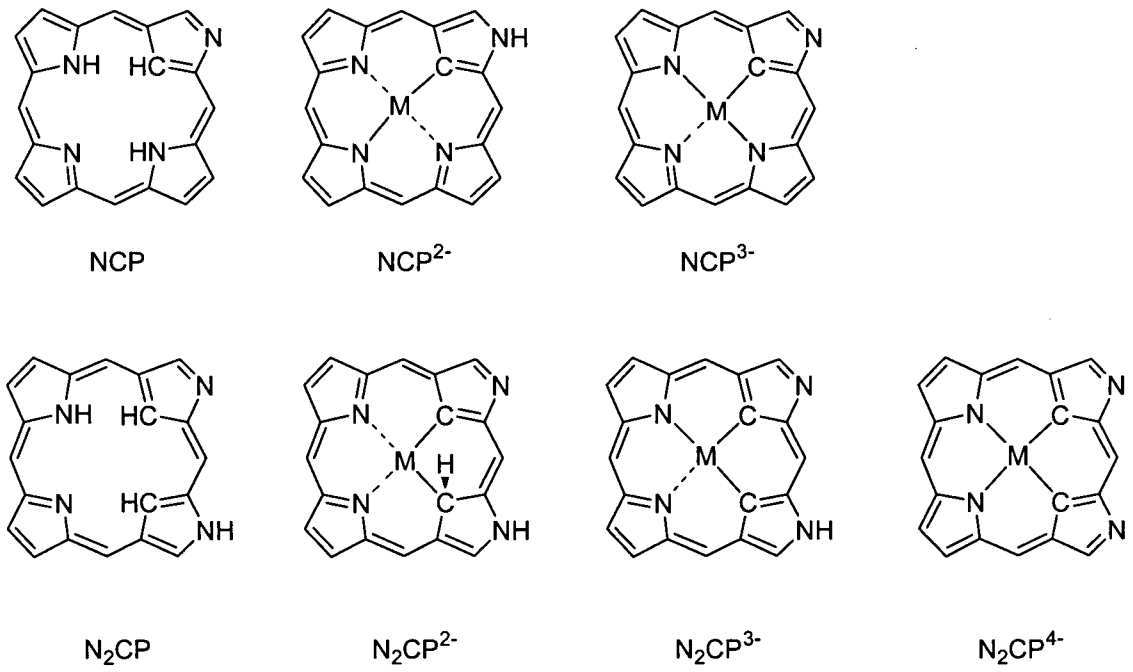

Figure 1.10 Multi-valence properties of NCP and N_2CP.

1.4.4.1 Alkylation of N-Confused Porphyrins

An outer N-methylated N-confused porphyrin, 2-aza-2-methyl-5,10,15,20-tetraphenyl-21-carbaporphyrin (N(2)-CH_3-NCTPP, **24**) is obtained quantitatively by reaction of NCTPP with CH_3I (Scheme 1.12).[25] The inner CH resonance at 0.43 ppm in the ^1H NMR spectrum of **24** shows that in **24** the aromaticity is preserved, though to a degree less than that of NCTPP, whose inner CH proton resonates at -5.1 ppm. The UV-vis spectrum of N(2)-CH_3-NCTPP is similar to that of a porphyrin, with the strongest absorption around 450 nm corresponding to the Soret band of a porphyrin, while the Q-band is red shifted to 710 nm. Compound N(2)-CH_3-NCTPP is readily metalated with $Ni(OAc)_2 \cdot 4H_2O$ at r. t. to yield (N(2)-CH_3-NCTPP)Ni^{II}, **25**.[25]

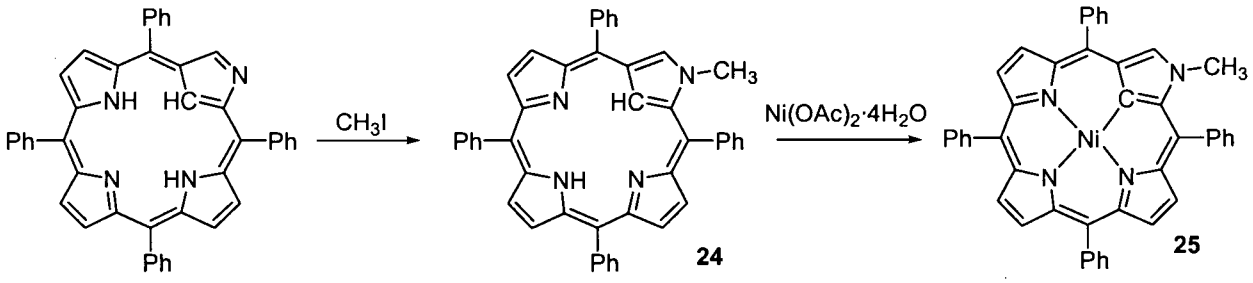

Scheme 1.12 Synthesis of N(2)-CH_3CTPP **24** and its Ni(II) complex **25**.

Methylation of (NCTPP)Ni^{II} was investigated by Latos-Grażyński *et al.* (Scheme 1.13).[26] After 24 h, the product of reaction between (NCTPP)Ni^{II} and CH_3I (1:30 molar ratio) is predominantly the diamagnetic inner C-methylated N-confused porphyrin (C(21)-CH_3-NCTPP)Ni^{II}, **26**.[26] Complete conversion to the dimethylated paramagnetic compound (N(2)-CH_3-C(21)-CH_3-NCTPP)$Ni^{II}I$, **27**, is observed after 7 days. Compound **27** can also be obtained quantitatively from the reaction of the Ni(II) N-confused porphyrin complex **25** with CH_3I.[26]

Upon reaction of compound **26** with a 1 % solution of HCl, a paramagnetic compound **28** is obtained. Demetalation of compounds **26** and **27** with conc. HCl yields N-confused porphyrins **29** and **30**, respectively.[26] The C-methylated N-confused porphyrins **29** and **30** preserve their coordination properties and can be remetalated to their parent N-confused metalloporphyrins. [26]

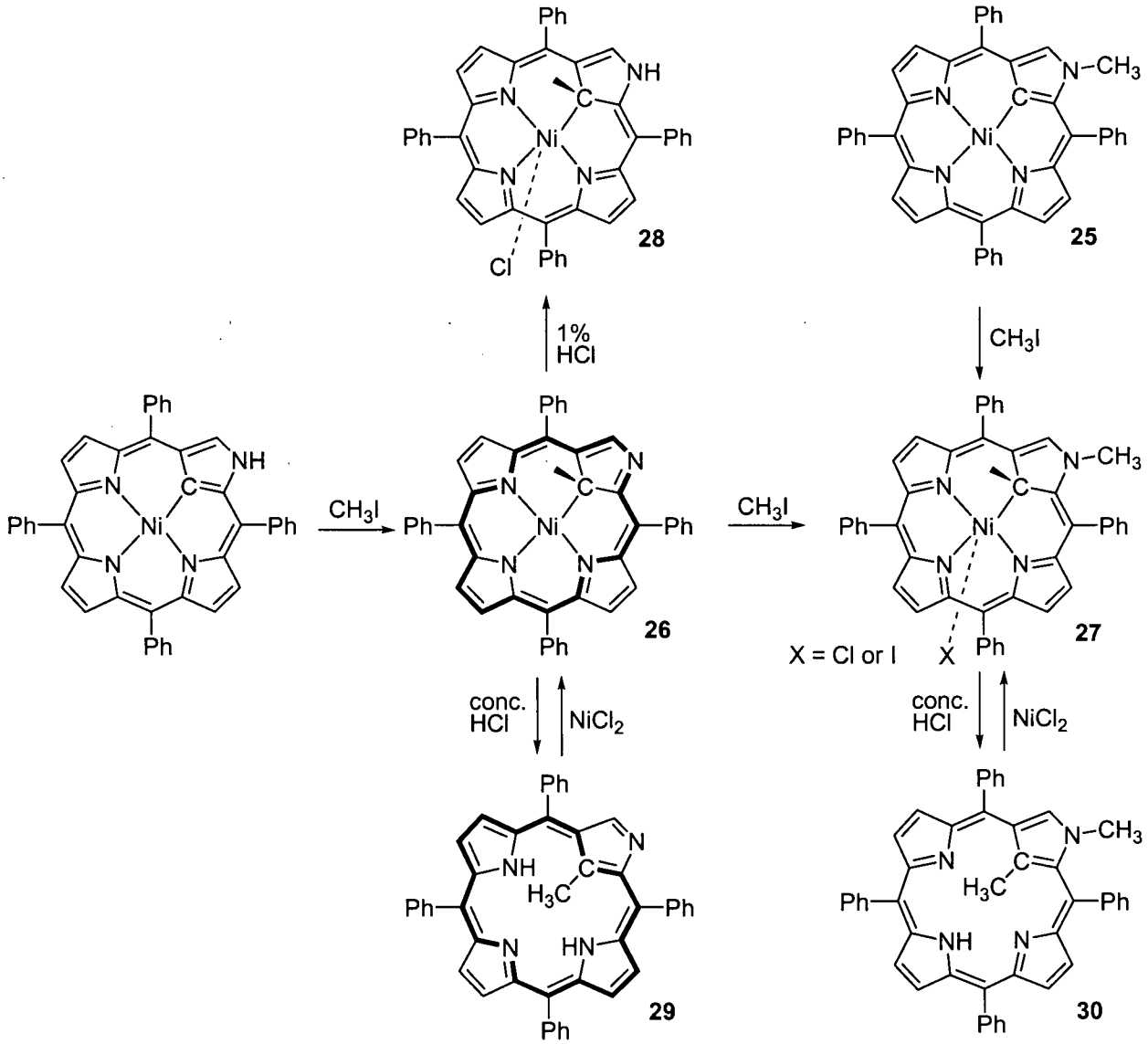

Scheme 1.13 Reactions of methylated (NCTPP)Ni^{II}.

It was proposed that CH_3I interacts directly with (NCTPP)Ni^{II} (Scheme 1.14), and oxidative addition of the methyl cation to the substrate at C(21) takes place.[26] The axially coordinated iodide is on the same side of the C-methyl group as the result of the *syn*-addition and thus the intermediate **32** is unstable due to the steric interaction. Dissociation of HI from the intermediate **32** results in the C-methylated compound **26**.

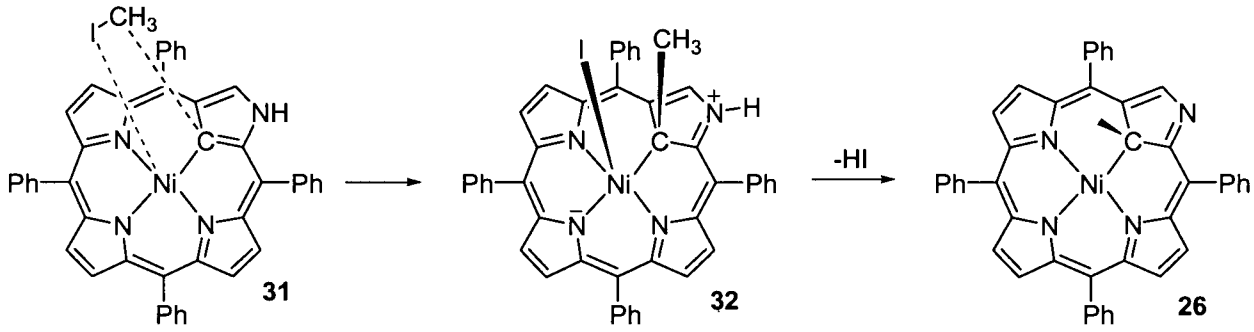

Scheme 1.14 Proposed mechanism for inner C-methylation of (NCTPP)Ni^{II}.

Compounds **27** and **28** have similar electronic absorption spectra, with broad absorptions around 730 nm ($\log\varepsilon$ is 3.88 and 3.80, respectively), whilst compound **26** has only a weak absorption between 650 - 900 nm.[26] Compounds **29** and **30** have strong absorptions at 740 nm ($\log\varepsilon = 3.95$) and 710 nm ($\log\varepsilon = 4.25$), respectively, and are thus potential photosensitizers for PDT.[26]

The ^1H NMR spectrum of compound **29** is similar to that of NCTPP, with the strongly upfield shifted C(21)H (-5.1 ppm) resonance being replaced by the resonance of C(21)-CH_3 (-4.84 ppm).[26] The ^1H NMR signal of C(21)-CH_3 in compound **30** appears at -1.40 ppm, suggesting weak aromaticity due to external N-methylation, as in the case of N(2)-CH_3-NCTPP,

24. The similarities of these ^{1}H NMR spectra between compound **29** and NCTPP, or compound **30** and **24**, respectively, suggest that inner C-methylation does not have a significant impact on the aromaticity nor the conjugation pathway.

The structure of compound **26** favors conjugation *via* the outer path at the inverted pyrrole unit, whilst compound **29** favors conjugation *via* the inner path at the inverted pyrrole unit (Scheme 1.13).[26] Consequently, the ^{1}H NMR signal of C(3)H in compound **29** appears at 7.11 ppm, compared to that in compound **26** at 9.90 ppm, as the result of a closer ring current.

The structures of compounds **26** and **27** were determined by X-ray crystallography (Figure 1.11).[26] In both compounds, the planarity of the macrocycles is severely distorted. The dihedral angles between the pyrrole unit and the plane defined by N(22)N(23)N(24) are as follows: C(21) -42.2°, N(22) 15.4°, N(23) 3.1°, and N(24) 15.8° for compound **26**, and C(21) -55.3°, N(22) 14.3°, N(23) 0.9°, and N(24) 14.4° for compound **27**. The confused pyrrole of compound **26** coordinates to Ni(II) through sp^3-hybridized C(21) resulting in a pyramidal geometry, while the coordinating carbon in compound **27** preserves the planar trigonal geometry indicating sp^2 hybridization.

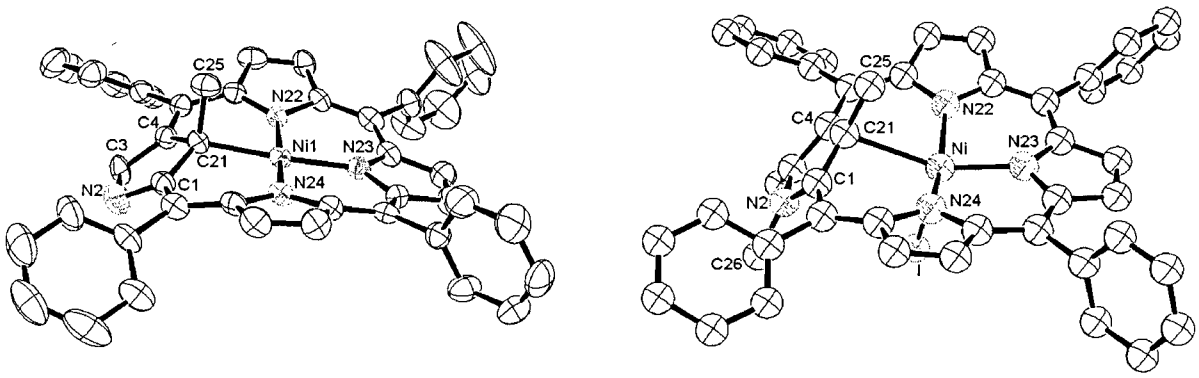

Figure 1.11 ORTEP drawings of compound **26** (left) and **27** (right) showing atomic labeling and thermal ellipsoids at 50 % probability. H atoms and solvent have been omitted for clarity.

(NCTPP)Ni^{II} reacts with CH_2Br_2 to yield 2,21'-CH_2-linked Ni(II) N-confused porphyrin dimer **33** (79 %) and 2,2'-linked dimer **34** (16 %) (Scheme 1.15).[38] If CH_2I_2 is used, only dimer **33** is formed.[38]

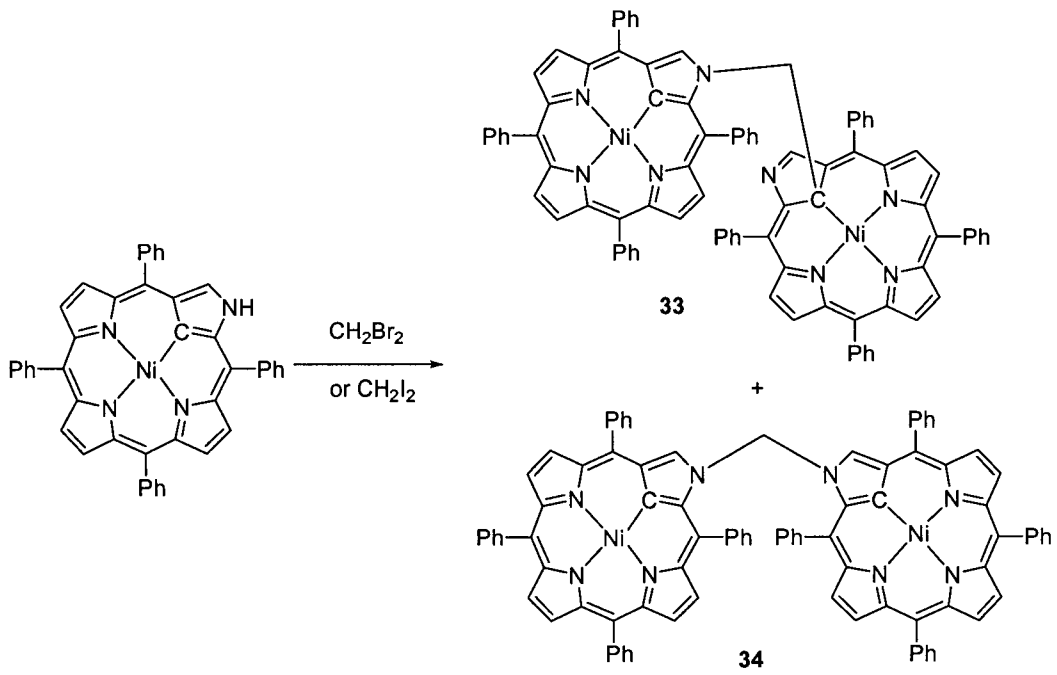

Scheme 1.15 Synthesis of dimeric Ni(II) N-confused porphyrins **33** and **34**.

1.4.4.2 Reactions of N-Confused Porphyrin Complexes

As mentioned before, NCTTP (section 1.4.1) and N(2)-CH_3-NCTPP, **24** (section 1.4.4.1), are readily metalated with $Ni(OAc)_2 \cdot 4H_2O$ at r. t. to yield Ni(II) complexes.[20,25] The structure of (NCTTP)Ni^{II} was determined by X-ray crystallography and the porphyrin skeleton is almost planar (Figure 1.12).[20]

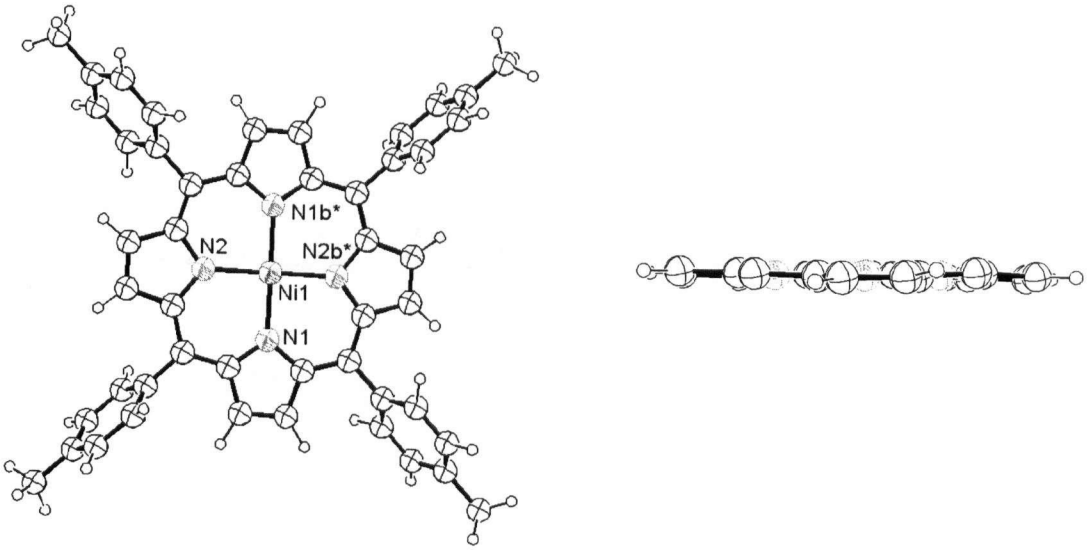

Figure 1.12 ORTEP drawings of (NCTTP)Ni^{II} showing thermal ellipsoids at 50 % probability: top view (left) and side view (right). *p*-Tolyl groups in side view have been omitted for clarity. The C(21) and N(2) atoms are disordered and not distinguishable in the X-ray structure.[20]

Reactions of Ni(II) dimethylated N-confused porphyrin **27** (X = Cl) with phenyl Grignard reagents, phenyllithium, and *n*-butyllithium were investigated by Chmielewski and Latos-Grażyński.[27] Reaction of compound **27** (X = Cl) with PhMgBr at 203 K leads to the substitution of an axial chloride by the phenyl anion to give (N(2)-CH_3-C(21)-CH_3-NCTPP)Ni^{II}Ph, **35**.[27]

Compound **35** can also be obtained by the titration of compound **27** (X = Cl) with phenyllithium, and a one-electron reduction of compound **35** with excess of phenyllithium gives [(N(2)-CH_3-C(21)-CH_3-NCTPP)$Ni^{II}Ph]^-$, **36**.[27] Reaction of **27** with *n*-butyllithium yields a single species [(N(2)-CH_3-C(21)-CH_3-NCTPP)$Ni^{II}Bu]^{n-}$, **37** (n =1 or 2), which is either one- or two-electron-reduced.[27] The exact value of "n" can not be determined, though the authors favor the formation of two electron reduced species (n = 2) for **37** based on its NMR spectra.[27]

Reaction of doubly N-confused porphyrin **23** with $Pd(OAc)_2$ in toluene results in Pd(II) complex **38**, the inner C-arylated product (Scheme 1.16).[28] A FAB peak at 1217.8 *m/e* suggests the addition of a tolyl group to the Pd-N_2CP complex. Signals corresponding to the tolyl protons were observed in the high-field region (5.61 - 6.36 ppm) in the ^{1}H NMR spectrum of compound **36**, suggesting that the tolyl group is located in the porphyrin core. The methyl groups on the tolyl substituent were found to be at the *para* and *meta* positions in a 1:2 ratio. This complexation reaction does not proceed if either chloroform or benzene is used as the solvent. However, both C-phenyl and C-tolyl Pd-N_2CP complexes are obtained when a 1:1 benzene/toluene solution is used.[28]

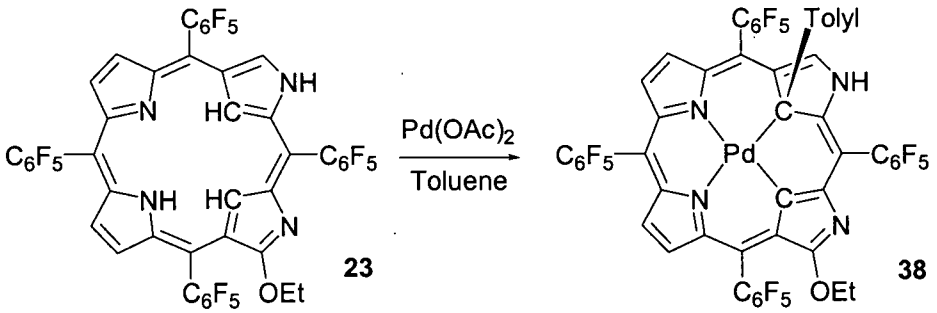

Scheme 1.16 C-arylation of doubly N-confused porphyrin **23**.

The structure of compound **38** was explicitly determined by single crystal X-ray diffraction analysis (Figure 1.13).[28] The arylation occurs on the inner carbon on the pyrrole without an ethoxy group. The tolyl-substituted inverted pyrrole ring is bent at 56.3° with respect to the mean plane defined by the four core nitrogen and carbon atoms, while the tolyl group stands almost vertically (88.6°) at the opposite side.

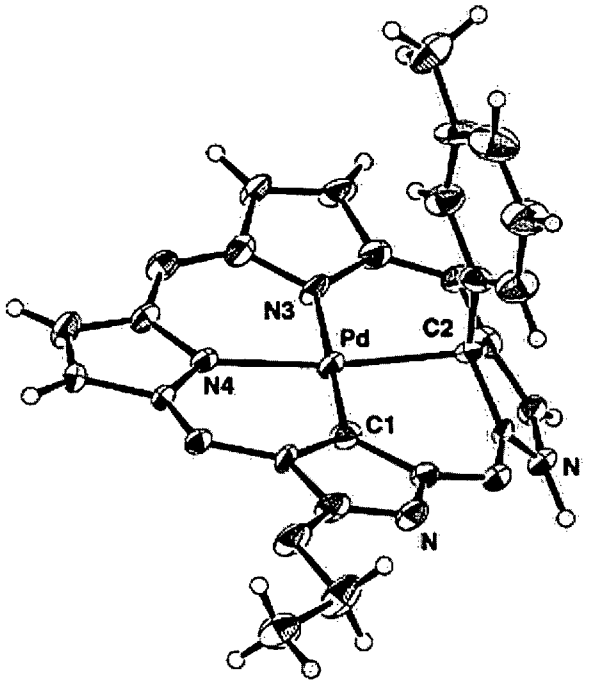

Figure 1.13[28] An ORTEP drawing of complex **38**. Solvents and pentafluorophenyl groups have been omitted for clarity.

The inner arylation reaction has not been observed in the reactions of N-confused porphyrins. When NCTTP and $Pd(OAc)_2$ are refluxed in chloroform, $(NCTTP)Pd^{II}$, **39**, is obtained in 50 % yield; if toluene is used as solvent, compound **39** and two red-colored products, **40a** and **40b,** are obtained in yields of 19 %, 27 %, and 36 %, respectively (Scheme 1.17).[29]

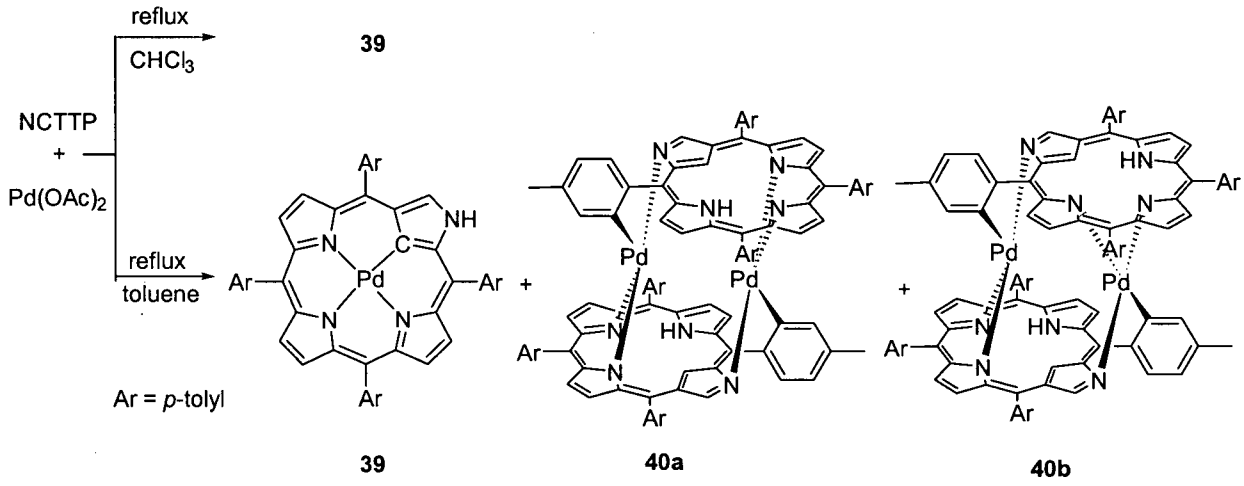

Scheme 1.17 Reactions of NCTTP with Pd(II).

The structure of compound **39** was determined by X-ray crystallography, and the Pd ion is located in the porphyrin core in a square-planar fashion.[29] The FAB mass spectra of both **40a** and **40b** have parent peaks at 1550 *m/e* suggesting they are dimeric species, (Pd-NCTTP)$_2$.[29] In the ^{1}H NMR spectra of complexes **40a** and **40b**, one set of inner proton (CH, NH) signals was observed at -4.40 and 0.09 ppm for **40a**, while two sets of signals for inner protons were observed at -3.83 and 0.04 ppm and -3.28 and 0.51 ppm for **40b**, suggesting the symmetrical and unsymmetrical structures of **40a** and **40b**, respectively.[29] The unsymmetrical structure of **40b** was elucidated by single crystal X-ray diffraction analysis.[29] Because of the lack of the crystal structure of **40a**, other isomeric structures which differ with respect to the coordinating nitrogen atoms can not be ruled out.[29]

A tetra-Zn(II)-coordinated NCTPP dimer **41** is quantitatively obtained when NCTPP is treated with 2 equiv. of $Zn(OAc)_2 \cdot 2H_2O$ in CH_2Cl_2 at r. t. (Scheme 1.18).[39] Removal of the acetate ligands of **41** by 1 % Et_4NOH aqueous solution leads to formation of dimer **42**, of which

the molecular mass was determined by molecular ion peak at 1353 *m/e* (FAB) as well as vapor pressure osmometry measurements at 1301 g/mol.[39] The Zn dimer **42** can be further transformed into monomeric pyridine complex **43** by adding pyridine.[39] The structures of complex **41** and **43** were determined by X-ray crystallography.[39]

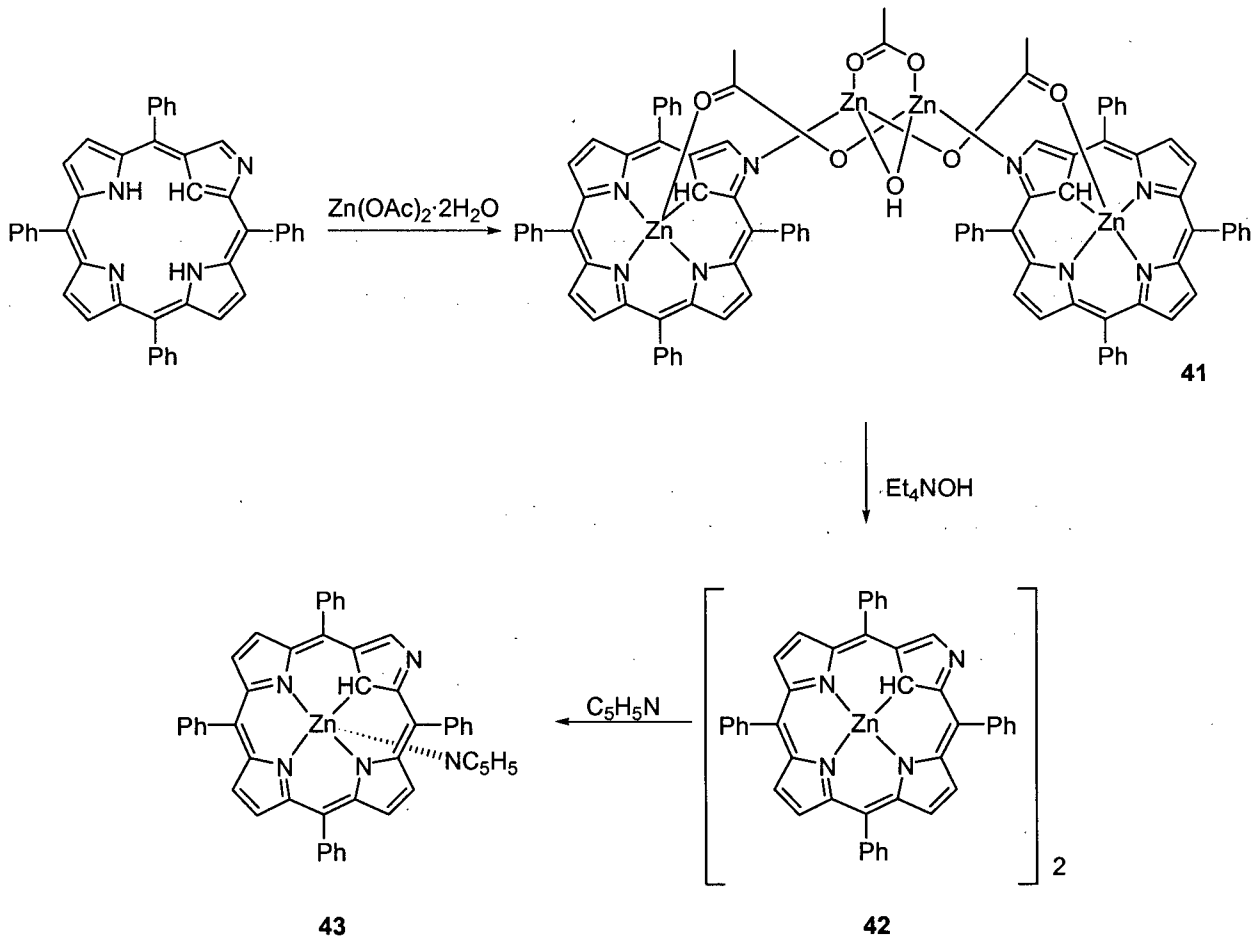

Scheme 1.18 Reactions of Zn complexes of NCTPP.

An inner and outer N-coordinated bis-Rh(I) N-confused porphyrin complex **44** is obtained from the reaction of N-confused porphyrin with $[Rh(CO)_2Cl]_2$ (Scheme 1.19).[40] The structure of complex **44** was explicitly demonstrated by single crystal X-ray diffraction

analysis.[40] Both Rh(I) ions are located above the NCP plane and the geometry around the metal centers is close to square planar.

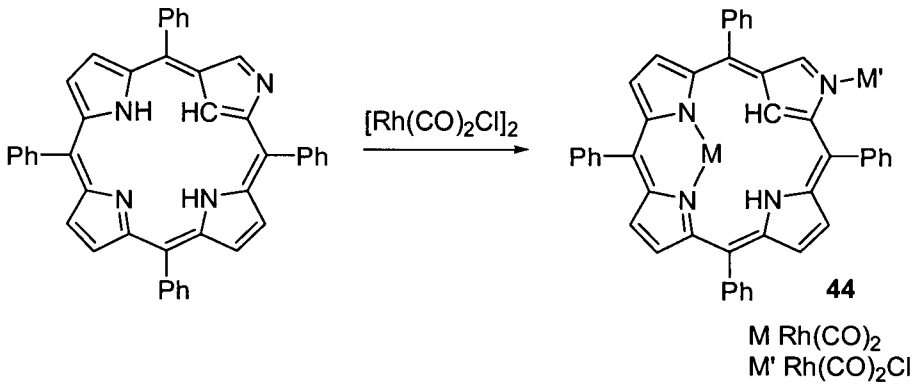

Scheme 1.19 Synthesis of bis-Rh(I) N-confused porphyrin complex **44**.

The Fe(II) complex (NCTPP)$Fe^{II}Br$, **45**, can be obtained through the reaction of NCTPP with $FeBr_2$ in 85 % yield, and the axial ligand Br^- can be changed to $C_7H_7S^-$ through the reaction of complex **45** with $NaSC_7H_7$ in 78 % yield (Scheme 1.20).[41] The r. t. effective magnetic moment of **45** obtained by Evan's method[42] is 4.85 μ_B, close to the spin only value (μ_{eff} = 4.90 μ_B) of a high spin d^6 Fe(II) center with four unpaired electrons, while the effective magnetic moment of **46** is 2.77 μ_B, suggesting an intermediate spin Fe(II) center with two unpaired electrons.[41] Structures of **45** and **46** were determined by single crystal X-ray diffraction analyses.[41] While the Fe···C(21) distances in **45** and **46**, 2.361(10) and 2.398(3) Å, respectively, are comparable, the Fe···H(21) distance of 1.971 Å in **45** is much shorter than that of **46**, 2.334 Å.[41] Importantly, the C(21)-H(21)···Fe in **45** is within the bond distance of an agostic interaction between the iron and pyrrolic C(21)-H(21) bond.[41] The iron center in **45** is relatively electron-deficient, as Br^- is less basic than $C_7H_7S^-$, resulting in the stronger three-center two-electron C(21)-H(21)···Fe interaction.[41]

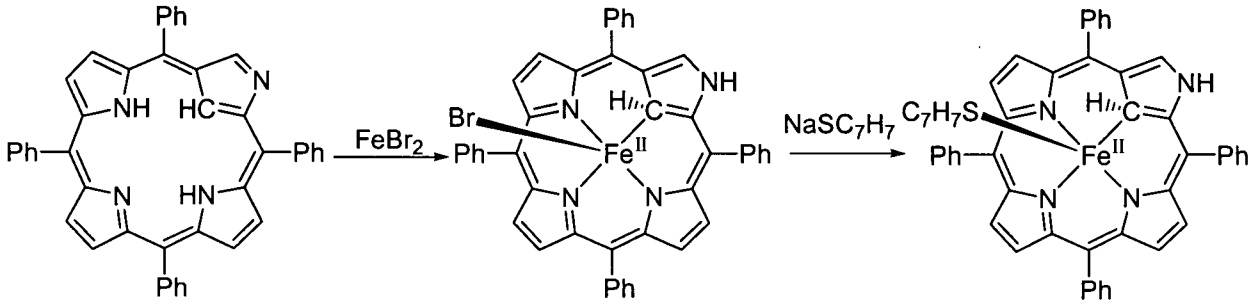

Scheme 1.20 Synthesis of Fe(II) N-confused porphyrin.

Stable NCP complexes with high oxidation state metals have been obtained, such as NCP complexes of Ni(III), Ag(III), Sb(V) and Cu(II).[43-47]

One-electron oxidations of (NCTPP)Ni^{II} and (N(2)-CH_3-NCTPP)Ni^{II}, **25**, result in formation of rare organonickel(III) derivatives **47** - **51** (Scheme 1.21).[43] Oxidation of (NCTPP)Ni^{II} occurs without deprotonation of the outer nitrogen and the additional charge is compensated by an anionic ligand. The oxidation processes are chemically reversible, and (NCTPP)Ni^{II} or (N(2)-CH_3NCTPP)Ni^{II} is recovered after addition of typical reducing agents, e.g. sodium dithionite.[43] EPR spectra of the one-electron oxidized species are heavily dependent on the axial group and the spin-Hamiltonian parameters in each case suggest a metal-centered oxidation rather than a cation radical formation.[43] The localization of the one-electron oxidation on the nickel ion is supported by the observation of ^{61}Ni hyperfine splitting in the EPR spectra.[43]

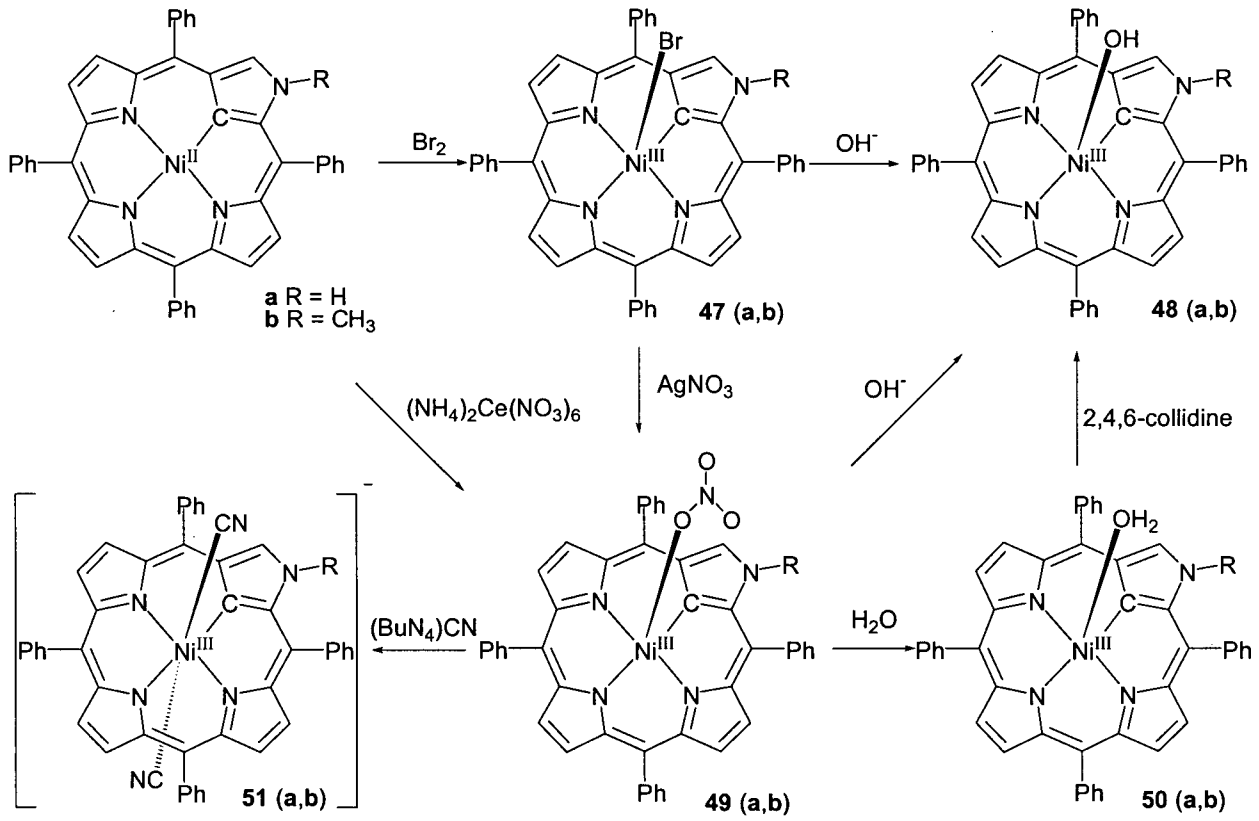

Scheme 1.21 Synthesis of organonickel(III) compounds.

A Ag(III) complex of N-confused porphyrin (NCTPP)Ag^{III}, **52**, can be obtained through the reaction of Ag(I) trifluoroacetate and NCTPP, and this was the first example of an air-stable Ag(III) complex.[44] Coordination of Ag(III) has a slightly distorted pseudo-square-planar geometry, shown by its X-ray structure (Figure 1.14).[44] The Ag(III) oxidation state of the silver ion is supported by the following points:[44]

- Absence of the counteranion indicates that the complex is neutral, and the outer nitrogen atom is deprotonated, as suggested by the ^{1}H NMR spectrum.
- Complex **52** is diamagnetic, whilst the Ag(II) complex is paramagnetic.

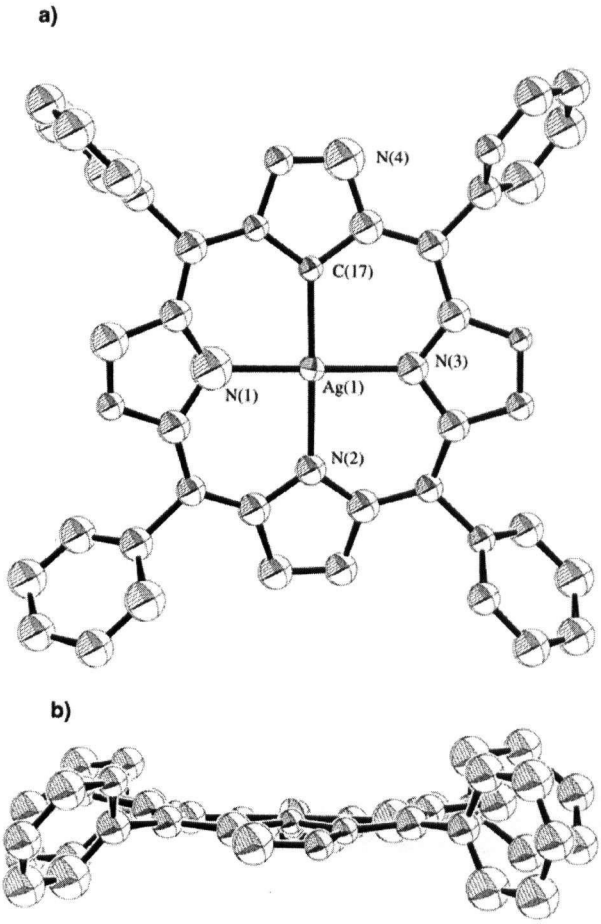

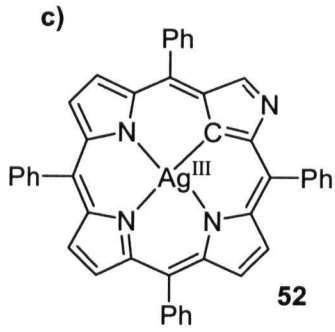

52

Figure 1.14[44] X-ray structure of (NCTPP)Ag^{III}, **52**: (a) top view and (b) side view; (c) chemdraw structure. H atoms and solvent molecule (CH_2Cl_2) are omitted for clarity.

Sb(V) N-confused porphyrins (NCTAP)$Sb^{V}(OCH_3)_2$ **53** (**a**,**b**) are prepared through the reactions of NCTAP and $SbBr_3$, followed by column chromatography with $MeOH/CH_2Cl_2$ as eluents (Scheme 1.22).[45] Compounds **53** are neutral as NCPs act as a tri-anionic ligand, which is suggested by the singlet peaks of C(3)H protons observed in the ^1H NMR spectra of **53a** and **53b** indicating no adjacent NH protons.[45] The fact that there is no counteranion in the X-ray crystal structure of **53b** also suggests that compounds **53** are neutral.[45]

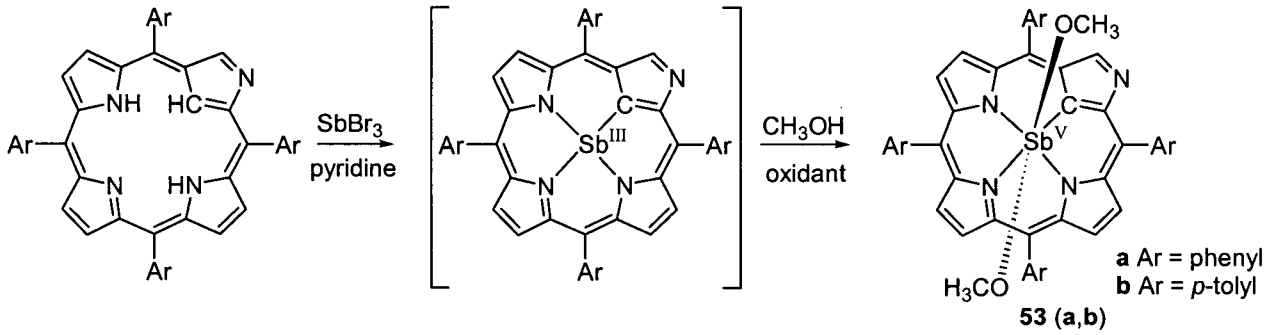

Scheme 1.22 Synthesis of $(NCTAP)Sb^{V}(OCH_3)_2$ **53**.

If **53** is refluxed in ethanol for 2 days, the axial group $-OCH_3$ is exchanged with $-OCH_2CH_3$ to give $(NCTAP)Sb^{V}(OCH_2CH_3)_2$ **54** quantitatively.[45] Addition of acid speeds up the exchange process and an "S_N1-like" mechanism is proposed (Scheme 1.23).[45]

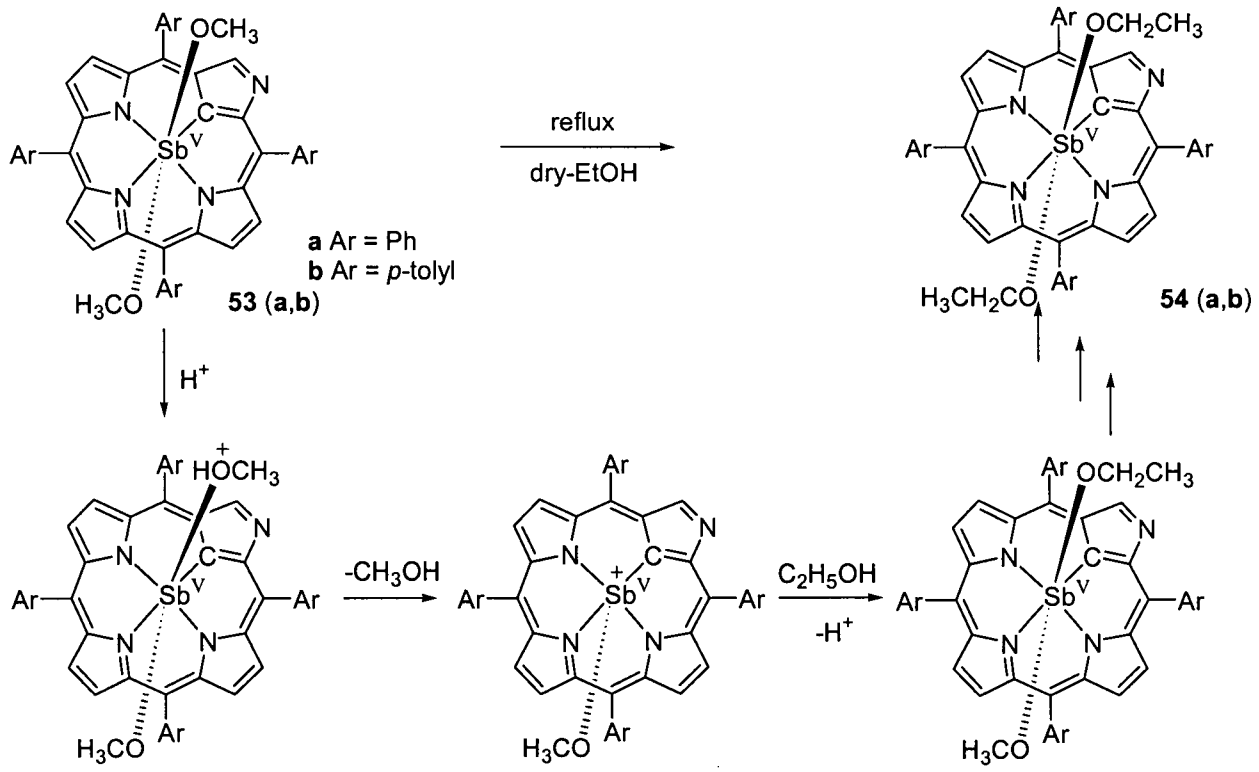

Scheme 1.23 Axial group exchange of complexes **53 (a, b)**.

Reactions of $Cu(OAc)_2$ with NCTPP or N(2)-CH_3-NCTPP, **24**, yield Cu(II) N-confused porphyrin **55** and **56**, respectively (Scheme 1.24).[46] Titration of **55** and **56** with acid results in formation of new species, **57**-X and **58**-X (X = Cl, CF_3COO), respectively, which can also be generated through the reaction of $CuCl_2$ with NCTPP and **24**, respectively.[46] Insertion of Cu(II) into dimethylated NCP **30** produces complex **59**-X (X = Cl, I), which can also be obtained through the reaction of **56** with CH_3I (Scheme 1.25).[46] Those compounds represent the first examples of stable monomeric organometallic complexes of Cu(II).[46] The isotropic ^{14}N EPR hyperfine pattern for **57**-X and **58**-X can be reproduced by a simulation assuming that all three inner nitrogen atoms are magnetically equivalent, indicating inner C(21) as the proton binding site.[46] The EPR spectrum of **59**-X resembles those of **57**-X and **58**-X due to the structure similarities between them.[46]

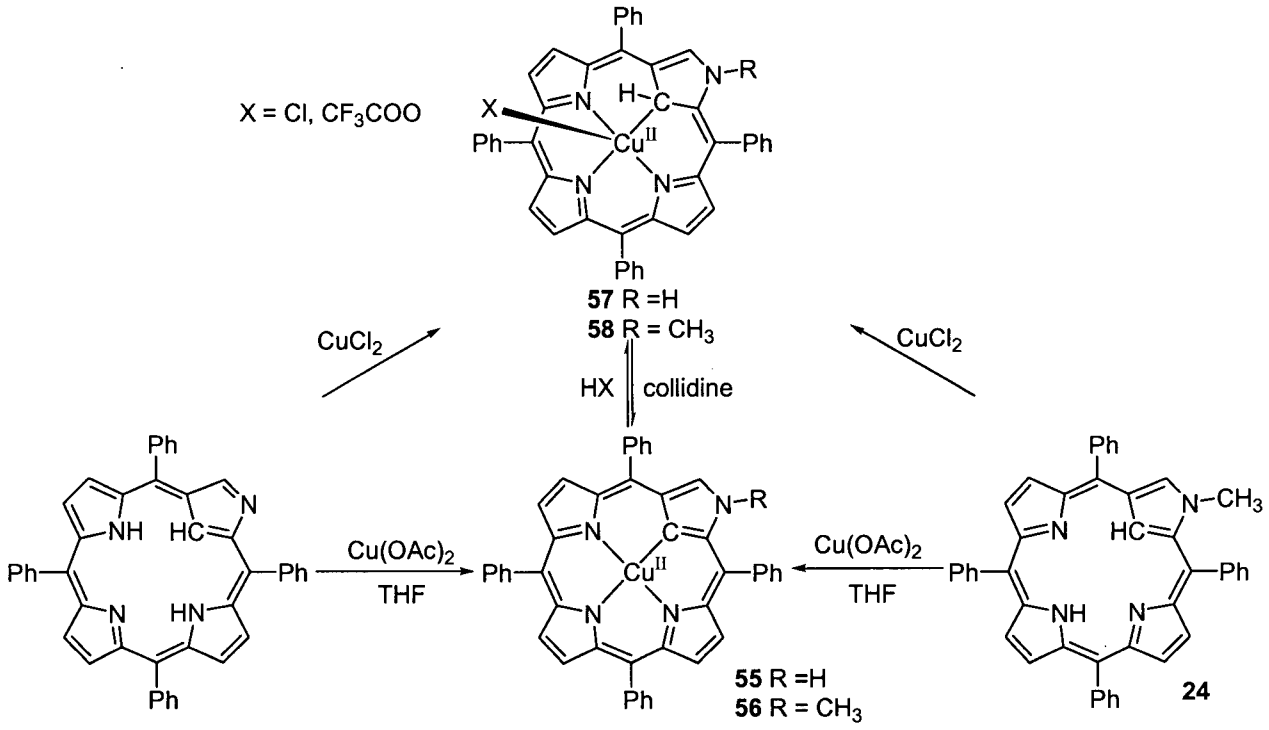

Scheme 1.24 Synthesis of Cu(II) N-confused porphyrin **55** - **58**.

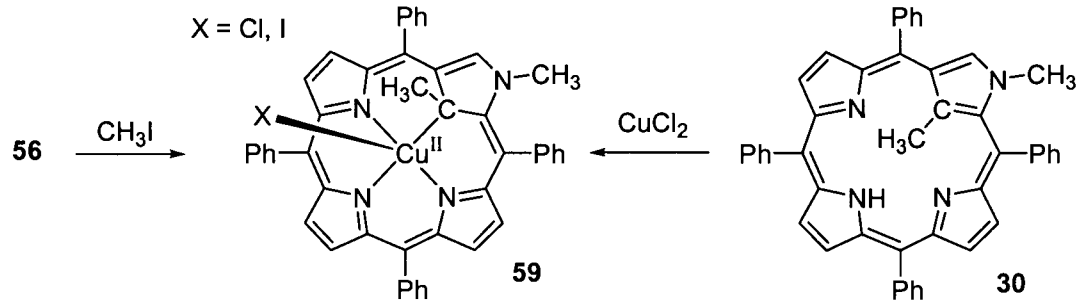

Scheme 1.25 Syntheses of dimethylated Cu(II) N-confused porphyrin **59**.

The Cu(II) complex can also be obtained through the metalation of N-confused calix[4]phyrin **60** (Scheme 1.26).[47] Compound **60** is prepared in 3 % yield by the acid catalyzed condensation of aryl aldehyde, acetone and pyrrole.[47] Metalation of **60** with $NiCl_2$ or $Cu(OAc)_2$ yields complex **61** and **62**, respectively, suggesting that the π-conjugated system is not necessary to stabilize the organometallic compounds.[47] Structures of both **61** and **62** were determined by single crystal X-ray diffraction analyses.[47] The Ni(II) complex **61** has a ruffled structure, with four pyrrole rings tilting 20.55, 11.37, 14.63, and 0.00°, whilst the Cu(II) complex **62** has a near planar structure and the four pyrrole rings are tilted 6.69, 4.25, 2.91, and 4.70°. Both complexes form dimeric structures through hydrogen bonding between the peripheral amide groups.[47] Although complex **62** is nearly planar in the solid state, differences between the EPR spectra of **62** in powder ($g_x = g_y = 2.031$, $g_z = 2.139$) and in DMF solution ($g_x = 2.01$, $g_y = 2.06$, $g_z = 2.13$) suggest a distortion from the square-planar form in DMF solution.[47]

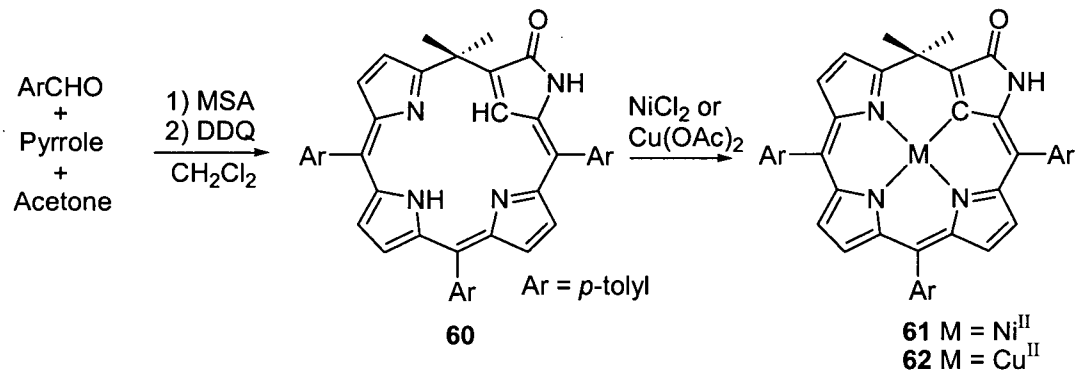

Scheme 1.26 Synthesis of metal complexes of N-confused calix[4]phyrin **61** and **62**.

Diamagnetic Ag(III) and Cu(III) complexes of doubly N-confused porphyrin, **63** and **64**, were prepared by Furuta *et al. via* the reaction of N_2CP **23** with AgOAc or $Cu(OAc)_2$ (Scheme 1.27).[37] Both complexes have a square-planar tetracoordination, shown by their X-ray crystal structures.[37]

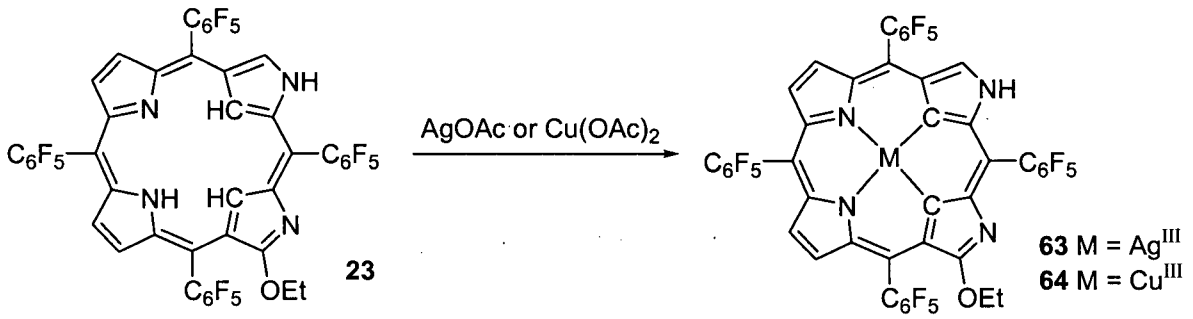

Scheme 1.27 Synthesis of N_2CP complexes **63** and **64**.

1.4.4.3 Electrophilic and Nucleophilic Substitution

As an aromatic system, an N-confused porphyrin undergoes electrophilic substitution. Nitration of NCTPP using either $NaNO_2$/HCl or 30 % HNO_3 occurs on inner C(21) and the resulting nitro-substituted NCTPP **65** (Scheme 1.28) is severely distorted due to the repulsion in the core, with the confused pyrrole ring canting 42.4° from the porphyrin plane.[48,49] Both nitronium (NO_2^+) and nitrosonium (NO^+) ions are plausible electrophiles, and electrophilic attack by nitrosonium ion followed by oxidation with O_2 in air is a candidate for the nitration process.[48]

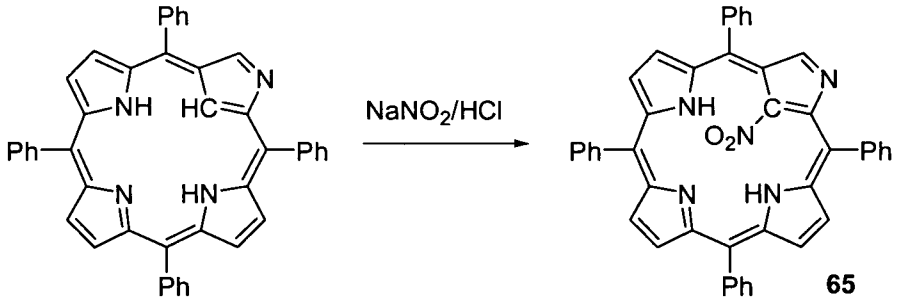

Scheme 1.28 Nitration of NCTPP.

When NCTPP is treated with 1 equiv. of N-bromosuccinimide (NBS), monobrominated NCTPP **66a** is obtained in 90 % yield, while 2 equiv. of NBS results to dibrominated NCTPP **67a** (Scheme 1.29).[49] When either N-chlorosuccinimide (NCS) or N-iodosuccinimide (NIS) is used in place of NBS, the corresponding monohalogenated NCTPP **66b** and **66c** are formed, but the dihalogenated products are not obtained, presumably due to the low reactivity of NCS and the instability of the diiodo product.[49] Bromination of **66b**, **66c**, and **65** is achieved by treatment with 1 equiv. of NBS.[49]

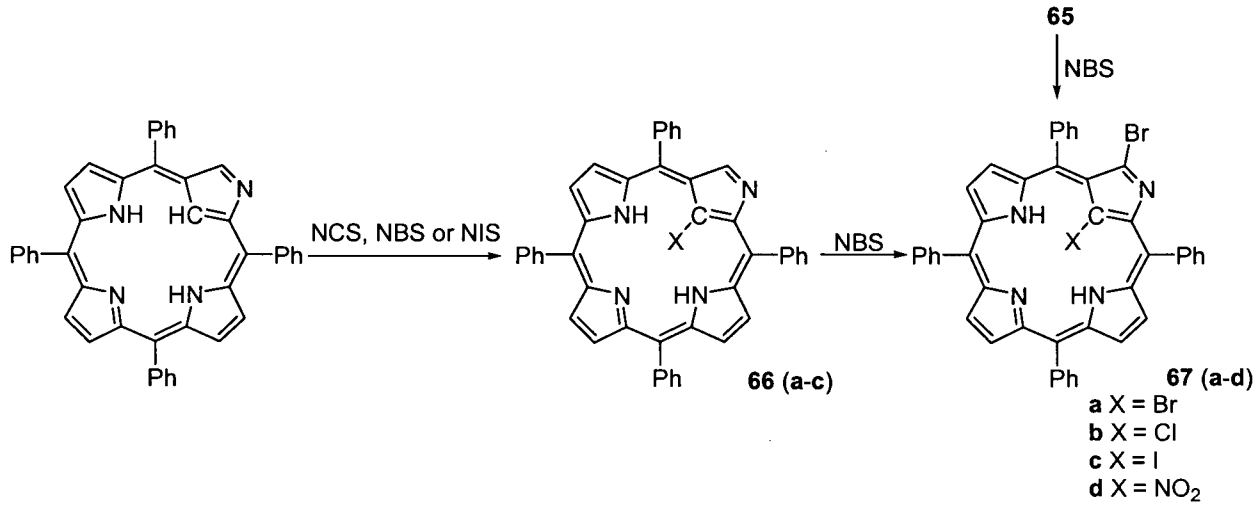

Scheme 1.29 Halogenation of NCTPP and substituted NCTPP.

A new type of porphyrinoid, N-fused porphyrin (NFP) **68** with a fused tripentacyclic pyrrole ring in the macrocyclic core is spontaneously obtained from a pyridine solution of dibrominated N-confused porphyrin **67a** in 91 % yield (Scheme 1.30).[49,50] Compounds **67** (**b** - **d**) undergo similar reactions.[49] An inversion of the confused pyrrole ring is believed to precede the reaction.[49] Compound **68** is aromatic, as it keeps the 18 π-electron pathway, and signals for the peripheral hydrogens are observed in the range of 7.55 - 8.96 ppm in the ^{1}H NMR spectrum.[49] The inner NH signal, expected to be highly shielded due to the ring current, appears at 8.38 ppm, as the result of strong hydrogen bonding overcoming ring current. Despite its crowded multi-ring structure, the porphyrinoid skeleton of **68** is almost planar, as revealed by its X-ray structure (Figure 1.15).[49,50]

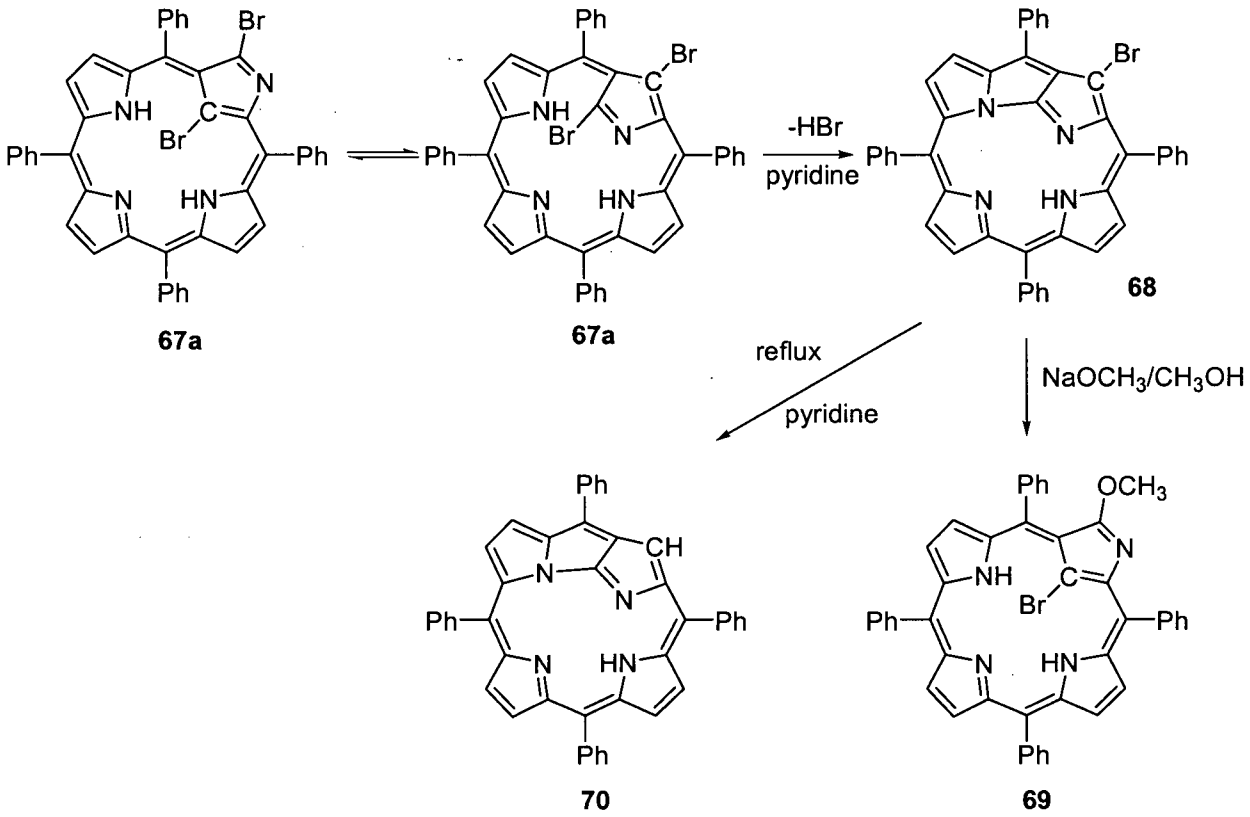

Scheme 1.30 Synthesis and reactions of N-fused porphyrins.

Compound **68** is unstable in basic media. Methoxy substituted N-confused porphyrin **69** is obtained in 72 % yield when compound **68** is treated with $NaOCH_3/CH_3OH$ for 30 min.[49] Debromination of compound **68** occurs when it is refluxed for 2 days in pyridine.[49] Presumably the hydrogen atom comes from the residual water in the solvent, as deuterium is introduced to NFP ring when D_2O is added to the pyridine solution.[49]

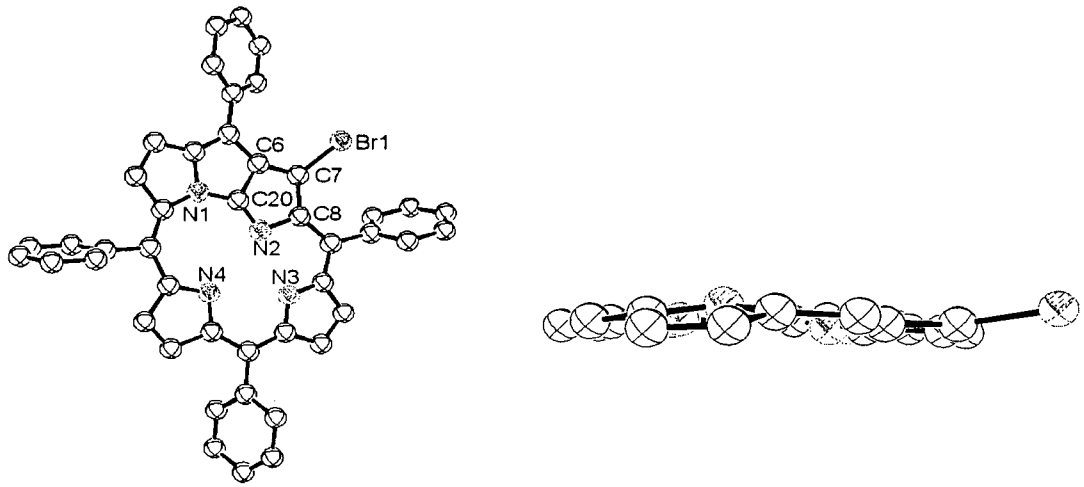

Figure 1.15 ORTEP drawings of compound **68** showing atomic labeling and thermal ellipsoids at 50 % probability: top view (left) and side view (right). H atoms in both view and phenyl groups in the side view have been omitted for clarity.

NCTPP reacts with excess of pyrrole in refluxing DMF containing a catalytic amount of $BF_3 \cdot OEt_2$ to give a pentapyrrolic NCP **71** with a yield of 60 % (Scheme 1.31).[51] Compound **71** can also be obtained through $BF_3 \cdot OEt_2$ catalyzed condensation of benzaldehyde and excess pyrrole with a yield of 1.5 %.[51]

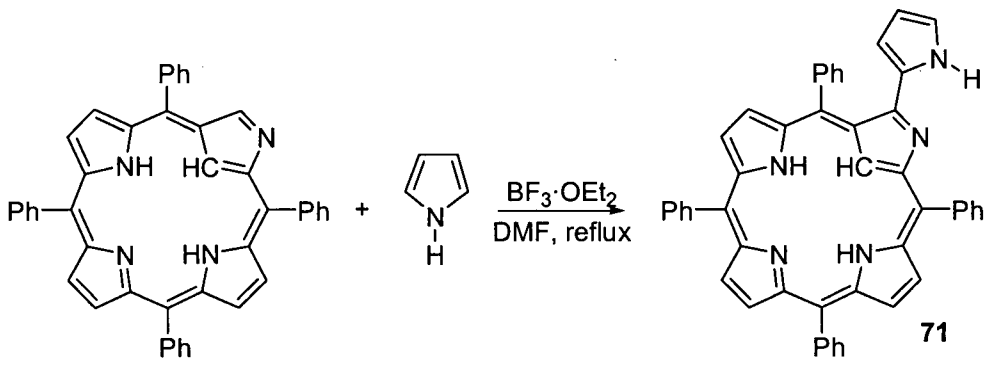

Scheme 1.31 Synthesis of N-confused porphyrin **71**.

1.4.4.4 Oxidative Degradation

It has been noticed that N-confused porphyrins are often unstable during the course of metalation with various transition metals such as Cu, Mn and Fe.[52] The complexation reaction of N-confused porphyrins with Cu(II) under an aerobic atmosphere was investigated by Furuta *et al.*[52] When NCTPP and $Cu(OAc)_2$ were refluxed in toluene for 24 h, a decomposing tripyrrolic complex **72** was obtained in 34 % yield (Scheme 1.32).[52] When the reaction was performed under rigorous anaerobic conditions, the inner core complex **55** was formed quantitatively (Scheme 1.24).[46] Complex **72** can be demetalated with conc. H_2SO_4 giving a free tripyrrolic ligand **73** which can bind a variety of transition metals (Scheme 1.32).[52]

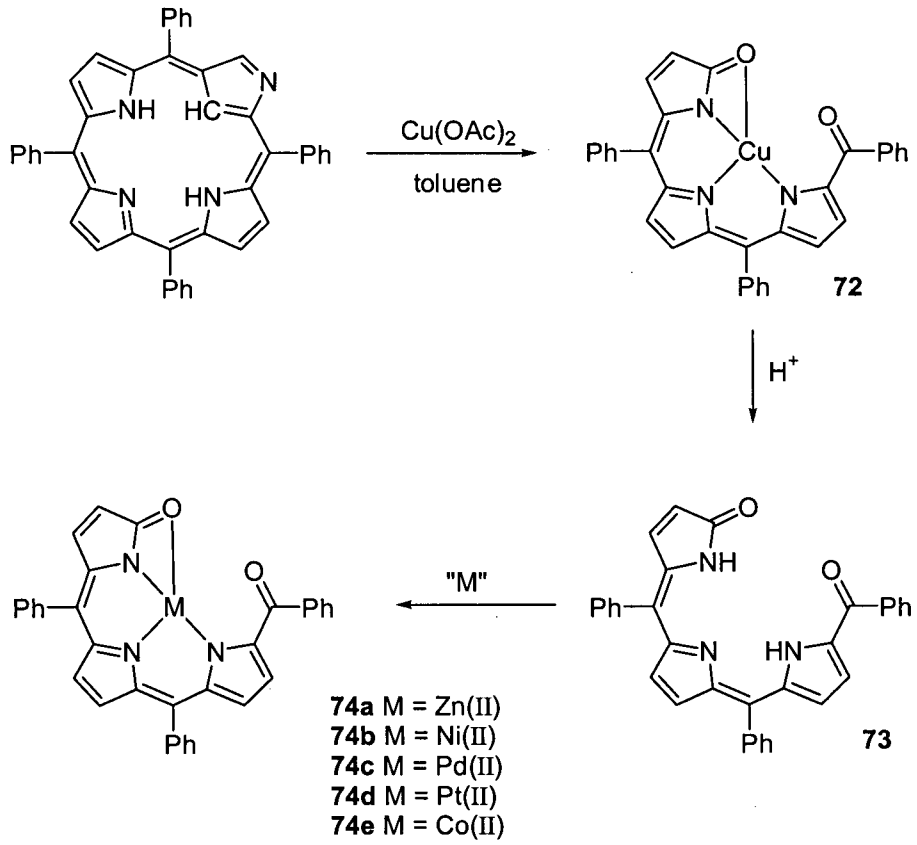

Scheme 1.32 Reactions of tripyrrolic ligand **73**.

The cleavage site of the *meso*-position, either 5-, 20- or both, was determined by using NCP **75** as the starting material (Scheme 1.33).[52] The isolated tripyrrolic complex **76** preserves the pyridine unit and no other tripyrrolic derivative was observed in this reaction, indicating that the removal of the *meso*-phenyl group is regioselective at the 5- position.

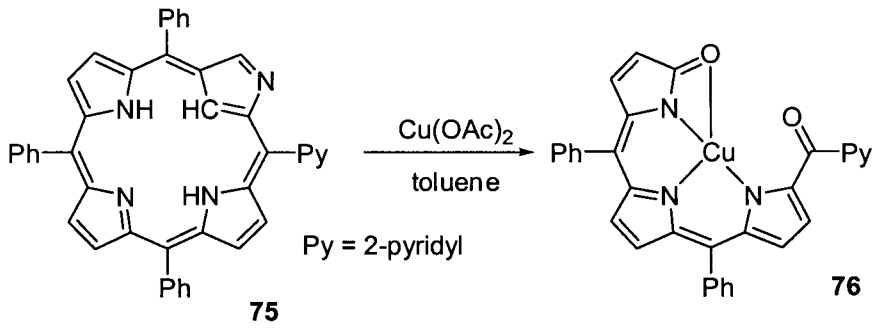

Scheme 1.33 Oxidative degradation of NCP **75**.

1.4.5 Other Porphyrin Analogues with a CH in the Inner Macrocycle

Carbaporphyrins are porphyrin analogues with one five-membered unsaturated all-carbon ring replacing one pyrrole ring. Carbaporphyrin **78 (a,b)** can be prepared by condensation of hydroxyfulvenedialdehyde **77 (a,b)** with tripyrrane **20** (Scheme 1.34).[30,31] In the ^{1}H NMR spectrum of compound **78a,** the inner NH protons and CH proton have signals at -4.2 and -7.2 ppm, respectively, indicating a strong ring current and the overall aromaticity of carbaporphyrins.

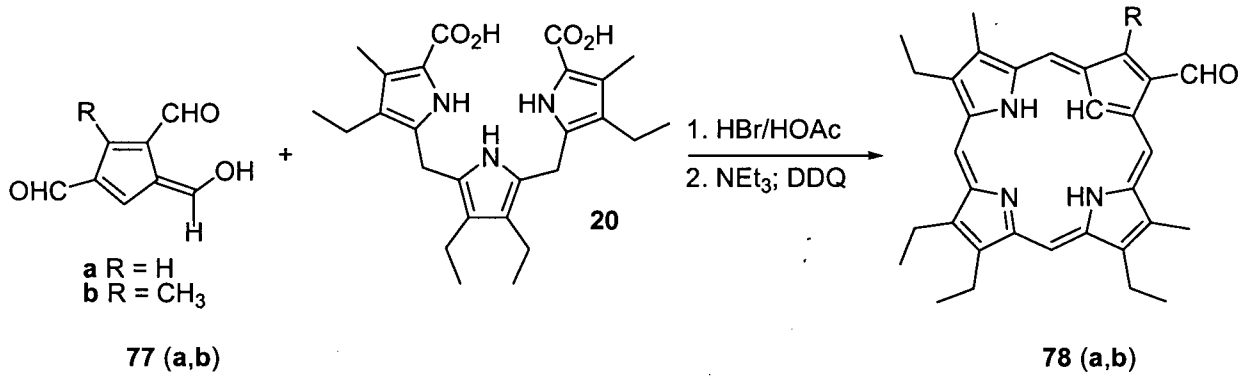

Scheme 1.34 Synthesis of carbaporphyrin **78 (a,b)**.

Benziporphyrin, a benzene containing porphyrin analogue, can be synthesized by acid catalyzed condensation of a tripyrrane dicarboxylic acid with isophthalaldehyde.[53] NMR data suggest that benziporphyrin exists as a mixture of two tautomers **79** and **80** (Scheme 1.35). The system does not exhibit aromatic properties as a whole, as the conjugation discontinues in the benzene ring.[54]

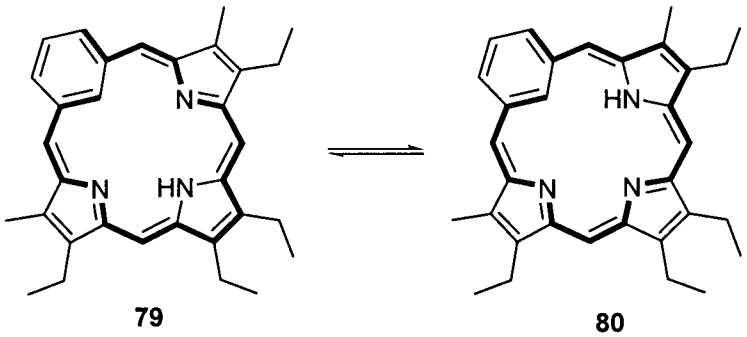

Scheme 1.35 Structures of the two tautomers for benziporphyrin.

Oxybenziporphyrin **82** was prepared by the reaction of tripyrrane dicarboxylic acid **20** and 5-formylsalicylaldehyde **81** (Scheme 1.36).[54-56] It has the 18 π-electron pathway and is aromatic.[54] The inner CH has a signal at -7.2 ppm in the ^{1}H NMR spectrum for compound **82**, indicating the presence of a macrocyclic ring current.

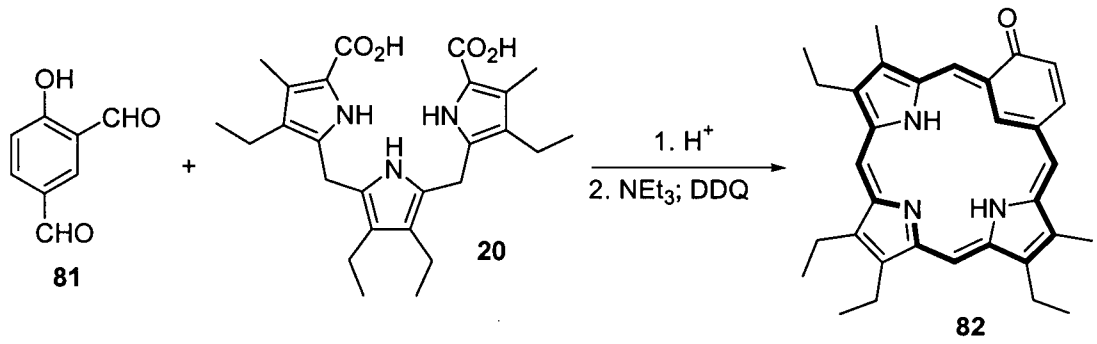

Scheme 1.36 Synthesis of oxybenziporphyrin **82**.

Compound **85**, a tetraphenylthiaporphyrin bearing one inverted pyrrole, was obtained by Lee and Kim *via* the [3 + 1] condensation of pyrrole **83** and thiotripyrrane **84** (Scheme 1.37).[57]

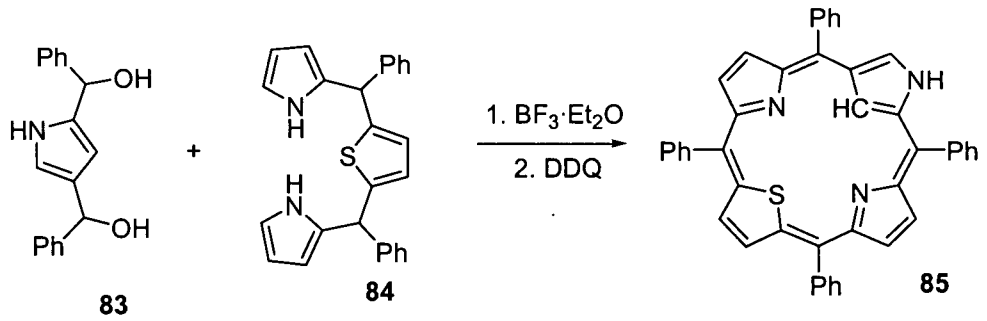

Scheme 1.37 Synthesis of compound **85**.

Compound **87**, a tetraphenylthiaporphyrin bearing one inverted thiophene ring, can be synthesized through condensation of thiophene **86** with pyrrole and benzaldehyde (Scheme 1.38).[58] The ^{1}H NMR spectrum of **87** shows that inner CH and NH resonate at 4.76 and 5.81 ppm, respectively, suggesting weak overall aromaticity of compound **87**.

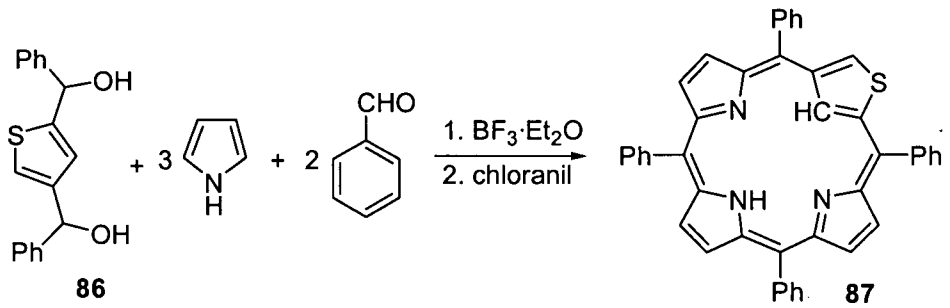

Scheme 1.38 Synthesis of compound **87**.

An aromatic isomer of 5,10,15,20-tetra(*p*-tolyl)-21,23-dithiaporphyrin with an inverted pyrrole ring, 5,10,15,20-tetra(*p*-tolyl)-2-aza-21-carba-22,24-dithiaporphyrin, **89**, can be prepared by the reaction of 2,5-bis(*p*-tolylhydroxymethyl)thiophene, **88**, with pyrrole (1:1 molar ratio) in dichloromethane, (Scheme 1.39).[59]

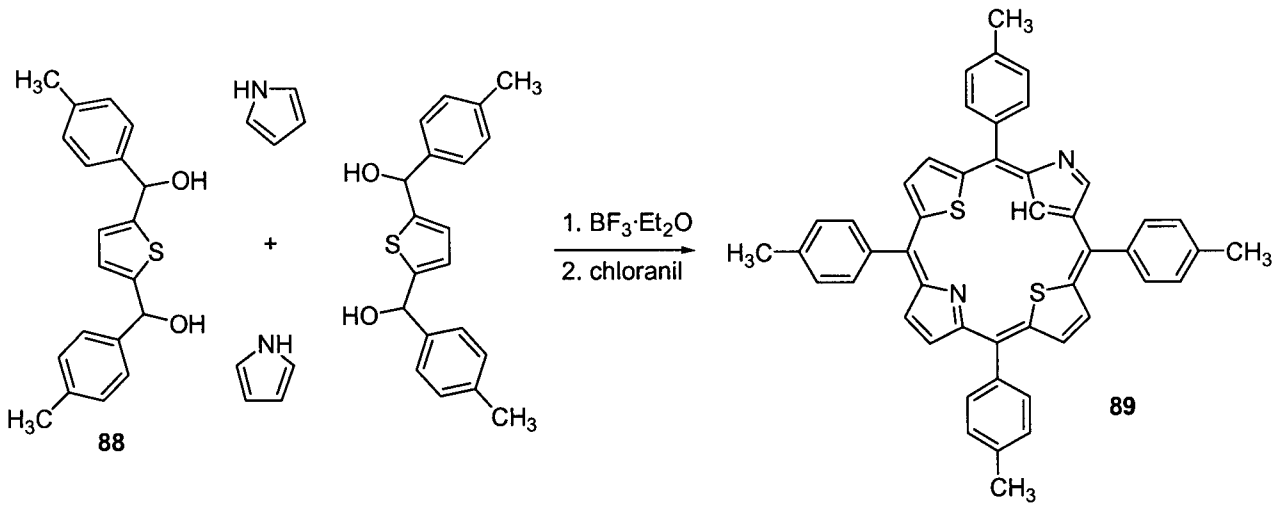

Scheme 1.39 Synthesis of compound **89**.

A [3 + 1] condensation of 2,5-bis(phenylhydroxymethyl)selenophene, **90**, and 5,10-ditolyltripyrrin **91** produces 5,10-diphenyl-15,20-bis(*p*-tolyl)-2-aza-21-carba-22-selenaporphyrin, **92** (Scheme 1.40), which preserves aromaticity.[60]

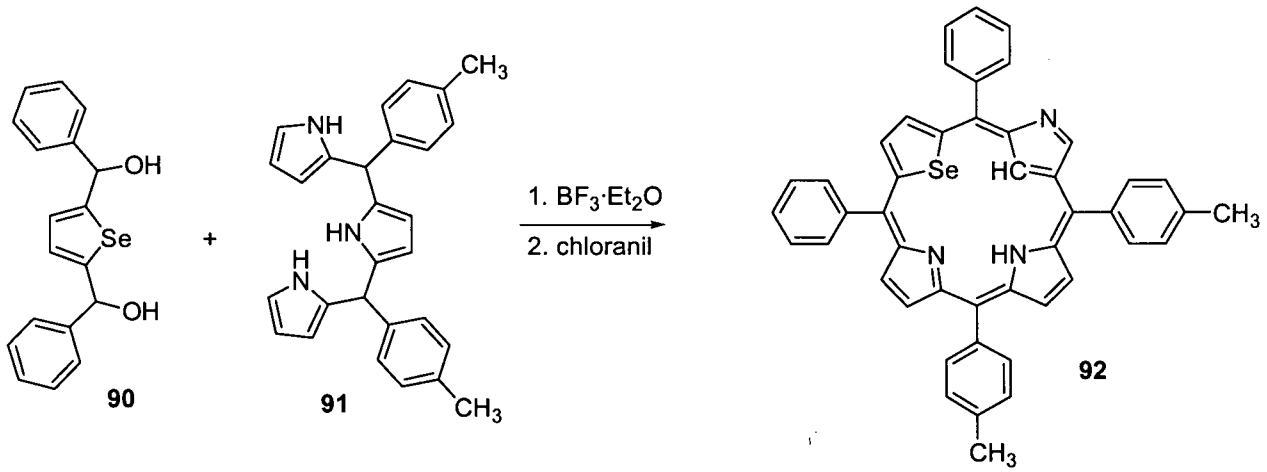

Scheme 1.40 Synthesis of compound **92**.

1.5 Research Objectives and Thesis Preview

The objectives of this work are to explore the chemistry of N-confused porphyrins and develop new photosensitizers for PDT.

In the presence of Na_2CO_3, N-confused tetraarylporphyrins reacted with CH_3I to yield novel N,N'-dimethylated N-confused porphyrin salts, which are mixtures of structural isomers (Chapter 2). The structures of the major isomers were determined by X-ray diffraction or NMR spectroscopic analyses. These N,N'-dimethylated N-confused tetraarylporphyrin salts can generate singlet oxygen when irradiated, and therefore, are potential photosensitizers for PDT.

It was postulated that similar to chlorins, N-confused chlorins might have much greater absorption intensity than N-confused porphyrins in the Q-bands region, and thus are better candidates as photosensitizers for PDT. Diels-Alder reactions of N-confused tetraarylporphyrins as dienophiles, and dihydroxylation of N-confused porphyrins with OsO_4 were proposed to prepare N-confused chlorins.

In the Diels-Alder reactions of Ni(II) N-confused tetraarylporphyrins as dienophiles with *o*-benzoquinodimethane, cycloaddition occurred selectively on the peripheral carbon-nitrogen bond and Ni(II) N-confused isoquinoporphyrins were obtained, presumably through oxidation of corresponding N-confused chlorins, the initial cycloaddition product (Chapter 3). This reaction suggested that the peripheral carbon-nitrogen bond of Ni(II) NCPs has some iminium character and might be reactive towards nucleophiles.

Nucleophilic reactions of Ni(II) N-confused porphyrins with $NaOCH_3$ were then studied. In the reactions of $(NCTTP)Ni^{II}$ with $NaOCH_3$ and DDQ, inner C- cyanide addition to

(NCTTP)Ni^{II} and subsequent electrophilic addition of CH_3O^- were observed and the products were structurally characterized (Chapter 4).

In our studies involving the reactions of Ni(II) N-confused porphyrins with OsO_4, an unexpected product, a Ni(III) complex of N-confused porphyrin inner C-oxide, was obtained and structurally characterized (Chapter 5).

References

1. Bonnett, R. Nomenclature. In *The Porphyrins;* Dolphin, D. Ed.; Academic Press: New York, 1978; Vol. 1; pp. 1.
2. Scheidt, W. R. Porphyrin Stereochemistry. In *The Porphyrins;* Dolphin, D. Ed.; Academic Press: New York, 1978; Vol. 3; pp. 463.
3. Smith, K. M. *Porphyrins and Metalloporphyrins: a new edition based on the original volume by J. E. Falk*; Elsevier Scientific Pub. Co.: Amsterdam, 1975.
4. Buchler, J. W. Synthesis and Properties of Metalloporphyrins. In *The Porphyrins;* Dolphin, D. Ed.; Academic Press: New York, 1978; Vol. 1; pp. 389.
5. Cowan, J. A. *Inorganic Biochemistry: an introduction*, 2nd ed.; Wiley-VCH: New York, 1997.
6. Gouterman, M. Optical Spectra and Electronic Structure of Porphyrins and Related Rings. In *The Porphyrins;* Dolphin, D. Ed.; Academic Press: New York, 1978; Vol. 3; pp. 1.
7. Sternberg, E. D., Dolphin, D. and Bruckner, C. *Tetrahedron* **1998,** *54*, 4151.
8. MacDonald, I. J. and Dougherty, T. J. *J. Porphyr. Phthalocya.* **2001,** *5*, 145.
9. Pandey, R. K. and Zheng, G. Porphyrins as Photosensitizers in Photodynamic Therapy. In *The Porphyrin Handbook;* Kadish, K. M.; Smith, K. M.; Guilard, R. Eds.; Academic Press: San Diego, 2000; Vol. 6; pp. 157.
10. Foote, C. S. Light, Oxygen, and Toxicity. In *Pathology of Oxygen;* Autor, A. P. Ed.; Academic Press: New York, 1982; pp. 21.

11. Foote, C. S. Mechanisms of Photooxygenation. In *Porphyrin Localization and Treatment of Tumors;* Doiron, D. R.; Gomer, C. J. Eds.; Alan R. Liss, Inc.: New York, 1983; pp. 3.

12. Pangka, V. S., Morgan, A. R. and Dolphin, D. *J. Org. Chem.* **1986,** *51*, 1094.

13. Morgan, A. R., Pangka, V. S. and Dolphin, D. *Chem. Commun.* **1984,** 1047.

14. Bruckner, C., Rettig, S. J. and Dolphin, D. *J. Org. Chem.* **1998,** *63*, 2094.

15. Tome, A. C., Lacerda, P. S. S., Neves, M. G. P. M. S. and Cavaleiro, J. A. S. *Chem. Commun.* **1997**, 1199.

16. Silva, A. M. G., Tome, A. C., Neves, M. G. P. M. S., Silva, A. M. S. and Cavaleiro, J. A. S. *Chem. Commun.* **1999**, 1767.

17. Whitlock, J. H. W., Hanamer, R., Oester, M. Y. and Bower, B. K. *J. Am. Chem. Soc.* **1969,** *91*, 7485.

18. Callot, H. *Bull. Chem. Soc. Chim. Fr.* **1972,** *11*, 4387.

19. Furuta, H., Asano, T. and Ogawa, T. *J. Am. Chem. Soc.* **1994,** *116*, 767.

20. Chmielewski, P. J., Latos-Grażyński, L., Rachlewicz, K. and Glowiak, T. *Angew. Chem., Int. Ed. Engl.* **1994,** *33*, 779.

21. Geier, G. R., Haynes, D. M. and Lindsey, J. S. *Org. Lett.* **1999,** *1*, 1455.

22. Narayanan, S. J., Sridevi, B., Srinivasan, A., Chandrashekar, T. K. and Roy, R. *Tetrahedron Lett.* **1998,** *39*, 7389.

23. Liu, B. Y., Bruckner, C. and Dolphin, D. *Chem. Commun.* **1996**, 2141.

24. Lash, T. D., Richter, D. T. and Shiner, C. M. *J. Org. Chem.* **1999,** *64*, 7973.

25. Chmielewski, P. J. and Latos-Grażyński, L. *J. Chem. Soc., Perkin Trans. 2* **1995**, 503.

26. Chmielewski, P. J., Latos-Grażyński, L. and Glowiak, T. *J. Am. Chem. Soc.* **1996,** *118*, 5690.

27. Chmielewski, P. J. and Latos-Grażyński, L. *Inorg. Chem.* **2000,** *39*, 5639.

28. Furuta, H., Maeda, H., Osuka, A., Yasutake, M., Shinmyozu, T. and Ishikawa, Y. *Chem. Commun.* **2000**, 1143.

29. Furuta, H., Kubo, N., Maeda, H., Ishizuka, T., Osuka, A., Nanami, H. and Ogawa, T. *Inorg. Chem.* **2000,** *39*, 5424.

30. Berlin, K. *Angew. Chem., Int. Ed. Engl.* **1996,** *35*, 1820.

31. Berlin, K., Steinbeck, C. and Breitmaier, E. *Synthesis* **1996**, 336.

32. Szterenberg, L. and Latos-Grażyński, L. *Inorg. Chem.* **1997,** *36*, 6287.

33. Ghosh, A. *Angew. Chem., Int. Ed. Engl.* **1995,** *34*, 1028.

34. Ghosh, A. *Acc. Chem. Res.* **1998,** *31*, 189.

35. Ghosh, A., Wondimagegn, T. and Nilsen, H. J. *J. Phys. Chem. B* **1998,** *102*, 10459.

36. Furuta, H., Ishizuka, T., Osuka, A., Dejima, H., Nakagawa, H. and Ishikawa, Y. *J. Am. Chem. Soc.* **2001,** *123*, 6207.

37. Furuta, H., Maeda, H. and Osuka, A. *J. Am. Chem. Soc.* **2000,** *122*, 803.

38. Schmidt, I. and Chmielewski, P. J. *Chem. Commun.* **2002**, 92.

39. Furuta, H., Ishizuka, T. and Osuka, A. *J. Am. Chem. Soc.* **2002,** *124*, 5622.

40. Srinivasan, A., Furuta, H. and Osuka, A. *Chem. Commun.* **2001**, 1666.

41. Chen, W. C. and Chen, C. H. *Inorg. Chem.* **2001,** *40*, 5070.

42. Evans, D. A. *J. Am. Chem. Soc.* **1959**, *81*, 2003.

43. Chmielewski, P. J. and Latos-Grażyński, L. *Inorg. Chem.* **1997,** *36*, 840.

44. Furuta, H., Ogawa, T., Uwatoko, Y. and Araki, K. *Inorg. Chem.* **1999,** *38*, 2676.

45. Ogawa, T., Furuta, H., Takahashi, M., Morino, A. and Uno, H. *J. Organomet. Chem.* **2000,** *611*, 551.

46. Chmielewski, P. J., Latos-Grażyński, L. and Schmidt, I. *Inorg. Chem.* **2000,** *39*, 5475.

47. Furuta, H., Ishizuka, T., Osuka, A., Uwatoko, Y. and Ishikawa, Y. *Angew. Chem., Int. Ed. Engl.* **2001,** *40*, 2323.

48. Ishikawa, Y., Yoshida, I., Akaiwa, K., Koguchi, E., Sasaki, T. and Furuta, H. *Chem. Lett.* **1997**, 453.

49. Furuta, H., Ishizuka, T., Osuka, A. and Ogawa, T. *J. Am. Chem. Soc.* **2000,** *122*, 5748.

50. Furuta, H., Ishizuka, T., Osuka, A. and Ogawa, T. *J. Am. Chem. Soc.* **1999,** *121*, 2945.

51. Schmidt, I. and Chmielewski, P. J. *Tetrahedron Lett.* **2001,** *42*, 1151.

52. Furuta, H., Maeda, H. and Osuka, A. *Org. Lett.* **2002,** *4*, 181.

53. Berlin, K. and Breitmaier, E. *Angew. Chem., Int. Ed. Engl.* **1994,** *33*, 1246.

54. Lash, T. D. *Angew. Chem., Int. Ed. Engl.* **1995,** *34*, 2533.

55. Lash, T. D., Chaney, S. T. and Richter, D. T. *J. Org. Chem.* **1998,** *63*, 9076.

56. Richter, D. T. and Lash, T. D. *Tetrahedron* **2001,** *57*, 3657.

57. Lee, C. H. and Kim, H. J. *Tetrahedron Lett.* **1997,** *38*, 3935.

58. Sprutta, N. and Latos-Grażyński, L. *Tetrahedron Lett.* **1999,** *40*, 8457.

59. Sprutta, N. and Latos-Grażyński, L. *Org. Lett.* **2001,** *3*, 1933.

60. Pacholska, E., Latos-Grażyński, L., Szterenberg, L. and Ciunik, Z. *J. Org. Chem.* **2000,** *65*, 8188.

Chapter 2

Alkylation of N-Confused Porphyrins

2.1 Introduction to Alkylation of Porphyrins and N-Confused Porphyrins

N-substituted porphyrins are of great importance to biological systems.[1] They can be produced *in vivo* from N-substitution of cytochrome P-450 enzymes or from reactions of hydrazines with hemoglobin and myoglobin[1] and have been shown to be powerful inhibitors of the enzyme ferrochelatase, which is the terminal enzyme of the heme biosynthetic pathway.[1] An N-substituted porphyrin, N-methyletioporphyrin I, was first reported by McEwen in 1936,[1,2] and the synthesis and characterization of this compound were subsequently reported with its Zn(II) complex in 1946.[3]

Many synthetic methods have been developed to prepare N-substituted porphyrins. For example, N,N'-dimethylated TPP **93** and **94** are obtained in the yield of 45 % when TPP and CH_3I are heated at 100 °C in a sealed tube with K_2CO_3 (Scheme 2.1).[1,4] However, N-methylated TPP (N-CH_3TPP **95**) is a stronger base than TPP and protonation occurs in the presence of AcOH, suppressing further methylation. Thus, when TPP is heated in chloroform at 65 - 70 °C in a sealed tube containing 7.5 % AcOH and 10 % CH_3I for 7 days, N-CH_3TPP is obtained as the major product (50 %) (Scheme 2.2).[1,5] Other N-substituted porphyrins, including N-ethyl, N-vinyl, N-phenyl and N-benzyl porphyrins, have also been prepared.[1]

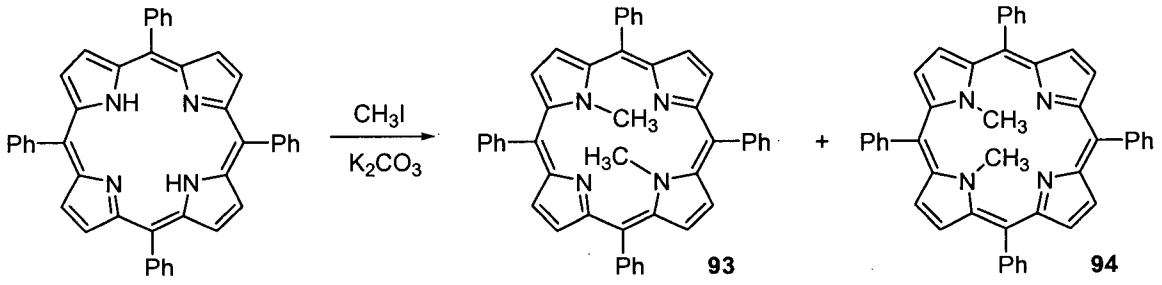

Scheme 2.1 N-methylation of TPP with base.

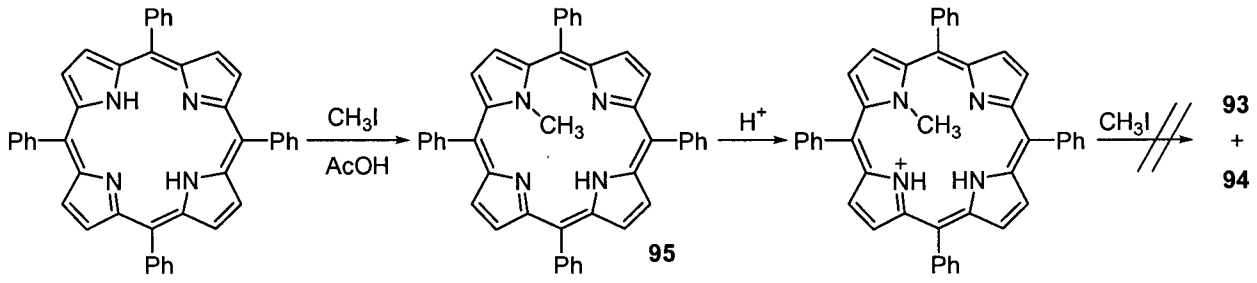

Scheme 2.2 N-methylation of TPP with CH_3I in the presence of acid.

Addition of a group to one of the central nitrogen atoms distorts the normally planar porphyrin skeleton.[1] The X-ray crystal structure of N-methyl-5,10,15,20-tetrakis(*p*-bromophenyl)porphyrin, reported by Lavallee and Anderson, shows that the N-methyl substituted pyrrole ring deviates 27.7° from the plane defined by the three unsubstituted nitrogen atoms.[6] X-ray crystal structures of other N-substituted porphyrins show similar deviations from planarity.[1]

The ^1H NMR spectrum of N-CH_3TPP shows a signal at -4.1 ppm for the inner methyl protons.[4] Other N-substituted porphyrins exhibit similar upfield signals for the inner substituent groups in their respective ^1H NMR spectra.[1] These signals suggest that even though the porphyrin ring is severely distorted, N-substituted porphyrins preserve aromaticity.

N-substituted porphyrins have UV-vis absorptions with molar extinction coefficients of 10^5 $M^{-1}cm^{-1}$ in the Soret region (400 - 500 nm) and 10^4 $M^{-1}cm^{-1}$ in the Q-bands region (500 - 700 nm), and the bands are generally red-shifted about 10 nm compared to those of corresponding non-N-substituted porphyrins.[1] The absorption intensities are similar to those of non-N-substituted porphyrins, indicating again that the high degree of aromaticity typical of nearly planar porphyrins is retained.[1]

Alkylation of N-confused porphyrins was reviewed in section 1.4.4.1. In short, both outer N(2) and inner C(21) atoms can be alkylated and outer N(2)-methylated N-confused porphyrin **24**, C(21)-methylated N-confused porphyrin **29**, C(21),N(2)-dimethylated N-confused porphyrin **30**, and their Ni(II) derivatives were prepared by Latos-Grażyński *et al.*[7,8]

Other than the N(2) and C(21) atoms, the three inner nitrogen atoms in N-confused porphyrins might be expected to react similarly as the inner nitrogen atoms of porphyrins. Their susceptibility to alkylation in particular was studied in this thesis work. The resulting alkylated products are potential photosensitizers for PDT. These alkylated N-confused porphyrins may also be interesting for their possible novel coordination properties.

Another aspect of this investigation with alkylated N-confused porphyrins is the synthesis of intramolecular C,N-strapped N-confused porphyrins, which have novel structural properties. Intramolecular N-strapped porphyrins **97** have been prepared from their precursor **96** by Ishimaru *et al.* (Scheme 2.3).[9] Signals for the N-CH_2 protons of **97** in the ^{1}H NMR spectrum are observed upfield at -4.08 and -4.31 ppm, due to the ring current.[9]

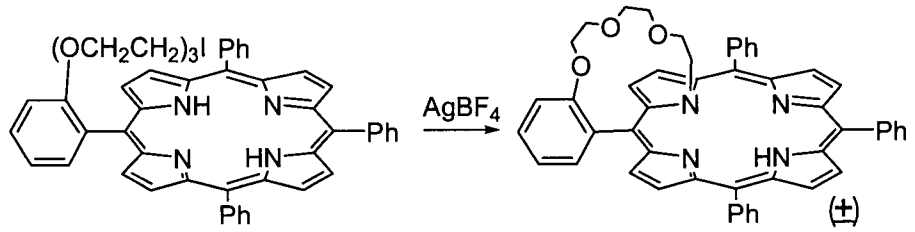

96 **97**

Scheme 2.3 Synthesis of N-strapped porphyrins **97**.

As Ni(II) N-confused porphyrins have at least two nucleophilic centers, the N(2) located outside and the C(21) located inside of the porphyrin ring, intramolecular C,N-strapped Ni(II) N-confused porphyrins **98** may be readily synthesized (Scheme 2.4).

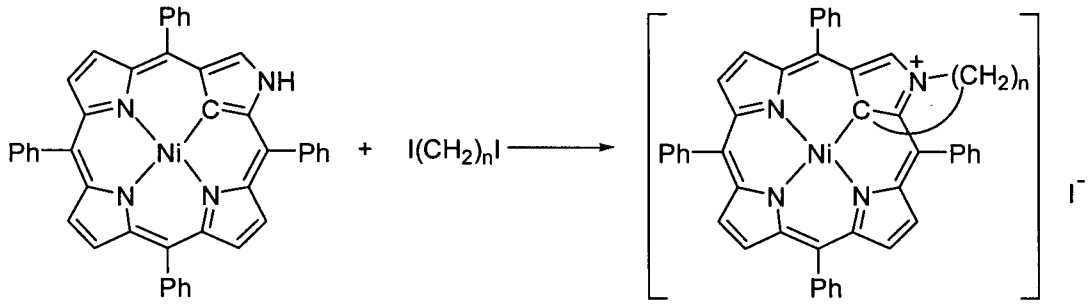

Scheme 2.4 Proposed synthesis of intramolecular C,N-strapped Ni(II) N-confused porphyrins.

2.2 Results and Discussion

2.2.1 N-Confused Porphyrins

N-confused porphyrins were synthesized according to the procedure of Lindsey and coworkers [10] *via* condensation of pyrrole and aryl aldehyde under catalysis of MSA (section 1.4.3) (Scheme 2.5).

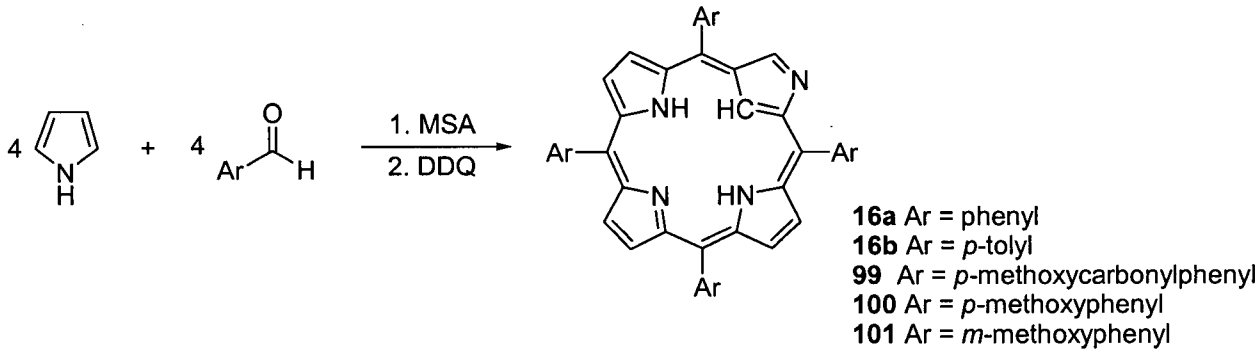

Scheme 2.5 Synthesis of N-confused tetraarylporphyrins.

2.2.2 N,N'-Dimethylated N-Confused Porphyrins

Methylation of NCTPP with CH_3I in CH_2Cl_2 yields N(2)-CH_3-NCTPP, **24** (section 1.4.4.1).[7] It is assumed that protonation of compound **24** by HI generated from the methylation reaction prevents subsequent inner N-methylation (Scheme 2.6). Therefore, addition of a base, such as Na_2CO_3, might neutralize the intermediate N(2)-CH_3-NCTPP·HI, **102**, making the inner nitrogen atoms more nucleophilic towards methylation and resulting in N,N'-dimethylation. In fact, dimethylation of N-confused porphyrins was carried out in CH_2Cl_2 solution using CH_3I and Na_2CO_3 (Scheme 2.7), and addition of two methyl groups was confirmed by the low and high resolution LSIMS spectra of the products. For example, product **103** resulting from the reaction of CH_3I and NCTPP ($C_{44}H_{30}N_4$) has the molecular ion peak at 643.28623 *m/e* (HRLSIMS), and the molecular formula search results in $C_{46}H_{35}N_4$ (*m/e* Calcd 643.28617) for the molecular ion peak, as expected for the dimethylated product.

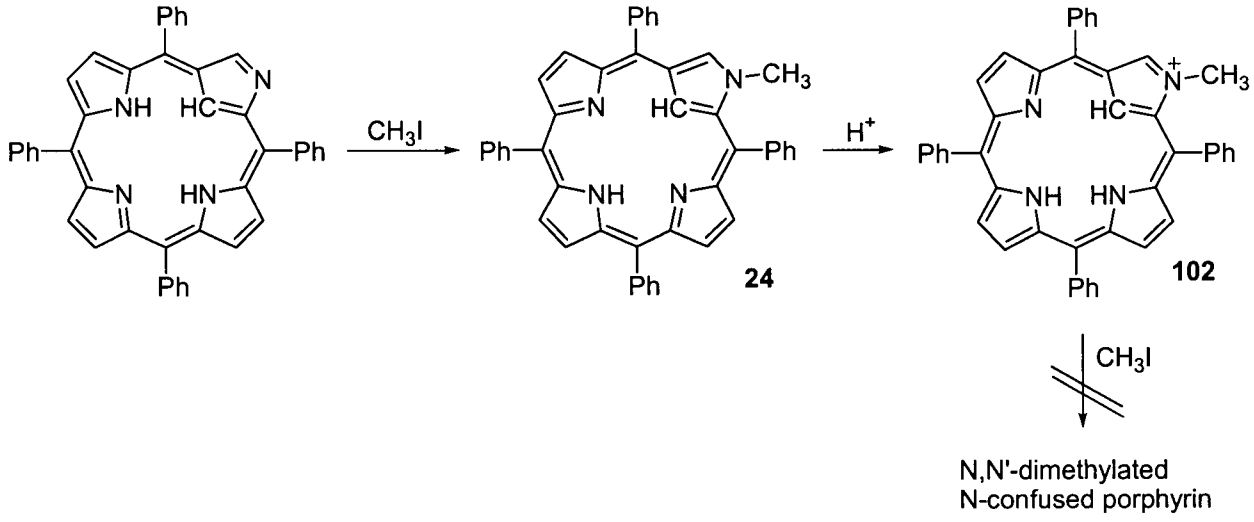

Scheme 2.6 Reactions of NCTPP with CH_3I without base.

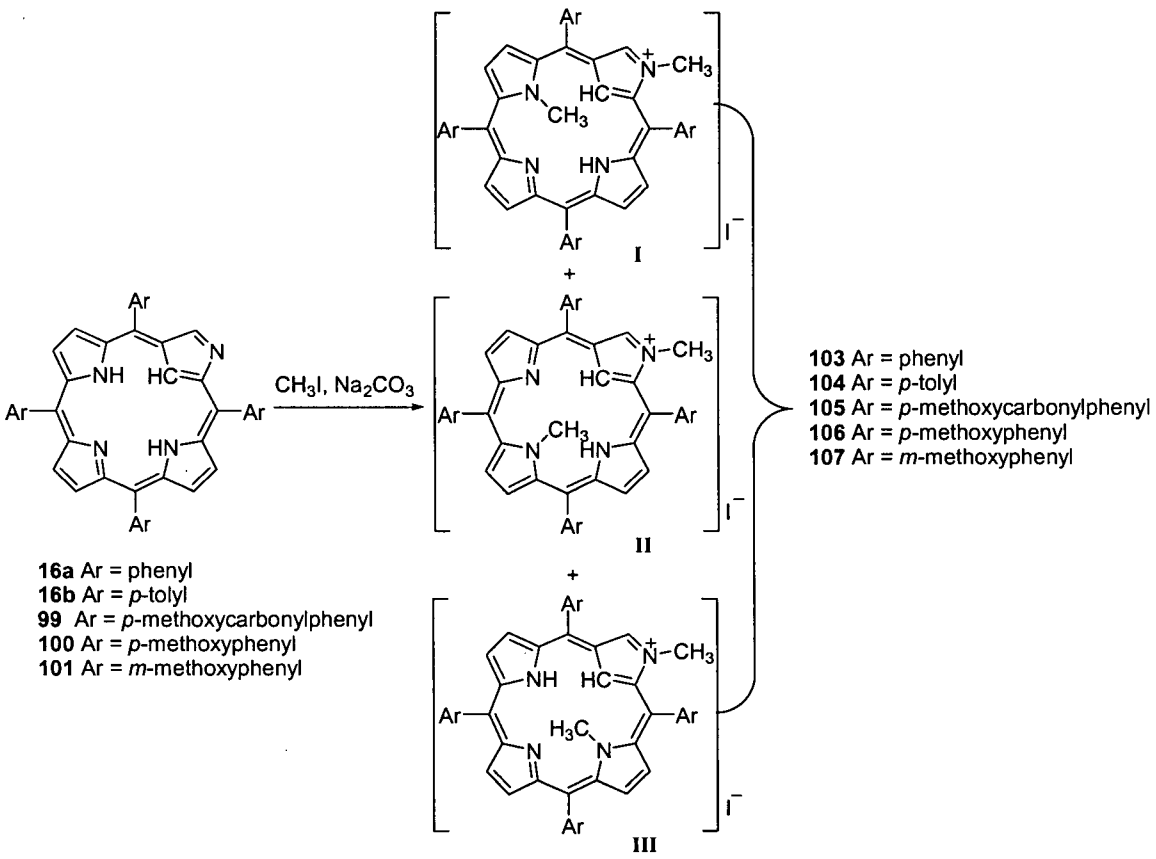

Scheme 2.7 Dimethylation of N-confused porphyrins.

Elemental analysis of **103** (C, 68.96; H, 4.76; N, 6.86; I, 15.82) agrees with the formation of iodide salts (Anal. Calcd for $C_{46}H_{34}N_4 \cdot HI \cdot 1.5H_2O$: C, 69.26; H, 4.80; N, 7.02; I, 15.91). Elemental analyses of **104** - **107** show similar results.

Each of the N,N'-dimethylated N-confused porphyrin salts **103** - **107** can consist of up to three structural isomers (**I** - **III**, Scheme 2.7), as there are three possible positions, N(22), N(23), and N(24), for inner N-methylation. ^{1}H NMR spectra data suggest that each of compounds **103** - **106** consists of two isomers, with the ratio of about 2:1 (Figure 2.1), while compound **107** has at least three isomers.

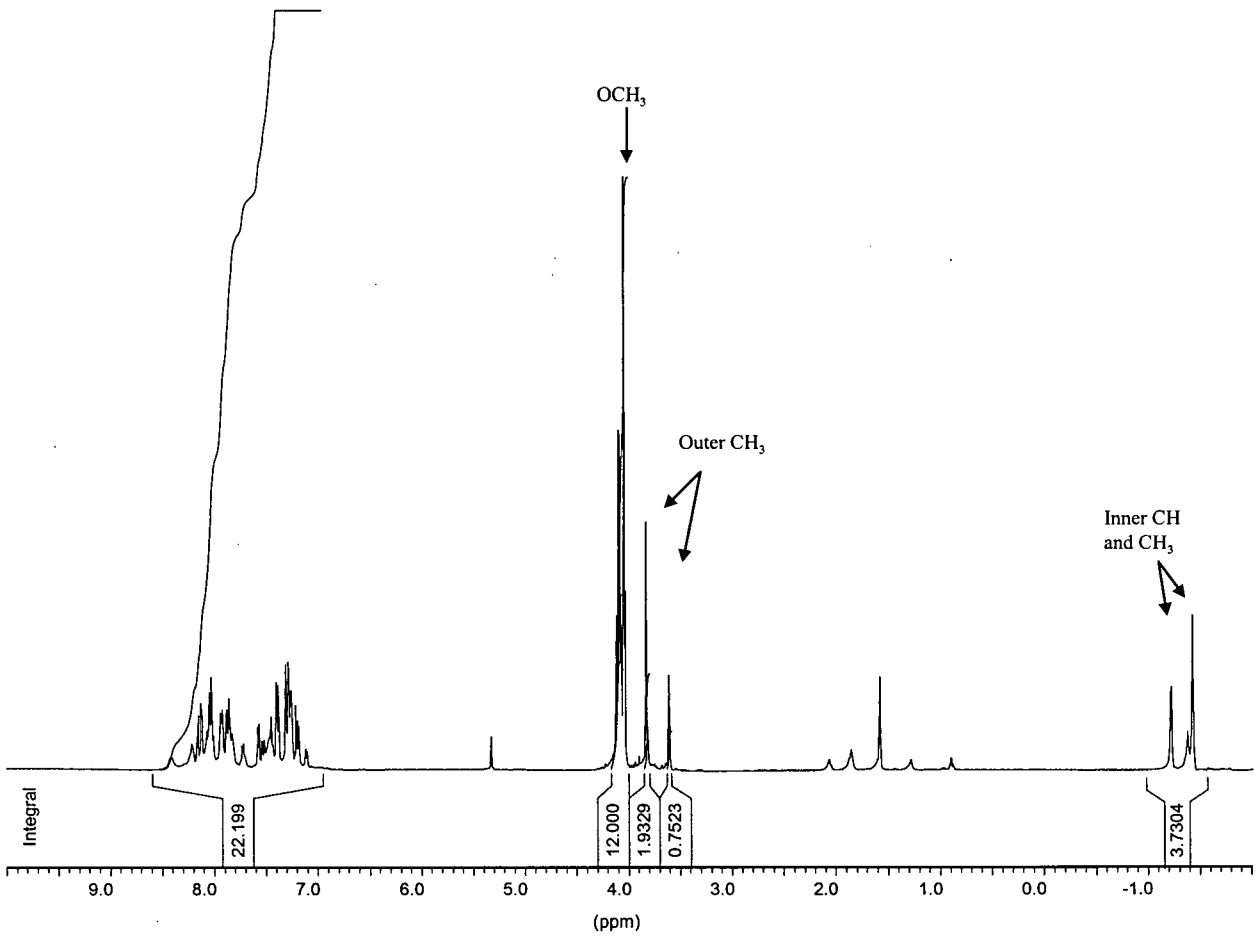

Figure 2.1 ^{1}H NMR spectrum of **106** in CD_2Cl_2 (400 MHz).

Each compound **103** - **107** showed only one spot on TLC plates (silica gel or alumina) with various developing solvents. Isolation attempts of the isomers by flash column chromatography using various developing solvents with different stationary phases, including silica gel (230 - 400 mesh), basic alumina, neutral alumina and acidic alumina, were not successful. Only the major isomers of compounds **103** - **106** were isolated by recrystallization with CH_2Cl_2/hexanes and structures of the major isomers were determined by X-ray diffraction and NMR spectroscopic analyses to be isomers **III** (Scheme 2.7).

Unlike the synthesis of N-methylated porphyrin, e.g. N-CH_3TPP, which requires heating at 65 - 70 °C in a sealed tube for 7 days,[5] synthesis of dimethylated N-confused porphyrins was

performed at room temperature for 2 days. The inner CH resonance at 0.43 ppm in the ^{1}H NMR spectrum of N(2)-CH_3-NCTPP shows that its ring current is weaker than that of NCTPP, of which the inner CH proton resonates at -5.1 ppm.[7] Aromaticity is often associated with planarity and the weak ring current of N(2)-CH_3-NCTPP may indicate the distortion of planarity. N(2)-CH_3-NCTPP is the intermediate to N,N'-dimethylated N-confused porphyrins and the distortion of its planarity can make the inner nitrogen atoms less sterically hindered towards methylation, resulting in the rate increase of inner methylation.

In the presence of solid Na_2CO_3 (pK_a value of the conjugate acid is 10.2),[11] the final dimethylation products were iodide salts instead of the free base, suggesting that the basicity of N,N'-dimethylated N-confused porphyrin free base is similar to or stronger than that of Na_2CO_3. While significant differences of polarity are expected between the protonated form and free base of N,N'-dimethylated N-confused porphyrins, no change on TLC was observed when Et_3N (pK_a value of the conjugate acid is 11.0)[11] was added to a solution of N,N'-dimethylated N-confused porphyrin salt in CH_2Cl_2, suggesting again their strong basicity. For comparison, the pK_a values of mono-protonated N-CH_3TPP and mono-protonated TPP in nitrobenzene are 5.6 and 4.4, respectively.[1,12]

The cyclic π conjugation is discontinued in the inverted pyrrole ring for N,N'-dimethylated N-confused porphyrin free base, while the cyclic delocalized pathway is retained in the protonated form (Scheme 2.8). In the cases of N-CH_3TPP or TPP, both the protonated form and free base retain their aromaticity (Scheme 2.9). Therefore, it is expected that the energy difference between the protonated form and the free base N,N'-dimethylated N-confused porphyrins is smaller than that of N-CH_3TPP or TPP, which explains the stronger basicity of N,N'-dimethylated N-confused porphyrins.

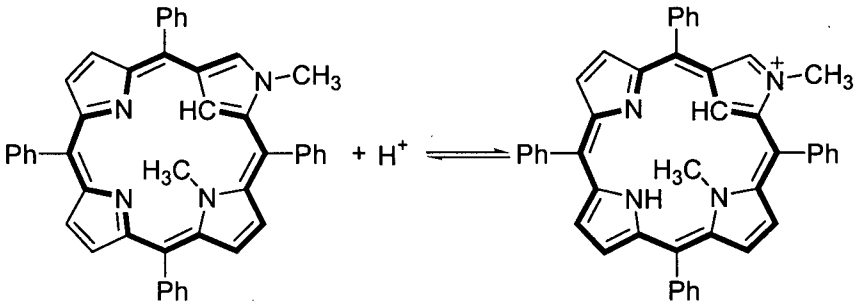

103-III (free base) **103-III** (protonated)

Scheme 2.8 Protonation equilibrium of **103-III** .

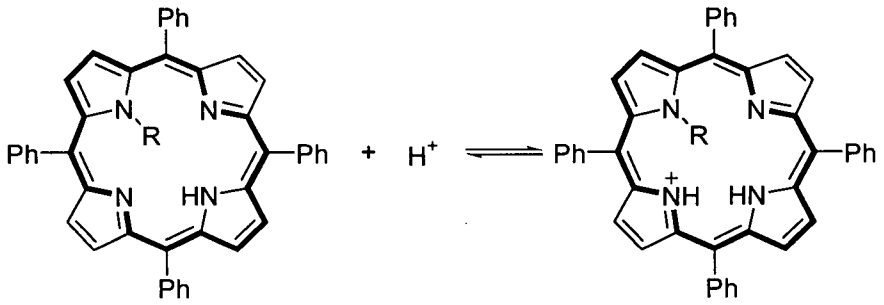

R = H, TPP
R = CH_3, N-CH_3TPP

Scheme 2.9 Protonation equilibrium of TPP and N-CH_3TPP.

In an attempt to prepare neutral dimethylated N-confused porphyrins, the major isomers of **103** - **106** were washed with 0.1 % aqueous NaOH solution, and many spots were observed on TLC plates afterwards, suggesting that the dimethylated N-confused porphyrins are not stable in the presence of strong base. Isolation of the neutral dimethylated N-confused porphyrins was not successful.

Metalation of N-methylated porphyrins is faster than that of non-N-substituted porphyrins, as the planarity of N-methylated porphyrins is distorted and thus N-methylated

porphyrins are "predeformed" for complexation.[1] Metalation reactions of Cd(II) and Zn(II) with N-methyletioporphyrin are about 10^5 times faster than that of etioporphyrin.[1,13] NCTTP and N(2)-CH_3-NCTPP react with $Ni(OAc)_2 \cdot 4H_2O$ at room temperature to yield corresponding Ni(II) complexes.[7,14] Therefore, it was expected that metalation of dimethylated N-confused porphyrins should readily proceed. However, when the dimethylated porphyrin salts were refluxed with $Ni(OAc)_2 \cdot 4H_2O$ or $Zn(OAc)_2$ in CH_2Cl_2/CH_3OH (1:1) for 24 h, no reaction was observed.

2.2.2.1 Structural Determination by NMR Spectroscopy

The structure of **106-III** (Figure 2.2), the major isomer of N,N'-dimethylated 2-aza-5,10,15,20-tetrakis(*p*-methoxyphenyl)-21-carbaporphyrin·HI, **106**, was determined by NMR spectroscopic analyses (^1H, ^{13}C, selective NOE, HMQC and HMBC) (Figure 2.2, 2.3, 2.4 and 2.5). The ^1H 3.81 ppm peak is assigned to H(25) based on the observed cross peak with the ^{13}C 39.5 ppm peak using HMQC (Figure 2.4). Selective NOE experiments show correlations of H(25) (3.81 ppm) with H(43a) (8.40 ppm) and H(43b) (8.04 ppm), correlations of H(43a) with H(43b) and H(18) (7.56 ppm) and correlation of H(18) with H(17) (7.16 ppm), respectively. The N(2)-methyl group hinders rotation of the adjacent *p*-methoxyphenyl group. The rotation is slow and H(43a) and H(43b) can be distinguished by NMR spectroscopy. However, there is still some rotation, which results in H(43a) and H(43b) being interchangeable with their peaks broadened. The negative peak at 8.04 ppm, upon irradiation at 8.40 ppm, shows that the two hydrogens are interchangeable. The -1.47 ppm peak is assigned to the inner methyl group, as suggested by the chemical shift, and integration. The observed cross peaks of ^{13}C 150.75 ppm with H(17) (7.16 ppm), H(18) (7.56 ppm) and H(26) (-1.47 ppm) in an HMBC experiment (Figure 2.5) clearly show that the inner methyl group is connected to the pyrrole unit containing H(17) and H(18).

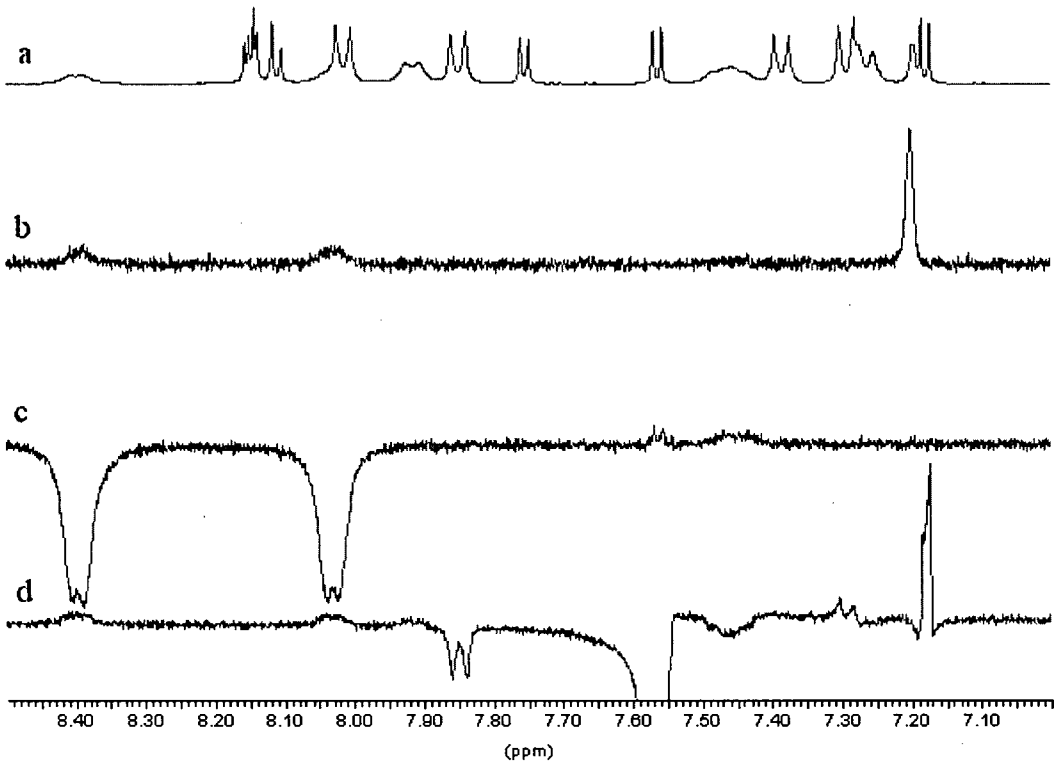

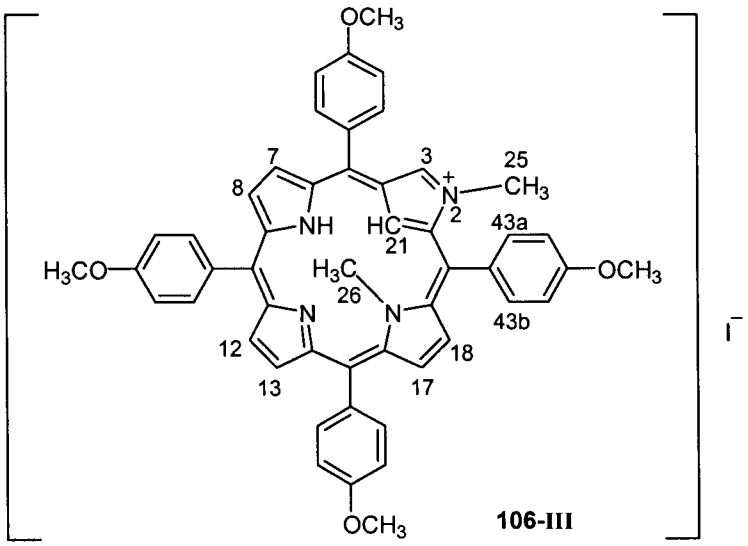

106-III

Figure 2.2 ^{1}H NMR spectra of **106-III** in CD_2Cl_2 (400 MHz): (a) no irradiation; (b) upon irradiation at 3.81 ppm; (c) upon irradiation at 8.40 ppm; (d) upon irradiation at 7.56 ppm.

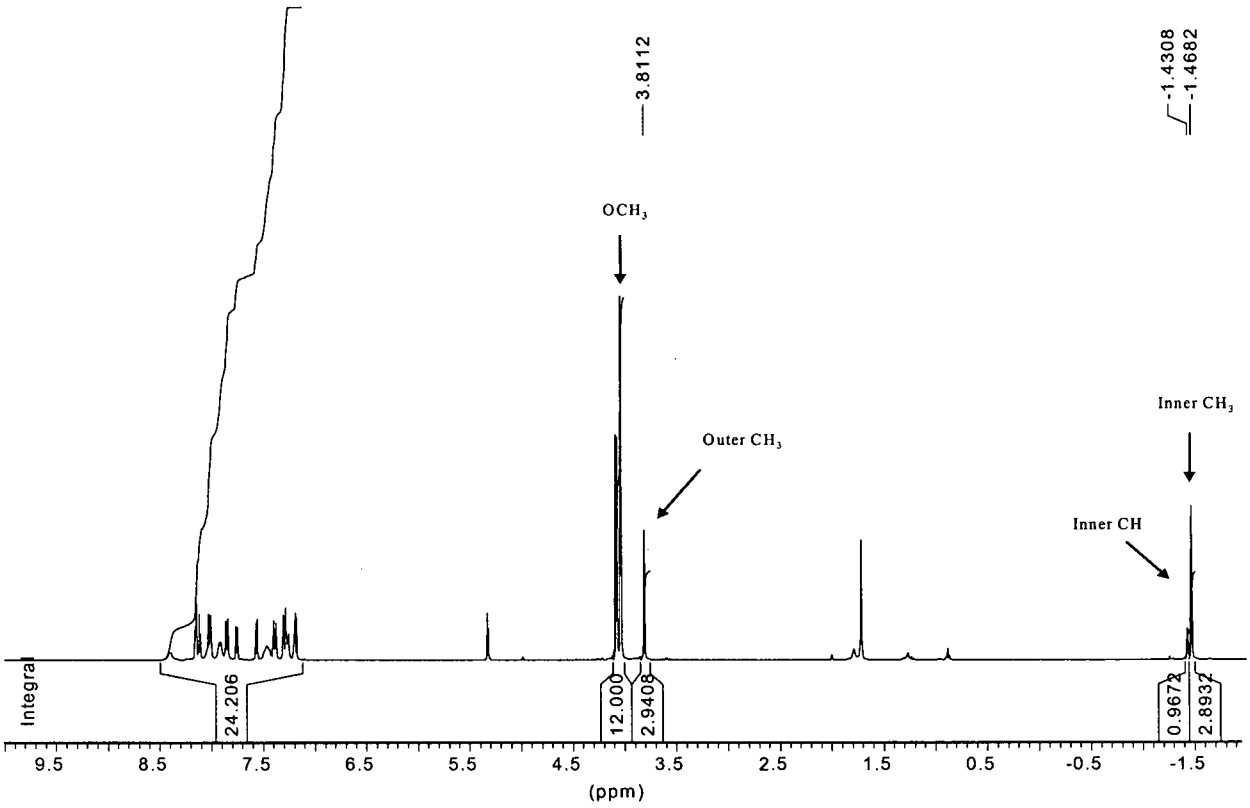

Figure 2.3 ^{1}H NMR spectrum of **106-III** in CD_2Cl_2 (400 MHz).

The ^{1}H NMR signal of C(21)H in **106-III** appears at -1.47 ppm, similar to that of N(2)-CH_3-NCTPP at 0.31 ppm,[7] suggesting that inner N-methylation does not have a significant impact on the aromaticity.

The structures of **104-III** and **105-III**, the major isomers of compounds **104** and **105,** respectively, were determined in a similar way by NMR spectroscopic analyses.

The N(2)-methyl group hinders rotation of the adjacent *p*-methoxyphenyl group in compound **106-III** , as suggested by NMR spectra data. It is expected that the hindrance would be greater in the case of compounds **107**, which have *m*-methoxyphenyl group adjacent to the N(2)-methyl group, resulting in atropisomers in addition to structural isomers, making

compounds **107** a more complicated mixture than compounds **103** - **106**. Purification by recrystallization was not successful for compounds **107**.

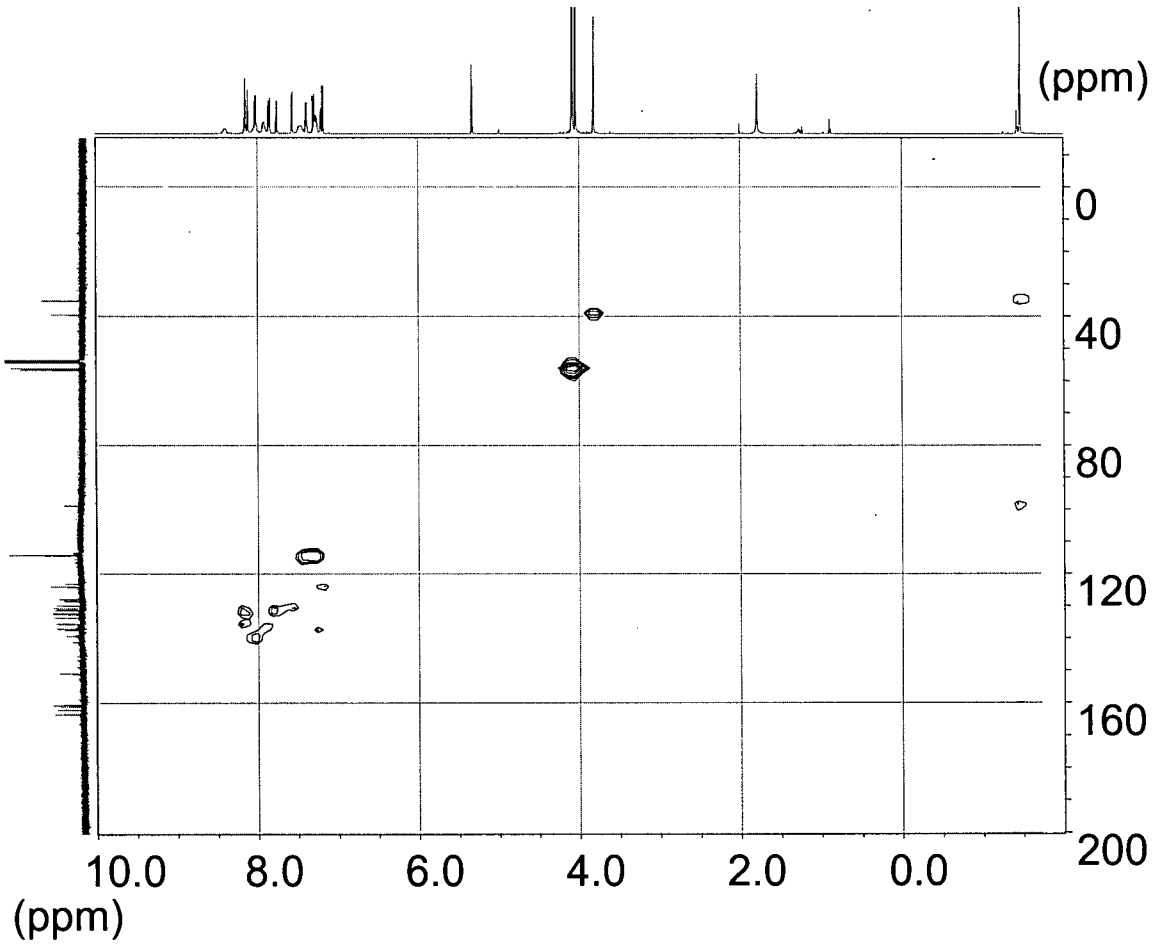

Figure 2.4 ^{1}H, ^{13}C HMQC spectrum of **106-III** in CD_2Cl_2 (400 MHz).

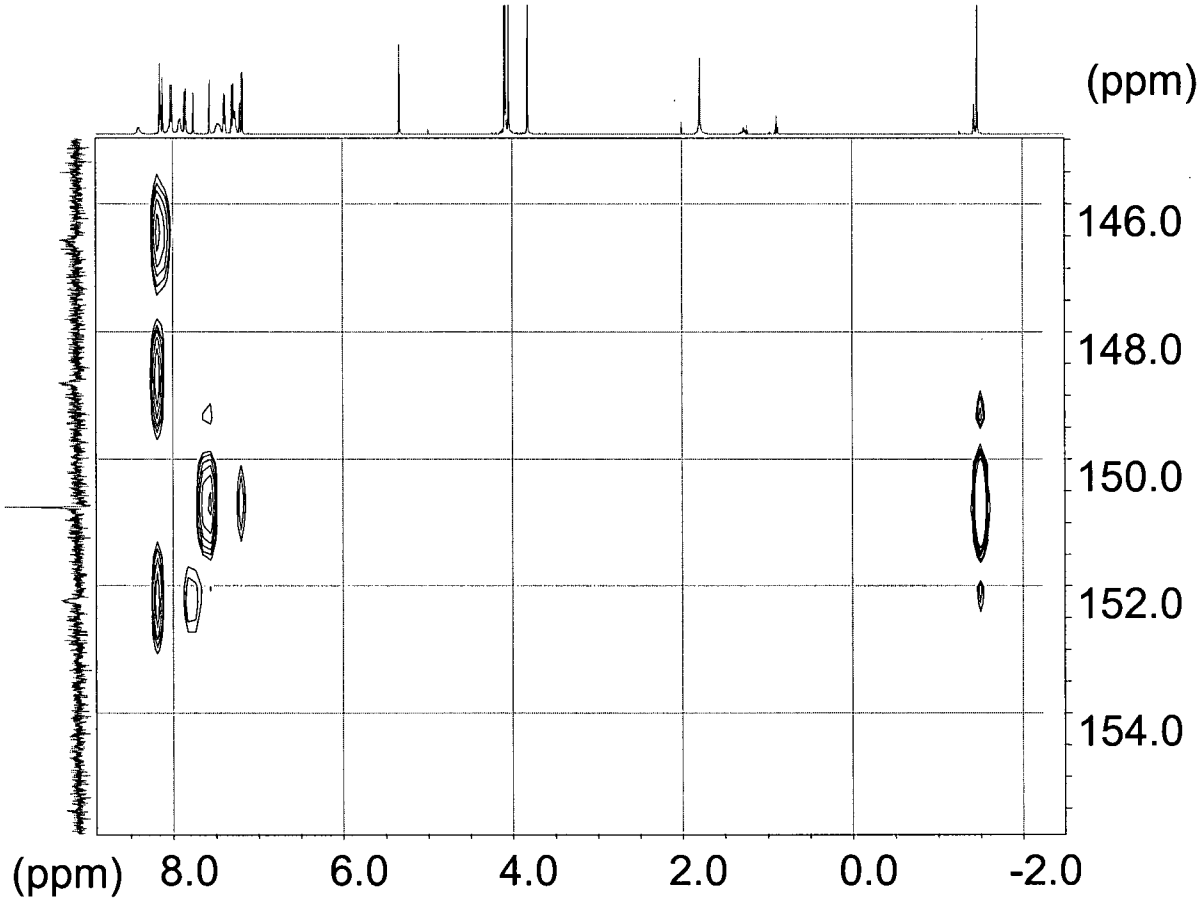

Figure 2.5 Portion of the ^{1}H, ^{13}C HMBC spectrum of **106-III** in CD_2Cl_2 (400 MHz).

2.2.2.2 Structural Determination by X-ray Diffraction Analysis

Compound **103-III** is the major isomer of N,N'-dimethylated 2-aza-5,10,15,20-tetraphenyl-21-carbaporphyrin·HI, **103**. The I^- was exchanged for $CF_3SO_3^-$ in **103-III** giving N(2)-CH_3-N(24)-CH_3-NCTPP·HCF_3SO_3, **108** (Figure 2.6). Crystals of **108** were obtained by solvent diffusion of hexanes into a CH_2Cl_2 solution of **108** and the structure of **108** was determined by X-ray crystallography, which confirms that the porphyrin is N,N'-dimethylated (Figure 2.7). Similar to N-methylated porphyrins, the planarity of **108** is severely distorted (Figure 2.8).

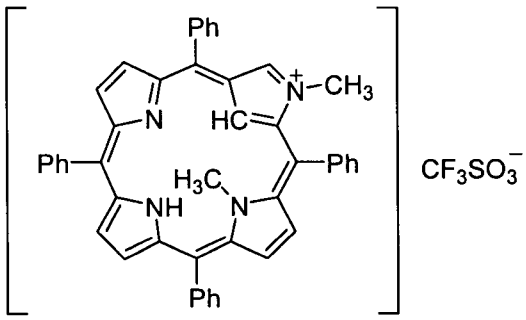

108

Figure 2.6 Structure of **108**.

Selected bond lengths and angles of compound **108** are included in Table 2.1 and Table 2.2 (Selected bond lengths and angles of NCTPP obtained by Furuta *et al.*[15] are included for comparison). Bond lengths of the regular pyrroles for **108** have the same pattern as of porphyrins: $C_\alpha - C_\beta > C_\alpha - N > C_\beta - C_\beta$. Changes of bond lengths in the inverted pyrrole from NCTPP to **108** is severe, -0.038, -0.046, and 0.034 Å, respectively for C(1)-N(2), C(3)-C(4), and C(1)-C(21), indicating that the change of N(2) from diagonal to trigonal changes the π-delocalization pattern.

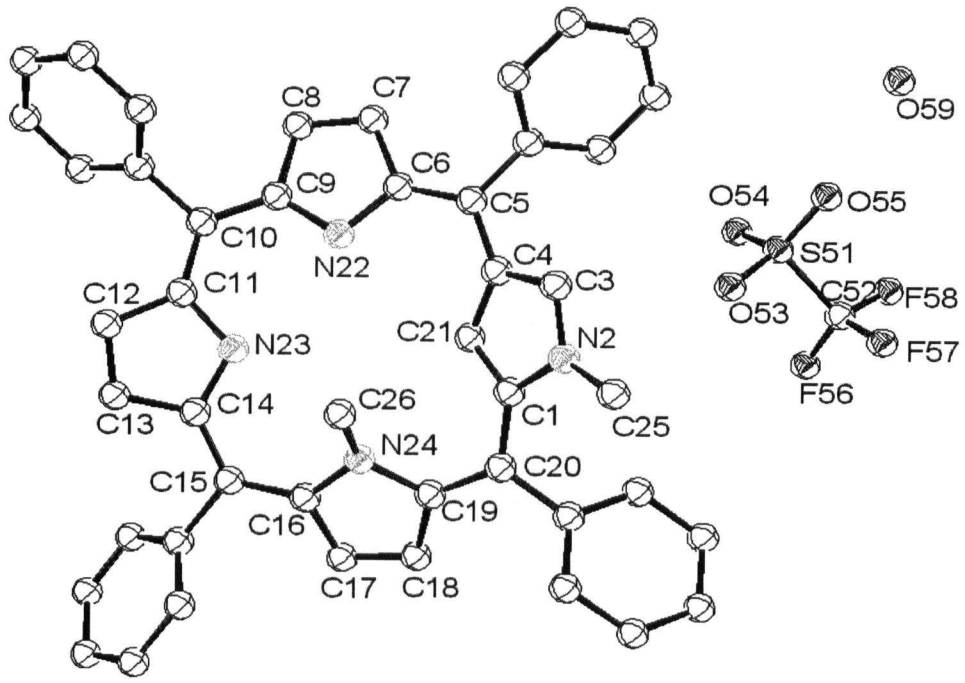

Figure 2.7 An ORTEP drawing of **108** showing atomic labeling and thermal ellipsoids at the 50 % probability level (top view). H atoms have been removed for clarity.

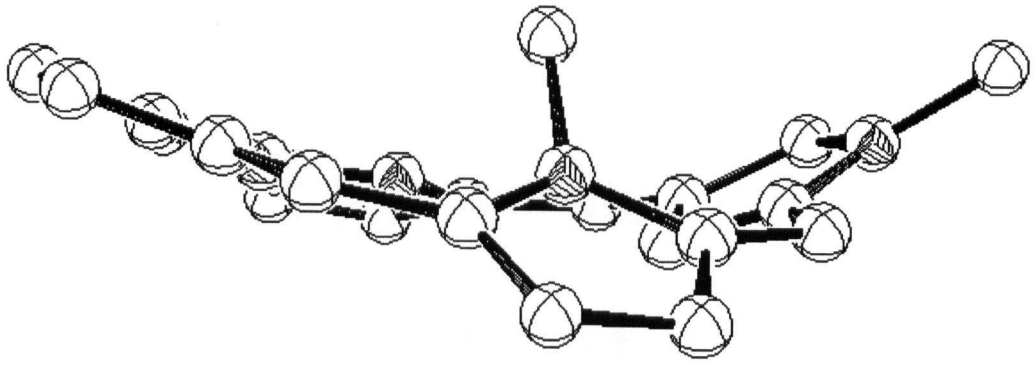

Figure 2.8 An ORTEP drawing of **108** showing thermal ellipsoids at the 50 % probability level (side view). Phenyl groups, residual H_2O, counteranion and H atoms have been removed for clarity.

Table 2.1 Selected bond lengths (Å) for N(2)-CH_3-N(24)-CH_3-NCTPP and NCTPP.

Bond Lengths (Å)	N(2)-CH_3-N(24)-CH_3-NCTPP	NCTPP
N(2)-C(25)	1.457(5)	N/A[a]
N(24)-C(26)	1.478(5)	N/A
C(1)-N(2)	1.405(5)	1.443
C(1)-C(20)	1.422(5)	1.436
C(1)-C(21)	1.389(5)	1.355
N(2)-C(3)	1.339(5)	1.336
C(3)-C(4)	1.408(5)	1.454
C(4)-C(5)	1.434(5)	1.410
C(4)-C(21)	1.391(5)	1.378
C(5)-C(6)	1.386(5)	1.366
C(6)-C(7)	1.454(5)	1.441
C(6)-N(22)	1.386(5)	1.430
C(7)-C(8)	1.348(6)	1.352
C(8)-C(9)	1.447(5)	1.475
C(9)-C(10)	1.422(6)	1.411
C(9)-N(22)	1.361(5)	1.366
C(10)-C(11)	1.388(5)	1.402
C(11)-C(12)	1.432(6)	1.439
C(11)-N(23)	1.391(5)	1.391
C(12)-C(13)	1.351(5)	1.325
C(13)-C(14)	1.439(5)	1.480
C(14)-C(15)	1.418(5)	1.403

C(14)-N(23)	1.374(5)	1.412
C(15)-C(16)	1.396(5)	1.381
C(16)-C(17)	1.423(5)	1.408
C(16)-N(24)	1.381(5)	1.393
C(17)-C(18)	1.358(5)	1.388
C(18)-C(19)	1.425(5)	1.414
C(19)-C(20)	1.391(5)	1.399
C(19)-N(24)	1.408(5)	1.393

a: N/A stands for "Not Applicable".

Bond angles for C(25)-N(2)-C(1), C(25)-N(2)-C(3), C(26)-N(24)-C(16), and C(26)-N(24)-C(19) are in the range of 122 - 128° (Table 2.2), indicating that both substituted nitrogen atoms keep sp^2 hybridization. Bond angles for both C(1)-N(2)-C(3) and C(16)-N(24)-C(19) are 108.5°, smaller than the optimum bond angle of 120° for sp^2 hybridized atoms, and this deviation is the result of the strain from planar five-membered pyrrolic ring. N(24) atom is trigonal in both compound **108** and NCTPP, and the N(24) centered bond angles are very close in these two compounds with the difference been 0.1°, 3.6°, and 0.5° (Table 2.2), suggesting that changes of the π electron conjugation of the porphyrin skeleton due to inner N-methylation is small.

Table 2.2 Selected bond angles (°) for N(2)-CH_3-N(24)-CH_3-NCTPP and NCTPP.

Bond Angles (°)	N(2)-CH_3-N(24)-CH_3-NCTPP	NCTPP
C(25)-N(2)-C(1)	127.2(4)	N/A[a]
C(25)-N(2)-C(3)	123.4(4)	N/A
C(1)-N(2)-C(3)	108.5(3)	103.5
C(26)-N(24)-C(16) / H(24)-N(24)-C(16)	122.6(3)	122.5
C(26)-N(24)-C(19) / H(24)-N(24)-C(19)	122.4(3)	126.0
C(16)-N(24)-C(19)	108.5(3)	109.0

a: N/A stands for "Not Applicable".

2.2.2.3 Optical Absorption Spectra

N,N'-dimethylated porphyrin salts have strong absorptions around 475 nm and 800 nm, corresponding to the Soret and Q-bands of porphyrins, respectively (Figure 2.9). The long wavelength absorption around 800 nm is broad, with a molar extinction coefficient around 20,000 $M^{-1}cm^{-1}$, making the N,N'-dimethylated porphyrin salts good candidates as photosensitizers for PDT.

The absorption spectra of the salt mixture and the corresponding major isomer are almost identical (Figure 2.9), suggesting that the position of the inner N-methylation does not significantly affect the overall porphyrin π electron conjugation.

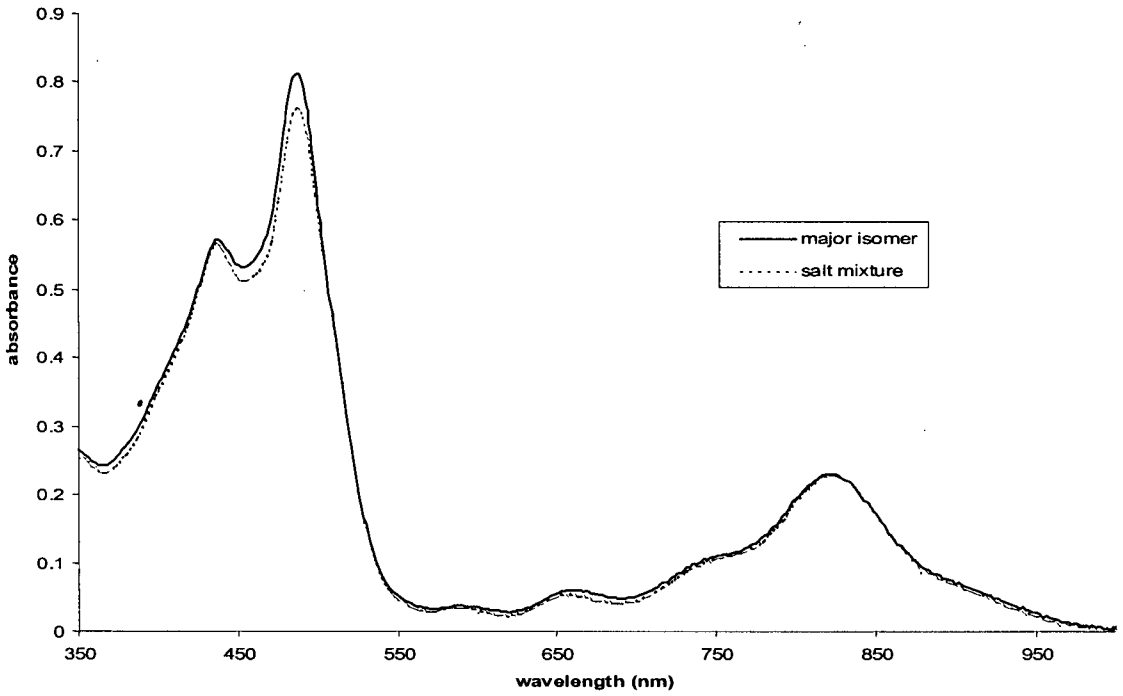

Figure 2.9 UV-vis spectra of **106** (salt mixture) and **106-III** (major isomer) in CH_2Cl_2.

2.2.2.4 Generation of Singlet Oxygen

DPBF (1,3-diphenylisobenzofuran) was used to determine the ability of these N,N'-dimethylated N-confused porphyrin salts to generate singlet oxygen ($^1O_2$).[16] DPBF reacts quickly with singlet oxygen (Scheme 2.10) and its absorption decay around 418 nm can be readily monitored.[17] The reaction products of DPBF have no absorption in the visible region and do not quench singlet oxygen. A solution containing DPBF (~17 μM) and N,N'-dimethylated N-confused porphyrin salts (e.g. **104**, ~13 μM) was irradiated with a halogen lamp using a filter (~700 nm) and monitored by UV-vis spectroscopy at 418 nm. Substantial decay of the UV-vis signal at 418 nm was observed confirming that N,N'-dimethylated N-confused porphyrin salts generate singlet oxygen (Figure 2.10). No change in UV-vis spectra was observed after a sample containing DPBF and an N,N'-dimethylated N-confused porphyrin salts was left in the dark for

10 min, and there is also no change in the UV-vis spectra after irradiating a solution containing only either DPBF or an N,N'-dimethylated N-confused porphyrin salts for 1 min.

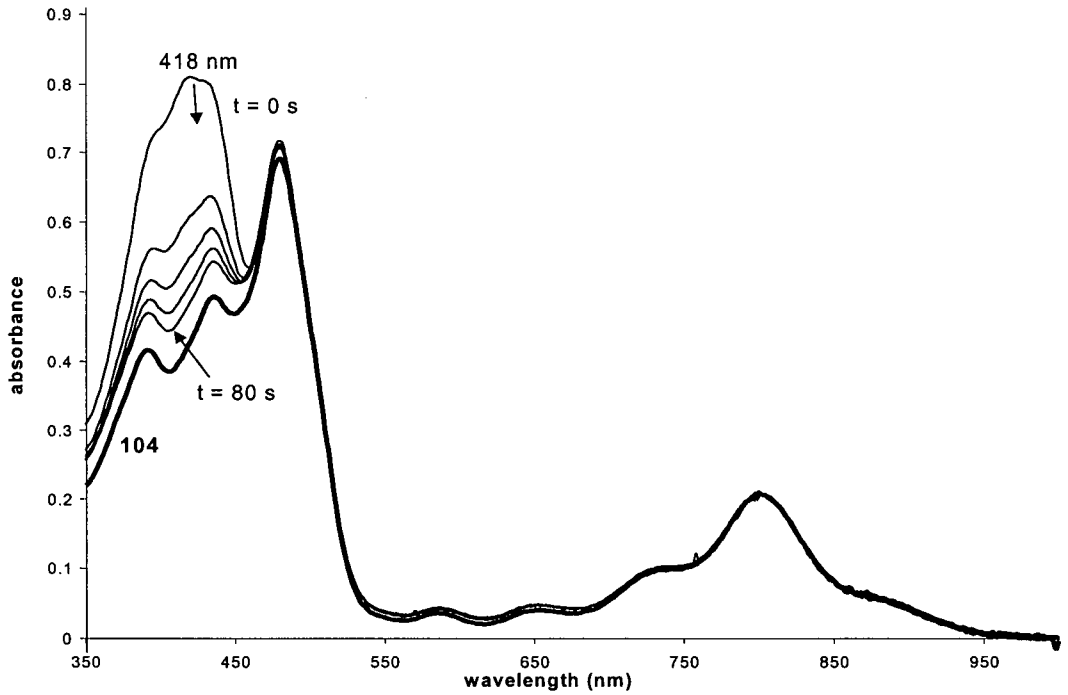

Figure 2.10 UV-vis spectra of a solution of DPBF and compound **104** before and after irradiation (irradiation intervals at 20 s). The UV-vis spectrum of compound **104** is shown in the thicker line.

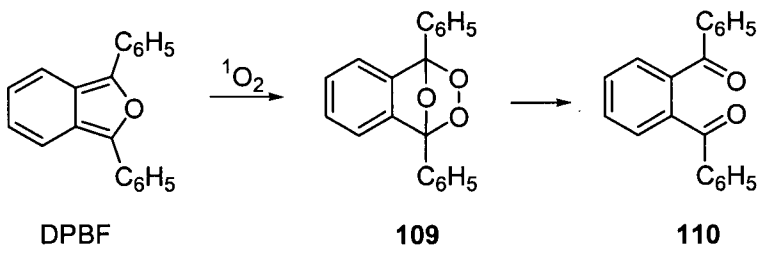

Scheme 2.10 Reactions of DPBF with $^1O_2$.

2.2.3 C,N-Strapped N-Confused Porphyrins

Attempts to directly synthesize C,N-strapped N-confused porphyrin, using Ni(II) N-confused porphyrin and diiodooctane with $AgBF_4$, were not successful (Scheme 2.11). A mixture of products with molecular ion peaks at 1485 and 1498 *m/e* (LSIMS) was obtained.

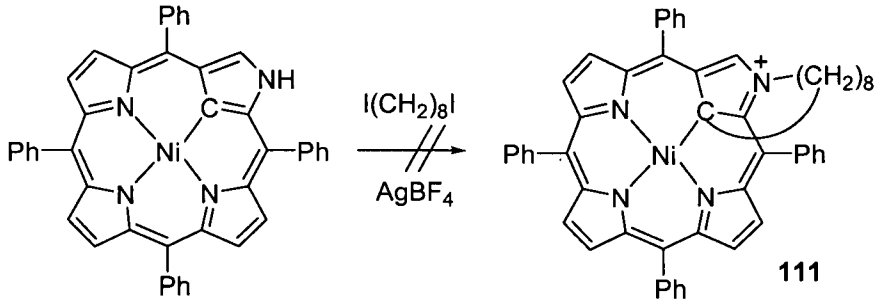

Scheme 2.11 Direct synthesis of C,N-strapped N-confused porphyrin.

As outer N(2) of N-confused porphyrin can be selectively alkylated in the absence of a base[7] and inner C(21) can be alkylated after metalation,[8] a stepwise synthesis of the C,N-strapped Ni(II) N-confused porphyrins was designed (Scheme 2.12).

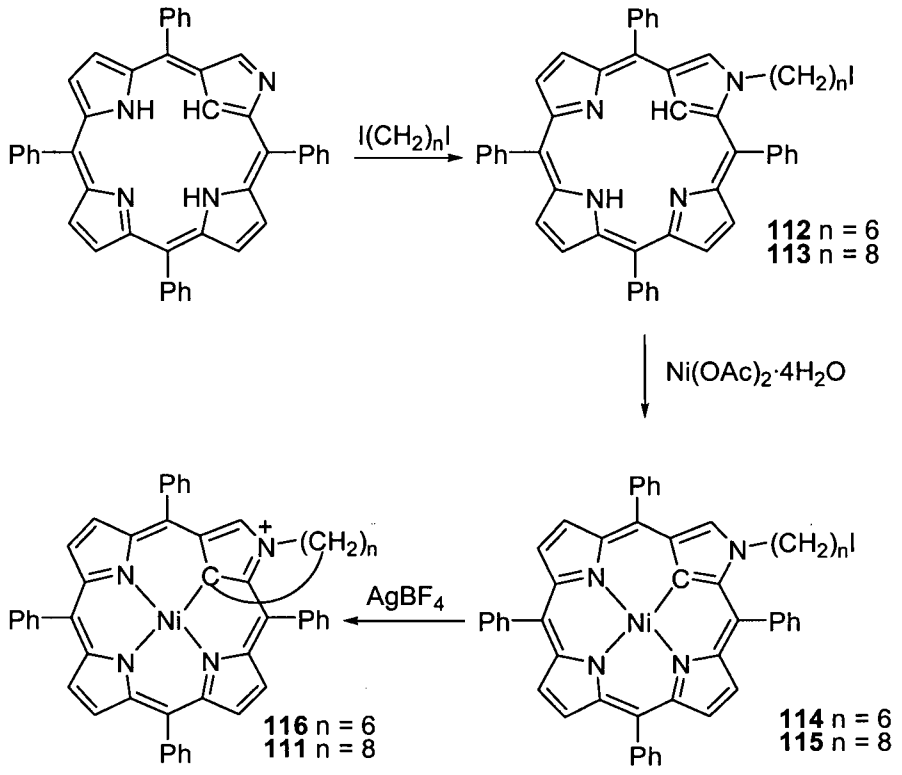

Scheme 2.12 Proposed synthesis of C,N-strapped N-confused porphyrins **116** and **111**.

NCTPP was reacted with a large excess of alkyl diiode (1:20 molar ratio) to avoid dimerization of N-confused porphyrin with an alkyl linkage. Iodoalkylated N-confused porphyrin **112** and **113** were obtained in the yields of 69 % and 65 %, respectively. Dimerization was not observed in these reactions.

Metalation of compounds **112** and **113** with $Ni(OAc)_2 \cdot 4H_2O$ readily proceeded at room temperature to give corresponding Ni(II) complexes **114** and **115** with yields of 92 % and 95 %, respectively.

When compound **115** was refluxed with $AgBF_4$ in freshly distilled CH_3CN/CH_2Cl_2 (1:1), a compound was obtained in 52 % yield. An observed molecular ion peak of 781 *m/e* (LSIMS)

suggests that this paramagnetic compound is the C,N-strapped N-confused porphyrin **111**. A similar result was obtained for compound **114**.

The coordination environments of Ni(II) in complexes **111** and **116** are similar to that of paramagnetic dimethylated Ni(II) NCP **27** (section 1.4.4.1), thus it is expected that complex **111** and **116** are paramagnetic as well. Broad peaks were observed in the ^{1}H NMR spectra of complexes **111** and **116**, and their structures were not determined by NMR spectroscopy. Efforts to determine the structures of **111** and **116** by X-ray crystallography have yet to be successful.

2.2.3.1 Structural Determination of Ni(II) Iodooctylated N-Confused Porphyrin

Crystals of Ni(II) iodooctylated N-confused tetraphenylporphyrin **115** were obtained by solvent diffusion of hexanes into a CH_2Cl_2 solution of the complex, and the structure of **115** was determined by X-ray crystallography (Figure 2.11). The iodine atom was found to be disordered over two sites, with relative populations of 0.9 and 0.1 for the major and minor fragments, respectively. Only the major form is shown in Figure 2.11. Unlike planar (NCTPP)Ni^{II}, the porphyrin skeleton of complex **115** is slightly distorted from planarity (Figure 2.12).

The Ni-N(C) bond distances (Å) of complex **115** are: C(21) 1.904(3), N(22) 1.951(3), N(23) 1.975(2), and N(24) 1.934(3), close to that of (NCTPP)Ni^{II} (1.955 or 1.963 Å). The bond angles of C(1)-N(2)-C(3), C(1)-N(2)-C(25) and C(3)-N(2)-C(25), are 107.7(3), 130.8(3), and 121.4(3)°, respectively. The large bond angles of C(1)-N(2)-C(25) and C(3)-N(2)-C(25) indicates that N(2) atom is sp^2 hybridized.

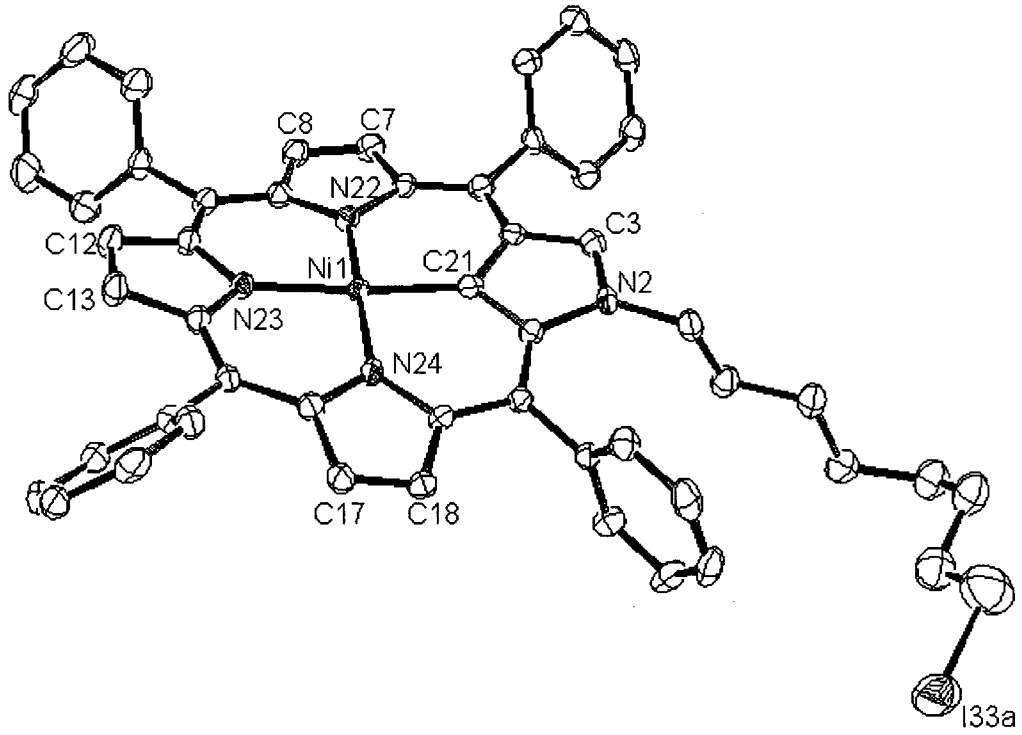

Figure 2.11 An ORTEP drawing of **115** showing atomic labeling and thermal ellipsoids at the 50 % probability level (top view). H atoms have been removed for clarity.

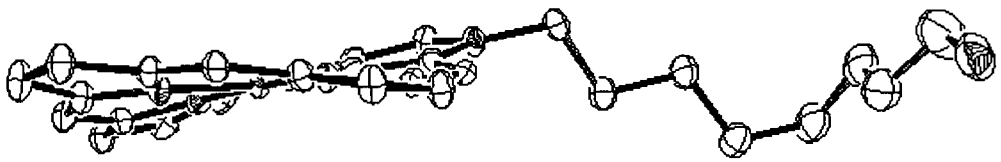

Figure 2.12 An ORTEP drawing of **115** showing thermal ellipsoids at the 50 % probability level (side view). Phenyl groups and H atoms have been removed for clarity.

The bond length of N(2)-C(3) in **115** is 1.311(4) Å, shorter than that of NCTPP (1.336 Å), in which the N(2)-C(3) is a partially isolated double bond.[15] It is also shorter than those of the C_β - C_β bonds in **115** (1.345(5), 1.346(5), and 1.345(5) Å, respectively for C(7)-C(8), C(12)-C(13), and C(17)-C(18)). This can be explained by the resonance structures of the complex **115** (Scheme 2.13). Structure **115a**, in which the N(2)-C(3) bond contains more of a single bond character, has no charge separation, however, the conjugation is not continued at the inverted pyrrole subunit. Structure **115b** has a 18 π-electron pathway and should be reasonably stable. The N(2)-C(3) bond exhibit a double bond nature in structure **115b** and the short bond length of N(2)-C(3) can be the result of structure **115b** being a significant contributor to the resonance hybrid.

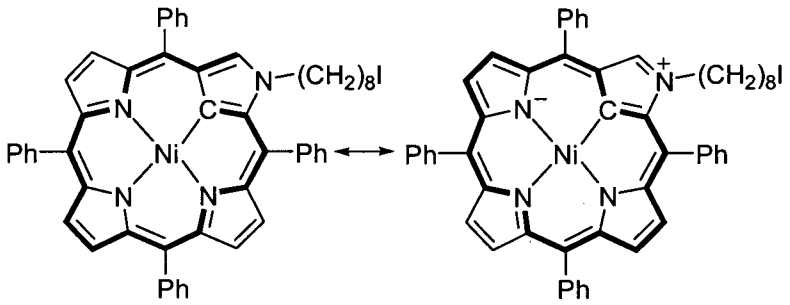

Scheme 2.13 Resonance structures of the compound **115**.

2.3 Conclusions

N-confused tetraarylporphyrins react with CH_3I in the presence of Na_2CO_3 to yield N,N'-dimethylated N-confused porphyrin salts, which are mixtures of structural isomers. The structures of the major isomers are determined by X-ray diffraction and/or NMR spectroscopic analyses. These N,N'-dimethylated N-confused tetraarylporphyrin salts can generate singlet oxygen when irradiated and are potential photosensitizers for PDT.

Ni(II) iodoalkylated N-confused porphyrins were prepared as the intermediate to synthesize C,N-strapped N-confused porphyrins. Ni(II) iodooctylated N-confused tetraphenylporphyrin was structurally characterized.

References

1. Lavallee, D. K. *The Chemistry and Biochemistry of N-Substituted Porphyrins*; VCH Publishers, INC: New York, 1987.
2. McEwen, W. K. *J. Am. Chem. Soc.* **1936,** *58*, 1124.
3. McEwen, W. K. *J. Am. Chem. Soc.* **1946,** *68*, 711.
4. Al-Hazimi, H. M. G., Jackson, A. H., Johnson, A. W. and Winter, M. *J. Chem. Soc., Perkin Trans. 1* **1977**, 98.
5. Aida, T., Kawaguchi, K. and Inoue, S. *Macromolecules* **1990**, *23*, 3887.
6. Lavallee, D. K. and Anderson, O. P. *J. Am. Chem. Soc.* **1982,** *104*, 4707.
7. Chmielewski, P. J. and Latos-Grażyński, L. *J. Chem. Soc., Perkin Trans. 2* **1995**, 503.
8. Chmielewski, P. J., Latos-Grażyński, L. and Glowiak, T. *J. Am. Chem. Soc.* **1996,** *118*, 5690.
9. Ishimaru, Y., Sumida, S. and Iida, T. *Chem. Commun.* **1997**, 2187.
10. Geier, G. R., Haynes, D. M. and Lindsey, J. S. *Org. Lett.* **1999,** *1*, 1455.
11. Weast, R. C. Handbook of Chemistry and Physics; CRC Press: Cleveland, Ohio, 1986.
12. Lavallee, D. K. and Gebala, A. E. *Inorg. Chem.* **1974,** *19*, 2004.
13. Shah, B., Shears, B. and Hambright, P. *Inorg. Chem.* **1971,** *10*, 1828.
14. Chmielewski, P. J., Latos-Grażyński, L., Rachlewicz, K. and Glowiak, T. *Angew. Chem., Int. Ed. Engl.* **1994,** *33*, 779.
15. Furuta, H., Asano, T. and Ogawa, T. *J. Am. Chem. Soc.* **1994,** *116*, 767.
16. Spiller, W., Kliesch, H., Wohrle, D., Hackbarth, S., Roder, B. and Schnurpfeil, G. *J. Porphyr. Phthalocya.* **1998,** *2*, 145.

17. Young, R. H. and Brewer, D. R. The Mechanism of Quenching of Singlet Oxygen. In *Singlet Oxygen Reactions with Organic Compounds and Polymers*.Ranby, B.; Rabek, J. F. Eds.; Wiley: London, 1978; pp. 36.

Chapter 3

Cycloaddition Reactions of N-Confused Porphyrins

3.1 Cycloaddition Reactions

Cycloaddition reactions involve the reaction of two molecules resulting in the formation of a new ring.[1] Many cycloaddition reactions are concerted: there is a single transition state, and therefore, no intermediate lies on the reaction path between reactants and the adduct.[1] Two examples of cycloaddition reactions involving a concerted mechanism are the Diels-Alder reactions and the 1,3-dipolar cycloaddition reactions.

The Diels-Alder reaction is the addition of a diene to a dienophile, e.g. an alkene, to form a cyclohexene (Scheme 3.1).[1] This is called a [4 + 2] cycloaddition reaction as four π electrons from the diene and two π electrons from the dienophile are directly involved in the bonding change.

Scheme 3.1 Diels-Alder reaction.

A 1,3-dipolar cycloaddition reaction is an addition reaction of a 1,3-dipole with a dipolarophile (Scheme 3.2).[1] 1,3-Dipoles are isoelectronic with the allyl anion and have four π electrons. Each such dipole (Scheme 3.3) has at least one charge-separated resonance structure with opposite charges in a 1,3-relationship. The 1,3-dipolar cycloaddition reaction is analogous to the Diels-Alder reaction, as both are [4 + 2] cycloaddition reactions.

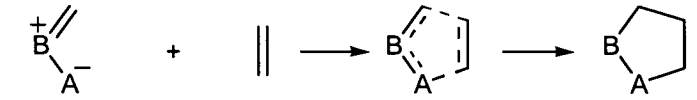

Scheme 3.2 1,3-Dipolar cycloaddition reaction.

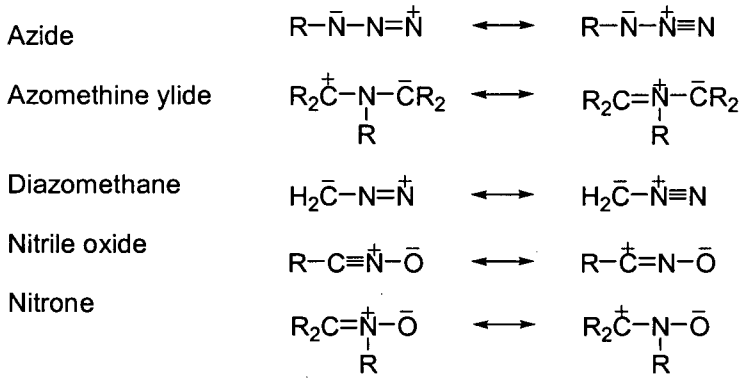

Scheme 3.3 Some examples of 1,3-dipoles.

While dienophiles and dipolarophiles are typically alkenes or alkynes, all that is essential is a π bond. For example, different types of imines can act as dienophiles.[2] Bohlmann *et al.* found that the simple imine **118** reacted thermally with butadiene carboxylate **119** to afford a Diels-Alder type adduct **121** (Scheme 3.4).[3] Only the conjugated ester **121**, presumably formed by isomerization of the initial adduct **120**, was isolated. In general, electron-deficient imines are the most reactive imine type dienophiles, particularly those of the N-sulfonyl, N-acyl, and iminium salt types.[2]

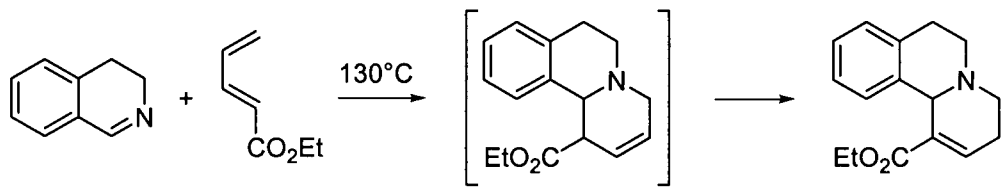

118 119 120 121

Scheme 3.4 Diels-Alder reaction of imine **118** with diene **119**.

3.1.1 Cycloaddition Reactions of Porphyrins

Cycloaddition reactions of porphyrins have been extensively studied and porphyrins have been used as dienes, 1,3-dipoles, dipolarophiles and dienophiles.[4-10]

Porphyrin **122**, which has a β–fused 3-sulfolene on one of the pyrrole rings, acts as a porphodimethylidene precursor and can be used for a variety of Diels-Alder reactions. For example, it reacts with DMAD to yield the cycloaddition adduct **123** (Scheme 3.5).[4]

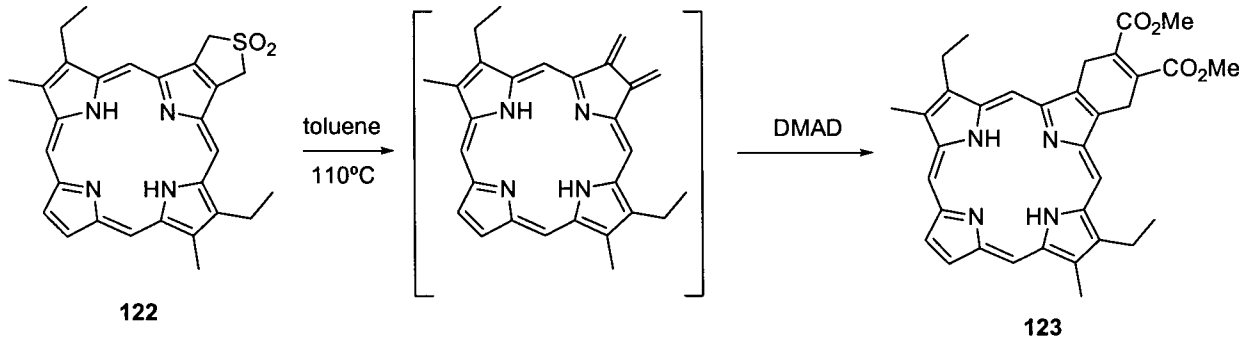

122 123

Scheme 3.5 Diels-Alder reaction of porphyrin **122** with DMAD.

Porphyrinic azomethine ylide **125** can be generated from the reaction of β-formyl porphyrin **124** with N-methylglycine and this ylide reacts with a range of dipolarophiles (Scheme 3.6).[5,6] For example, reaction of porphyrin **125** with N-phenylmaleimide yields the

cycloaddition adduct **126** (61 %) and **127** (35 %).[6] In the absence of a dipolarophile, intramolecular cycloaddition of **125** occurs to give porphyrin **128**.[5]

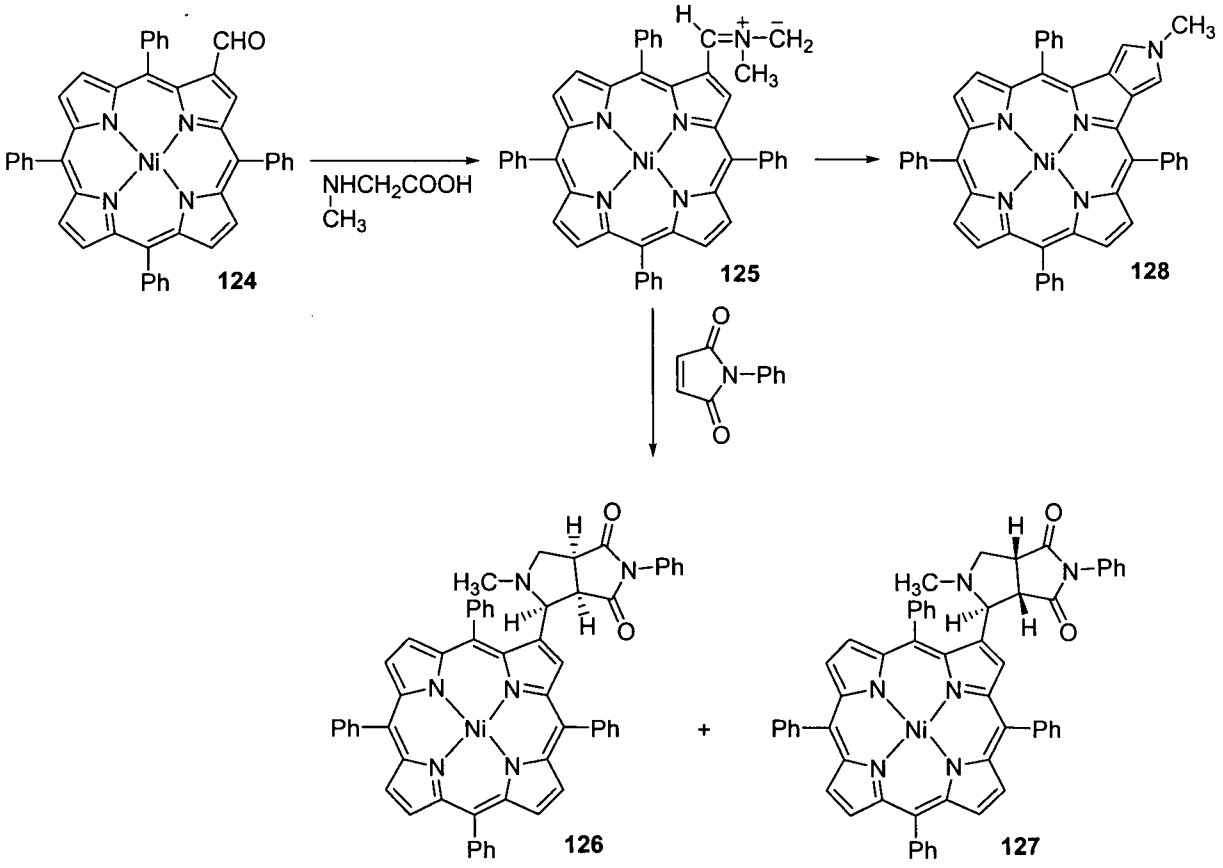

Scheme 3.6 Synthesis and reactions of porphyrin **125**.

Diels-Alder reactions of porphyrins with β-vinyl groups as dienes, Diels-Alder reactions of porphyrins as dienophiles, and 1,3-dipolar cycloaddition reactions of porphyrins as dipolarophiles have been discussed in sections 1.3.1 and 1.3.3.

Similar to those of porphyrins, the peripheral C-C or C-N bonds of N-confused porphyrins are cross-conjugated and thus might react as alkenes or imines. Cycloaddition reactions of N-confused porphyrins as dienophiles or dipolarophiles were studied in this thesis

work. This work demonstrates the reactivity of the cross-conjugated peripheral bonds of N-confused porphyrins and offers a simple method to modify N-confused porphyrins. Furthermore, the cycloaddition adducts are of interest as potential photosensitizers for PDT.

3.2 Results and Discussion

3.2.1 Ni(II) N-Confused Porphyrins

N-confused porphyrins were synthesized according to Lindsey's procedure[11] *via* condensation of pyrrole and aryl aldehydes under catalysis of MSA (section 1.4.3). The condensation product mixture was passed through a silica gel column under vacuum to remove the less polar side product tetraarylporphyrin and some baseline impurities. The crude N-confused porphyrin product was used without further purification and reacted with $Ni(OAc)_2 \cdot 4H_2O$ to provide Ni(II) N-confused porphyrins **129** (**a-e**) with overall yield ranging from 6.4 % to 16 % (Scheme 3.7).[12]

Metalation of N-confused porphyrins gave products that are much less polar than their free base counterparts. This decrease in polarity allowed for a cleaner gradient elution during column chromatographic purifications (silica gel, 230 - 400 mesh). The desired products came off the column with CH_2Cl_2 (0.4 % CH_3OH in CH_2Cl_2 was used for **129d** and **129e**), and the impurities normally co-eluted with the free base NCP as the polarity was increased to 1.2 % CH_3OH in CH_2Cl_2. The additional metalation step was more than offset by the resultant facile purification of the desired products.

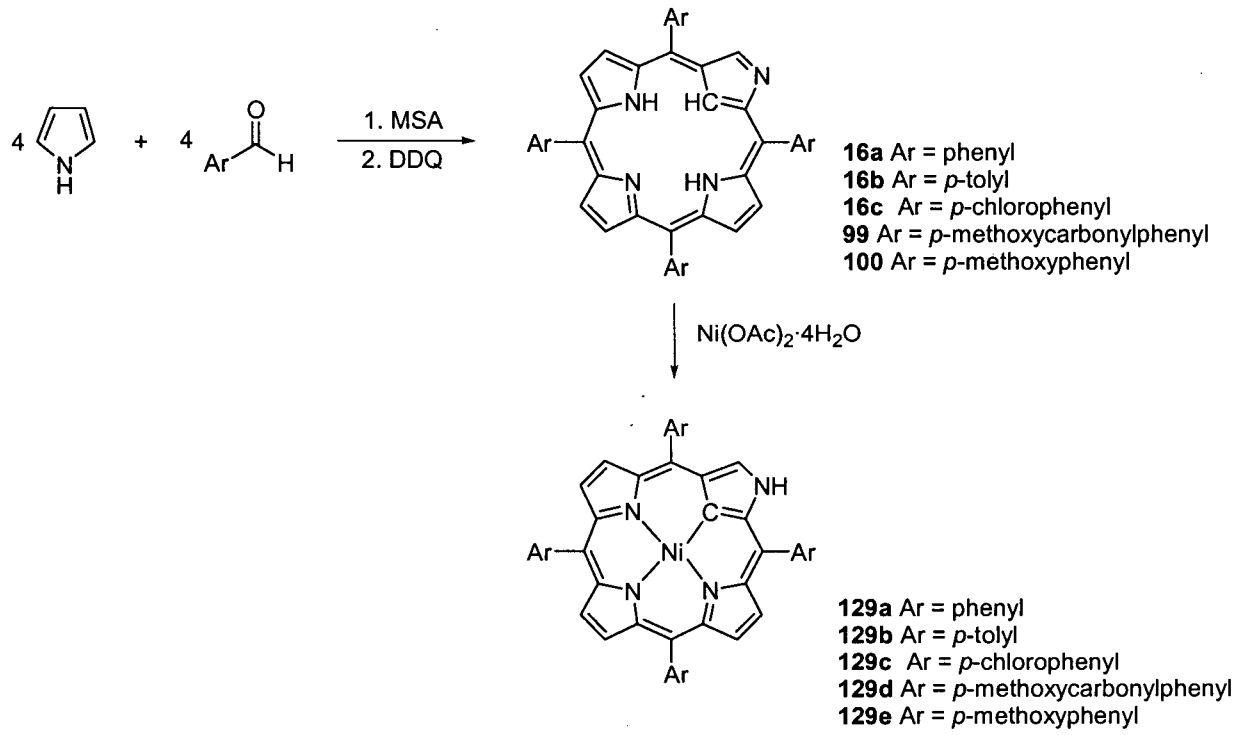

Scheme 3.7 Synthesis of Ni(II) N-confused tetraarylporphyrins.

3.2.2 Diels-Alder Reactions of Ni(II) N-confused Porphyrins

o-Benzoquinodimethane, **8**, was selected as the diene in the Diels-Alder reactions. Compound **8** is exceedingly reactive as a diene because cycloaddition re-establishes a benzenoid ring resulting in aromatic stabilization (Scheme 3.8).

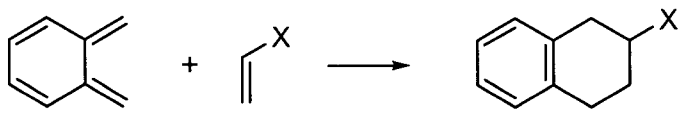

8

Scheme 3.8 Diels-Alder reaction of *o*-benzoquinodimethane **8**.

o-Benzoquinodimethane can be generated from sultine **130**, which was synthesized from the reaction of sodium hydroxymethanesulfinate (rongalite) and α,α'-dibromo-*o*-xylene, **131**, with a catalytic amount of tetrabutylammonium bromide (TBAB) (Scheme 3.9).[13] Sultine **130** is an ideal precursor of *o*-benzoquinodimethane because it decomposes smoothly around 80 °C and does not produce organic or inorganic byproducts except for gaseous sulfur dioxide.

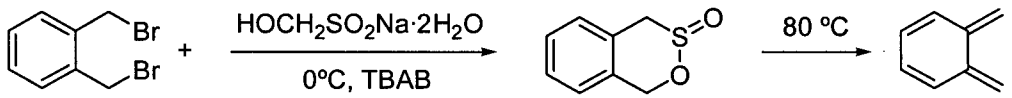

131 **130** **8**

Scheme 3.9 Synthesis and reactions of sultine **130**.

No reaction was observed when NCTPP was refluxed with sultine **130** in benzene for two days (Scheme 3.10). However, when (NCTPP)Ni^{II} was used instead of NCTPP, Diels-Alder adducts were obtained (Scheme 3.11). The major product, which has a higher R_f value on silica gel than that of (NCTPP)Ni^{II}, was obtained in 23 % yield and identified as the N-confused isoquinoporphyrin **133a** based on its mass and NMR spectra (^1H, ^{13}C, selective NOE, COSY and $^1H/^{15}N$ HSQC) data (Figure 3.1, 3.2 and 3.3). Compound **133a** was presumably formed by oxidation of the chlorin **132a**. There is also a product with a higher R_f value than that of compound **133a** with a parent ion observed at 879 *m/e* (LSIMS), presumably from the addition of two equivalents of *o*-benzoquinodimethane to (NCTPP)Ni^{II}. However, the yield of this second compound was too low to allow characterization by NMR spectroscopy.

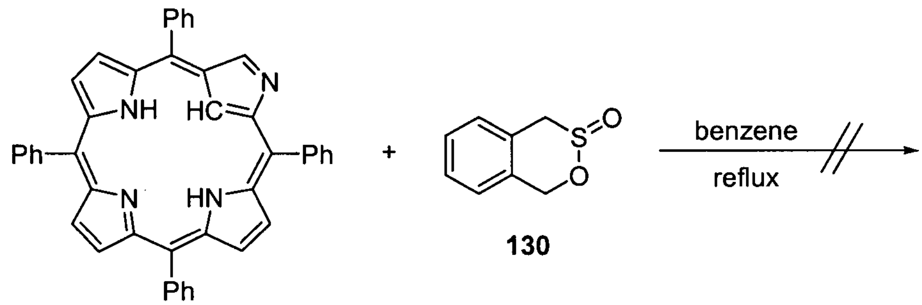

Scheme 3.10 Diels-Alder reaction of NCTPP with sultine **130**.

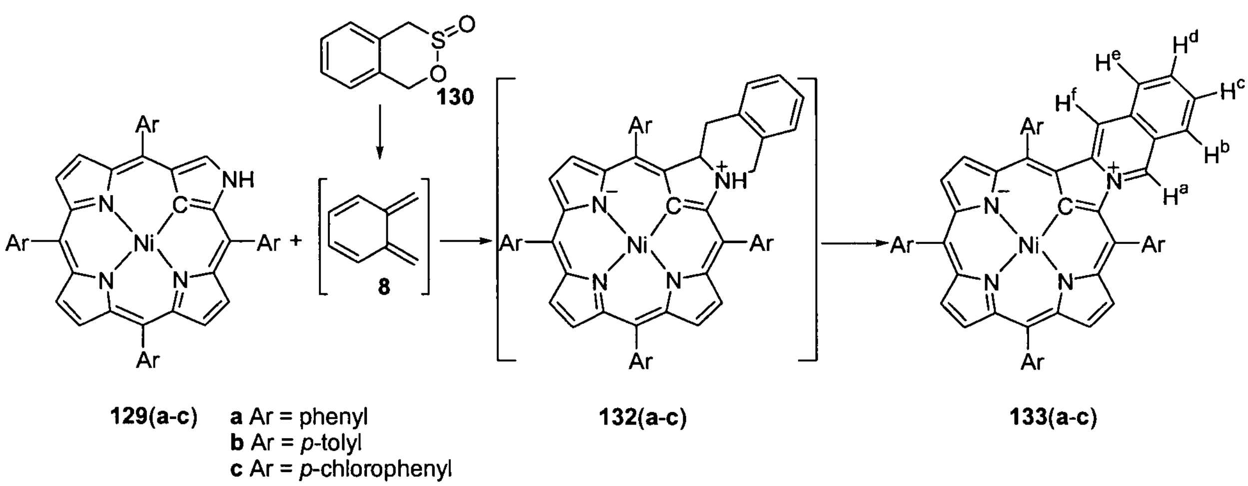

Scheme 3.11 Diels-Alder reactions of Ni(II) N-confused porphyrins with sultine **130**.

The parent ion of compound **133a** is observed at 770 *m/e* (LSIMS), suggesting the addition of one *o*-benzoquinodimethane and the loss of four hydrogen atoms. This is corroborated by the formula search result of $C_{52}H_{32}N_4Ni$ (*m/e* Calcd 770.19799,) from the HRLSIMS result (770.19797 *m/e*). These results suggest that a four-electron oxidation occurred and **133a** is either a Ni(II) N-confused naphthoporphyrin (Diels-Alder addition on a peripheral carbon-carbon bond) or a Ni(II) N-confused isoquinoporphyrin (addition on the peripheral carbon-nitrogen bond).

Attempts to synthesize Diels-Alder adducts of **129d** and **129e** with sultine **130** were not successful, probably because of the poor solubilities in either benzene or toluene.

3.2.2.1 Structural Determination by NMR Spectroscopy

Based on correlations shown in a COSY experiment (Figure 3.2), signals for the H^a/H^f protons of complex **133a** appear as singlets at 6.91 and 8.57 ppm (see Scheme 3.11 for proton assignments) and signals for the H^b - H^e protons appear at 7.11, 7.27 (2H) and 7.46 ppm. The large difference in chemical shift between H^a and H^f protons in complex **133a** suggests that the addition is on the peripheral carbon-nitrogen bond rather than on a peripheral carbon-carbon bond, as a nominal difference of chemical shift between H^a and H^f protons would be observed in the peripheral carbon-carbon bond addition product. A large chemical shift difference between H^a and H^f protons has also been observed in isoquinolinium salt **134** (Figure 3.4).[14] Cycloaddition on the peripheral carbon-nitrogen bond is confirmed by the cross peak of ^1H 6.91 ppm with ^{15}N 17 ppm in a $^1H/^{15}N$ HSQC experiment of **133a** (Figure 3.3), which indicates that H^a is either two or three bonds away from a nitrogen atom. Similar results were obtained for complex **133b** and **133c**. Thus, the combined solution NMR results suggest cycloaddition of *o*-benzoquinodimethane to Ni(II) N-confused porphyrins on the peripheral carbon-nitrogen bond giving N-confused isoquinoporphyrins.

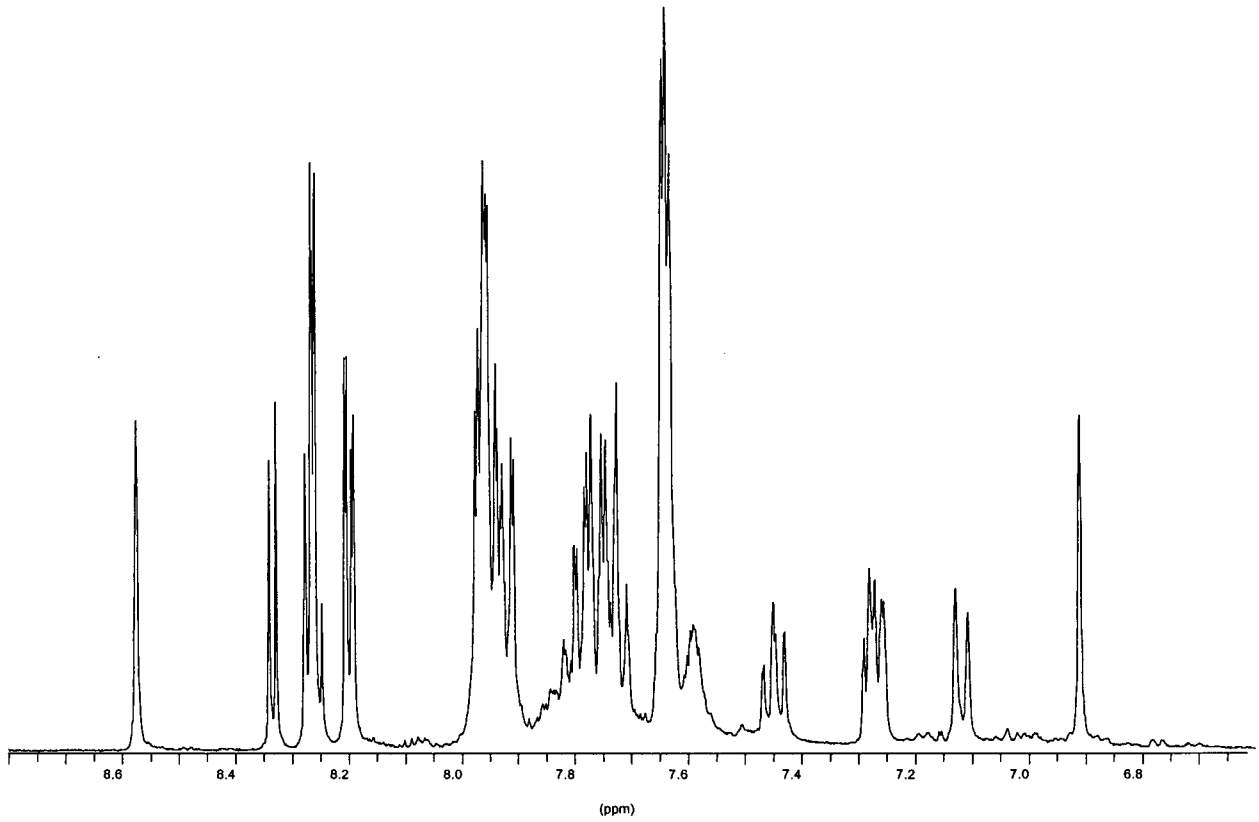

Figure 3.1 ^{1}H NMR spectrum of **133a** in CD_2Cl_2 (400 MHz).

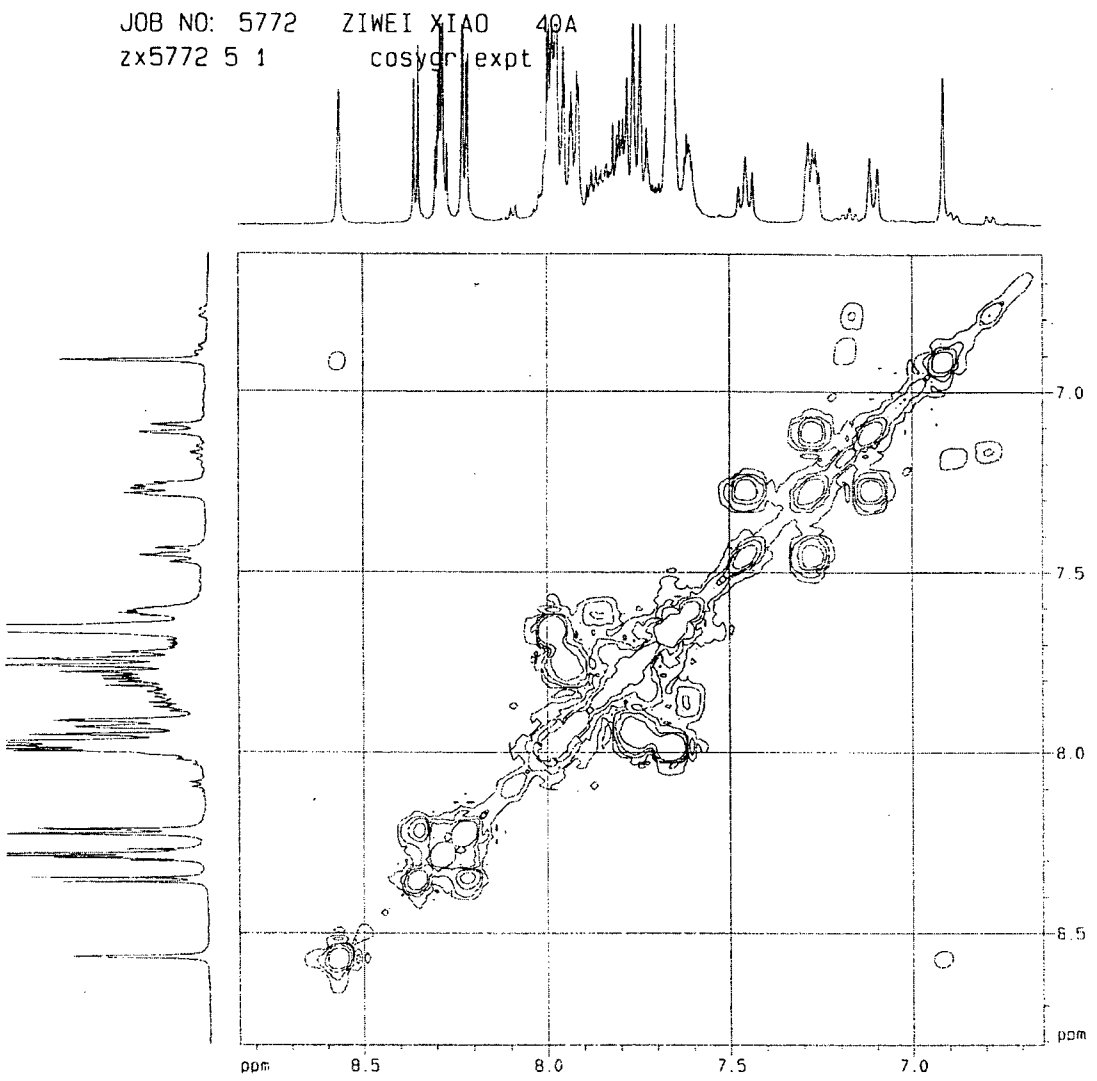

Figure 3.2 COSY spectrum of **133a** in CD_2Cl_2 (400 MHz).

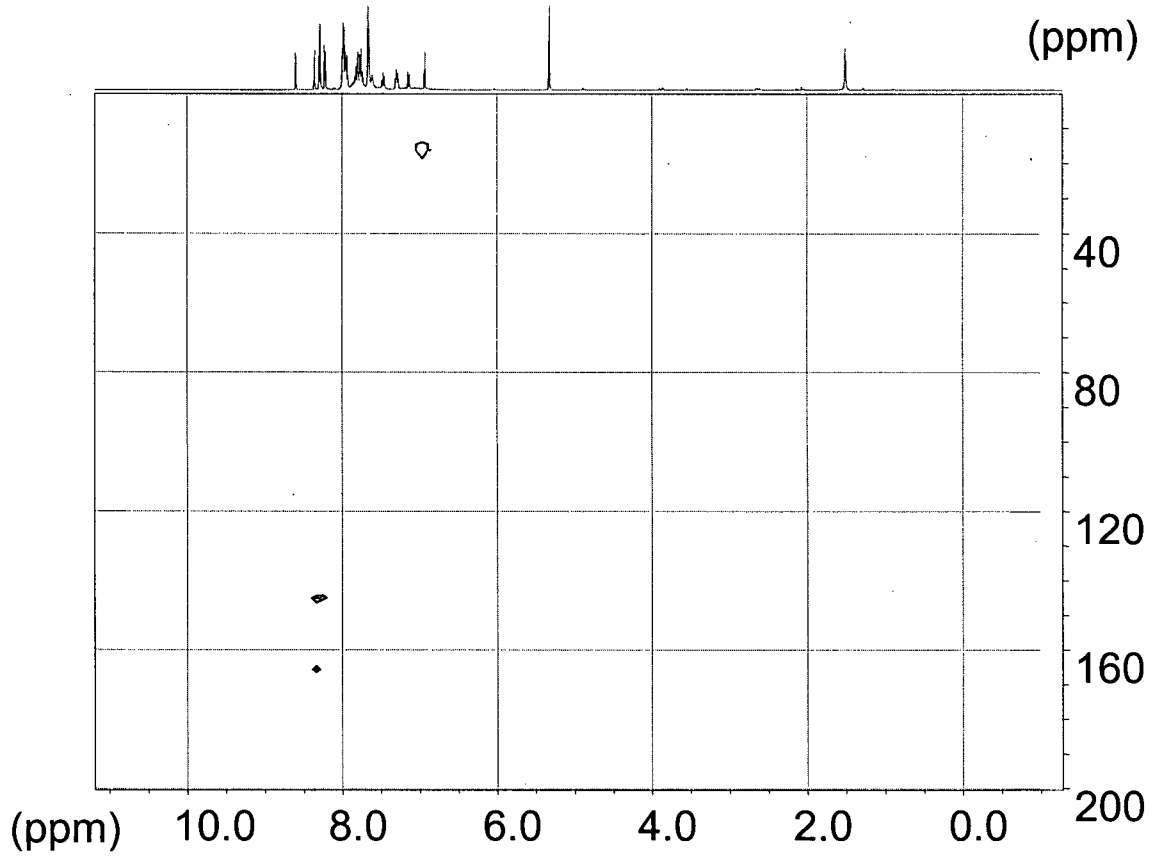

Figure 3.3 $^{1}H/^{15}N$ HSQC spectrum of **133a** (400 MHz, CD_2Cl_2).

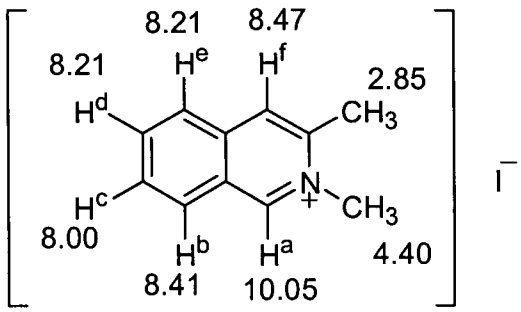

134

Figure 3.4 ^{1}H chemical shift (ppm) assignments of isoquinolinium iodide salt **134** in d_6-DMSO (300 MHz).

3.2.2.2 Structural Determination of Ni(II) N-Confused Tetraphenylisoquinoporphyrin by X-ray Diffraction Analysis

Crystals of compound **133a** were obtained by solvent diffusion of hexanes into a CH_2Cl_2 solution of **133a** and the structure of Ni(II) N-confused tetraphenylisoquinoporphyrin was determined by X-ray crystallography (Figure 3.5). However, the N(2) and C(3) atoms are disordered and not distinguishable in the X-ray crystal structure.

The X-ray crystal structure shows that the isoquino group is in the same plane with the linked pyrrole subunit. Deviation from planarity for the isoquinopyrrole unit is 0.066 Å. Unlike planar (NCTTP)Ni^{II},[12] the porphyrin skeleton of compound **133a** is ruffled (Figure 3.6). The dihedral angles between the pyrrole planes of **133a** and the plane defined by N(22)N(23)N(24) are as follows: C(21) 19.88°, N(22) 16.85°, N(23) -15.98°, N(24) -13.87°. The Ni-N(C) bond distances (Å) of **133a** are: C(21) 1.904(2), N(22) 1.9239(18), N(23) 1.949(2), and N(24) 1.9276(18), which are shorter than that of (NCTTP)Ni^{II} (1.955 or 1.963 Å),[12] and the shortened bond lengths are typical of the difference between planar Ni(II) porphyrins and ruffled Ni(II) porphyrins.[15]

For complex **133a**, there are three resonance structures with charge separation (**133a-I**, **133-II** and **133a-III**) and one resonance structure with no charge separation (**133a-IV**) (Scheme 3.12). Resonance structures with bonding differences outside of the isoquinopyrrole unit are omitted in Scheme 3.12 as the focus is on the bonds involving N(2) and C(3). Table 3.1 shows the bond lengths of N(2)-C(1), N(2)-C(3), N(2)-C(25), C(3)-C(4), and C(3)-C(32), as well as their bond orders in the charge separated resonance structures (**133a-I**, **133-II** and **133a-III**) and in structure **133a-IV**. The charge separated resonance structures are the main contributors to the overall resonance hybrid of **133a**, as indicated by the good match between the bond lengths and the bond orders derived from charge separated resonance structures.

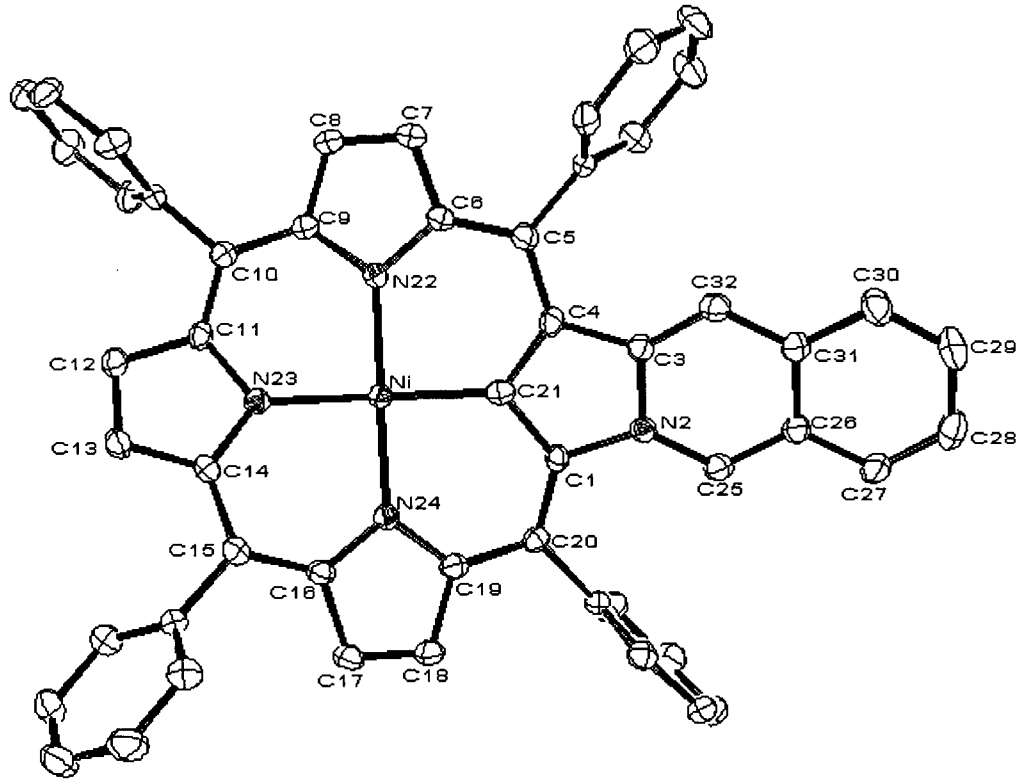

Figure 3.5 An ORTEP drawing of compound **133a** showing atomic labeling and thermal ellipsoids at the 50 % probability level. Only one of two possible forms is shown.

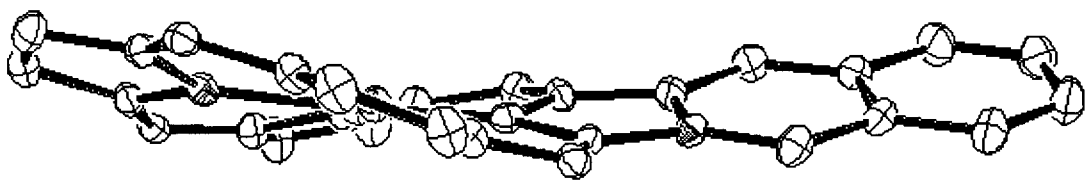

Figure 3.6 An ORTEP drawing of **133a** showing thermal ellipsoids at the 50 % probability level (side view). Phenyl groups and H atoms have been removed for clarity.

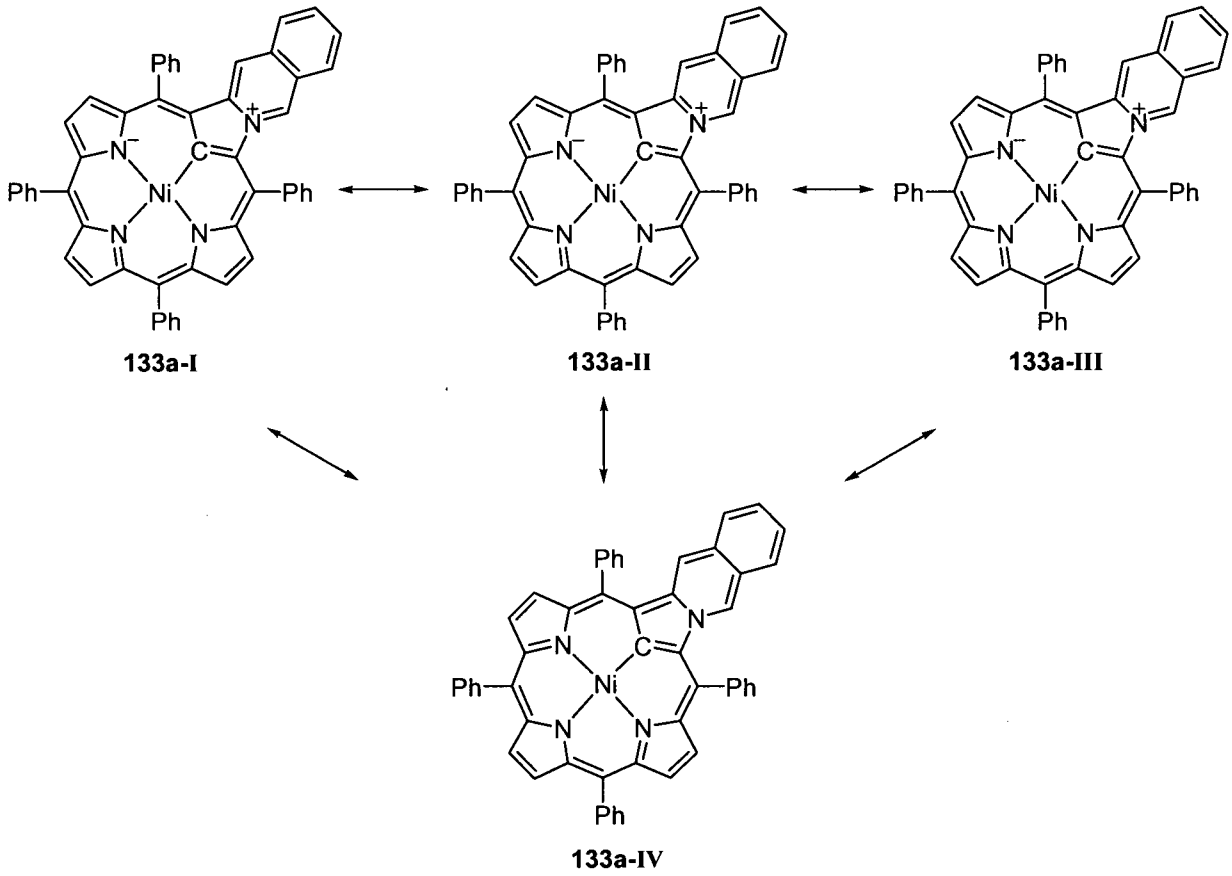

Scheme 3.12 Resonance structures for complex **133a**.

Table 3.1 Bond lengths (Å) and bond orders from selected resonance structures for selected bonds in complex **133a**.

Bond	Bond order in **133a-I**, **133-II** and **133a-III**	Bond order in **133a-IV**	Bond length (Å)
N(2)-C(1)	1	1	1.445(3)
N(2)-C(3)	4/3	1	1.389(3)
N(2)-C(25)	5/3	1	1.357(3)
C(3)-C(4)	1	2	1.452(3)
C(3)-C(32)	5/3	1	1.366(3)

3.2.2.3 Optical Absorption Spectra

Broad peaks at 438 and 628 nm, corresponding to the Soret and Q-bands of porphyrins respectively, were observed in the UV-vis spectrum for complex **133a** (Figure 3.7). The intensity of the 628 nm peak (42000 $M^{-1}cm^{-1}$) is about 5 times larger than that of the Q-bands of (NCTPP)Ni^{II}, **129a**. The difference between the absorption spectra of **133a** with (NCTPP)Ni^{II} reflects the changes in the conjugation pathway of **133a** due to the fused isoquino group.

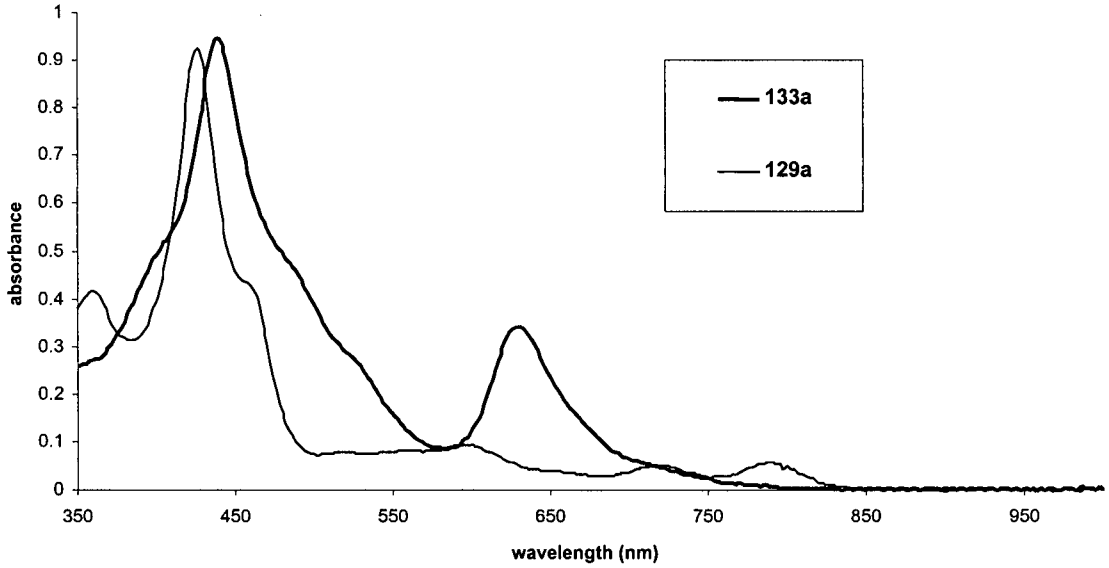

Figure 3.7 UV-vis spectra of **133a** and (NCTPP)Ni^{II}, **129a**.

3.2.2.4 Regioselectivity

The high selectivity of the peripheral carbon-nitrogen bond over the carbon-carbon bonds in the Diels-Alder reactions with *o*-benzoquinodimethane can be rationalized by the resonance contributions to the overall structure of Ni(II) N-confused porphyrins.[16] Scheme 3.13 shows two such resonance structures. In canonical form **II**, the C=N is both "cross conjugated" and in the

iminium form which is known to be electron-deficient and an active dienophile.[2] The reported X-ray structure of (NCTTP)Ni^{II} was disordered: the peripheral carbon-nitrogen bond could not be distinguished with the peripheral carbon-carbon bonds,[12] and thus this X-ray structure is not very helpful in determining the importance of each resonance structure (**I** and **II**) to the overall resonance hybrid. Ni(II) N(2)-iodooctyl N-confused tetraphenylporphyrin **115** is isoelectronic with (NCTTP)Ni^{II} and its bond lengths (Figure 3.8) clearly demonstrate the uniqueness of the $C=N^{+}R$ bond and confirm that it should be an effective dienophile (Section 2.2.3.1).

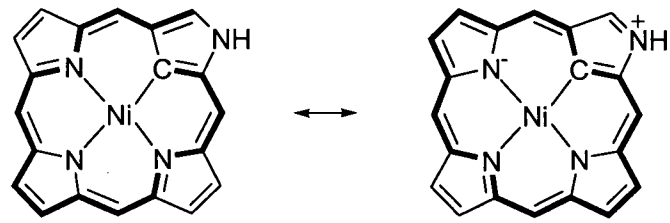

I **II**

Scheme 3.13 Two canonical forms for a Ni(II) N-confused porphyrin.

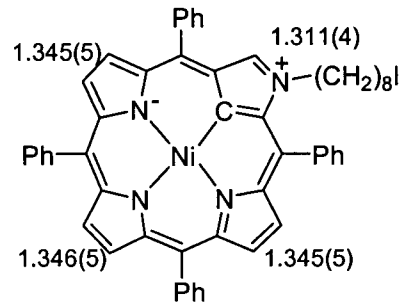

115

Figure 3.8 Peripheral bond lengths (Å) for compound **115**.

3.2.3 Demetalation of Ni(II) N-confused Isoquinoporphyrins

Demetalation of Ni(II) N-confused isoquinoporphyrin **133a** occurred with 10 % TFA in CH_2Cl_2 giving a 63 % yield (Scheme 3.14). The product was confirmed to be **135** on the basis of its mass and NMR (^1H, and COSY) spectra.

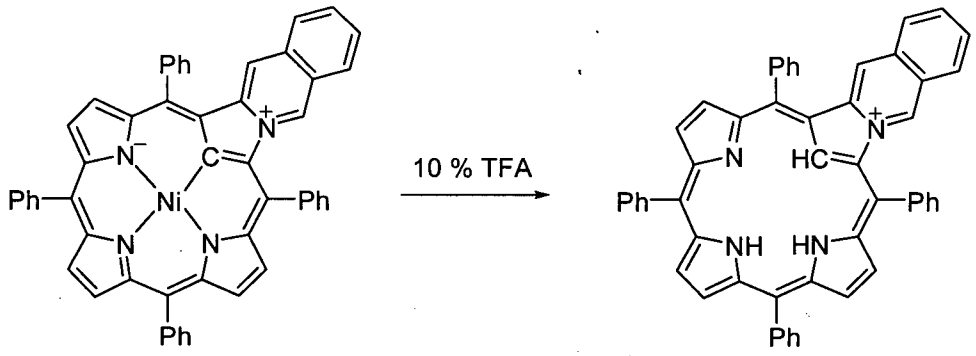

133a **135**

Scheme 3.14 Demetalation of Ni(II) N-confused isoquinoporphyrin **133a**.

3.2.3.1 Structural Determination of N-Confused Tetraphenylisoquinoporphyrin by X-ray Diffraction Analysis

Crystals of N-confused tetraphenylisoquinoporphyrin, **135**, were obtained by solvent diffusion of hexanes into a CH_2Cl_2 solution of **135** and the structure of **135** was determined by X-ray crystallography (Figure 3.9). X-ray diffraction analysis indicates electron density equivalent to about two electrons in the porphyrin core. This electron density presumably comes from a hydrogen atom of **135** and nickel in an impurity, precursor **133a**, present in about 3.8 % based on the electron density. This electron density is not shown in Figure 3.9 or 3.10. An X-ray structure report on **135** is not available because of the impurity.

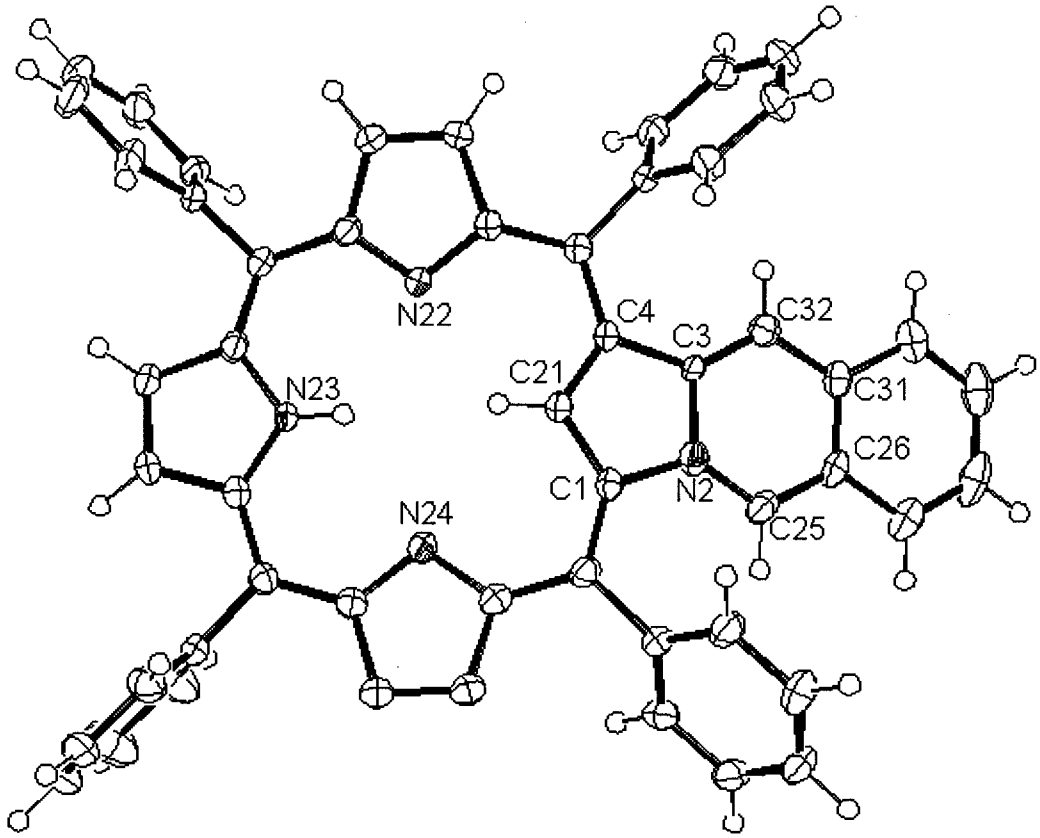

Figure 3.9 An ORTEP drawing of compound **135** showing atomic labeling and thermal ellipsoids at the 50 % probability level.

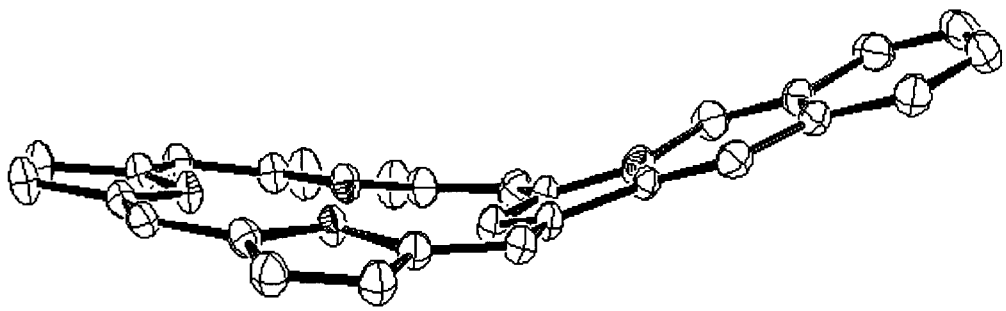

Figure 3.10 An ORTEP drawing of **135** showing thermal ellipsoids at the 50 % probability level (side view). Phenyl groups and H atoms have been removed for clarity.

As shown in Figure 3.10, the isoquinopyrrole unit is severely tilted from the porphyrin plane, presumably due to the steric repulsion between the isoquinopyrrole group and the neighboring phenyl group.

3.2.3.2 Optical Absorption Spectra of N-Confused Tetraphenylisoquinoporphyrin

Optical absorption spectra of **135** and **133a** are shown in Figure 3.11. Compared to that of **133a**, the Q-bands of **135** are red-shifted about 50 nm to 678 nm, implying potential use as a photosensitizer for PDT.

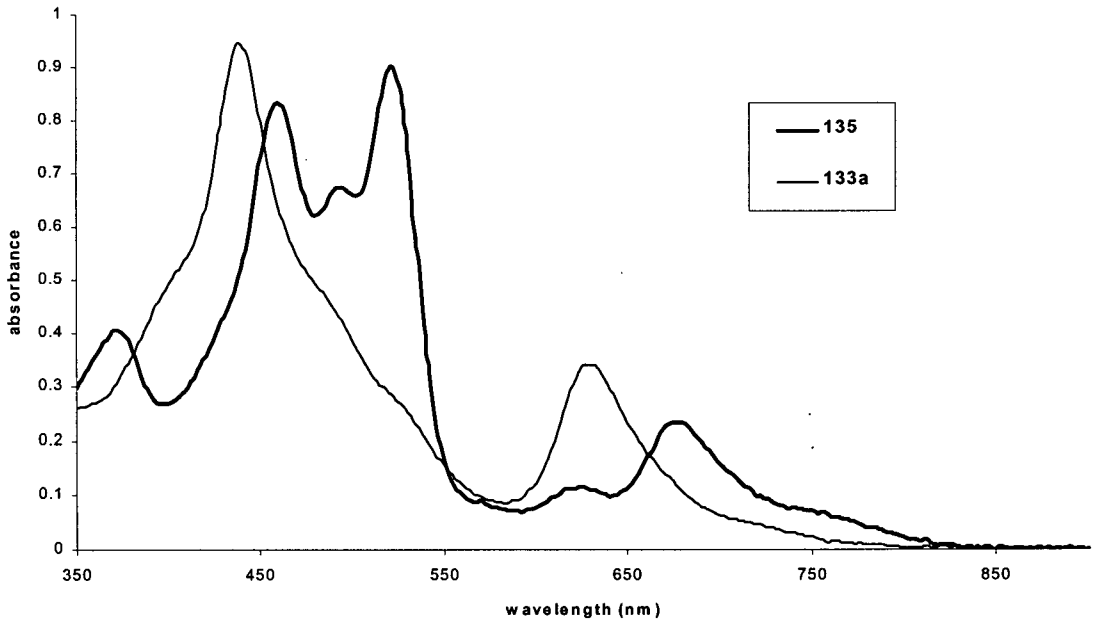

Figure 3.11 UV-vis spectra of **135** and Ni(II) complex **133a**.

3.2.4 Other Cycloaddition Reactions of N-confused Porphyrins

3.2.4.1 Diels-Alder Reactions of Non-Metalated N-Confused Porphyrins

A Diels-Alder reaction did not occur when NCTPP was refluxed with sultine **130** in benzene. However, similar to that of Ni(II) NCP, the peripheral carbon nitrogen bond of the protonated NCP is in iminium form (Figure 3.12) and thus protonated NCP may be expected to react faster than NCP in the Diels-Alder reaction with *o*-benzoquinodimethane.

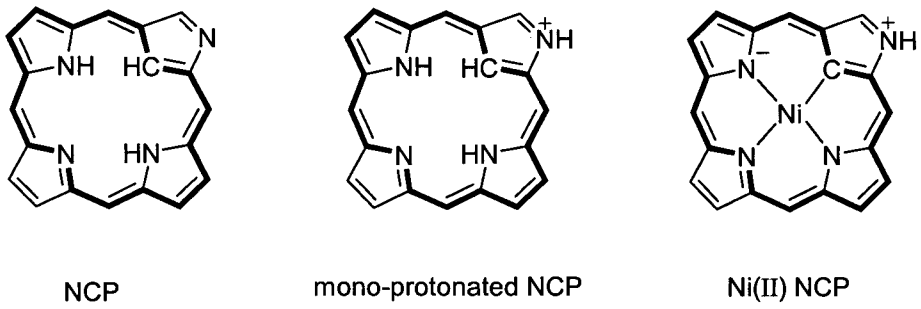

Figure 3.12 Structures of mono-protonated NCP and Ni(II) NCP.

NCTPP was refluxed with sultine **130** in benzene with 5 % acetic acid for 4 h. The major product and compound **135** are not distinguishable on TLC plates with various developing solvents. The parent ion peak of this product is observed at 715 *m/e*, the same as observed for compound **135**. However, purification of this compound was not successful.

3.2.4.2 Diels-Alder Reactions of Ni(II) N-Methylated N-confused Porphyrins

In an attempt to isolate the Diels-Alder adduct as a chlorin, Ni(II) N(2)-methylated N-confused tetra(*p*-tolyl)porphyrin[17] was used as a dienophile. Formula search results of the major

product, **137** ($C_{57}H_{46}N_4NiO$), based on its HRLSIMS spectrum (860.30121 *m/e*) suggests the additions of one *o*-benzoquinodimethane and one oxygen atom. The addition sites for the *o*-benzoquinodimethane and oxygen were not determined as purification of **137** was not successful.

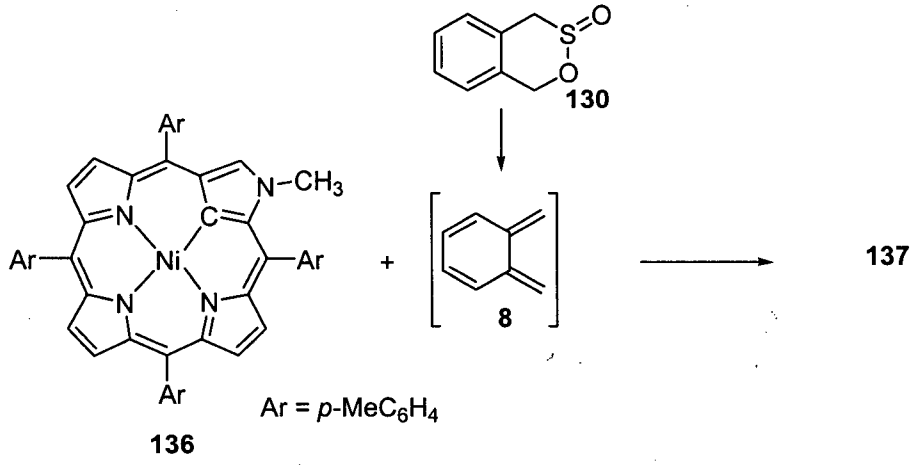

Scheme 3.15 Attempted Diels-Alder reaction of complex **136**.

3.2.4.3 1,3-Dipolar Cycloaddition of Ni(II) N-Confused Porphyrins

1,3-Dipole **13**[10] was used to react with (NCTTP)Ni^{II}, **129b**, to obtain the 1,3-dipolar cycloaddition product (Scheme 3.16). The molecular ion peak of the major product **138** was observed at 782 *m/e* (LSIMS), suggesting the addition of one dipole **13** and the loss of two hydrogen atoms. Purification of **138** was not successful. A possible structure for **138** is shown in Scheme 3.16.

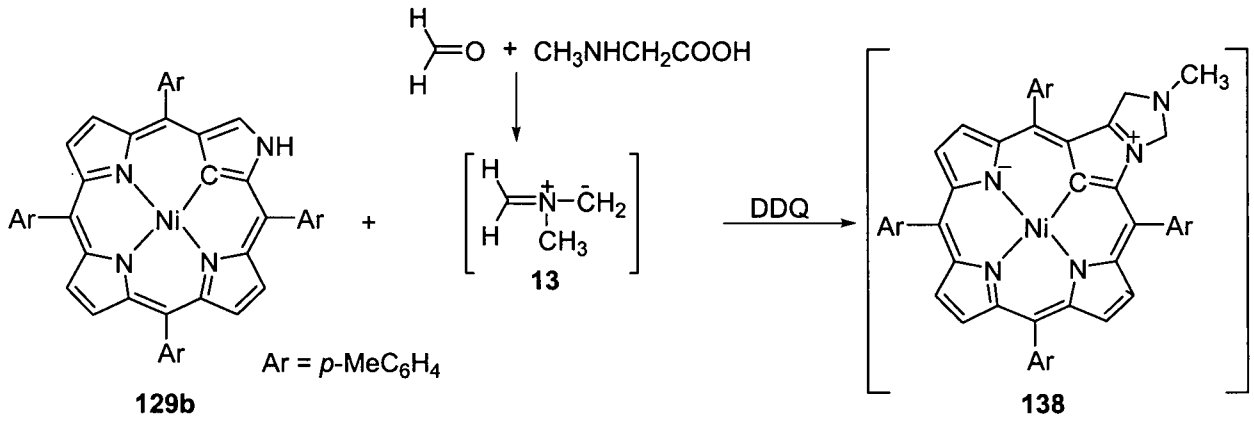

Scheme 3.16 1,3-Dipole cycloaddition reactions of Ni(II) NCP **129b**.

3.3 Conclusions

The peripheral carbon-nitrogen double bonds of Ni(II) N-confused porphyrins are partially isolated from the 18π conjugated aromatic system and react as dienophiles in Diels-Alder reactions with *o*-benzoquinodimethane yielding novel Ni(II) N-confused isoquinoporphyrins. Ni(II) N-confused tetraphenylisoquinoporphyrin has been structurally characterized.

As suggested by the mass spectra of the major products, Diels-Alder reactions of *o*-benzoquinodimethane with NCP in acid, Diels-Alder reactions of *o*-benzoquinodimethane with Ni(II) N(2)-methylated NCP, and 1,3-dipolar cycloaddition reaction of azomethine **13** with Ni(II) NCP do proceed, though purification of these cycloaddition adducts was not successful.

References

1. Carey, F. A. and Sundberg, R. J. *Advanced Organic Chemistry*, 3rd ed.; Plenum Press: New York, 1990.
2. Boger, D. L. and Weinreb, S. N. Organic Chemistry. In *Hetero Diels-Alder Methodology in Organic Synthesis;* Wasserman, H. H. Ed.; Academic Press: San Diego, 1987; Vol. 47; pp. 34.
3. Bohlmann, F., Habeck, D., Poetsch, E. and Schumann, D. *Chem. Ber.* **1967,** *100*, 2742.
4. Gunter, M. J., Tang, H. and Warrener, R. N. *Chem. Commun.* **1999**, 803.
5. Silva, A. M. G., Faustino, M. A. F., Tome, A. C., Neves, M. G. P. M. S., Silva, A. M. S. and Cavaleiro, J. A. S. *J. Chem. Soc., Perkin Trans. 1* **2001**, 2752.
6. Silva, A. M. G., Tome, A. C., Neves, M. G. P. M. S., Silva, A. M. S. and Cavaleiro, J. A. S. *J. Org. Chem.* **2002,** *67*, 726.
7. Pangka, V. S., Morgan, A. R. and Dolphin, D. *J. Org. Chem.* **1986**, *51*, 1094.
8. Morgan, A. R., Pangka, V. S. and Dolphin, D. *Chem. Commun.* **1984**, 1047.
9. Tome, A. C., Lacerda, P. S. S., Neves, M. G. P. M. S. and Cavaleiro, J. A. S. *Chem. Commun.* **1997**, 1199.
10. Silva, A. M. G., Tome, A. C., Neves, M. G. P. M. S., Silva, A. M. S. and Cavaleiro, J. A. S. *Chem. Commun.* **1999**, 1767.
11. Geier, G. R., Haynes, D. M. and Lindsey, J. S. *Org. Lett.* **1999,** *1*, 1455.
12. Chmielewski, P. J., Latos-Grażyński, L., Rachlewicz, K. and Glowiak, T. *Angew. Chem., Int. Ed. Engl.* **1994,** *33*, 779.
13. Hoey, M. D. and Dittmer, D. C. *J. Org. Chem.* **1991,** *56*, 1947.
14. Pitts, M. R., Harrison, J. R. and Moody, C. J. *J. Chem. Soc., Perkin Trans. 1* **2001**, 955.

15. Scheidt, W. R. The Porphyrins. In *Porphyrin Stereochemistry;* Dolphin, D. Ed.; Academic Press: New York, 1978; Vol. III; pp. 465.

16. Lash, T. D., Richter, D. T. and Shiner, C. M. *J. Org. Chem.* **1999,** *64*, 7973.

17. Chmielewski, P. J. and Latos-Grażyński, L. *J. Chem. Soc., Perkin Trans. 2* **1995**, 503.

Chapter 4

Inner C- Cyanide Addition and Nucleophilic Addition Reactions to Ni(II) N-Confused Porphyrins

4.1 Introduction

Electrophilic substitution and nucleophilic addition reactions commonly occur in porphyrin chemistry.[1] For electrophilic substitution reactions such as halogenation, formylation and nitration reactions, metalloporphyrins are often used to avoid the deactivating effect which would occur upon protonation of inner pyrrolic nitrogen atoms.[1] For instance, (TPP)Cu^{II}, **139**, reacts with a large excess of Vilsmeier reagent (prepared by mixing DMF and $POCl_3$) to give formylation product **140** in excellent yield (95 %) (Scheme 4.1).[1,2] Porphyrins are also susceptible to attack by nucleophiles.[1] For example, nucleophilic addition of butyllithium to TPP at low temperature produces a mixture of phlorin **141** (26 %) and chlorin **142** (18 %) (Scheme 4.2).[3]

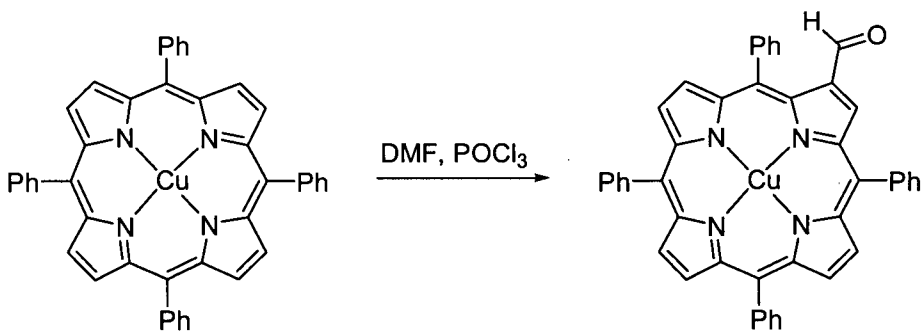

139 **140**

Scheme 4.1 Formylation of (TPP)Cu^{II} **139**.

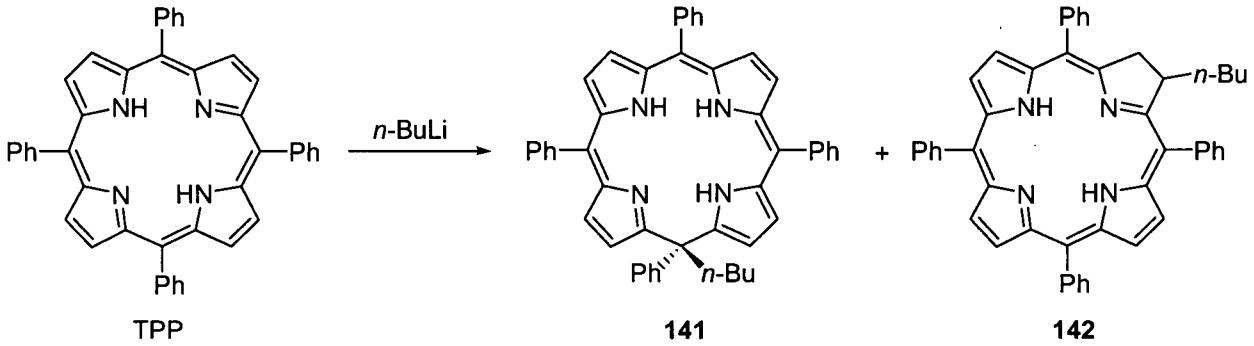

Scheme 4.2 Nucleophilic addition of butyllithium to TPP.

Some electrophilic and nucleophilic reactions of N-confused porphyrins were introduced in section 1.4.4.3. Additionally, as discussed in section 3.2.2.4, the peripheral carbon-nitrogen bond of Ni(II) N-confused porphyrins seems to have some iminium character. Thus, it was expected that, similar to iminium compounds, Ni(II) N-confused porphyrins might be reactive toward nucleophiles, and their reactions with $NaOCH_3$ were studied.

4.2 Results and Discussion

When (NCTTP)Ni^{II} was added to a solution of $NaOCH_3$ in 1:1 CH_2Cl_2/CH_3OH, no reaction was observed. It was postulated that the addition product, N-confused chlorin **143**, is not stable (Scheme 4.3). The reaction, however, might be driven toward a more stable product, **144**, with the addition of an oxidant, e.g. DDQ, to convert the N-confused chlorin **143** to N-confused porphyrin **144**.

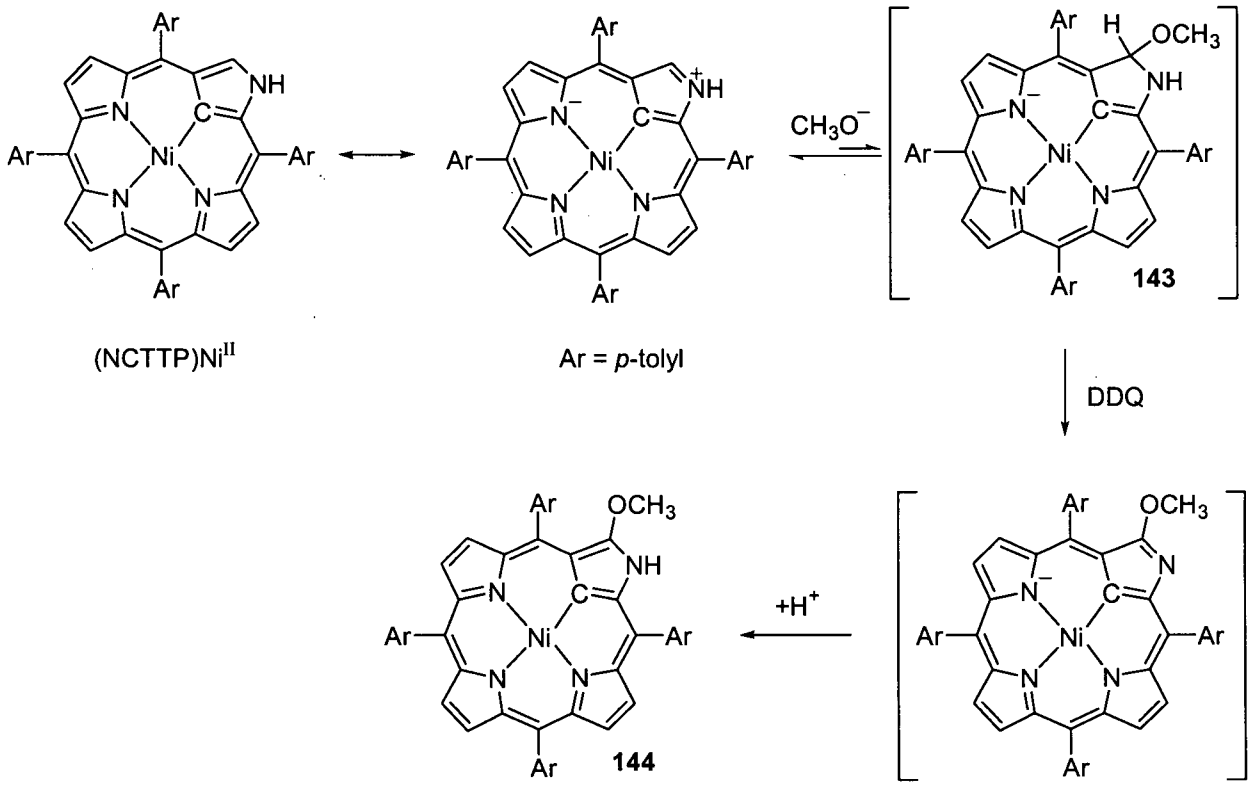

Scheme 4.3 Postulated reaction of (NCTTP)Ni^{II} with $NaOCH_3$ and DDQ.

Thus, to a 1:1 CH_2Cl_2/CH_3OH (70 mL) solution of $NaOCH_3$ (200 mg) were added (NCTTP)Ni^{II} (110 mg) and DDQ (400 mg). The solution was stirred at room temperature for 24 h and then washed with saturated aqueous $NaHCO_3$ solution. The solvent was removed *in vacuo* and the residue was subjected to column chromatography (silica gel, 230 - 400 mesh, 16 g). Using 1:1 CH_2Cl_2/hexanes, (NCTTP)Ni^{II} was eluted first; 3:1 CH_2Cl_2/hexanes eluted the first new compound, **145** (11.7 mg), and the second new compound, **146** (30.3 mg), was eluted with CH_2Cl_2.

However, based on the observed parent ion peak at 752 *m/e* (LSIMS), the major product **146** was not the product expected from simple nucleophilic addition of CH_3O^-. The formula search result of $C_{49}H_{36}N_5Ni$ (*m/e* Calcd 752.23237) for **146** from the HRLSIMS result

(752.23242 *m/e*) suggested the addition of one carbon atom and one nitrogen atom to (NCTTP)Ni^{II} ($C_{48}H_{36}N_4Ni$). Similarly, compound **145** appeared to involve the addition of one methanol, one carbon atom, and one nitrogen atom to (NCTTP)Ni^{II} with the loss of two hydrogen atoms, also suggested by the formula search result of $C_{50}H_{38}N_5ONi$ (*m/e* Calcd 782.24294) based on its HRLSIMS result (782.24344 *m/e*).

4.2.1 Structural Determination by X-ray Diffraction Analyses

Full identification of the new complexes could only be obtained through crystal structure analyses. Crystals of complexes **145** and **146** were obtained by solvent diffusion of CH_3OH into CH_2Cl_2 solutions of each complex, and the structures of complexes **145** and **146** were determined by X-ray diffraction analyses (Figure 4.1, 4.2 and 4.3). Cyanide addition had been found to occur in both complexes on the inner C(21) site. Additionally, the expected methoxy addition on the peripheral C(3) site was observed in complex **145**, the minor product.

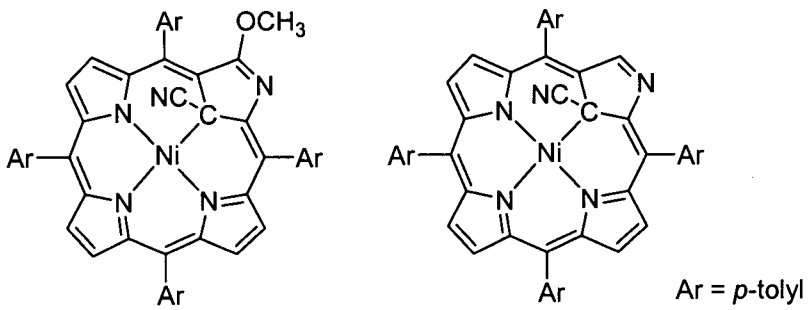

145 **146**

Figure 4.1 Structures of complexes **145** and **146**.

The structure of complex **145** displayed disorder in the locations of the methoxy fragment. The structure has been refined to give 63 % occupancy with -OCH_3 as shown in

Figure 4.2 and 37 % occupancy with -OCH_3 attached to the C(3) which replaces N(2) of the major form. Figures 4.2 and 4.4 only show the major form.

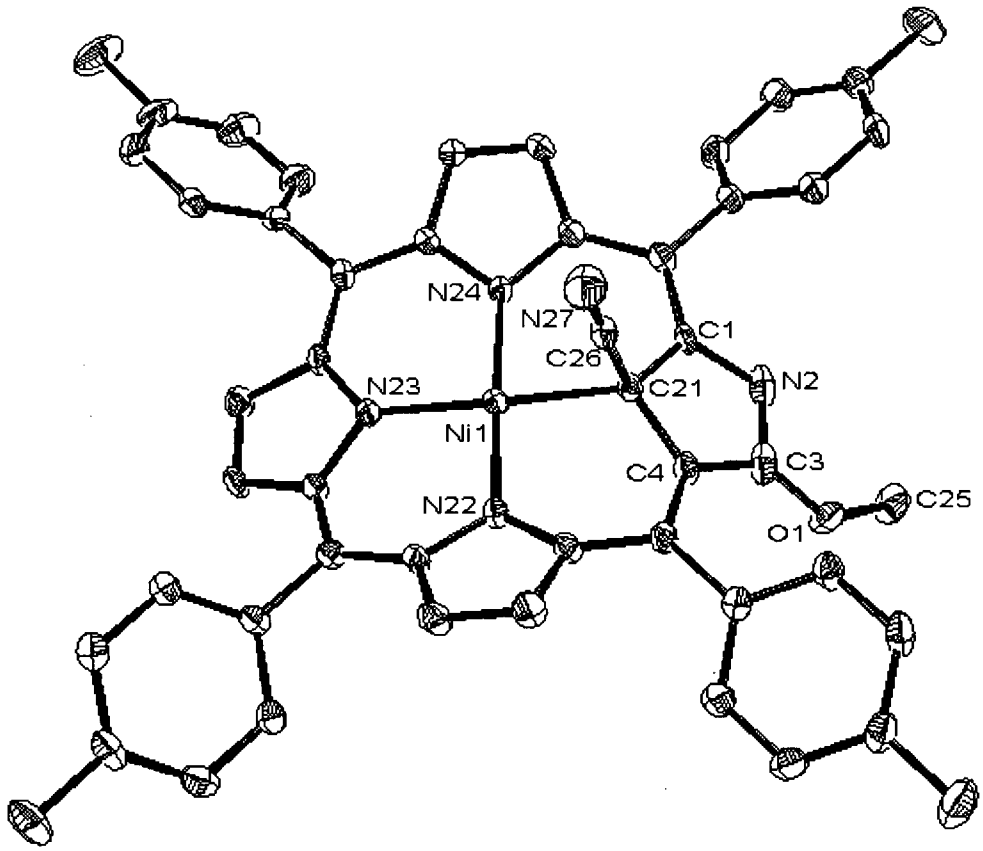

Figure 4.2 An ORTEP drawing of compound **145** showing atomic labeling and thermal ellipsoids at the 50 % probability level. H atoms and the disorder of the OCH_3 fragment have been removed for clarity.

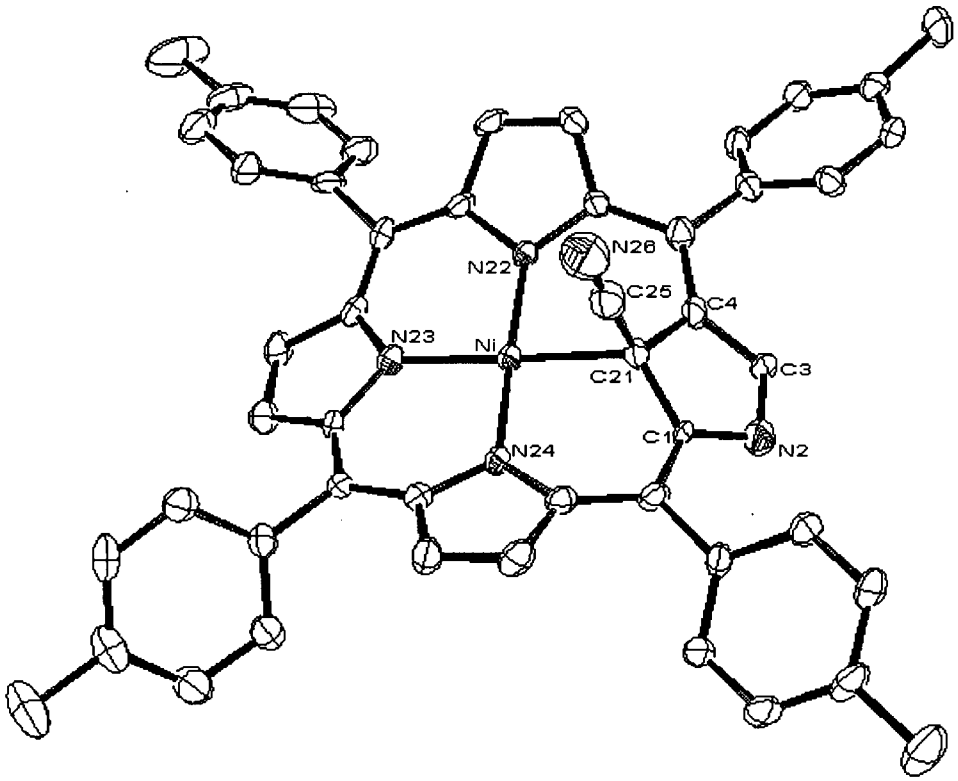

Figure 4.3 An ORTEP drawing of compound **146** showing atomic labeling and thermal ellipsoids at the 50 % probability level. H atoms and solvent have been removed for clarity.

The porphyrin skeletons of complexes **145** and **146** are distorted from planarity (Figure 4.4 and 4.5). In the X-ray structure of complex **145**, the dihedral angles between the pyrrole planes and the plane defined by N(22)N(23)N(24) are as follows: C(21) 39.52(13)°, N(22) -21.01(14)°, N(23) 12.77(13)°, and N(24) -20.56(16)°. For complex **146**, the dihedral angles between the pyrrole planes and the plane defined by N(22)N(23)N(24) are as follows: C(21) 40.4(2)°, N(22) -21.0(3)°, N(23) 13.4(3)°, and N(24) -18.5(2)°. The degree of distortion for **145** and **146** is similar to that observed in the C(21)-methylated Ni(II) N-confused porphyrin **26** (Figure 1.11), in which the inverted pyrrole plane deviates from the N(22)N(23)N(24) plane by 42.2°.[4]

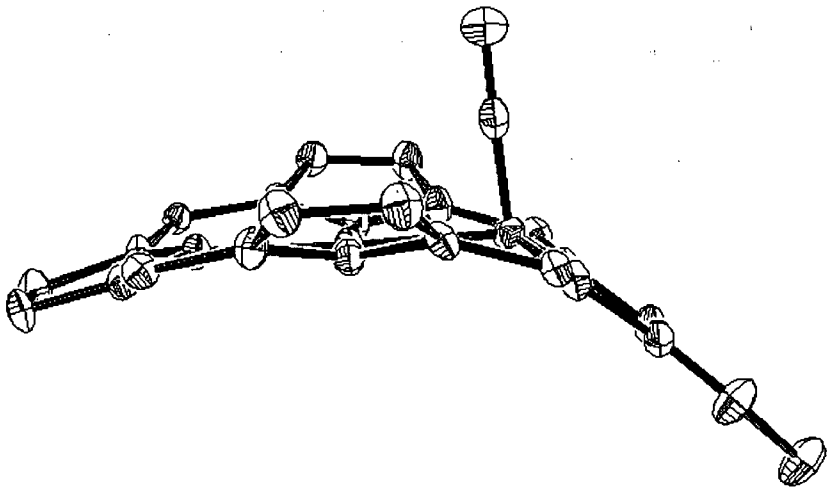

Figure 4.4 An ORTEP drawing of **145** showing thermal ellipsoids at the 50 % probability level (side view). *p*-Tolyl groups, H atoms and the disorder of the OCH_3 fragment have been removed for clarity.

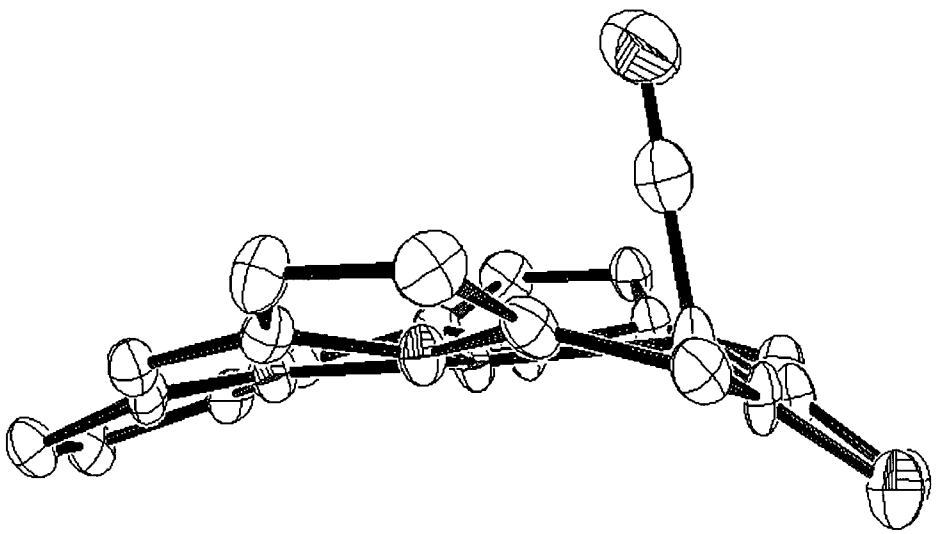

Figure 4.5 An ORTEP drawing of **146** showing thermal ellipsoids at the 50 % probability level (side view). *p*-Tolyl groups, H atoms and solvent have been removed for clarity.

In the X-ray crystal structure of complex **145**, the bond distances of N(2)-C(1), N(2)-C(3), and C(3)-C(4) are markedly shorter than those of C(21)-C(1) and C(21)-C(4) (Table 4.1), suggesting that the C(21) atom approaches sp^3 hybridization. The distance between Ni and C(26) is 2.429 Å, suggesting possible interaction between these two atoms. However, the bond lengths of C(26)-N(27) and C(21)-C(26) at 1.144(4) and 1.462(4) Å, respectively, and the bond angle of 178.3(3)° for C(21)-C(26)-C(27) are characteristic of N≡C−C bonding, suggesting no bonding between Ni and C(26). These structural features were also observed in the structure of complex **146.**

Table 4.1 Selected bond lengths for complexes **145** and **146**.

Bond	Bond length in complex **145** (Å)	Bond length in complex **146** (Å)
N(2)-C(1)	1.376(4)	1.363(6)
N(2)-C(3)	1.372(4)	1.339(6)
C(3)-C(4)	1.394(4)	1.396(6)
C(21)-C(1)	1.470(4)	1.468(6)
C(21)-C(4)	1.462(4)	1.442(6)
C(21)-C(25)	N/A[a]	1.469(8)
C(21)-C(26)	1.462(4)	N/A
C(25)-N(26)	N/A	1.157(8)
C(26)-N(27)	1.144(4)	N/A
Ni-C(21)	2.018(3)	2.024(4)
Ni-N(22)	1.946(2)	1.948(4)
Ni-N(23)	1.926(2)	1.926(4)
Ni-N(24)	1.951(2)	1.953(3)

a: N/A stands for "Not Applicable".

4.2.2 NMR Spectra of the Cyanide Addition Products

In the ^{1}H NMR spectra of **145** and **146**, signals representative of the pyrrole protons, excluding C(3)H, are observed in the region of 8.29 - 8.51 ppm and 8.54 - 8.78 ppm, respectively (Figure 4.6, 4.7), and are downfield compared to those of (NCTTP)Ni^{II}, which are observed in the 7.65 - 8.12 ppm region. The 4.21 ppm peak in the ^{1}H NMR spectrum of **145** was assigned to the OCH_3 protons. The 10.03 ppm peak observed in the spectrum of **146** was assigned to C(3)H proton and this signal was not located in the ^{1}H NMR spectrum of **145**, suggesting addition may have occurred at the C(3) position of complex **145**.

Notably, the position of the C(3)H chemical shift for **146** is approximately 1.5 ppm downfield from the starting material, (NCTTP)Ni^{II}. A similar effect is observed in the case of inner C-methylated Ni(II) N-confused porphyrin (C(21)-CH_3-NCTPP)Ni^{II}, **26** (Scheme 1.12), and signal for the C(3)H of complex **26** is observed at 9.90 ppm.[4] Complexes **145** and **146** seem to favor the π delocalization *via* the outer path C(1)-N(2)-C(3)-C(4) at the inverted pyrrole fragment, as C(21) atoms in both complexes approach sp^3 hybridization and inner conjugation C(1)-C(21)-C(4) is not possible (Figure 4.1). The downfield of C(3)H signal may be the result of a closer ring current.

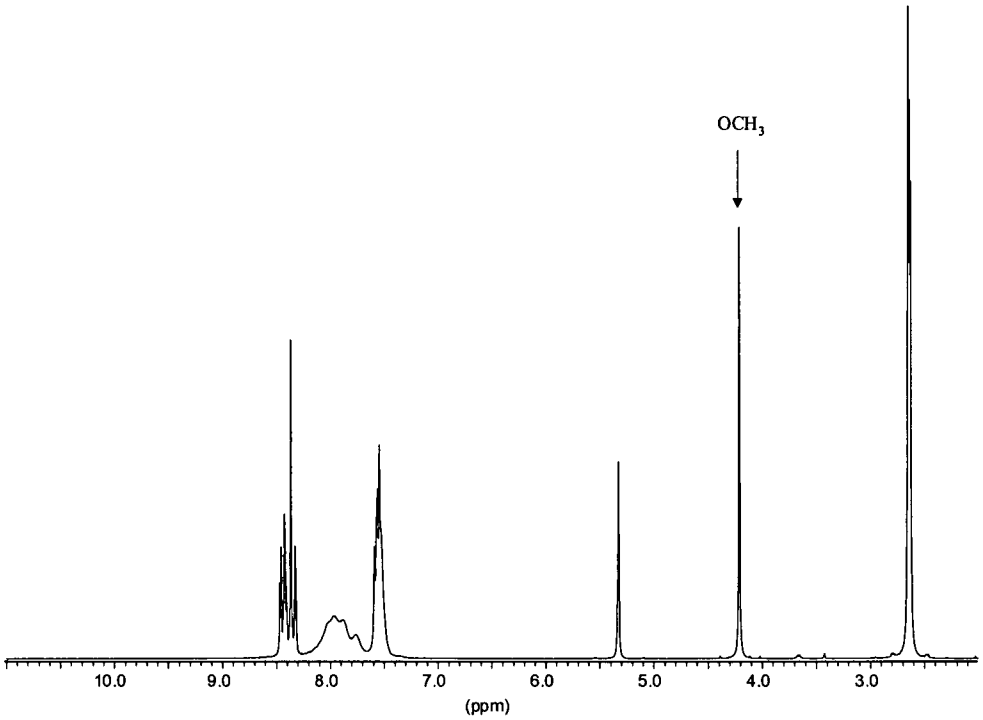

Figure 4.6 ^{1}H NMR spectrum of **145** in CD_2Cl_2 (400 MHz).

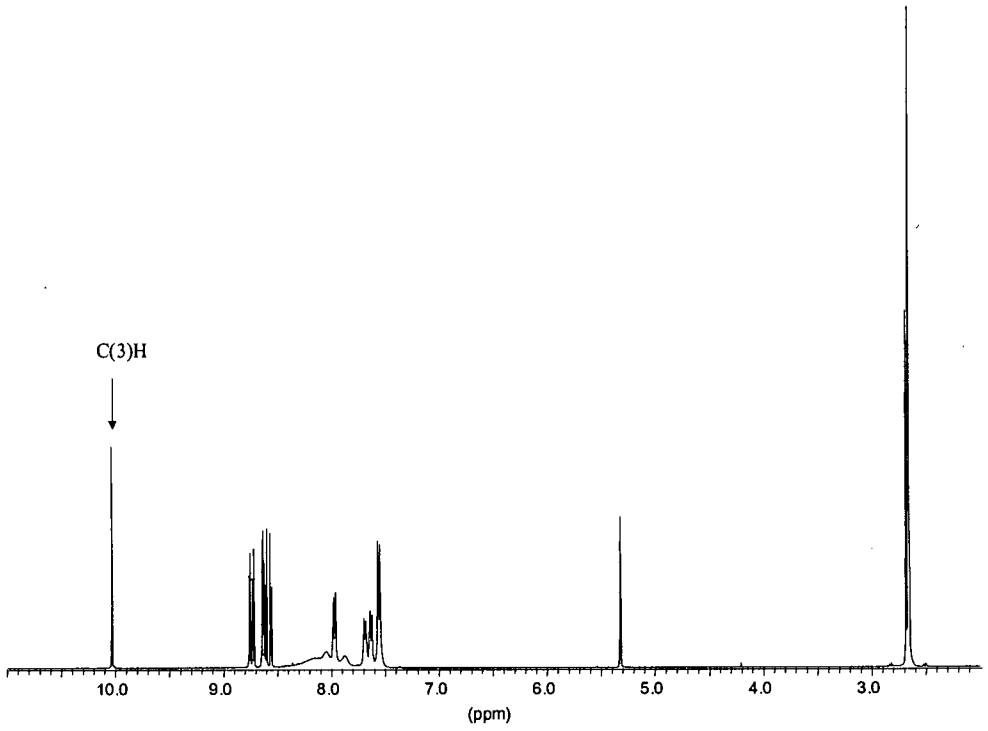

Figure 4.7 ^{1}H NMR spectrum of **146** in CD_2Cl_2 (400 MHz).

4.2.3 Optical Absorption Spectra

The UV-vis spectra of complexes **145** and **146** both exhibit absorptions around 434 nm and 720 nm (Figure 4.8), corresponding to the Soret band and Q-bands of porphyrins, respectively. The single broad Q-bands of complexes **145** and **146** are much different from those of the starting material, (NCTTP)Ni^{II}, which exhibits three distinctive Q-bands, suggesting that inner cyanide addition changes the conjugation pathway. This change of conjugation pathway has also been suggested by the downfield C(3)H signal in the ^1H NMR spectrum of **145**, and is presumably caused by sp^3 hybridization of C(21).

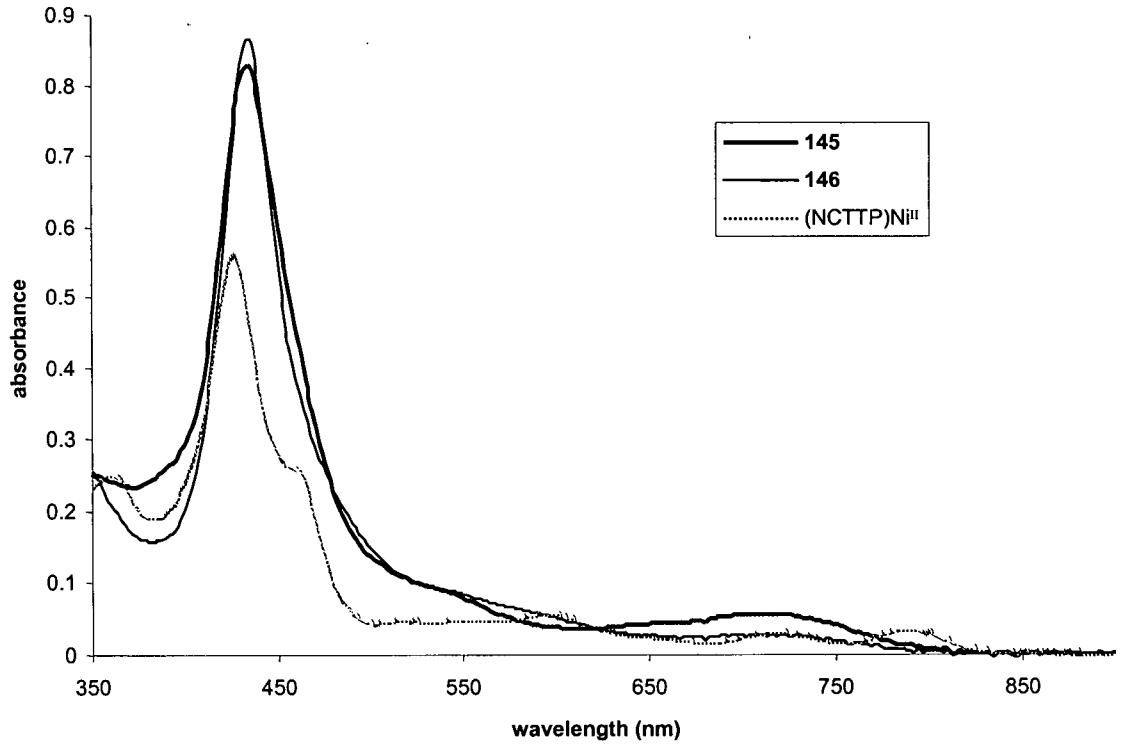

Figure 4.8 UV-vis spectra of complexes **145**, **146**, and (NCTTP)Ni^{II}.

4.2.4 Reaction Mechanism

A possible mechanism for the generation of complexes **145** and **146** is shown in Scheme 4.4. Electrophilic addition of compound **148**, the reduction product of DDQ, to the deprotonated

(NCTPP)Ni^{II}, **147**, results in **149**, which tautomerizes to **150**. Elimination of **151** from **150** gives complex **146**. Nucleophilic addition of CH_3O^- to **146** at C(3) followed by protonation gives Ni(II) N-confused chlorin **152.** Oxidation of **152** with DDQ results in complex **145**.

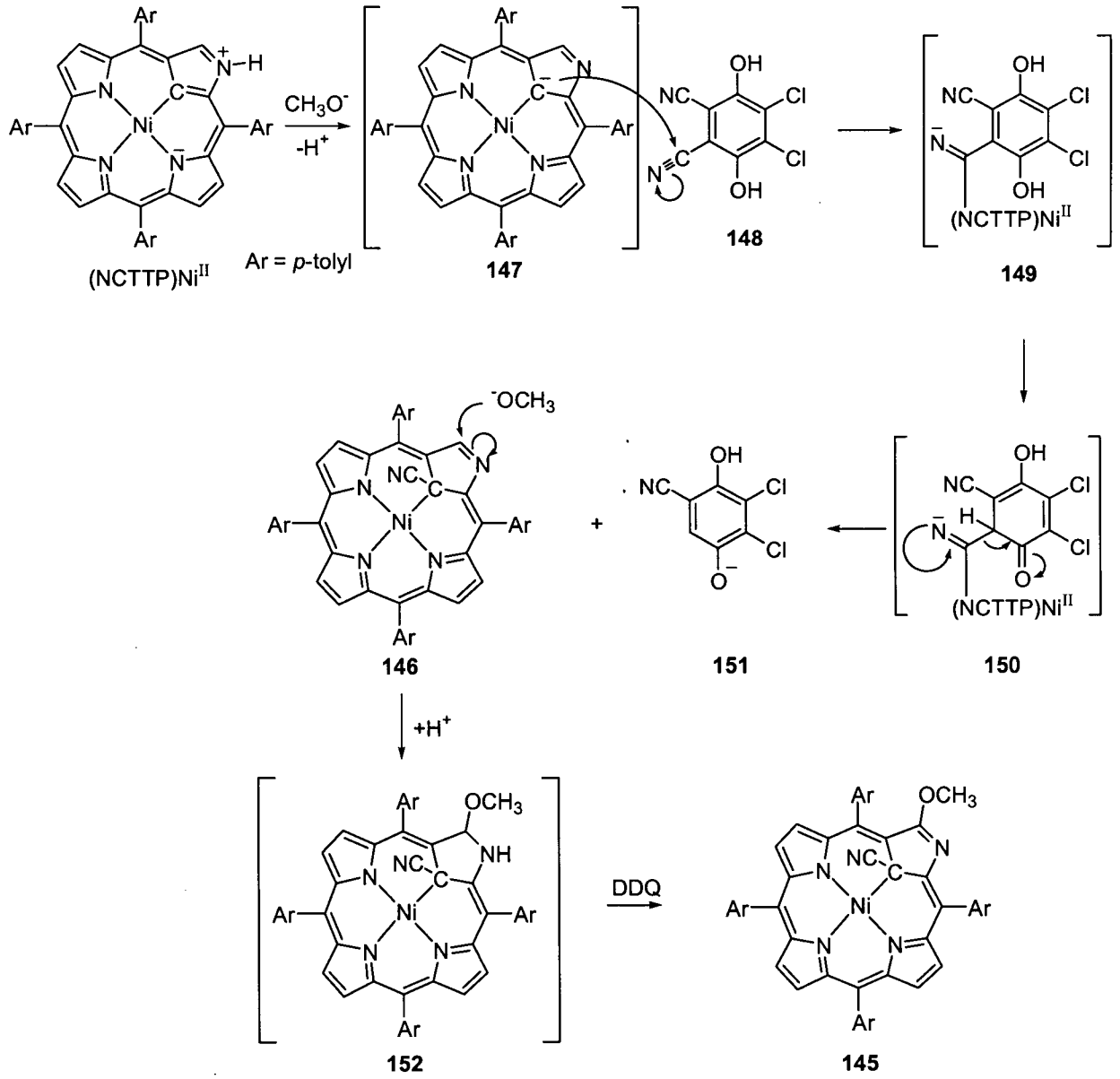

Scheme 4.4 A possible mechanism for the generation of complexes **145** and **146**.

The UV-vis spectra of (NCTTP)Ni^{II} in CH_2Cl_2/CH_3OH (1:1) with and without $NaOCH_3$ are shown in Figure 4.9. The difference between the spectra suggests that (NCTTP)Ni^{II} is deprotonated in the presence of $NaOCH_3$.

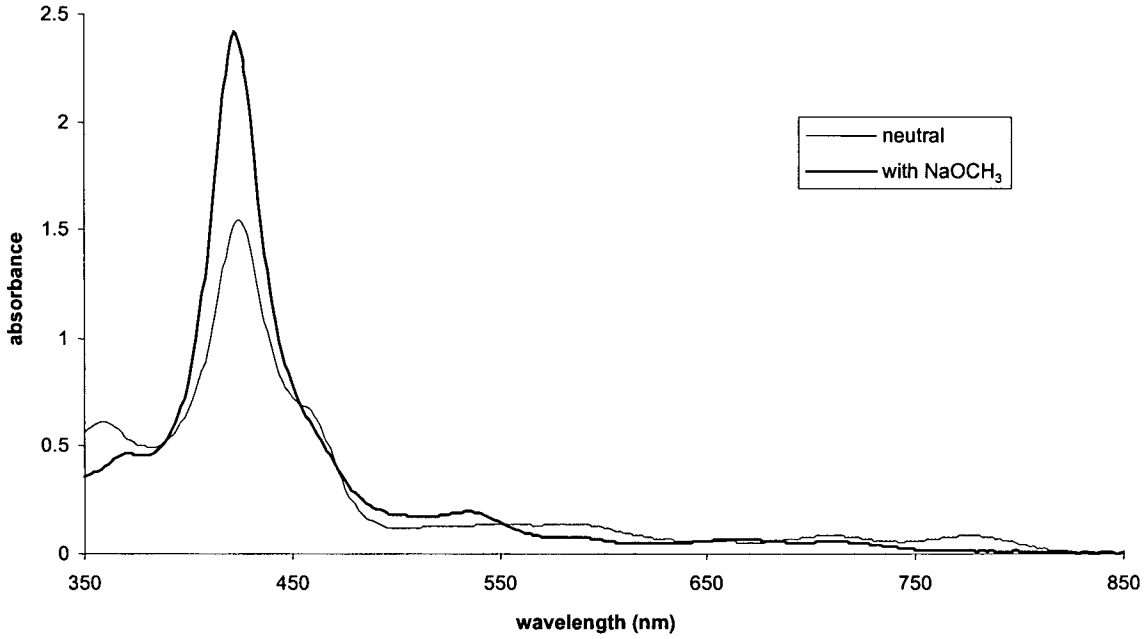

Figure 4.9 UV-vis spectra of (NCTTP)Ni^{II} in CH_2Cl_2/CH_3OH (1:1) with and without $NaOCH_3$.

4.3 Conclusions

Reaction of $(NCTTP)Ni^{II}$ with $NaOCH_3$ and DDQ resulted in the unexpected inner C-cyanide addition product **146**. Subsequent nucleophilic addition of CH_3O^- to **146** followed by oxidation with DDQ gave complex **145**. Structures of both complexes **145** and **146** were determined by X-ray diffraction analyses. The cyanide additions in both complexes are on the inner C(21) while the methoxy addition for **145** is on the peripheral C(3).

Complexes **145** and **146** seem to favor the π delocalization *via* the outer path C(1)-N(2)-C(3)-C(4) at the inverted pyrrole fragment as the result of sp^3 hybridization of C(21). The resulting increase of the ring current effect in the inverted pyrrole fragment is demonstrated by the remarkable ^1H NMR chemical shift of C(3)H at 10.03 ppm for complex **146**, while the signal for C(3)H of $(NCTTP)Ni^{II}$ is observed at 8.56 ppm.

Electrophilic addition of compound **148**, the reduction product of DDQ, to the deprotonated $(NCTPP)Ni^{II}$, was proposed as the critical step for the inner cyanide addition. The generality of the cyanide addition to other nucleophiles with DDQ and base is worthy of study in the future.

References

1. Jaquinod, L. Functionalization of 5,10,15,20-Tetra-Substituted Porphyrins. In *The Porphyrin Handbook;* Kadish, K. M.; Smith, K. M.; Guilard, R. Eds.; Academic Press: San Diego, 2000; Vol. 1; pp. 201.

2. Momenteau, M., Loock, B. and Bisagni, E. *Can. J. Chem.* **1979,** *57,* 1804.

3. Krattinger, B. and Callot, H. J. *Tetrahedron Lett.* **1996,** *37,* 7699.

4. Chmielewski, P. J., Latos-Grażyński, L. and Glowiak, T. *J. Am. Chem. Soc.* **1996,** *118,* 5690.

Chapter 5

Ni(III) Complex of N-Confused Porphyrin Inner C-Oxide

5.1 Introduction

Ni(III) tetrapyrrolic macrocycles have been intensively studied.[1] Wolberg and Manassen reported on the generation of a Ni(III) porphyrin cation *via* electrochemical oxidation of Ni(II) tetraphenylporphyrin at 77 K.[2] This reaction was re-examined by Dolphin *et al.* and it was observed that a Ni(II) porphyrin π cation radical is formed at room temperature and a low spin Ni(III) porphyrin is generated upon cooling to 77 K, showing intramolecular electron transfer.[3,4] N-confused porphyrins[5,6] can stabilize transition metals in high oxidation states[7-11] and Ni(III) complexes were prepared by Chmielewski and Latos-Grażyński. (section 1.4.2).[7] Factor 430 (F430), a nickel tetrapyrrole, is the cofactor of methyl-coenzyme M reductase, which catalyzes the final steps of CO_2 conversion to methane by methanogenic *Archaea*, and a methyl-Ni(III) transient is suggested to be a key intermediate.[12] Ni(III)-alkyl intermediates are also considered to be involved in the reactions of Ni(I) macrocycles with alkyl halides.[13]

In our attempts to synthesize N-confused chlorins *via* dihydroxylation reactions of Ni(II) N-confused porphyrins with OsO_4, an unexpected product, a Ni(III) complex of N-confused porphyrin inner C-oxide **153**, was obtained and structurally characterized.

5.2 Results and Discussion

A solution of the (NCTTP)Ni^{II} complex, **129b** (130 mg),[5] and OsO_4 (60 mg) in 15 % pyridine/CH_2Cl_2 (50 mL) was stirred at room temperature for 24 h and then filtered through a silica gel plug using 10 % CH_3OH in CH_2Cl_2. The solvent was removed *in vacuo* and the residue was separated on a silica gel column (230 - 400 mesh, 16 g). Compound **153** was eluted with 1.5 % CH_3OH in CH_2Cl_2 and was obtained in 42 % yield.

A molecular ion peak of **153** was observed at 742 *m/e* (LSIMS in the positive mode) and the molecular formula search resulted in $C_{48}H_{36}N_4NiO$ (*m/e* Calcd 742.22421) based on the HRLSIMS result (742.22443 *m/e*), suggesting the addition of one oxygen atom to (NCTTP)Ni^{II} ($C_{48}H_{36}N_4Ni$). However, location of the oxygen atom could not be determined, as addition of oxygen to either N(2) or peripheral C-C bonds and dehydration of the dihydroxylation product are all possible.

Broad peaks were observed in the ^1H NMR spectrum of **153** (Figure 5.1), suggesting that complex **153** is paramagnetic. Characterization of compound **153** with NMR spectroscopy was thus not successful.

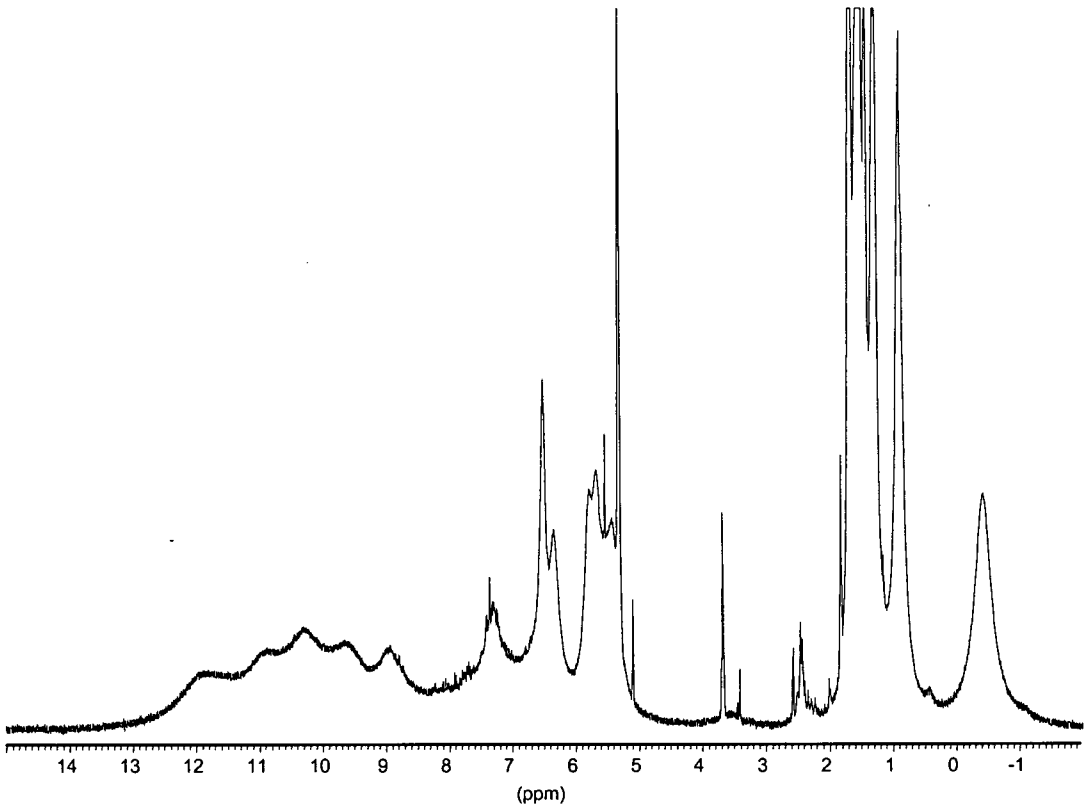

Figure 5.1 ^1H NMR spectrum of **153** in CD_2Cl_2 (400 MHz).

X-ray crystallography was relied upon to determine the structure of **153**. After numerous unsuccessful attempts to grow crystals of **153** by solvent diffusion of hexanes or CH_3OH into a CH_2Cl_2 solution of **153**, crystals of **153** were finally obtained by solvent diffusion of hexanes into a CH_2Cl_2/pyrindine solution of **153**. The structure of compound **153** was determined by single crystal X-ray diffraction analysis (Figure 5.2, 5.3).

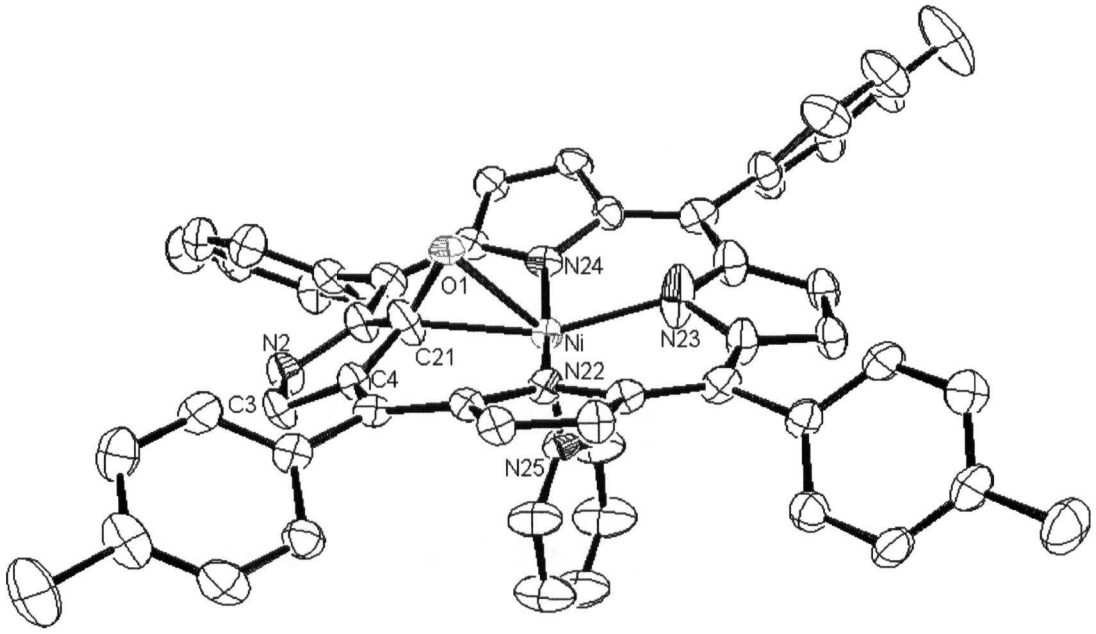

Figure 5.2 An ORTEP drawing of compound **153** showing atomic labeling and thermal ellipsoids at 50 % probability. H atoms, solvent and the disorder of the O(1) atom have been removed for clarity.

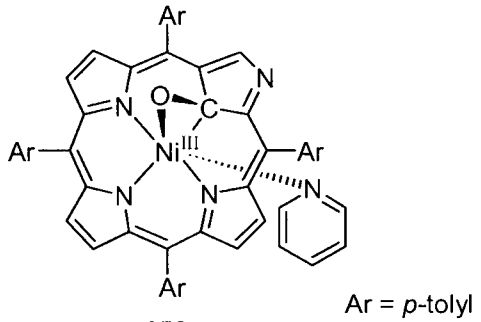

153

Figure 5.3 Structure of complex **153**.

The X-ray crystal structure of **153** shows that an oxygen atom has been added to C(21) and is coordinated to the center nickel ion as well. There is also an axial pyridine ligand *trans* to the bridging oxygen atom. A counteranion was not detected. However, the nature of the nickel complex **153** was still not determined as the origin of the unpaired electrons that result in a paramagnetic compound can be from one of the following sources:

- A high spin Ni(II) ion (two unpaired electrons).
- A low spin Ni(II) ion with a porphyrin π cation radical (one unpaired electron).
- A Ni(III) ion (one unpaired electron for a low spin Ni(III) ion and three unpaired electrons for a high spin Ni(III) ion).

To determine the position of the unpaired electrons in complex **153**, the EPR spectrum of **153** in toluene glass was taken at 130 K (Figure 5.4). The spectrum is similar to that observed for a Ni(III) complex of N-confused tetraphenylporphyrin containing an axial hydroxyl group (**48a**, Scheme 1.21).[7] The g-factor ($g > 2.1$) is indicative of the unpaired electron located on the metal center rather than in a porphyrin π cation radical ($g_{iso} \approx 2.002$ for porphyrin π cation radical).[3,7]

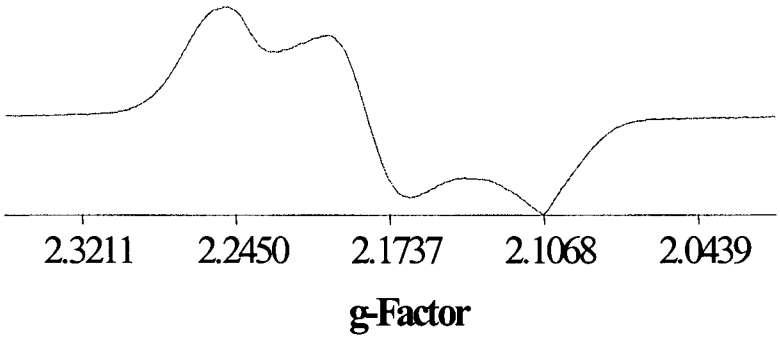

Figure 5.4 EPR spectrum (X-band, 130 K, toluene) of complex **153**.

Evan's method[14,15] was used to measure the room temperature effective magnetic moment (μ_{eff}) of complex **153** in CD_2Cl_2, which was then used to determine the number of unpaired electrons in **153**. A dilute CD_2Cl_2 solution of cyclohexane (reference) was placed in the NMR sample tube while the solvent containing a known concentration of complex **153** and cyclohexane was incorporated in an inner narrow-bore tube. The ^1H NMR spectrum of cyclohexane in the two coaxial tubes exhibits a chemical shift difference (Figure 5.5) which was used to calculate the room temperature effective magnetic moment. The experimental result is 1.87 μ_B, close to the spin-only value for a low spin d^7 Ni(III) center with one unpaired electron ($\mu_{eff} = (n(n+2))^{0.5} = 1.73\ \mu_B$, n = 1). In comparison, a high spin Ni(II) ion would have $\mu_{eff} = 2.83\ \mu_B$ (n = 2). The room temperature effective magnetic moment of complex **153** and its EPR spectrum lead to the conclusion that complex **153** is a Ni(III) complex of N-confused porphyrin inner C-oxide. This is corroborated by the parent ion peak of **153** at 741 *m/e* detected using LSIMS in the negative mode, together with the absence of the counteranion in the X-ray crystal structure. The corresponding Ni(II) complex would require protonation of either N(2) or O(1) to balance the charge, resulting in a parent ion peak observed at 742 *m/e*.

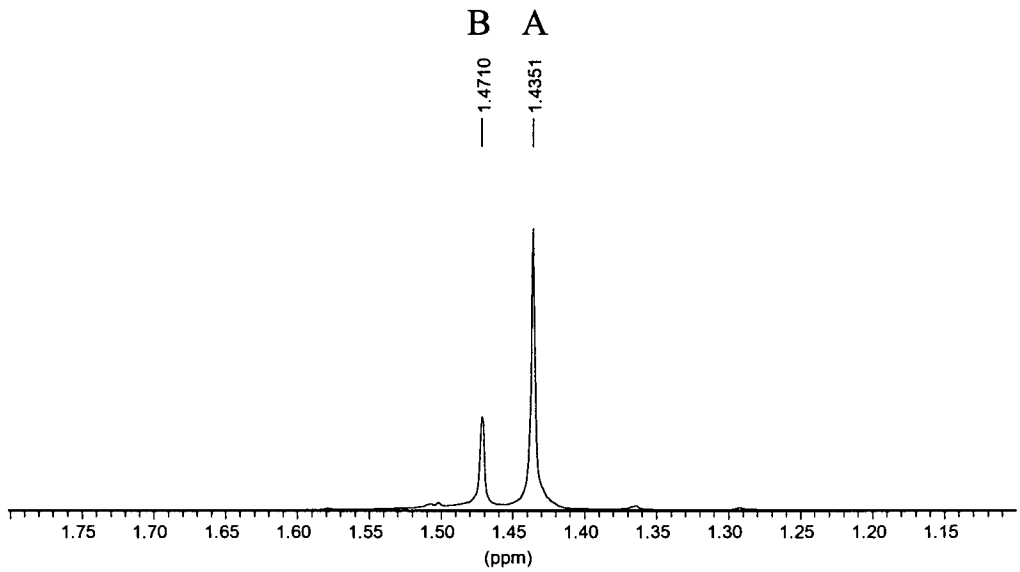

Figure 5.5 The ^{1}H NMR (400 MHz, CD_2Cl_2) spectrum of cyclohexane showing the paramagnetic shift caused by complex **153** (6.9 x 10^{-3} M). (**A** = cyclohexane in CD_2Cl_2, and **B** = cyclohexane peak shifted by complex **153**).

5.2.1 X-ray Crystal Structure of Ni(III) N-Confused Porphyrin Inner C-Oxide

The X-ray crystal structure of complex **153** was found to contain a 6-coordinate nickel ion with an axial pyridine ligand. The nickel ion in complex **153** is bonded to both the oxygen atom and C(21). However, disorder was observed in the location of the O(1) atom. The structure was refined to give 64 % occupancy with O(1) coordinated to the Ni and the C(21), as shown in Figure 5.2, and 36 % occupancy with O(1) attached to the Ni and the N(23). The unit cell also contains one molecule of disordered CH_2Cl_2.

The planarity of the porphyrin skeleton of **153** is distorted (Figure 5.6), but not as severely as that of the C(21)-methylated Ni(II) N-confused porphyrin **26** (Figure 1.11), in which the inverted pyrrole plane deviates from the N(22)N(23)N(24) plane by 42.2°.[16] For complex **153**, the dihedral angles between the pyrrole planes and the plane defined by N(22)N(23)N(24) are as follows: C(21) 20.5(2)°, N(22) -17.61(7)°, N(23) 22.5(2)°, and N(24) -15.3(2)°.

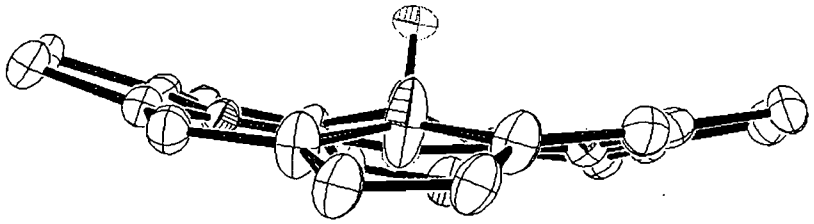

Figure 5.6 An ORTEP drawing (side view) of compound **153** showing distortion from planarity (thermal ellipsoids at 50 % probability). Solvent, *p*-tolyl group, H atoms and the disorder of the O(1) atom have been removed for clarity.

The Ni-N bond distances (2.005 - 2.100 Å) in **153**, listed in Table 5.1, are longer than those of the high spin Ni(II) complex of N(2),C(21)-dimethylated N-confused porphyrin **27** (section 1.4.4.1) (1.979 - 2.057 Å),[16] contrary to what might be expected for the smaller Ni(III) ion.[1] However, a similar elongation of Ni(III)-C bond lengths has also been observed in the case of $[Ni^{III}(C_6Cl_5)_4]^-$, of which the mean Ni-C distance is 2.007(8) Å.[17]

The fact that the bond distances of N(2)-C(1), N(2)-C(3), and C(3)-C(4) are markedly shorter than those of C(21)-C(1) and C(21)-C(4) suggests that the C(21) atom approaches sp^3 hybridization. The Ni-O(1)-C(21) ring distorts the octahedral coordination geometry of the central metal. While the pyridine ring is almost perpendicular to the N(22)N(23)N(24) plane with a dihedral angle of 83.3(2)°, the O-Ni-C(21) angle is only 39.19(16)°.

Table 5.1 Selected bond lengths (Å) for complex **153**.

Bond	Bond length (Å)	Bond	Bond length (Å)
Ni-C(21)	2.069(4)	N(2)-C(1)	1.393(5)
Ni-N(22)	2.088(3)	N(2)-C(3)	1.348(5)
Ni-N(23)	2.005(4)	C(3)-C(4)	1.409(5)
Ni-N(24)	2.100(3)	C(21)-C(1)	1.444(5)
Ni-N(25)	2.003(3)	C(21)-C(4)	1.427(5)
Ni-O(1)	2.037(4)	C(21)-O(1)	1.377(5)

Notably, complex **153** is structurally similar to an Fe(III) porphyrin N-oxide **154**, which was proposed as an alternative candidate of compound I, **155**, for the active intermediate of cytochrome P-450 (Figure 5.7).[18] An Fe(III) porphyrin N-oxide **157** was prepared from oxidation of an Fe(III) porphyrin **156** (Scheme 5.1) and was structurally characterized by Groves and Watanabe.[19] Octaethylporphyrin N-oxide, **159**, can be prepared by oxidation of octaethylporphyrin with maleic peracid (Scheme 5.2).[20] Metalations of **159** with $Ni(OAc)_2$ or $Cu(OAc)_2$ result in complexes **160 (a,b)**.[20,21] The X-ray crystal structures of **159** and the Ni(II) porphyrin N-oxide **160a** were reported by Balch *et al.*[21,22] The nitrogen atom bonded to oxygen is not bonded to the metal ion in complex **157** and **160a**.[19,21]

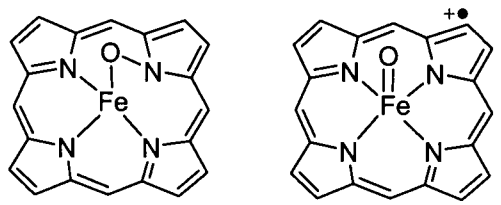

154 **155**

Figure 5.7 Structures of Fe(III) porphyrin N-oxide **154**, compound I, **155**.

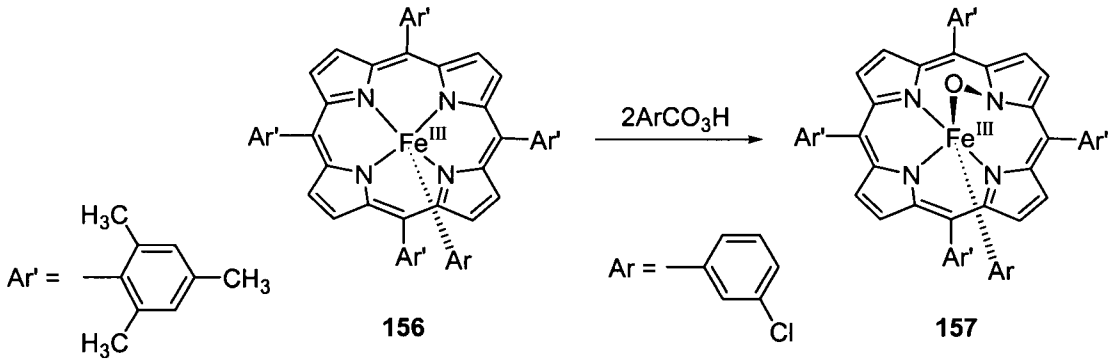

156 **157**

Scheme 5.1 Synthesis of Fe(III) porphyrin N-oxide **157**.

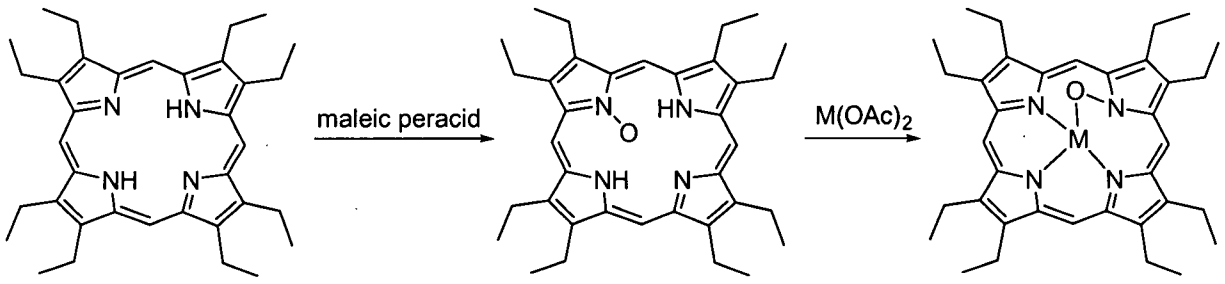

158 **159** **160a** M = Ni^{II} **160b** M = Cu^{II}

Scheme 5.2 Synthesis of porphyrin N-oxide **159** and metalloporphyrin N-oxide **160 (a,b)**.

5.2.2 Reaction Mechanism

Reactions at C(21) are not uncommon for N-confused porphyrin complexes. Methylations of (NCTPP)Ni^{II} and Cu(II) N(2)-methylated NCP **59** with CH_3I at the C(21) position readily proceed at room temperature (Scheme 1.13, Scheme 1.25).[8,16] Inner cyanide addition at C(21) was observed for (NCTTP)Ni^{II} in the presence of DDQ and $NaOCH_3$ (Chapter 4).

Three canonical forms for a Ni(II) N-confused porphyrin are shown in Scheme 5.3. The X-ray crystal structure of Ni(II) N(2)-iodooctyl N-confused tetraphenylporphyrin, **115** (section 2.2.3.1), shows that its N(2)-C(3) bond length, 1.311(4) Å, is markedly shorter than those of peripheral C-C bonds, 1.345(5) or 1.346(5) Å. Complex **115** is isoelectronic to Ni(II) N-confused porphyrins, and those bond lengths suggest that dipolar canonical forms **II** and **III**, which reserve the 18 π-electron pathway and have more double bond character for the N(2)-C(3) bond than canonical form **I**, are important contributors to the overall resonance hybrid.

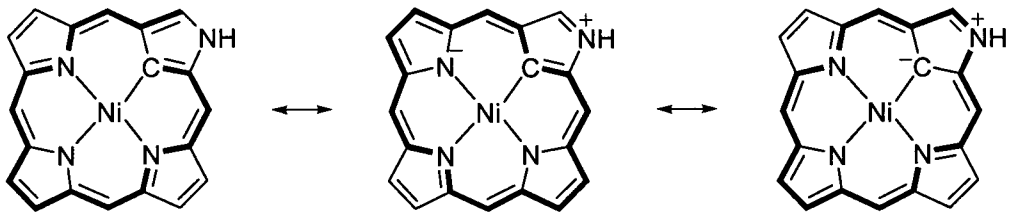

I **II** **III**

Scheme 5.3 Three canonical forms for a Ni(II) N-confused porphyrin.

In canonical form **III**, C(21) is negatively charged, which might explain why Ni(II) N-confused porphyrins readily methylate at C(21). Canonical form **III** could also be used to explain the susceptibility of C(21) towards oxidation. A possible mechanism for the oxidation of

(NCTTP)Ni^{II} with OsO_4 is shown in Scheme 5.4. Electrophilic addition of OsO_4 to (NCTTP)Ni^{II}, **129b**, at C(21) results in intermediate **161**. Rearrangement of **161** gives **162** and cleavage of the (C-)O-Os bond in **162** results in Ni(II) N-confused porphyrin C-oxide **163**. One-electron oxidation of **163**, followed by deprotonation and coordination of a pyridine gives Ni(III) N-confused porphyrin C-oxide **153**. The coordination of pyridine to the nickel ion at earlier steps is also possible.

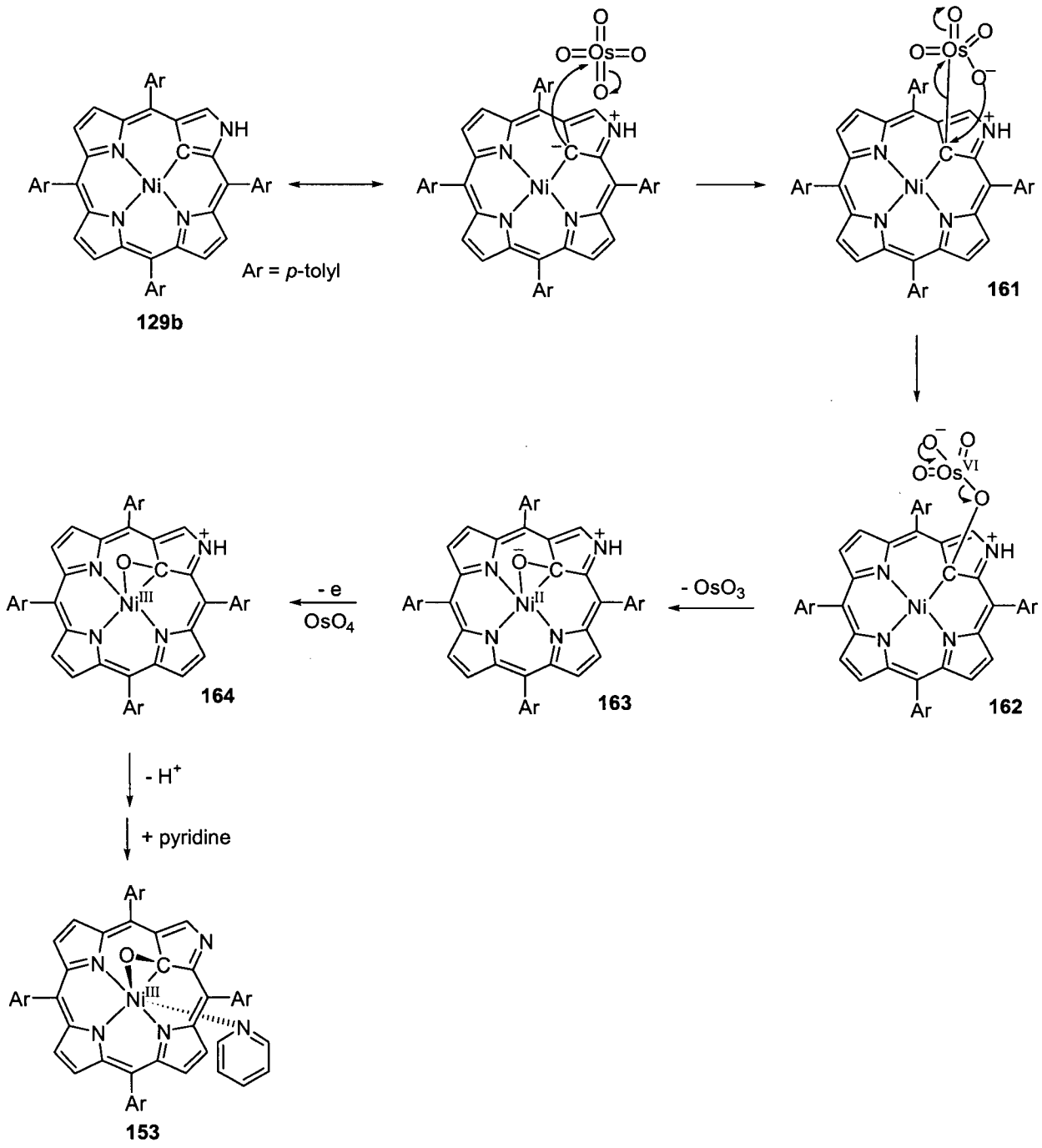

Scheme 5.4 A possible mechanism for the generation of complex **153**.

5.2.3 Optical Absorption Spectra

The UV-vis spectrum of complex **153** displays a broad absorption at 380 nm (50,000 M^{-1} cm^{-1}) with shoulder peaks at 428 nm and 470 nm (Figure 5.8). The absorption spectrum of **153** is much different from that of (NCTTP)Ni^{II}, suggesting a change of conjugation pathway after oxidation. Structure of **153** favors the outer C(1)-N(2)-C(3)-C(4) conjugation pathway as C(21) is sp^3 hybridized (Figure 5.9), while both inner C(1)-C(21)-C(4) and outer pathways are possible for (NCTTP)Ni^{II}. This change of conjugation pathway was also suggested for Ni(II) C(21)-methylated N-confused porphyrin **26** (section 1.4.4.1), and the UV-vis spectra of **26** and **153** are similar to each other.

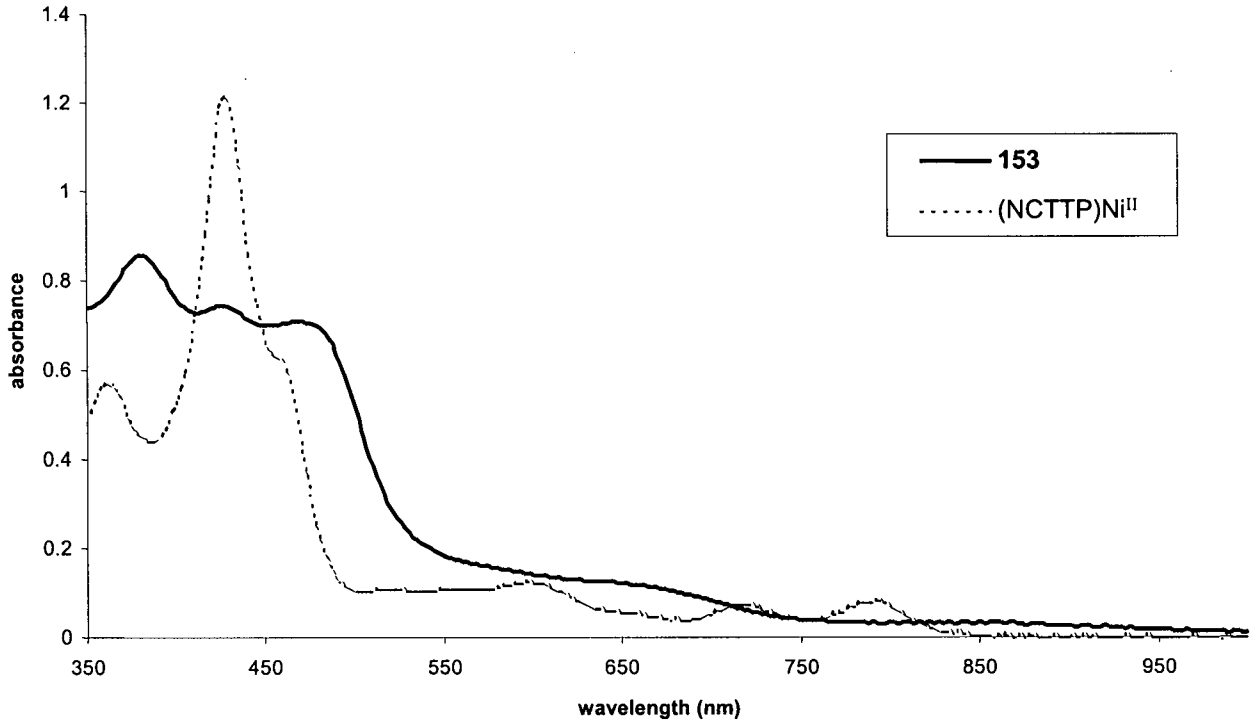

Figure 5.8 UV-vis spectra of **153** and (NCTTP)Ni^{II}.

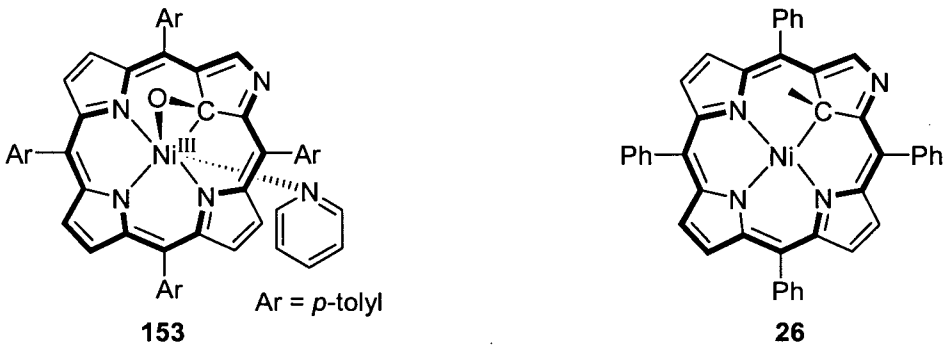

Figure 5.9 Structures of complexes **153** and **26** showing possible conjugation pathways.

5.3 Conclusion

A novel nickel complex of N-confused porphyrin inner C-oxide **153** was synthesized from the oxidation of the precursor Ni(II) N-confused porphyrin using OsO_4. This complex was characterized to be a Ni(III) complex based on its X-ray crystal structure, room temperature effective magnetic moment, and mass, NMR and EPR spectra.

Complex **153** was not the expected product, as dihydroxylation occurs for the reactions of Ni(II) porphyrins and OsO_4. However, reactions on C(21) are not uncommon for N-confused porphyrin complexes. In a dipole canonical form (**III**) of Ni(II) N-confused porphyrins (Scheme 5.3), the 18 π-electron pathway is reserved and C(21) is negatively charged. This canonical form could be used to explain the high reactivity of C(21) in NCP complexes.

References

1. Renner, M. W. and Fajer, J. *J. Biol. Inorg. Chem.* **2001,** *6*, 823.
2. Wolberg, A. and Manassen, J. *J. Am. Chem. Soc.* **1970,** *92*, 2982.
3. Dolphin, D., Niem, T., Felton, R. H. and Fujita, E. *J. Am. Chem. Soc.* **1975,** *97*, 5288.
4. Johnson, E. C., Niem, T. and Dolphin, D. *Can. J. Chem.* **1978,** *56*, 1381.
5. Chmielewski, P. J., Latos-Grażyński, L., Rachlewicz, K. and Glowiak, T. *Angew. Chem., Int. Ed. Engl.* **1994,** *33*, 779.
6. Furuta, H., Asano, T. and Ogawa, T. *J. Am. Chem. Soc.* **1994,** *116*, 767.
7. Chmielewski, P. J. and Latos-Grażyński, L. *Inorg. Chem.* **1997,** *36*, 840.
8. Chmielewski, P. J., Latos-Grażyński, L. and Schmidt, I. *Inorg. Chem.* **2000,** *39*, 5475.
9. Furuta, H., Ishizuka, T., Osuka, A., Uwatoko, Y. and Ishikawa, Y. *Angew. Chem., Int. Ed. Engl.* **2001,** *40*, 2323.
10. Furuta, H., Ogawa, T., Uwatoko, Y. and Araki, K. *Inorg. Chem.* **1999,** *38*, 2676.
11. Ogawa, T., Furuta, H., Takahashi, M., Morino, A. and Uno, H. *J. Organomet. Chem.* **2000,** *611*, 551.
12. Ermler, U., Grabarse, W., Shima, S., Goubeaud, M. and Thauer, R. K. *Science* **1997,** *278*, 1457.
13. Lahiri, G. K. and Stolzenberg, A. M. *Inorg. Chem.* **1993,** *32*, 4409.
14. Evans, D. A. *J. Am. Chem. Soc.* **1959,** *81*, 2003.
15. Sur, S. K. *J. Magn. Reson.* **1989,** *82*, 169.
16. Chmielewski, P. J., Latos-Grażyński, L. and Glowiak, T. *J. Am. Chem. Soc.* **1996,** *118*, 5690.

17. Alonso, P. J., Falvello, L. R., Fornies, J., Martin, A., Menjon, B. and Rodriguez, G. *Chem. Commun.* **1997**, 503.

18. Watanabe, Y. *J. Biol. Inorg. Chem.* **2001,** *6*, 846.

19. Groves, J. T. and Watanabe, Y. *J. Am. Chem. Soc.* **1986,** *108*, 7836.

20. Andrews, L. E., Bonnett, R., Ridge, R. J. and Appelman, E. H. *J. Chem. Soc., Perkin Trans. 1* **1983**, 103.

21. Balch, A. L., Chan, Y. W., Olmstead, M. and Renner, M. W. *J. Am. Chem. Soc.* **1985,** *107*, 2393.

22. Balch, A. L., Chan, Y. W. and Olmstead, M. *J. Am. Chem. Soc.* **1985,** *107*, 6510.

Chapter 6

Experimental

6.1 Instrumentation and General Materials

All chemicals for syntheses were purchased from Sigma-Aldrich fine chemicals, Across Chemicals, or Fisher Scientific. If necessary, chemicals were purified by published procedures.[1] Deuterated solvents for NMR measurements were purchased from Cambridge Isotope Laboratories or Aldrich. The silica gel was 230 - 400 mesh (Silicycle). Activity III basic alumina was obtained by adding 6 % water to activity I Brockman basic alumina, 60 - 325 mesh (Fisher). Analytical thin-layer chromatography was performed using pre-coated silica gel aluminum plates which contain a fluorescent indicator (GF 254 Merck).

The NMR spectra were recorded on a Bruker WH-400, a Bruker AV-400 or a Bruker AMX-500 in the solvents indicated and were referenced to residual solvent peaks. Elemental analyses were performed on a Carlo Erba Elemental Analyzer 1108. As N-confused porphyrins obtained are often hydroscopic, and H_2O has been observed in the X-ray crystal structures of N,N'-dimethylated N-confused porphyrin **108** and inner C(21)-cyano Ni(II) N-confused porphyrin **146**, H_2O was added to the formula in some cases to obtain acceptable elemental analysis results. The UV-vis spectra were measured with absorption in the range of 0.1 -1.0, on a Varian Cary 50 scan UV-visible spectrophotometer. Mass spectra were determined on a KRATOS Concept IIHQ hybrid mass spectrometer. X-ray crystallographic data were collected on a Rigaku/ADSC CCD. EPR spectrum was recorded on a Bruker ECS-106 spectrometer. Irradiations in the singlet oxygen test were carried with a 250 W Osram HLX 64655 arc lamp in an Oriel lamp housing (model 66184) and the light output passed through a filter: P70-700-S-Corion.

6.2 Experimental Data for Chapter 2

6.2.1 N-Confused Tetraarylporphyrins

General Procedure:

N-confused porphyrins were synthesized using a modification of the procedure of Lindsey and coworkers.[2] To a solution of pyrrole (0.52 mL, 7.5 mmol) and arylaldehyde (7.5 mmol) in CH_2Cl_2 (750 mL) was added methanesulfonic acid (MSA) (0.34 mL, 5.2 mmol). The mixture was stirred for 30 min after which DDQ (1.50 g, 6.6 mmol) was added. After 1 min, triethylamine (1.5 mL) was added. The crude reaction mixture was passed through a silica gel (14 × 4.4 cm) column under vacuum and eluted with CH_2Cl_2. 1.2 % Methanol/CH_2Cl_2 eluted the product with impurities. The fractions were collected and concentrated *in vacuo* and then absorbed onto 7.5 g of activity III basic alumina. The absorbed sample was added to the top of a column with 150 g activity III basic alumina in 2:1 hexanes/CH_2Cl_2. The polarity of the eluent was increased from 2:1 to 1:1 to 1:2 hexanes/CH_2Cl_2, the N-confused porphyrins were eluted with 1:2 hexanes/CH_2Cl_2 (in the case of compound **99** and **100**, the polarity of the eluent was increased from CH_2Cl_2 to 0.2 % methanol/CH_2Cl_2 to elute the product). The solvent was removed *in vacuo* and the residue was triturated with CH_2Cl_2/hexanes to yield the product. Compound **16a**, yield: 373 mg (32 %); compound **16b**, yield: 274 mg (22 %); compound **99**, yield: 259 mg (16 %); compound **100**, yield: 208 mg (15 %); compound **101**, yield: 316 mg (23 %).

2-Aza-5,10,15,20-tetraphenyl-21-carbaporphyrin (16a)

R_f (silica-CH_2Cl_2/5 % CH_3OH/2 % Et_3N) 0.54; ^{1}H-NMR (200 MHz, CD_2Cl_2) δ = -3.88 (s, 1H), -2.40 (br s, 2H), 7.69 - 7.94 (m, 12H), 8.12 - 8.26 (m, 4H), 8.31 - 8.45 (m, 4H), 8.53 -

8.66 (m, 4H), 8.78 (s, 1H), 8.94 (d, J = 4.9 Hz, 1H), 9.01 (d, J = 4.9 Hz, 1H); λ_{max}/nm (log ε) 438 (5.27), 542 (3.95), 582 (4.10), 726 (4.06); MS (EI) 614 (M^+, 100 %); HRMS (EI) *m/e* Calcd for $C_{44}H_{30}N_4$: 614.24705, found 614.24691 (M^+); Anal. Calcd for $C_{44}H_{30}N_4 \cdot H_2O$: C, 83.52; H, 5.10; N, 8.85. Found: C, 83.86; H, 4.77; N, 8.71. These data agree with the literature data.[3]

2-Aza-5,10,15,20-tetrakis(*p*-tolyl)-21-carbaporphyrin (16b)

R_f (silica-CH_2Cl_2/5 % CH_3OH/2 % Et_3N) 0.51; ^{1}H-NMR (400 MHz, CD_2Cl_2) δ = -5.00 (s, 1H), -2.43 (br s, 2H), 2.67 (s, 3H), 2.69 (s, 6H), 2.70 (s, 3H), 7.52 - 7.78 (m, 8H), 7.98 - 8.13 (m, 4H), 8.16 - 8.30 (m, 4H), 8.51 - 8.61 (m, 3H), 8.63 (d, J = 4.9 Hz, 1H), 8.70 (s, 1H), 8.93 (d, J = 4.9 Hz, 1H), 8.99 (d, J = 4.9 Hz, 1H); λ_{max}/nm (log ε) 440 (5.27), 542 (3.93), 586 (4.16), 732 (4.11); MS (LSIMS) 671 (MH^+, 100 %); Anal. Calcd for $C_{48}H_{38}N_4$: C, 85.94; H, 5.71; N, 8.35. Found: C, 86.01; H, 5.52; N, 8.45. These data agree with the literature data.[4]

2-Aza-5,10,15,20-tetrakis(*p*-methoxycarbonylphenyl)-21-carbaporphyrin (99)

R_f (silica-CH_2Cl_2/5 % CH_3OH/2 % Et_3N) 0.46; ^{1}H-NMR (400 MHz, CD_2Cl_2) δ = -5.24 (s, 1H), -2.56 (br s, 2H), 4.08 (d, 12H), 8.18 - 8.58 (m, 19H), 8.60 (d, J = 4.7 Hz, 1H), 8.70 (s, 1H), 8.84(d, J = 4.7 Hz, 1H), 8.94 (d, J = 4.7 Hz, 1H); UV-vis (CH_2Cl_2) λ_{max}/nm (log ε) 444 (5.31), 544 (4.07), 586 (4.22), 728 (4.15); MS (LSIMS) 847 (MH^+, 100 %); HRMS (LSIMS) *m/e* Calcd for $C_{52}H_{39}N_4O_8$: 847.27679, found 847.27667 (MH^+); Anal. Calcd for $C_{52}H_{38}N_4O_8$: C, 73.75; H, 4.52; N, 6.62. Found: C, 73.95; H, 4.49; N, 6.72.

2-Aza-5,10,15,20-tetrakis(*p*-methoxyphenyl)-21-carbaporphyrin (100)

R_f (silica-CH_2Cl_2/5 % CH_3OH/2 % Et_3N) 0.38; ^{1}H-NMR (400 MHz, CD_2Cl_2) δ = -4.92 (s, 1H), -2.31 (br s, 2H), 4.04 (s, 3H), 4.07 (s, 6H), 4.09 (s, 3H), 7.25 - 7.49 (m, 8H), 8.00 -

8.13(m, 4H), 8.25 (d, J = 8.6 Hz, 4H), 8.55(d, J = 5.2 Hz, 3H), 8.61 (d, J = 4.7 Hz, 1H), 8.64 (s, 1H), 8.89 (d, J = 4.4 Hz, 1H), 8.97 (d, J = 4.7 Hz, 1H); UV-vis (CH_2Cl_2) λ_{max}/nm (log ε) 442 (5.38), 514 (sh), 548 (sh), 592 (4.32), 736 (4.24); MS (LSIMS) 735 (MH^+, 100 %); HRMS (LSIMS) *m/e* Calcd for $C_{48}H_{39}N_4O_4$: 735.29713, found 735.29721 (MH^+); Anal. Calcd for $C_{48}H_{38}N_4O_4$: C, 78.45; H, 5.21; N, 7.62. Found: C, 78.11; H, 5.10; N, 7.71.

2-Aza-5,10,15,20-tetrakis(*m*-methoxyphenyl)-21-carbaporphyrin (101)

R_f (silica-CH_2Cl_2/5 % CH_3OH/2 % Et_3N) 0.50; ^{1}H-NMR (400 MHz, CD_2Cl_2) δ = -5.12 (s, 1H), -2.45 (br s, 2H), 3.98 (s, 6H), 4.02 (s, 3H), 4.06 (s, 3H), 7.22 - 7.45 (m, 4H), 7.58 - 7.82 (m, 8H), 7.82 - 8.00 (m, 4H), 8.55 - 8.66 (m, 3H), 8.68 (d, J = 4.7 Hz, 1H), 8.78 (s, 1H), 8.96(d, J = 4.7 Hz, 1H), 9.05(d, J = 5.2 Hz, 1H); UV-vis (CH_2Cl_2) λ_{max}/nm (log ε) 440 (5.34), 540 (4.06), 582 (4.13), 726 (4.11); MS (LSIMS) 735 (MH^+, 100 %); HRMS (LSIMS) *m/e* Calcd for $C_{48}H_{39}N_4O_4$: 735.29713, found 735.29827 (MH^+); Anal. Calcd for $C_{48}H_{38}N_4O_4$: C, 78.45; H, 5.21; N, 7.62. Found: C, 78.44; H, 5.18; N, 7.71.

6.2.2 N,N'-Dimethylated N-Confused Porphyrins

General Procedure:

N-confused porphyrin (100 mg) was dissolved in a minimal amount of CH_2Cl_2 (about 10 mL). To this solution, CH_3I (8 mL) and Na_2CO_3 (250 mg) were added. The mixture was stirred for 2 days in the absence of light, and then filtered through Celite. The filtrate was evaporated to dryness *in vacuo* and the residue was triturated with CH_2Cl_2/hexanes to yield the products. Compounds **103**, yield: 110 mg (88 %); compounds **104**, yield: 105 mg (85 %); compounds **105**, yield: 103 mg (87 %); compounds **106**, yield: 112 mg (92 %); compounds **107**, yield: 99 mg (82 %).

N,N'-Dimethylated 2-aza-5,10,15,20-tetraphenyl-21-carbaporphyrin·I^- (103)

R_f (silica-CH_2Cl_2/5 % CH_3OH/2 % Et_3N) 0.36; ^{1}H-NMR (400 MHz, CD_2Cl_2) δ = -1.62 (d, *J* = 1.4 Hz, 0.65H), -1.57 (d, *J* = 1.5 Hz, 0.35H), -1.48 (s, 3×0.65H), -1.39 (s, 3×0.35H), 3.62 (s, 3×0.35H), 3.82 (s, 3×0.65H), 7.18 - 8.54 (m, 27H); UV-vis (CH_2Cl_2) λ_{max}/nm (log ε) 382 (sh), 476 (4.85), 582 (3.79), 650 (3.73), 724 (sh), 788 (4.39); MS (LSIMS) 643 (M^+, 100 %); HRMS (LSIMS) *m/e* Calcd for $C_{46}H_{35}N_4$: 643.28617, found 643.28623 (M^+); Anal. Calcd for $C_{46}H_{35}N_4$·I·1.5H_2O: C, 69.26; H, 4.80; N, 7.02; I, 15.91. Found: C, 68.96; H, 4.76; N, 6.86; I, 15.82.

2-Aza-2,24-dimethyl-5,10,15,20-tetraphenyl-21-carbaporphyrin·$CF_3SO_3^-$ (108)

Compounds **103** (86 mg) were dissolved in 20 mL of CH_2Cl_2. Silver triflate (1.3 g) was added and the solution was stirred for 2 h. The mixture was passed through a silica gel column (14 g) and eluted with CH_2Cl_2 under vacuum. CH_2Cl_2 /1% CH_3OH eluted the porphyrin triflate salts. The compounds were recrystallized three times with CH_2Cl_2/hexanes giving **108** (29 mg). Crystals of **108** were obtained by solvent diffusion of hexanes into a CH_2Cl_2 solution of **108**. R_f (silica-CH_2Cl_2/5 % CH_3OH/2 % Et_3N) 0.36; ^{1}H-NMR (400 MHz, CD_2Cl_2) δ = -1.60 (s, 1H), -1.49 (s, 3H), 3.81 (s, 3H), 7.24 (d, *J* = 5.0 Hz, 1H), 7.43 (s, 1H), 7.62 (d, *J* = 5.0 Hz, 1H), 7.70 - 8.13 (m, 20H), 8.16 (d, *J* = 5.1 Hz, 1H), 8.20 (d, *J* = 5.1 Hz, 1H), 8.33 (d, *J* = 4.8 Hz, 1H), 8.47 (d, *J* = 6.4 Hz, 1H); ^{13}C-NMR (100 MHz, CD_2Cl_2) δ = 35.47, 39.93, 98.91, 123.55, 124.13, 127.42, 128.06, 128.11, 128.64, 129.00, 129.50, 130.00, 130.23, 131.51, 131.70, 131.88, 132.97, 134.38, 134.93, 136.03, 136.16, 136.92, 137.24, 137.63, 138.70, 139.69, 139.86, 140.54, 141.16, 150.96; UV-vis (CH_2Cl_2) λ_{max}/nm (log ε) 385 (sh), 475 (4.85), 580 (3.74), 650 (3.67), 724 (sh), 790 (4.41); MS (LSIMS) 643 (M^+, 100 %); Anal. Calcd for $C_{46}H_{35}N_4$·CF_3SO_3·1.5H_2O: C, 68.85;

H, 4.67; N, 6.83; S, 3.91. Found: C, 68.99; H, 4.61; N, 6.78; S, 4.00.

N,N'-Dimethylated 2-aza-5,10,15,20-tetrakis(*p*-tolyl)-21-carbaporphyrin·I⁻ (104)

R_f (silica-CH_2Cl_2/5 % CH_3OH/2 % Et_3N) 0.36; ^{1}H-NMR (400 MHz, CD_2Cl_2) δ = -1.53 (d, *J* = 1.7 Hz, 0.65H), -1.48 (s, 3×0.65H), -1.45 (d, *J* = 1.7 Hz, 0.35H), -1.34 (s, 3×0.35H), 2.65 (m, 12H), 3.61 (s, 3×0.35H), 3.81 (s, 3×0.65H), 7.1 - 8 .5 (m, 23H); UV-vis (CH_2Cl_2) λ_{max}/nm (log ε) 392 (sh), 478 (4.85), 588 (3.64), 646 (3.69), 798 (4.22); MS (LSIMS) 699 (M^+, 100 %); HRMS (LSIMS) *m/e* Calcd for $C_{50}H_{43}N_4$: 699.34877, found 699.34859 (M^+); Anal. Calcd for $C_{50}H_{43}N_4$·I·0.5H_2O: C, 71.85; H, 5.31; N, 6.70. Found: C, 71.85; H, 5.41; N, 6.70.

2-Aza-2,24-dimethyl-5,10,15,20-tetrakis(*p*-tolyl)-21-carbaporphyrin·I⁻ (104-III)

Compounds **104** (109 mg) were recrystallized three times with CH_2Cl_2/hexanes to give the major isomer **104-III** (34 mg). R_f (silica-CH_2Cl_2/5 % CH_3OH/2 % Et_3N) 0.36; ^{1}H-NMR (400 MHz, CD_2Cl_2) δ = -1.55 (d, *J* = 1.7 Hz, 1H), -1.49 (s, 3H), 2.63 (s, 6H), 2.66 (s, 6H), 3.82 (s, 3H), 7.22 (d, *J* = 5.2 Hz, 1H), 7.33 (d, *J* = 1.3 Hz, 1H), 7.51 - 8.05 (m, 17H), 8.15 (d, *J* = 5.2 Hz, 1H), 8.18 (d, *J* = 5.2 Hz, 1H), 8.29 (d, *J* = 4.7 Hz, 1H), 8.34 (br s, 1H); ^{13}C-NMR (100 MHz, CD_2Cl_2) δ = 21.54, 21.56, 21.61, 21.83, 35.21, 39.72, 98.64, 114.12, 123.50, 123.96, 127.53, 128.60, 128.79, 128.89, 129.33, 130.01, 130.51, 130.68, 131.30, 131.60, 132.75, 134.25, 134.79, 135.06, 135.90, 136.85, 137.09, 137.45, 137.86, 137.89, 139.08, 139.76, 140.67, 141.30, 142.83, 147.10, 149.30, 150.88, 152.18, 160.56, 160.76; UV-vis (CH_2Cl_2) λ_{max}/nm (log ε) 390 (sh), 435 (sh), 480 (4.78), 585 (3.54), 650 (3.56), 800 (4.26); MS (LSIMS) 699 (M^+, 100 %); Anal. Calcd for $C_{50}H_{43}N_4$·I·H_2O: C, 71.08; H, 5.37; N, 6.63; I, 15.02. Found: C, 71.05; H, 5.31; N, 6.58; I, 14.95.

N,N'-Dimethylated 2-aza-5,10,15,20-tetrakis(*p*-methoxycarbonylphenyl)-21-carba-porphyrin·I⁻ (105)

R_f (silica-CH_2Cl_2/5 % CH_3OH/2 % Et_3N) 0.36; ^{1}H-NMR (400 MHz, CD_2Cl_2) δ = -1.79 (m, 1H), -1.49 (m, 3H), 3.65 (s, 3×0.27H), 3.87 (s, 3×0.73H), 4.05 (m, 12H), 7.20 - 8.73 (m, 23H); UV-vis (CH_2Cl_2) λ_{max}/nm (log ε) 386 (sh), 478 (4.84), 576 (3.86), 652 (3.81), 726 (sh), 792 (4.24); MS (LSIMS) 875 (M^+, 100 %); HRMS (LSIMS) *m/e* Calcd for $C_{54}H_{43}N_4O_8$: 875.30809, found 875.30815 (M^+); Anal. Calcd for $C_{54}H_{43}N_4O_8$·I·2.5H_2O: C, 61.89; H, 4.62; N, 5.35. Found: C, 61.99; H, 4.42; N, 5.20.

2-Aza-2,24-dimethyl-5,10,15,20-tetrakis(*p*-methoxycarbonylphenyl)-21-carbaporphyrin·I⁻ (105-III)

Compounds **105** (78.5 mg) were recrystallized three times with CH_2Cl_2/hexanes to give the major isomer **105-III** (29 mg). R_f (silica-CH_2Cl_2/5 % CH_3OH/2 % Et_3N) 0.36; ^{1}H-NMR (400 MHz, $CDCl_3$) δ = -1.45 (d, 4H), 3.91 (s, 3H), 4.06 (s, 12H), 7.19 (s, 1H), 7.52 (s, 2H), 7.82 - 8.85 (m, 20H); ^{13}C-NMR (125 MHz, CD_2Cl_2) δ = 35.83, 40.50, 52.73, 52.78, 52.83, 52.94, 99.08, 114.20, 122.42, 123.95, 126.95, 128.01, 128.86, 129.15, 129.52, 129.59, 129.99, 130.27, 130.49, 130.76, 130.82, 130.89, 130.96, 131.18, 131.47, 131.55, 132.17, 132.81, 133.03, 134.28, 134.53, 135.19, 135.98, 136.06, 136.17, 137.05, 139.68, 139.90, 141.03, 143.82, 144.00, 144.46, 150.73, 160.48, 166.74, 167.02, 167.08; UV-vis (CH_2Cl_2) λ_{max}/nm (log ε) 385 (sh), 480 (4.83), 585 (3.67), 655 (3.16), 725 (sh), 790 (4.26); MS (LSIMS) 875 (M^+, 100 %); Anal. Calcd for $C_{54}H_{43}N_4O_8$·I·H_2O: C, 63.53; H, 4.44; N, 5.49; I, 12.43. Found: C, 63.26; H, 4.55; N, 5.48; I, 12.20.

N,N'-Dimethylated 2-aza-5,10,15,20-tetrakis(*p*-methoxyphenyl)-21-carbaporphyrin·I⁻ (106)

R_f (silica-CH_2Cl_2/5 % CH_3OH/2 % Et_3N) 0.36; ^{1}H-NMR (400 MHz, CD_2Cl_2) δ = -1.43 (s, 3×0.7H), -1.37 (d, J = 1.5 Hz, 1×0.7H), -1.22 (d, 4×0.3H), 3.60 (s, 3×0.3H), 3.82 (s, 3×0.7H), 4.00 - 4.14 (m, 12H), 7.07 - 8.50 (m, 23H); UV-vis (CH_2Cl_2) λ_{max}/nm (log ε) 436 (4.82), 486 (4.97), 592 (3.62), 662 (3.82), 818 (4.40); MS (LSIMS) 763 (M^+, 100 %); Anal. Calcd for $C_{50}H_{43}N_4O_4 \cdot I \cdot 1.5H_2O$: C, 65.43; H, 5.05; N, 6.10. Found: C, 65.67; H, 4.88; N, 5.98.

2-Aza-2,24-dimethyl-5,10,15,20-tetrakis(*p*-methoxyphenyl)-21-carbaporphyrin·I⁻ (106-III)

Compounds **106** (89 mg) were recrystallized three times with CH_2Cl_2/hexanes to give the major isomer **106-III** (37 mg). R_f (silica-CH_2Cl_2/5 % CH_3OH/2 % Et_3N) 0.36; ^{1}H-NMR (500 MHz, $CDCl_3$) δ = -1.47 (s, 3H), -1.44 (s, 1H), 3.81 (s, 3H), 4.01 - 4.13 (m, 12H), 7.16 (d, J = 4.9 Hz, 1H), 7.19 (s, 1H), 7.28 (m, 4H), 7.38 (d, J = 8.6 Hz, 2H), 7.46 (m, 2H), 7.56 (d, J = 4.9 Hz, 1H), 7.75 (d, J = 4.7 Hz, 1H), 7.84 (d, J = 8.7 Hz, 2H), 7.91 (d, J = 7.0 Hz, 2H), 8.04 (m, 3H), 8.11 (d, J = 5.1Hz, 1H), 8.14 (d, J = 4.6 Hz, 1H), 8.15 (d, J = 5.1 Hz, 1H), 8.40 (d, J = 6.4 Hz, 1H); ^{13}C-NMR (125 MHz, CD_2Cl_2) δ = 35.02, 39.48, 55.97, 56.04, 56.21, 56.38, 98.68, 113.27, 113.51, 113.64, 113.79, 113.97, 114.08, 115.24, 116.37, 122.90, 123.70, 127.73, 128.25, 129.77, 130.56, 130.60, 130.99, 131.19, 132.17, 132.37, 132.40, 133.37, 135.49, 135.93, 136.44, 136.52, 136.88, 137.24, 138.78, 139.19, 141.06, 146.55, 148.80, 150.75, 152.21, 160.39, 160.54, 160.94, 161.95, 163.24; UV-vis (CH_2Cl_2) λ_{max}/nm (log ε) 436 (4.78), 486 (4.91), 590 (3.56), 658 (3.74), 824 (4.37); MS (LSIMS) 763 (M^+, 100 %); HRMS (LSIMS) *m/e* Calcd for $C_{50}H_{43}N_4O_4$: 763.32843, found 763.32857 (M^+); Anal. Calcd for $C_{50}H_{43}N_4O_4 \cdot I$: C, 67.40; H, 4.87; N, 6.29; I, 14.25. Found: C, 67.11; H, 4.97; N, 6.16; I, 14.09.

N,N'-Dimethylated 2-aza-5,10,15,20-tetrakis(*m*-methoxyphenyl)-21-carbaporphyrin·I⁻ (107)

R_f (silica-CH_2Cl_2/5 % CH_3OH/2 % Et_3N) 0.36; ^{1}H-NMR (400 MHz, CD_2Cl_2) δ = -1.61 (m, 1H), -1.48 (d, 3×0.7H), -1.39 (s, 3×0.3H), 3.68 (s, 3×0.3H), 3.86 (s, 3×0.7H), 3.95- 4.17 (m, 12H), 7.21 - 8.42 (m, 23H); UV-vis (CH_2Cl_2) λ_{max}/nm (log ε) 378 (sh), 478 (4.95), 584 (3.81), 654 (3.74), 724 (sh), 788 (4.38); MS (LSIMS) 763 (M^+, 100 %); HRMS (LSIMS) *m/e* Calcd for $C_{50}H_{43}N_4O_4$: 763.32843, found 763.32854 (M^+); Anal. Calcd for $C_{50}H_{43}N_4O_4 \cdot I \cdot 0.5H_2O$: C, 66.74; H, 4.93; N, 6.23; I, 14.10. Found: C, 66.72; H, 4.93; N, 6.30; I, 13.97.

Singlet Oxygen Tests of N,N'-Dimethylated N-Confused Porphyrin Salts

A solution containing DPBF and an N,N'-dimethylated N-confused porphyrin salt (one of compounds **103 - 107** or the major isomer of **103 - 106**) (OD = 0.8 - 1.0 at 418 nm, OD = ~0.2 at irradiation wavelength) was prepared and the UV-vis spectra were measured. The solution was then irradiated with a halogen lamp (a 250 W Osram HLX 64655 arc lamp in an Oriel lamp housing, model 66184, at 30V) using a filter (~700 nm, P70-700-S-Corion) for four 20 second intervals (the UV cell is about 1 cm away from the filter) and UV-vis spectra were taken after each interval. Substantial decay of the signal around 418 nm was observed in all cases.[5] No change in UV-vis spectra was observed after a sample containing DPBF and an N,N'-dimethylated N-confused porphyrin salt was left in the dark for 10 min, and there was also no change in UV-vis spectra after irradiating a solution containing only DPBF or an N,N'-dimethylated N-confused porphyrin salt for 1 min.

6.2.3 Synthesis towards C,N-Strapped N-Confused Porphyrins

6.2.3.1 Synthesis of Iodoalkylated N-Confused Porphyrins

A $CHCl_3$ solution (25 mL) of NCTPP (153 mg) and $I(CH_2)_6I$ (1.76 g) was refluxed for three days under N_2, shielded from light. The reaction mixture was then chromatographed with silica gel (14 g) under vacuum and eluted with CH_2Cl_2/methanol. 0.8 % Methanol/CH_2Cl_2 eluted NCTPP with some impurities and 2 % methanol/CH_2Cl_2 eluted **112** (142 mg, 69 %).

2-Aza-2-iodohexyl-5,10,15,20-tetraphenyl-21-carbaporphyrin (112)

R_f (silica-CH_2Cl_2/5 % CH_3OH/2 % Et_3N) 0.43; ^{1}H-NMR (300 MHz, CD_2Cl_2) δ = -2.90 (s, 1H), 0.62 (m, 2H), 0.89 (m, 2H), 1.19 (m, 2H), 1.36 (m, 2H), 2.87 (t, J = 6.8 Hz, 2H), 4.01 (t, J = 7.7 Hz, 2H), 7.59 (s, 1H), 7.70 – 8.42 (m, 24H), 8.67 (d, J = 5.1 Hz, 1H), 8.85 (d, J = 5.0 Hz, 1H); MS (LSIMS) 825 (M^+, 100 %); HRMS (LSIMS) *m/e* Calcd for $C_{50}H_{42}N_4I$: 825.24542, found 825.24554 (M^+); Anal Calcd for $C_{50}H_{42}N_4I \cdot HI \cdot 2.5H_2O$: C, 60.19; H, 4.75; N, 5.62. Found: C, 60.17; H, 4.40; N, 5.72.

6.2.3.2 Synthesis of Ni(II) Iodoalkylated N-Confused Porphyrins

N-confused porphyrin **112** (73 mg) and $Ni(OAc)_2 \cdot 4H_2O$ (0.36 g) were dissolved in CH_2Cl_2/CH_3OH (2:3) and the solution was stirred for 24 h.[4] The solvent was then removed *in vacuo*, and the residue was separated with silica gel (12 g) column eluting with CH_2Cl_2 to give Ni(II) complex **114** (92 %). Ni(II) complex **115** was obtained similarly with a yield of 95 %.

2-Aza-2-iodohexyl-5,10,15,20-tetraphenyl-21-carbaporphyrinatonickel(II) (114)

R_f (silica-CH_2Cl_2/hexanes 1:1) 0.47; ^{1}H-NMR (400 MHz, CD_2Cl_2) δ= 0.96 (m, 2H), 1.21 (m, 2H), 1.67 (m, 4H), 3.10 (t, J = 7.0 Hz, 2H), 3.80 (t, J = 7.8 Hz, 2H), 7.56 - 7.69 (m, 12H),

7.77 (d, J = 5.0 Hz, 1H), 7.80 - 7.97 (m, 12H), 8.09 (d, J = 5.1 Hz, 1H), 8.44 (s, 1H); ^{13}C-NMR (100 MHz, CD_2Cl_2) δ = 7.12, 25.85, 30.15, 32.13, 33.61, 52.41, 127.20, 127.38, 127.46, 127.65, 127.80, 127.96, 128.27, 128.75, 130.20, 132.20, 132.34, 132.84,133.51, 133.55, 133.80, 141.80, 152.44; UV-vis (CH_2Cl_2) λ_{max}/nm (log ε) 364 (4.68), 430 (4.98), 462 (sh), 562 (4.05), 718 (3.71), 786 (3.70); MS (LSIMS) 881 (M^+, 100 %).

2-Aza-2-iodooctyl-5,10,15,20-tetraphenyl-21-carbaporphyrinatonickel(II) (115)

R_f (silica-CH_2Cl_2/hexanes 1:1) 0.20; ^{1}H-NMR (400 MHz, CD_2Cl_2) δ = 0.95 (m, 2H), 1.14 (m, 4H), 1.32 (m, 2H), 1.68 (m, 4H), 3.48 (t, J = 6.7 Hz, 2H), 3.78 (t, J = 7.8 Hz, 2H), 7.55 - 7.68 (m, 12H), 7.75 - 7.98 (m, 13H), 8.09 (d, J = 5.1 Hz, 1H), 8.45 (s, 1H); ^{13}C-NMR (100 MHz, CD_2Cl_2) δ = 26.79, 27.02, 28.96, 29.14, 32.26, 32.90, 45.60, 52.46, 117.51, 118.65, 122.03, 124.31, 126.13, 127.18, 127.38, 127.46, 127.65, 127.77, 127.95, 128.24, 128.70, 130.18, 131.34, 132.20, 132.33, 133.45, 133.52, 133.56, 133.80, 134.16, 139.71, 140.27, 141.83, 144.36, 146.24, 148.04, 149.47, 150.97, 152.52, 153.09; MS (LSIMS) 909 (M^+, 33 %), 818 (100 %).

6.2.3.3 Synthesis of C,N Strapped N-Confused Porphyrins

Compound **115** (63.1 mg) was refluxed with $AgBF_4$ (253 mg) in 150 mL fresh distilled CH_3CN/CH_2Cl_2 (1:1) for 24 h. The solvent was then removed *in vacuo*, and the residue was chromatographed with silica gel (12 g) eluting with 1.5 % methanol/CH_2Cl_2 to give complex **111** (28.3 mg, 52 %), MS (LSIMS) 781 (M^+, 100 %). Complex **116** was obtained similarly with a yield of 56 %, MS (LSIMS) 753 (M^+, 100 %).

6.3 Experimental Data for Chapter 3

6.3.1 Ni(II) N-Confused Porphyrins

To a solution of pyrrole (1.04 mL, 15 mmol) and arylaldehyde (15 mmol) in CH_2Cl_2 (750 mL) was added MSA (0.98 mL, 15 mmol).[2] The mixture was stirred for 8 min after which DDQ (3.00 g, 13.2 mmol) was added. After 1 min, triethylamine (1.5 mL) was added. The crude reaction mixture was passed through a silica gel column (14 × 4.4 cm) under vacuum and eluted with CH_2Cl_2. CH_2Cl_2/1.2 % methanol eluted the product with impurities. The fractions were collected and dried *in vacuo*. The residue and $Ni(OAc)_2 \cdot 4H_2O$ (3.50 g) were dissolved in 500 mL CH_2Cl_2/CH_3OH (1:1) and the solution was stirred for 24 h.[4] The solvent was then removed *in vacuo*, and the residue was purified with a silica gel column (12 × 4.4 cm) under vacuum eluting with CH_2Cl_2 (in the cases of **129d** and **129e**, 0.4 % methanol/CH_2Cl_2 eluted the product) to give the Ni(II) complex. Compound **129a**, yield: 405 mg, (16 %); compound **129b**, yield: 306 mg, (11 %); compound **129c**, yield: 257 mg, (7.5 %); compound **129d**, yield: 216 mg, (6.4 %); compound **129e**, yield: 389 mg, (13 %).

2-Aza-5,10,15,20-tetraphenyl-21-carbaporphyrinatonickel(II) (129a)

R_f (silica-CH_2Cl_2/hexanes 3:1) 0.59; ^{1}H-NMR (400 MHz, CD_2Cl_2) δ = 7.56 - 7.64 (m, 9H), 7.65 - 7.71 (m, 3H), 7.77 - 7.86 (m, 6H), 7.86 - 7.95 (m, 6H), 8.06 (d, J = 4.7 Hz, 1H), 8.09 (d, J = 5.2 Hz, 1H), 8.57 (d, J = 3.9 Hz, 1H), 10.24 (br s, 1H); UV-vis (CH_2Cl_2) λ_{max}/nm (log ε) 359 (sh), 426 (4.92), 596 (3.92), 718 (3.66), 788 (3.71); MS (LSIMS) 670 (M^+, 100%). These data agree with the literature data.[6]

2-Aza-5,10,15,20-tetrakis(*p*-tolyl)-21-carbaporphyrinatonickel(II) (129b)

R_f (silica-CH_2Cl_2/hexanes 3:1) 0.70; ^{1}H-NMR (400 MHz, CD_2Cl_2) δ = 2.57 (d, 12H), 7.37-7.52 (m, 8H), 7.65-7.81 (m, 9H), 7.83 (d, *J* = 5.2 Hz, 1H), 7.88 (d, *J* = 5.2 Hz, 1H), 7.92 (d, *J* = 5.2 Hz, 1H), 8.05 (d, *J* = 4.7 Hz, 1H), 8.09 (d, *J* = 5.2 Hz, 1H), 8.56 (d, *J* = 3.4 Hz, 1H), 10.20 (br s, 1H); UV-vis (CH_2Cl_2) λ_{max}/nm (log ε) 362 (4.62), 428 (4.95), 598 (3.97), 720 (3.73), 792 (3.77); MS (LSIMS) 726 (M^+, 100%); HRMS (LSIMS) *m/e* Calcd for $C_{48}H_{36}N_4Ni$: 726.22930, found 726.22923 (M^+); Anal. Calcd for $C_{48}H_{36}N_4Ni \cdot 0.5H_2O$: C, 78.28; H, 5.06; N, 7.61. Found: C, 78.00; H, 4.87; N, 7.41. These data agree with the literature data.[4]

2-Aza-5,10,15,20-tetrakis(*p*-chlorophenyl)-21-carbaporphyrinatonickel(II) (129c)

R_f (silica-CH_2Cl_2/hexanes 3:1) 0.75; ^{1}H-NMR (400 MHz, CD_2Cl_2) δ = 7.56 - 7.95 (m, 20H), 8.04 (d, *J* = 4.9 Hz, 1H), 8.07 (d, *J* = 5.7 Hz, 1H), 8.56 (d, *J* = 3.8 Hz, 1H), 10.17 (br s, 1H); UV-vis (CH_2Cl_2) λ_{max}/nm (log ε) 362 (sh), 426 (4.95), 600 (3.99), 720 (3.71), 792 (3.71); MS (LSIMS) 809 (MH^+ [$C_{44}H_{25}{}^{35}Cl_3{}^{37}ClN_4Ni$], 100%).

2-Aza-5,10,15,20-tetrakis(*p*-methoxycarbonylphenyl)-21-carbaporphyrinatonickel(II) (129d)

R_f (silica-CH_2Cl_2/1 % CH_3OH) 0.22; ^{1}H-NMR (400 MHz, CD_2Cl_2) δ = 4.02 (d, 12H), 7.77 (d, *J* = 4.9 Hz, 1H), 7.81 (d, *J* = 4.9 Hz, 1H), 7.85 - 8.10 (m, 12H), 8.22 - 8.39 (m, 8H), 8.56 (d, *J* = 3.8 Hz, 1H), 10.19 (br s, 1H); UV-vis (CH_2Cl_2) λ_{max}/nm (log ε) 364 (4.52), 428 (4.88), 598 (3.90), 722 (3.60), 794 (3.62); MS (LSIMS) 903 (MH^+, 100%); HRMS (LSIMS) *m/e* Calcd for $C_{52}H_{37}N_4O_8Ni$: 903.19643, found 903.19619 (MH^+); Anal. Calcd for $C_{52}H_{36}N_4O_8Ni$: C, 69.12; H, 4.02; N, 6.20. Found: C, 69.14; H, 4.06; N, 6.44.

2-Aza-5,10,15,20-tetrakis(*p*-methoxyphenyl)-21-carbaporphyrinatonickel(II) (129e)

R_f (silica-CH_2Cl_2/1 % CH_3OH) 0.68; ^{1}H-NMR (400 MHz, CD_2Cl_2) δ = 3.96 - 4.01 (m, 12H), 7.10 - 7.25 (m, 8H), 7.69 - 7.87 (m, 10H), 7.90 (d, *J* = 5.3 Hz, 1H), 7.93 (d, *J* = 5.3 Hz, 1H), 8.07 (d, *J* = 4.9 Hz, 1H), 8.10 (d, *J* = 4.9 Hz, 1H), 8.59 (d, *J* = 3.8 Hz, 1H), 10.22 (br s, 1H); UV-vis (CH_2Cl_2) λ_{max}/nm (log ε) 368 (4.59), 428 (4.94), 600 (3.99), 722 (3.80), 794 (3.85); MS (LSIMS) 791 (MH^+, 100%); HRMS (LSIMS) *m/e* Calcd for $C_{48}H_{37}N_4O_4Ni$: 791.21679, found 791.21730 (MH^+); Anal. Calcd for $C_{48}H_{36}N_4O_4Ni$: C, 72.84; H, 4.58; N, 7.08. Found: C, 73.18; H, 4.51; N, 7.38.

6.3.2 Preparation of Sultine

A suspension of sodium hydroxymethanesulfinate (rongalite) (6.0 g, 40 mmol) was stirred with a solution of α,α'-dibromo-*o*-xylene (20 mmol) and TBAB (4 mmol) in DMF (40 mL) at 0 °C for 4 h.[7] Water (300 mL) was then added and the precipitate was removed by filtration. The filtrate was extracted with ethyl ether and chromatographed on silica gel (16 g) with hexanes/CH_2Cl_2 (1:1) to yield sultine **130** 2.31 g (69 %).

1,4-Dihydro-2,3-benzoxathiin 3-oxide (130)

^{1}H-NMR (400 MHz, CD_2Cl_2) δ= 3.56 (d, *J* = 15.6 Hz, 1H), 4.38 (d, *J* = 15.6 Hz, 1H), 4.96 (d, *J* = 13.7 Hz, 1H), 5.28 (d, *J* = 13.7 Hz, 1H), 7.20 - 7.31 (m, 2H), 7.33 - 7.45 (m, 2H); MS (LSIMS) 169 (MH^+, 100%). These data agree with the literature data.[7]

6.3.3 Diels-Alder Reactions of Ni(II) N-Confused Porphyrins as Dienophiles

A solution of (NCTPP)Ni^{II} (**129a**, 100 mg) and sultine **130** (1.50 g) was refluxed in benzene (50 mL) for 2 days. The solvent was removed *in vacuo* and the residue was purified

with a silica gel column (14 g) using hexanes/CH_2Cl_2 (1:1). The product, **133a**, which has a higher R_f value than that of **129a**, was obtained in 23 % yield. Complexes **133b** and **133c** were synthesized in a similar way with the yield of 25 % and 18 %, respectively.

Ni(II) N-confused tetraphenylisoquinoporphyrin (133a)

R_f (silica-CH_2Cl_2/hexanes 2:1) 0.77; ^{1}H-NMR (400 MHz, CD_2Cl_2) δ = 6.91 (s, 1H), 7.11 (d, *J* = 8.6 Hz, 1H), 7.27 (m, 2H), 7.46 (m, 1H), 7.55 - 8.05 (m, 20H), 8.22 (m, 2H), 8.29 (m, 3H), 8.36 (d, *J* = 4.9 Hz, 1H), 8.57 (s, 1H); UV-vis (CH_2Cl_2) λ_{max}/nm (log ε) 438 (5.07), 628 (4.62); MS (LSIMS) 770 (M^+, 100%); HRMS (LSIMS) *m/e* Calcd for $C_{52}H_{32}N_4Ni$: 770.19799, found 770.19797 (M^+); Anal. Calcd for $C_{52}H_{32}N_4Ni{\cdot}0.5H_2O$: C, 80.02; H, 4.26; N, 7.18. Found: C, 79.88; H, 4.11; N, 6.95.

Ni(II) N-confused tetrakis(*p*-tolyl)isoquinoporphyrin (133b)

R_f (silica-CH_2Cl_2/hexanes 2:1) 0.77; ^{1}H-NMR (300 MHz, CD_2Cl_2) δ = 2.61 (s, 3H), 2.63 (s, 6H), 2.70 (s, 3H), 6.87 (s, 1H), 6.90 (s, 1H), 7.14 - 7.25 (m, 2H), 7.36 - 7.55 (m, 9H), 7.64 (d, *J* = 7.9 Hz, 2H), 7.76 (d, *J* = 7.9 Hz, 2H), 7.87 (d, *J* = 7.5 Hz, 4H), 8.19 - 8.27 (m, 3H), 8.28 - 8.35 (m, 3H), 8.42 (s, 1H); UV-vis (CH_2Cl_2) λ_{max}/nm (log ε) 440 (5.07), 628 (4.75); MS (LSIMS) 827 (MH^+, 100%); HRMS (LSIMS) *m/e* calc'd for $C_{56}H_{41}N_4Ni$: 827.26842, found 827.27036 (MH^+).

Ni(II) N-confused tetrakis(*p*-chlorophenyl)isoquinoporphyrin (133c)

R_f (silica-CH_2Cl_2/hexanes 2:1) 0.44; ^{1}H-NMR (400 MHz, CD_2Cl_2) δ = 7.06 (s, 1H), 7.18 (d, *J* = 8.6 Hz, 1H), 7.37 (m, 2H), 7.49 - 7.95 (m, 17H), 8.15 - 8.33 (m, 6H), 8.66 (s, 1H); MS (LSIMS) 908 (M^+ [$C_{52}H_{28}{}^{35}Cl_3{}^{37}ClN_4Ni$], 100%); HRMS (LSIMS) *m/e* Calcd for $C_{52}H_{28}{}^{35}Cl_3{}^{37}ClN_4Ni$: 908.03916, found 908.03956 (M^+).

6.3.4 Demetalation of Ni(II) N-Confused Tetraphenylisoquinoporphyrin

Complex **133a** (40 mg) was dissolved in 10 % TFA/CH_2Cl_2. After 24 h, the solution was washed with saturated aqueous Na_2CO_3 solution. The solvent was then removed *in vacuo* and the residue was purified on a silica gel column (12 g). CH_2Cl_2/4 % CH_3OH/0.5 % Et_3N eluted the product. This collection was concentrated and washed with aqueous NaCl solution. The solvent was removed *in vacuo* and the residue was triturated with CH_2Cl_2/hexanes to give demetalation product **135** 24.6 mg (63 %).

N-confused tetraphenylisoquinoporphyrin 135

R_f (silica-CH_2Cl_2/5 % CH_3OH/2 % Et_3N) 0.29; ^{1}H-NMR (500 MHz, CD_2Cl_2) δ = 7.19 (s, 1H), 7.29 - 7.58 (m, 4H), 7.70 (s, 6H), 7.78 - 7.94 (m, 6H), 8.00 - 8.30 (m, 10H), 8.31 - 8.45 (m, 4H), 8.84 (s, 1H); MS (LSIMS) 715 (MH^+, 100%); HRMS (LSIMS) *m/e* Calcd for $C_{52}H_{35}N_4$: 715.28617, found 715.28614 (MH^+).

6.3.5 Diels-Alder Reactions of Ni(II) N(2)-Methylated N-Confused Porphyrins

A solution of Ni(II) N(2)-methylated N-confused tetra(*p*-tolyl)porphyrin (80 mg) and sultine **130** (1.50 g) was refluxed in benzene (60 mL) for 2 days. The solvent was removed *in vacuo* and the residue was subjected to column chromatography with a silica gel (14 g) using hexanes/CH_2Cl_2. Compound **137** was obtained with impurities. MS (LSIMS) 860 (100%); HRMS (LSIMS) 860.30121 *m/e*.

6.3.6 1,3-Dipolar Cycloaddition of Ni(II) N-Confused Porphyrins

A solution of (NCTPP)Ni^{II} (**129a**, 50 mg), sarcosine (N-methylglycine, 0.70 g), paraformaldehyde (1.1 g) and DDQ (200 mg)was refluxed in toluene (70 mL) for 24 h. The

solvent was removed *in vacuo* and the residue was subjected to column chromatograph with silica gel (14 g) using 2 % CH_3OH/CH_2Cl_2. Compound **138** was obtained with impurities. MS (LSIMS) 782 (100%).

6.4 Experimental Data for Chapter 4

(NCTTP)Ni^{II} (110 mg) and DDQ (400 mg) were added to a 1:1 CH_2Cl_2/CH_3OH (70 mL) solution of $NaOCH_3$ (200 mg). The solution was stirred for 24 h at r. t. and then washed with saturated aqueous $NaHCO_3$ solution for three times. The solvent was removed *in vacuo* and the residue was subjected to column chromatography (silica gel, 16 g). Using 1:1 CH_2Cl_2/hexanes. (NCTTP)Ni^{II} was eluted first; 3:1 CH_2Cl_2/hexanes eluted the first new compound, **145** (11.7 mg, 9.9 %), and the second new compound, **146** (30.3 mg, 27 %), was eluted with CH_2Cl_2.

2-Aza-21-cyano-3-methoxy-5,10,15,20-tetrakis(*p*-tolyl)-21-carbaporphyrinatonickel(II) (145)

R_f (silica-CH_2Cl_2/hexanes 2:1) 0.63; ^{1}H-NMR (400 MHz, CD_2Cl_2) δ = 2.63 (m, 12H), 4.21 (s, 3H), 7.41 - 7.62 (m, 9H), 7.65 - 8.20 (m, 7H), 8.32 (d, J = 4.8 Hz, 1H), 8.36 (s, 2H), 8.38 - 8.51 (m, 3H); ^{13}C-NMR (100 MHz, CD_2Cl_2) δ = 21.57, 21.67, 57.72, 108.28, 123.02, 125.60, 126.28, 128.09, 128.18, 128.41, 128.88, 129.77, 131.75, 131.81, 132.55, 133.55, 133.86, 133.93, 135.50, 136.38, 137.19, 137.31, 137.76, 137.96, 138.31, 138.68, 138.80, 138.94, 146.64, 147.21, 148.60, 149.23, 155.29, 159.99, 164.85, 172.83; UV-vis (CH_2Cl_2) λ_{max}/nm (log ε) 434 (5.12), 716 (3.96); MS (LSIMS) 782 (MH^+, 100%); HRMS (LSIMS) *m/e* Calcd for $C_{50}H_{38}N_5NiO$: 782.24294, found 782.24344 (MH^+); Anal Calcd for $C_{50}H_{37}N_5NiO{\cdot}H_2O$: C, 75.02; H, 4.91; N, 8.75. Found: C, 74.74; H, 4.68; N, 8.68.

2-Aza-21-cyano-5,10,15,20-tetrakis(*p*-tolyl)-21-carbaporphyrinatonickel(II) (146)

R_f (silica-CH_2Cl_2/hexanes 2:1) 0.37; ^{1}H-NMR (400 MHz, CD_2Cl_2) δ = 2.66 (m, 12H), 7.56 (d, *J* = 7.7 Hz, 4H), 7.63 (d, *J* = 7.7 Hz, 2H), 7.69 (d, *J* = 7.5 Hz, 2H), 7.78 - 8.32 (m, 8H), 8.56 (d, *J* = 4.8 Hz, 1H), 8.58 - 8.66 (m, 3H), 8.73 (d, *J* = 5.0 Hz, 1H), 8.76 (d, *J* = 5.0 Hz, 1H), 10.03 (s, 1H); ^{13}C-NMR (100 MHz, CD_2Cl_2) δ = 21.59, 106.75, 125.86, 127.50, 128.00, 128.13, 128.91, 129.40, 132.30, 133.01, 133.40, 133.71, 134.09, 134.27, 135.04, 135.57, 135.82, 135.90,137.52, 137.86, 137.98, 138.78, 138.84, 138.97, 139.96, 143.72, 147.80, 148.88, 149.25, 149.96, 154.63, 157.48, 158.15, 168.43; UV-vis (CH_2Cl_2) λ_{max}/nm (log ε) 434 (5.14), 716 (3.65); MS (LSIMS) 752 (MH^+, 100%); HRMS (LSIMS) *m/e* Calcd for $C_{49}H_{36}N_5Ni$: 752.23237, found 752.23242 (MH^+); Anal Calcd for $C_{49}H_{35}N_5Ni{\cdot}CH_3OH{\cdot}0.5H_2O$: C, 75.68; H, 5.08; N, 8.83. Found: C, 75.97; H, 4.76; N, 9.09.

6.5 Experimental Data for Chapter 5

6.5.1 Synthesis of Ni(III) N-Confused Porphyrin Inner C-Oxide

A solution of the (NCTTP)Ni^{II} complex, **129b** (130 mg), and OsO_4 (60 mg) in 15 % pyridine/CH_2Cl_2 (50 mL) was stirred at r. t. for 24 h and then filtered through a silica gel plug using 10 % CH_3OH in CH_2Cl_2. The solvent was removed *in vacuo* and the residue was subjected to column chromatography (silica gel, 16 g). Compound **153** was eluted with 1.5 % CH_3OH in CH_2Cl_2 and was obtained in a 42 % yield.

Ni(III) complex of N-confused porphyrin inner C-oxide 153

R_f (silica-CH_2Cl_2/5% CH_3OH/2% Et_3N) 0.70; UV-vis (CH_2Cl_2) λ_{max}/nm (log ε) 380 (4.70), 428 (sh), 470 (sh); MS (LSIMS) 742 (MH^+, 100%); HRMS (LSIMS) *m/e* Calcd for

$C_{48}H_{36}N_4NiO$: 742.22421, found 742.22443 (MH^+); MS (-LSIMS) 741 (M^-, 100%); HRMS (-LSIMS) *m/e* Calcd for $C_{48}H_{35}N_4NiO$: 741.21639, found 741.21609 (M^-); Anal. Calcd for $C_{48}H_{35}N_4NiO.C_5H_5N$: C, 77.47; H, 4.91; N, 8.52. Found: C, 77.36; H, 4.97; N, 8.61.

6.5.2 Measurement of Room Temperature Effective Magnetic Moment

A dilute CD_2Cl_2 solution of cyclohexane (reference) was placed in the NMR sample tube while the solvent containing complex **153** and cyclohexane was incorporated in an inner narrow-bore tube and held in place with a Teflon spacer. The ^1H NMR spectrum of cyclohexane in the two coaxial tubes exhibits a chemical shift difference, which was used to calculate the room temperature effective magnetic moment.[8-11]

6.6 Crystal Data and Details of the Structure Determination

Table 6.1 Crystal data and details of the structure determination for **108**.

Empirical Formula	$C_{47}H_{35}N_4SO_3F_3 \cdot H_2O$
Formula Weight	810.88
Crystal Color, Habit	Dark, chip
Crystal Dimensions	0.50 x 0.25 x 0.15 mm
Crystal System	Triclinic
Lattice Type	Primitive
Lattice Parameters	a = 11.922(2) Å b = 13.505(2) Å c = 15.090(3) Å α = 110.043(6)° β = 94.106(6)° γ = 113.859(7)° V = 2023.9(6) Å^3
Space group	$P\bar{1}$ (#2)
Z value	2
D_{calc}	1.330 g/cm^3
F_{000}	844.00
μ(MoKα)	1.44 cm^{-1}
Temperature	198 K
Diffractometer	Rigaku/ADSC CCD
Radiation	MoKα (λ = 0.71069 Å) graphite monochromated
Detector Aperture	94 mm x 94 mm
Data Images	4620 exposures @ 51.0 seconds
ø oscillation Range (χ = -90.0)	0.0 - 190.0°

Table 6.1 Crystal data and details of the structure determination for **108** (continued).

ω oscillation Range (χ = -90.0)	-22.0 - 18.0°
Detector Position	38.33 mm
Detector Swing Angle	-10.50°
$2\theta_{max}$	50.4°
No. of Reflections Measured	Total: 11514 Unique: 5815 (R_{int} = 0.056)
Corrections	Lorentz-polarization Absorption/scaling/decay (trans. factors: 0.6115 - 1.0000)
Structure Solution	Direct Methods (SIR97)
Refinement	Full-matrix least-squares
Function Minimized	$\Sigma w(Fo^2 - Fc^2)^2$
p-factor	0.0000
Anomalous Dispersion	All non-hydrogen atoms
No. Observations (I>0.00σ(I))	5815
No. Variables	544
Reflection/Parameter Ratio	10.69
Residuals (refined on F^2, all data): R; Rw	0.122; 0.176
Goodness of Fit Indicator	1.69
Max Shift/Error in Final Cycle	0.01
No. Observations (I>2σ(I))	3078
Residuals (refined on F, I>2σ(I)): R; Rw	0.061; 0.074
Maximum peak in Final Diff. Map	0.60 $e^-/Å^3$
Minimum peak in Final Diff. Map	-0.53 $e^-/Å^3$

Table 6.2 Crystal data and details of the structure determination for **115**.

Empirical Formula	$C_{52}H_{43}N_4NiI$
Formula Weight	909.54
Crystal Color, Habit	purple, needle
Crystal Dimensions	0.50 x 0.15 x 0.15 mm
Crystal System	Triclinic
Lattice Type	Primitive
Lattice Parameters	a = 10.0178(8) Å b = 14.2261(6) Å c = 16.329(1) Å α = 108.764(2)° β = 94.009(2)° γ = 109.291(3)° V = 2038.9(2) Å^3
Space group	$P\bar{1}$ (#2)
Z value	2
D_{calc}	1.481 g/cm^3
F_{000}	928.00
μ(MoKα)	12.76 cm^{-1}
Temperature	173 K
Diffractometer	Rigaku/ADSC CCD
Radiation	MoKα (λ = 0.71069 Å) graphite monochromated
Detector Aperture	94 mm x 94 mm
Data Images	462 exposures @ 19.0 seconds
ø oscillation Range (χ = -90.0)	0.0 - 190.0°

Table 6.2 Crystal data and details of the structure determination for **115** (continued).

ω oscillation Range (χ = -90.0)	-23.0 - 18.0°
Detector Position	40.30 mm
Detector Swing Angle	-10.52°
$2\theta_{max}$	60.3°
No. of Reflections Measured	Total: 17463 Unique: 8533 (R_{int} = 0.036)
Corrections	Lorentz-polarization Absorption/scaling/decay (trans. factors: 0.7367 - 1.0000)
Structure Solution	Patterson Methods (DIRDIF92 PATTY)
Refinement	Full-matrix least-squares
Function Minimized	$\Sigma w(Fo^2 - Fc^2)^2$
p-factor	0.0000
Anomalous Dispersion	All non-hydrogen atoms
No. Observations (I>0.00σ(I))	8533
No. Variables	527
Reflection/Parameter Ratio	16.19
Residuals (refined on F^2, all data): R; Rw	0.076; 0.134
Goodness of Fit Indicator	1.69
Max Shift/Error in Final Cycle	0.01
No. Observations (I>2σ(I))	6180
Residuals (refined on F, I>2σ(I)): R; Rw	0.046; 0.062
Maximum peak in Final Diff. Map	1.02 $e^-/Å^3$
Minimum peak in Final Diff. Map	-1.69 $e^-/Å^3$

Table 6.3 Crystal data and details of the structure determination for **133a**.

Empirical Formula	$C_{52}H_{32}N_4NiI$
Formula Weight	771.55
Crystal Color, Habit	dark, needle
Crystal Dimensions	0.50 x 0.15 x 0.05 mm
Crystal System	Monoclinic
Lattice Type	Primitive
Lattice Parameters	a = 13.2484(19) Å b = 15.1197(17) Å c = 19.255(3) Å β = 110.821(3)° V = 3605.1(9) Å^3
Space group	$P2_1/c$ (#14)
Z value	4
D_{calc}	1.421 g/cm^3
F_{000}	1600.00
μ(MoKα)	5.84 cm^{-1}
Temperature	173 K
Diffractometer	Rigaku/ADSC CCD
Radiation	MoKα (λ = 0.71069 Å) graphite monochromated
Detector Aperture	94 mm x 94 mm
Data Images	460 exposures @ 49.0 seconds
ø oscillation Range (χ = -90.0)	0.0 - 190.0°

Table 6.3 Crystal data and details of the structure determination for **133a** (continued).

ω oscillation Range (χ = -90.0)	-17.0 - 23.0°
Detector Position	38.10 mm
Detector Swing Angle	-5.59°
$2\theta_{max}$	55.7°
No. of Reflections Measured	Total: 33795 Unique: 8021 (R_{int} = 0.085)
Corrections	Lorentz-polarization Absorption/scaling/decay (trans. factors: 0.7875 - 1.0000)
Structure Solution	Direct Methods (SIR97)
Refinement	Full-matrix least-squares
Function Minimized	$\Sigma w(Fo^2 - Fc^2)^2$
p-factor	0.0000
Anomalous Dispersion	All non-hydrogen atoms
No. Observations (I>0.00σ(I))	7755
No. Variables	514
Reflection/Parameter Ratio	15.09
Residuals (refined on F^2, all data): R; Rw	0.076; 0.090
Goodness of Fit Indicator	0.80
Max Shift/Error in Final Cycle	0.00
No. Observations (I>2σ(I))	4167
Residuals (refined on F, I>2σ(I)): R; Rw	0.036; 0.039
Maximum peak in Final Diff. Map	0.50 $e^-/Å^3$
Minimum peak in Final Diff. Map	-0.59 $e^-/Å^3$

Table 6.4 Crystal data and details of the structure determination for **145**.

Empirical Formula	$C_{50}H_{37}N_5NiO$
Formula Weight	782.56
Crystal Color, Habit	Brown, platelet
Crystal Dimensions	0.20 x 0.20 x 0.10 mm
Crystal System	Triclinic
Lattice Type	Primitive
Lattice Parameters	a = 9.8239(4) Å b = 12.7674(6) Å c = 15.3382(7) Å α = 82.788(8)° β = 81.698(7)° γ = 82.301(8)° V = 1875.39(15) Å^3
Space group	Pī (#2)
Z value	2
D_{calc}	1.388 g/cm^3
F_{000}	818.00
μ(MoKα)	5.65 cm^{-1}
Temperature	173 K
Diffractometer	Rigaku/ADSC CCD
Radiation	MoKα (λ = 0.71069 Å) graphite monochromated
Detector Aperture	94 mm x 94 mm
Data Images	460 exposures @ 47.0 seconds
ø oscillation Range (χ = -90.0)	0.0 - 190.0°

Table 6.4 Crystal data and details of the structure determination for **145** (continued).

ω oscillation Range (χ = -90.0)	-17.0 - 23.0°
Detector Position	38.79 mm
Detector Swing Angle	-5.54°
$2\theta_{max}$	55.7°
No. of Reflections Measured	Total: 17139 Unique: 7723 (R_{int} = 0.066)
Corrections	Lorentz-polarization Absorption/scaling/decay (corr. factors: 0.7797 - 1.0000)
Structure Solution	Direct Methods (SIR97)
Refinement	Full-matrix least-squares
Function Minimized	$\Sigma w(Fo^2 - Fc^2)^2$
p-factor	0.0000
Anomalous Dispersion	All non-hydrogen atoms
No. Observations (I>0.00σ(I))	7709
No. Variables	538
Reflection/Parameter Ratio	14.33
Residuals (refined on F^2, all data): R; Rw	0.088; 0.112
Goodness of Fit Indicator	0.95
Max Shift/Error in Final Cycle	0.00
No. Observations (I>2σ(I))	5006
Residuals (refined on F, I>2σ(I)): R; Rw	0.048; 0.099
Maximum peak in Final Diff. Map	0.31 $e^-/Å^3$
Minimum peak in Final Diff. Map	-0.54 $e^-/Å^3$

Table 6.5 Crystal data and details of the structure determination for **146**.

Empirical Formula	$C_{49}H_{35}N_5Ni \cdot 0.5H_2O$
Formula Weight	761.55
Crystal Color, Habit	Dark, chip
Crystal Dimensions	0.15 x 0.15 x 0.10 mm
Crystal System	Triclinic
Lattice Type	Primitive
Lattice Parameters	a = 9.7125(10) Å b = 14.3732(15) Å c = 14.0565(15) Å α = 94.720(10)° β = 77.440(10)° γ = 76.150(10)° V = 1840.9(4) Å^3
Space group	$P\bar{1}$ (#2)
Z value	2
D_{calc}	1.376 g/cm^3
F_{000}	796.00
μ(MoKα)	5.73 cm^{-1}
Temperature	173 K
Diffractometer	Rigaku/ADSC CCD
Radiation	MoKα (λ = 0.71073 Å) graphite monochromated
Detector Aperture	94 mm x 94 mm
Data Images	460 exposures @ 55.0 seconds
ø oscillation Range (χ = -90.0)	0.0 - 190.0°

Table 6.5 Crystal data and details of the Structure determination for **146** (continued).

ω oscillation Range (χ = -90.0)	-17.0 - 23.0°
Detector Position	38.72 mm
Detector Swing Angle	-5.60°
$2\theta_{max}$	50.1°
No. of Reflections Measured	Total: 44912 Unique: 10104 (R_{int} = 0.063)
Corrections	Lorentz-polarization Absorption/scaling/decay (corr. factors: 0.4343 - 1.0000)
Structure Solution	Direct Methods
Refinement	Full-matrix least-squares
Function Minimized	$\Sigma w(Fo^2 - Fc^2)^2$
Anomalous Dispersion	All non-hydrogen atoms
No. Observations (I>0.00σ(I))	10104
No. Variables	509
Residuals (refined on F^2, all data): R; Rw	0.134; 0.160
Goodness of Fit Indicator	0.96
Max Shift/Error in Final Cycle	0.00
No. Observations (I>2σ(I))	5521
Residuals (refined on F, I>2σ(I)): R; Rw	0.064; 0.142
Maximum peak in Final Diff. Map	0.58 $e^-/Å^3$
Minimum peak in Final Diff. Map	-0.43 $e^-/Å^3$

Table 6.6 Crystal data and details of the structure determination for **153**.

Empirical Formula	$C_{53}H_{40}N_5NiO \cdot CH_2Cl_2$
Formula Weight	906.56
Crystal Color, Habit	Green, platelet
Crystal Dimensions	0.35 x 0.30 x 0.03 mm
Crystal System	Monoclinic
Lattice Type	Primitive
Lattice Parameters	a = 21.2291(14) Å b = 8.6451(5) Å c = 25.7622(17) Å β = 93.004(3)° V = 4721.6(5) Å^3
Space group	P2/a (#13)
Z value	4
D_{calc}	1.275 g/cm^3
F_{000}	1884.00
μ(MoKα)	5.68 cm^{-1}
Temperature	173 K
Diffractometer	Rigaku/ADSC CCD
Radiation	MoKα (λ = 0.71069 Å) graphite monochromated
Detector Aperture	94 mm x 94 mm
Data Images	460 exposures @ 47.0 seconds
ø oscillation Range (χ = -90.0)	0.0 - 190.0°

Table 6.6 Crystal data and details of the structure determination for **153** (continued).

ω oscillation Range (χ = -90.0)	-17.0 - 23.0°
Detector Position	37.98 mm
Detector Swing Angle	-5.59°
$2\theta_{max}$	55.8°
No. of Reflections Measured	Total: 40883 Unique: 11220 (R_{int} = 0.084)
Corrections	Lorentz-polarization Absorption/scaling/decay (trans. factors: 0.7145 - 1.0000)
Structure Solution	Direct Methods (SIR97)
Refinement	Full-matrix least-squares
Function Minimized	$\Sigma w(Fo^2 - Fc^2)^2$
p-factor	0.0000
Anomalous Dispersion	All non-hydrogen atoms
No. Observations (I>0.00σ(I))	10590
No. Variables	587
Reflection/Parameter Ratio	18.04
Residuals (refined on F^2, all data): R; Rw	0.112; 0.209
Goodness of Fit Indicator	0.94
Max Shift/Error in Final Cycle	0.00
No. Observations (I>2σ(I))	6256
Residuals (refined on F, I>2σ(I)): R; Rw	0.071; 0.187
Maximum peak in Final Diff. Map	0.98 $e^-/Å^3$
Minimum peak in Final Diff. Map	-0.77 $e^-/Å^3$

References

1. Perrin, D. D. and Armarego, W. L. F. *Purification of Laboratory Chemicals*, 3rd ed. ed.; Pergamon Press: New York, 1988.
2. Geier, G. R., Haynes, D. M. and Lindsey, J. S. *Org. Lett.* **1999,** *1*, 1455.
3. Furuta, H., Asano, T. and Ogawa, T. *J. Am. Chem. Soc.* **1994,** *116*, 767.
4. Chmielewski, P. J., Latos-Grażyński, L., Rachlewicz, K. and Glowiak, T. *Angew. Chem., Int. Ed. Engl.* **1994,** *33*, 779.
5. Spiller, W., Kliesch, H., Wohrle, D., Hackbarth, S., Roder, B. and Schnurpfeil, G. *J. Porphyr. Phthalocya.* **1998,** *2*, 145.
6. Chmielewski, P. J., Latos-Grażyński, L. and Glowiak, T. *J. Am. Chem. Soc.* **1996,** *118*, 5690.
7. Hoey, M. D. and Dittmer, D. C. *J. Org. Chem.* **1991,** *56*, 1947.
8. Cheu, E. *Thioether and Sulfoxide Complexes of Ruthenium; Preliminary In Vitro Studies of the Water-Soluble Species*, Ph.D. Thesis, University of British Columbia 2000.
9. Evans, D. A. *J. Am. Chem. Soc.* **1959,** *81*, 2003.
10. Sur, S. K. *J. Magn. Reson.* **1989,** *82*, 169.
11. Weast, R. C. Handbook of Chemistry and Physics; CRC Press: Cleveland, Ohio, 1986.

Chapter 7

Summary and Future Work

7.1 Thesis Summary

Inner nitrogen atoms of N-confused porphyrins are reactive towards alkylation. N,N'-dimethylated N-confused porphyrin salts, which are mixtures of structural isomers, were obtained in the reactions of N-confused porphyrins with CH_3I in the presence of Na_2CO_3 (Chapter 2). These N,N'-dimethylated N-confused porphyrin salts have been shown to generate singlet oxygen when irradiated with light of the appropriate wavelengths and are potential photosensitizers for PDT.

Two dipolar canonical forms (Scheme 7.1) were proposed to explain the reactivity of Ni(II) N-confused porphyrins. Unlike canonical form **I**, canonical forms **II** and **III** reserve the 18 π-electron pathway and have more of a double bond character for the N(2)-C(3) bond. The importance of canonical forms **II** and **III** to the overall resonance hybrid is suggested by the X-ray crystal structure of Ni(II) N(2)-iodooctyl N-confused tetraphenylporphyrin, **115** (section 2.2.3.1), which is isoelectronic with Ni(II) N-confused porphyrins, as the N(2)-C(3) bond length of **115**, 1.311(4) Å, is markedly shorter than those of the peripheral C-C bonds, 1.345(5) or 1.346(5) Å.

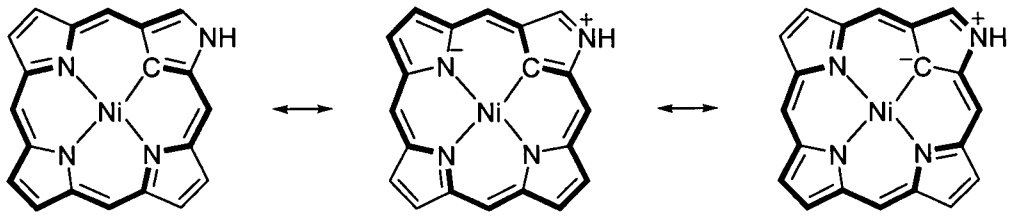

I **II** **III**

Scheme 7.1 Three canonical forms for a Ni(II) N-confused porphyrin. The negative charge in canonical form **II** can also be located on other inner nitrogen atoms.

In canonical forms **II** and **III**, the peripheral C-N bond is both "cross conjugated" and in the iminium form, which is known to be electron-deficient and an active dienophile.[1] Ni(II) N-confused porphyrins reacted selectively at the peripheral C-N bond with *o*-benzoquinodimethane giving novel Ni(II) N-confused isoquinoporphyrins, presumably formed by oxidation of the initially formed Diels-Alder adducts (Chapter 3).

The canonical form **III** of Ni(II) N-confused porphyrins suggests that Ni(II) N-confused porphyrins are electrophiles at C(21). Inner C(21)-methylation has been observed by Latos-Grażyński *et al.*[2] Inner C(21) cyanide addition and subsequent nucleophilic addition of CH_3O^- at C(3) followed by oxidation with DDQ were observed in reactions of $(NCTPP)Ni^{II}$ with $NaOCH_3$ and DDQ (Chapter 4). Electrophilic addition of the reduction product of DDQ to the deprotonated $(NCTPP)Ni^{II}$ was proposed as the critical step for the inner cyanide addition.

A Ni(III) complex of N-confused porphyrin inner C-oxide was obtained in the reactions of Ni(II) N-confused porphyrins with OsO_4, and the canonical form **III** of Ni(II) N-confused porphyrins can be used to explain the susceptibility of C(21) towards oxidation (Chapter 5).

In summary, N-confused porphyrins are involved in a variety of reactions, especially reactions involving the inner carbon and nitrogen atoms, as well as the peripheral C-N bond. These modified N-confused porphyrins can be potential photosensitizers for PDT, as well as interesting ligands with novel structural features.

7.2 Future Work

The canonical forms **II** and **III** of Ni(II) N-confused porphyrins suggest that the peripheral carbon-nitrogen bond of Ni(II) N-confused porphyrins has some iminium character and might be reactive towards nucleophiles. However, direct nucleophilic addition was not observed in the reactions of Ni(II) N-confused porphyrins with $NaOCH_3$ and DDQ, presumably because of the

deprotonation of Ni(II) N-confused porphyrins in strong basic conditions. Therefore, nucleophilic addition of a less basic nucleophile, such as **166**, to Ni(II) N-confused porphyrins, might be possible (Scheme 7.2).

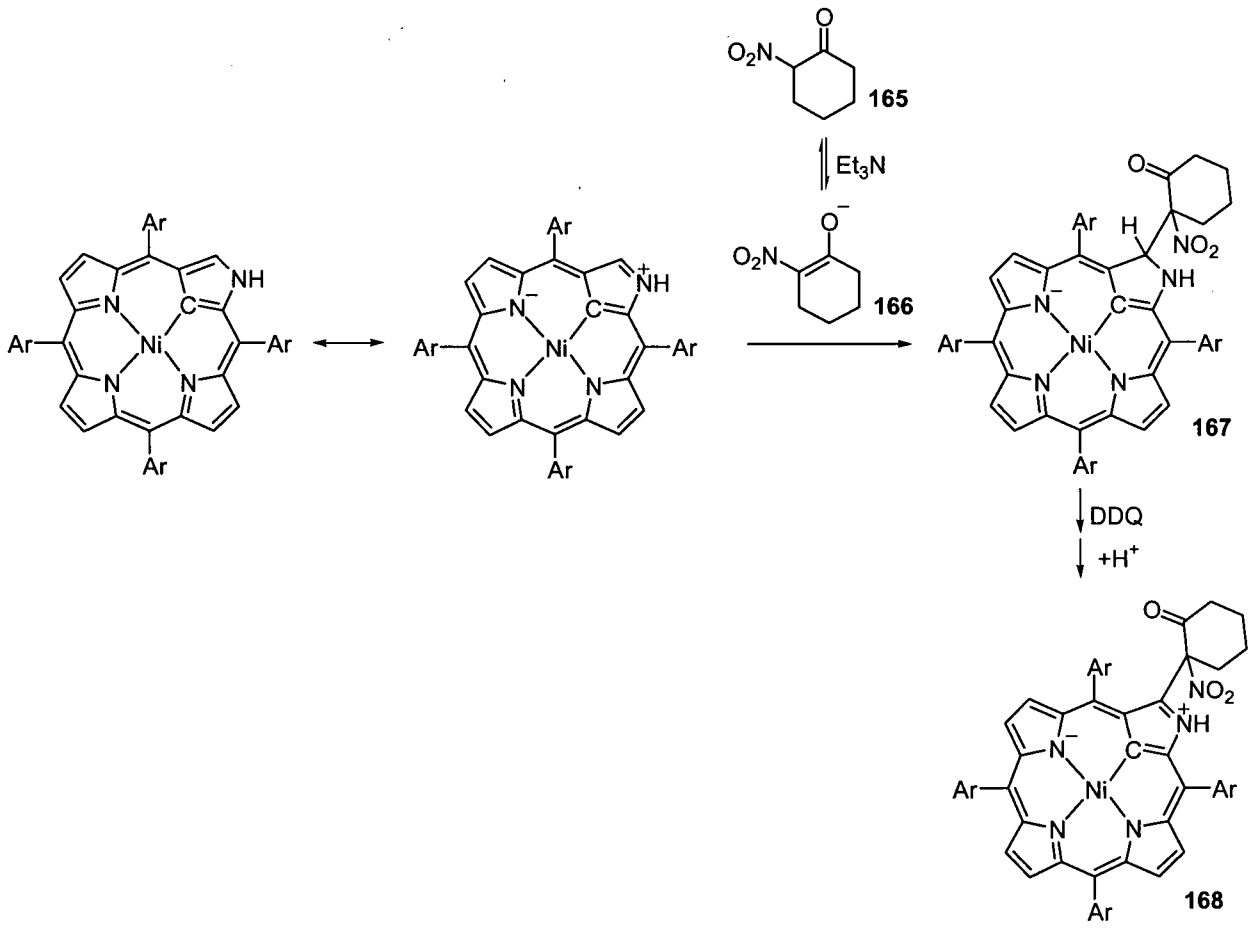

Scheme 7.2 Proposed nucleophilic addition of an enolate to a Ni(II) N-confused porphyrin.

The mechanism proposed for the inner C- cyanide addition (section 4.2.1) suggests that the cyanide addition might be general to other nucleophiles. Thus, reaction of **148**, the reduction product of DDQ, with an enolate, such as **166**, may result in cyanide addition to the enolate (Scheme 7.3). This would be a useful method in organic synthesis as the cyanide group can be easily transformed to other functional groups, such as an amine, a carboxylic acid, or an aldehyde.

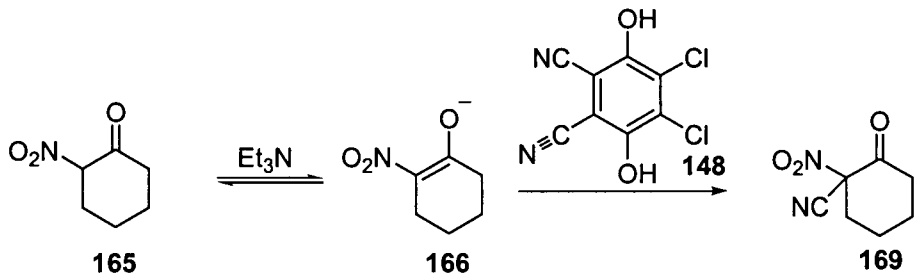

Scheme 7.3 Proposed cyanide addition to an enolate.

The Ni(III) complex of N-confused porphyrin inner C-oxide **153** is structurally similar to an Fe(III) porphyrin N-oxide **154**, which was proposed as an alternative candidate of compound I, **155**, for the active intermediate of cytochrome P-450 (Figure 5.7).[3] It will be interesting to study the reactions of Fe(II) N-confused porphyrins[4] with OsO_4. The possible product, an Fe complex of N-confused porphyrin inner C-oxide, might have a high oxidation state for the iron ion and still be stable. It will also be interesting to see whether this Fe complex has any catalytic activity toward epoxidation or hydroxylation reactions.

References

1. Boger, D. L. and Weinreb, S. N. Organic Chemistry. In *Hetero Diels-Alder Methodology in Organic Synthesis;* Wasserman, H. H. Ed.; Academic Press: San Diego, 1987; Vol. 47; pp. 34.

2. Chmielewski, P. J., Latos-Grażyński, L. and Glowiak, T. *J. Am. Chem. Soc.* **1996,** *118*, 5690.

3. Watanabe, Y. *J. Biol. Inorg. Chem.* **2001,** *6*, 846.

4. Chen, W. C. and Chen, C. H. *Inorg. Chem.* **2001,** *40*, 5070.